The use of 3D image analysis in the diagnosis and treatment planning of corrective surgery for mandibular asymmetry patients

Alhadidi, Abeer

Awarding institution:
King's College London

The use of 3D image analysis in the diagnosis and treatment planning of corrective surgery for mandibular asymmetry patients

A dissertation submitted to the Dental Institute, King's college London in fulfillment of the requirements for a PhD in Oral and maxillofacial Radiology

Abeer AlHadidi, DDS, MS

Supervisors KCL and UNC

Dr. Lucia Cevidanes, Dr. Beatriz Paniagua, Dr. Richard Cook, Dr. Frederic Festy, and Dr. Donald Tyndall

Postgraduate Coordinator

Dr. Lucy Di Silvio

Biomaterial, Biomimetics & Biophotonics
Dental Institute
King's College London

2014

ABSTRACT

The use of 3D image analysis in the diagnosis and treatment planning of corrective surgery for mandibular asymmetry patients

Background: mandibular asymmetry poses a challenge in craniofacial diagnosis and treatment planning. Variability in etiology and presentation necessitates accurate asymmetry diagnosis and quantification for treatment planning and follow-up. Conventional cephalometric radiographs have inherent superimpositions, magnifications and distortions, limiting their clinical value.

Aims: To develop and trial novel diagnostic Cone Beam CT image analysis procedures, to enhance treatment by quantification and localization of mandibular asymmetries. Development and trials employed simulation and patient datasets, including end-user clinicians' perception of simulation versus conventional surgical outcomes.

Methods: Twenty asymmetric patients' CBCT volumes were segmented, constructing surface models, allowing 3D image analyses, using voxel-based co-registration. Mirroring techniques computed left to right side dissimilarities and validation studies initially compared known introduced asymmetries. The SPHARM-PDM toolbox was then applied to a cohort of 60 patients with varying degrees of asymmetry to assess detection limits and functionality, including a Craniofacial

Microsomia dataset. Finally, an algorithm was developed to compute virtual mandibular surgical outcomes and a multi-centre study compared both real and virtual outcomes for 20 patients.

Results: SPHARM-PDM proved a valid technology to quantify degree and direction of mandibular asymmetries with probabilities of (0.99-1) and (0.84-1) respectively, that true asymmetry was within 0.5 mm (translation) or 5^0 (rotation). Whether right or left mandible was mirrored, no statistical output differences were identified, demonstrating consistency. The functional limit is identified as no anatomical correspondence e.g. where a complete structural loss or external augmentation has arisen.

Encouragingly, simulated outcomes based on virtual templates were better than actual outcomes, conventionally planned, in particular in difficult cases.

Conclusion: SPHARM-PDM is useful for diagnosis and quantification of mandibular asymmetries and virtual templates in treatment planning offer potentials to increase predictability and optimize craniofacial interventions.

ACKNOWLEDGEMENTS

I would like to express my profound gratitude and deep regards to my mentor Dr. Cevidanes for her exemplary guidance, monitoring and constant encouragement throughout the course of this work. Her enthusiasm and amazing energy has always been inspiring. I would also like to express my special appreciation and thanks to Dr. Paniagua for her support, guidance and her extraordinary passion throughout this work. I am gratefull to Dr. Cook for all the time and effort he dedicated to this work. I learned so much from his pricless advice, brilliant comments, and suggestions. I also thank Dr. Festy for his valuable feedback. I will always be in debt to Dr. Tyndall for his extreme help and support. Without your vision and extraordinary effort none of this would have been possible. I am beholden to my great family and best friends Sahar and Sandra, your prayer for me was what sustained me thus far.

TABLE OF CONTENTS

LIST OF FIGURES:

LIST OF TABLES:

List of abbreviations:

ANS: Anterior Nasal Spine

Ba: Basion

BEIR: Biological Effects of Ionizing Radiations

CASS: Computer Aided Surgical Simulation

CBCT: Cone Beam Computed Tomography

CMF: CranioMaxilloFacial software application

CP: Closest Point algorithm

CT: Computed Tomography

MRI: Magnetic Resonance Imaging

Na: Nasion

NIRAL: The Neuro-Image Research and Analysis Lab at the University of North Carolina

SPHARM: SPherical HARMonic representation

UNSCEAR: United Nations Scientific Commission on Effects of Atomic Radiation

“Cell and tissue, shell and bone, leaf and flower, are so many portions of matter, and it is in obedience to the laws of physics that their particles have been moved, moulded and conformed. They are no exceptions to the rule that God always geometrizes. Their problems of form are in the first instance mathematical problems, their problems of growth are essentially physical problems, and the morphologist is, ipso facto, a student of physical science.”

– D’Arcy Thompson

Chapter 1

Introduction

1.1 The clinical problem:

Craniofacial deformity occurs in around 5% of the US population, and 2% of these have facial asymmetry severe enough to be disabling and stigmatizing (Severt, Proffit 1997). Internationally prevalence rates of facial asymmetry range between 21% and 85% (Fong JH et al. 2010, Lee MS et al. 2010, Reyneke JP et al. 1997, Ferrario VF et al. 2001, Proffit WR and White RP Jr. 1990).

The variation on the prevalence rates may stem from sample characteristics, dental-facial deformity type, assessment methods and tools, and the criteria defining asymmetry used by the authors. In South East Asian populations asymmetry was reported in 21-35.8% of patients with dentofacial deformities, with the majority of cases in patients with class III occlusal deformity (Chew MT 2005, Samman N et al. 1992). Chew suggested that special attention be paid to class III patients to detect any asymmetry. Class III is more common in South East Asians than in Caucasians, so it is a reasonable assumption that there are more patients with facial asymmetry. In an adolescent group in (Jeddah, Kingdom of Suadi Arabia) mandibular asymmetry was reported as the presence of a midline shift and was reported to be 24% of the studied population (Al-Nowaiser et al. 2010). Others took an anthropometric approach to study the prevalence of facial asymmetry. Ponyi S et al. 1991 examined

10th-12th-century European skulls from burial sites in South-Eastern Hungary for mandibular asymmetry and concluded that asymmetry of the left and right sides was found between the measured individual mandibular dimensions on average in 41.4% of the males and 40.4% of the females.

Asymmetry occurs in 40% of dentofacial patients with Class III or long face problems, and in 28% of mandibular deficiency patients (Severt and Proffit 1997) Normally, the right side of the human face is slightly larger, and when an asymmetric mandible is observed in patients with mandibular deficiency or excess, there is a >80% chance that the chin is deviated to the left (Proffit et al. 2000, 1998). When excessive vertical growth of the maxilla occurs, left and right asymmetries are equally probable. Furthermore, correcting maxillary asymmetry usually involves moving one side up (and perhaps the other side down) to correct a canted occlusal plane and usually is done in conjunction with mandibular surgery. For the maxillary component of asymmetry surgery, downward movement of the maxilla is in the stability problematic category. Problematic stability in moving the maxilla down is due largely to changes within the first few postsurgical weeks, before bone healing is complete, as occlusal force tends to push it upward. There are three logical approaches to maintaining the position of the maxilla until it heals: heavy rigid fixation, a rigid hydroxyl apatite graft in the defect created by the downward movement, and simultaneous mandibular surgery to decrease the occlusal force. All are reasonably successful, but the rigid fixation has to be much heavier than typical

plates and screws and still is not completely effective (Proffit et al. 2007, Baily et al. 2004).

Facial asymmetry includes a spectrum of malformations that result from maxillary and/or mandibular relative hypoplasia or hyperplasia of the perceived affected side of the face (Proffit et al. 1998, Severt and Proffit 1997).

Facial asymmetry often poses a challenge in craniofacial diagnosis and treatment planning. The wide variability in the etiology and the presentation of asymmetry makes proper assessment and quantification of the differences between the right and left sides crucial for diagnosis, treatment planning, and follow up (Proffit et al. 2007). The choice of which side to use as a reference in the planning phase and the practical definition of a "healthy" side also added to the complexity of facial asymmetry as a 3 dimensional entity.

1.2 Symmetry and attractiveness:

Measures of symmetry in the human body and face correlate with attractiveness (Gangestad et al. 1994, Grammer and Thornhill 1994, Mealey and Bridgstock 1999). Such correlations may, however, be due to other factors co-varying with symmetry. For example, sex hormones may influence the symmetry of growth (Thornhill and Gangestad 1993) and chin shape, which independently affects attractiveness (Perrett et al. 1994).

Attractiveness is an important element of social life. A large body of research in social psychology has shown that “attractive” persons enjoy many advantages that “unattractive” persons do not have (Eagly et al. 1991, Bull and Rumsey 1988, Berscheid and Walster 1974). This well-known stereotype, described by social psychologists as the “What is beautiful is good” prototype (Dion et al. 1972), mainly applies to the formation of first impressions, but it can also extend into less superficial interactions (Frieze et al. 1991). For example, in a cross-sectional analytic interview study conducted by Newton JT et al. 2003, participants judged subjects with less dental disease to be more socially competent, to show greater intellectual achievement, and to have better psychologic adjustment.

Beauty was considered to lie in the eyes of the beholder (Bruce and Young 1998). In that sense, a person’s physical appearance is not the main aspect of his/her attractiveness. It is determined instead by the beholder, who probably takes personality into account in addition to physical appearance. Above all, it is believed that each beholder has personal likings that may differ from those of others. Thus, a face may be attractive for some people but unattractive for others. However, other studies have reported substantial agreement, not only within the sexes but also across sexes, ethnic groups, and ages (Cunningham et al. 1995, Langlois et al. 1991, Langlois and Roggman 1990).

Moreover, some facial characteristics have been shown to be factors of attractiveness, including closeness to the average (Langlois and Roggman 1990), symmetry (Thornhill and Gangestad 1993), and the physical characteristics of

individual facial features (Cunningham 1986). From an evolutionary standpoint, the fact that humans share views about which features are attractive suggests that there are species-typical psychological adaptations that have evolved because of a preference for healthy and fertile mates (Symons 1979, Thornhill and Gangestad 1999). Langlois and her colleagues (1990) demonstrated the appeal of computer-generated averaged composites of faces. These were generally more attractive than the component faces, and as faces were added the composites became more attractive.

Converging evidence for the appeal of average faces comes from studies using normal, un-manipulated faces. Typical faces, which are closer to the population average, are consistently rated as more attractive than distinctive faces (Light et al. 1981, Morris and Wickham 2001, O'Toole et al. 1994, Rhodes and Tremewan 1996, Rhodes et al. 1999, 2005, Vokey and Read 1992). Furthermore, the attractiveness of individual faces can be increased (or reduced) by moving their configurations toward (or away from) an average configuration for that sex (O'Toole et al. 1999, Rhodes et al. 1999, Rhodes and Tremewan 1996).

Early research on the attractiveness of facial symmetry was motivated by the idea that symmetry advertises mate quality (Polak 2003, Thornhill and Gangestad 1999, Gangestad and Thornhill 1997, Thornhill and Møller 1997, Gangestad et al. 1994, Watson and Thornhill 1994, Parsons 1990, Palmer and Strobeck 1986). Symmetric bodies are attractive to many animals, including humans (Gangestad and Simpson 2000, Concar 1995, Brooks and Pomiankowski 1994, Thornhill and

Gangestad 1994, Watson and Thornhill 1994).

But are symmetric faces attractive? Some studies suggested that they were not, with normal (slightly asymmetric) faces preferred to perfectly symmetric versions (Kowner 1996, Swaddle and Cuthill 1995, Langlois et al. 1994, Samuels et al. 1994). However, other studies found that perfectly symmetric faces were more attractive than the original, slightly asymmetric, faces (Perrett et al. 1999, Rhodes et al. 1998, 1999) and that their appeal could not be explained by any associated increase in averageness (Rhodes et al. 1999) or change in skin texture (Perrett et al. 1999, Rhodes et al. 1999).

Converging evidence for the appeal of facial symmetry comes from studies with normal faces. Natural variations in symmetry co-vary with attractiveness (Mealey et al. 1999, Scheib et al. 1999, Rikowski and Grammer 1999, Rhodes et al. 1998, 1999, Zebrowitz et al. 1996, Grammer and Thornhill 1994, Jones and Hill 1993). Symmetry remains attractive when the effects of averageness are statistically controlled, which suggests that the two contribute independently to attractiveness (Rhodes et al. 1999).

Facial bilateral symmetry is hypothesized to affect positive beauty judgments because symmetry is a certification of overall phenotypic quality and developmental health, it is hypothesized that human faces judged to be attractive by people possess two features; averageness and symmetry. That promoted adaptive mate selection in human evolutionary history.

Conditions affecting oral health, including malocclusion, are highly prevalent, and have consequences not only for physical and economical well being, but can also impair quality of life by affecting function, appearance, interpersonal relationships, socializing, self-esteem and psychological well-being (Adams 1977, Masood et al. 2013, Masood et al. 2012). In the UK, recent evidence has reported the prevalence of bullying in adolescents with a malocclusion aged between 10 and 14 at 12.8 per cent (Seehra et al. 2013). Facial features associated with being bullied include those with a higher need for orthodontic treatment when assessed using the aesthetic component of the Index of Orthodontic Treatment Need including asymmetry (Seehra et al. 2011).

1.3 Hard tissue support and soft tissue contour:

The interplay between the hard tissue scaffold and the overlaying soft tissue of the head and neck makes up the overall shape of the face. The pattern of later stages of growth and development of both hard and soft tissues is a major diagnostic and prognostic determinant of corrective orthognathic surgery. Growth of the nasomaxillary area is produced by two basic mechanisms: (1) passive displacement, created by growth in the cranial base that pushes the maxilla forward, and (2) active growth of the maxillary structures and nose (Profitt 2012).

Passive displacement of the maxilla is an important growth mechanism during the primary dentition years but becomes less important as growth at the synchondroses of the cranial base slows markedly with the completion of neural growth at about age 7 (Profitt 2012, Farkas et al. 1992).

Note that during the entire period between ages 7 and 15, about one third of the total forward movement of the maxilla can be accounted for on the basis of passive displacement. The rest is the result of active growth of the maxillary sutures in response to stimuli from the enveloping soft tissue. Growth of the mandible continues at a relatively steady rate before puberty (Profitt 2012, Farkas et al. 1992). On the average ramus height increases 1 to 2 mm per year and body length increases 2 to 3 mm per year. These cross sectional data tend to smooth out the juvenile and pubertal growth spurts, which do occur in growth of the mandible. One feature of mandibular growth is an accentuation of the prominence of the chin. The increase in chin prominence with maturity results from a combination of forward translation of the chin as a part of the overall growth pattern of the mandible and resorption above the chin that alters the bony contours. An important source of variability in how much the chin grows forward is the extent of growth changes at the glenoid fossa. If the area of the temporal bone to which the mandible is attached moved forward relative to the cranial base during growth, this would translate the mandible forward in the same way that cranial base growth translates the maxilla. However, this rarely happens. Usually, the attachment point moves straight down, so that there is no anteroposterior displacement of the mandible, but occasionally it moves posteriorly, thus subtracting from rather than augmenting the forward projection of the chin (Profitt 2012).

Maturational changes affect both the soft and hard tissues of the face and jaws, with greater long-term changes in the soft tissues. An important concept is that

changes in facial soft tissues not only continue with aging, they are much larger in magnitude than changes in the hard tissues of the face and jaws. The change of most significance for orthodontists is that the lips, and the other soft tissues of the face, sag downward with aging. With aging, the lips also become progressively thinner, with less vermilion display (Ackerman and Proffit 2007). Dynamically or statically, the soft tissue contours of the face are determined by three interacting factors: The skeletal foundation, which for the midface and lower face is provided by the jaws; The dental support system provided by the teeth; and the soft tissue mask influenced by both the underlying hard tissue and the components of the soft tissue itself (nose and chin, lip thickness, lip tonicity) (Ackerman and Proffit 2007).

1.4 Alternative diagnostic radiographic techniques:

Although cephalometric radiography has been and will probably continue to be the routine radiographic examination for many patients seeking orthodontic/orthognathic treatment, the ‘‘inappropriateness of conventional cephalometrics’’ was recognized as early as 1979 (Moyers and Bookstein 1979). The 2D radiographs conventionally used in orthodontic practice are particularly problematic when rotational or asymmetrical correction is required since surgical jaw displacements are inherently 3-dimensional (Sandor et al. 2007).

Since the discovery of radiography in early 1895 by Roentgen, many advances in radiologic practice have been proposed, and new devices for better imaging have been developed. However, intraoral and extraoral procedures, used individually or

in combination, suffer from the same inherent limitations of all planar two-dimensional (2D) projections: magnification, distortion, superimposition, and misrepresentation of structures. Numerous efforts have been made toward three-dimensional (3D) radiographic imaging (eg, Tomography, stereoscopy, and tuned aperture Computed Tomography) (Liang et al. 2001, Rashedi et al. 2003).

Cone beam computed tomography (CBCT) Imaging is accomplished by using a rotating gantry to which an x-ray source and detector are fixed. A divergent pyramidal or cone-shaped source of ionizing radiation is directed through the middle of the area of interest in the head and neck area, as well as the extremities in other clinical situations, of the patient onto an area x-ray detector on the opposite side. The x-ray source and detector rotate around a rotation fulcrum fixed within the center of the region of interest. During the rotation, multiple sequential planar projection images of the field of view (FOV) are acquired in a complete, or sometimes partial, arc. Because CBCT exposure incorporates the entire FOV, only one rotational sequence of the gantry is necessary to acquire enough data for image reconstruction.

Although Computed Tomography has been available for a long time, its application in dentistry has been limited because of cost, access, and dose considerations. The cone-beam geometry was developed as an alternative to conventional CT using either fan-beam or spiral-scan geometries, to provide more rapid acquisition of a data set of the entire field of view and it uses a comparatively

less expensive radiation detector. Obvious advantages of such a system, which provides a shorter examination time, include the reduction of image marginal resolution caused by the translation of the patient, reduced image distortion due to internal patient movements, and increased x-ray tube efficiency. However, its main disadvantage, especially with larger FOVs, is a limitation in image quality related to noise and contrast resolution because of the detection of large amounts of scattered radiation (Scarfe and Farman 2008, Robinson et al. 2005). Those disadvantages are still in favor of CBCT use in the maxillofacial region as larger field of view is not really needed and high signal to noise ratio is only needed in soft tissue applications (such as salivary gland disease and TMJ disk imaging) (White and Pharoah 2008). These applications are not routine in a typical dental practice and they already have other imaging modalities established as the standard of care in the management of such entities.

The introduction of cone-beam computed tomography (CBCT) specifically dedicated to imaging the maxillofacial region heralds a true paradigm shift from 2D to 3D approach to data acquisition and image reconstruction. After conventional CT scanners have been widely adopted in the medical field, some areas in dentistry still lack some breakthroughs for radiographic examination of the maxillofacial field. With the development and involvement of computer science and mathematical algorithms (the Feldkamp-Davis-Kress reconstruction method), cone beam computed tomography (CBCT), machines were turned to imaging devices sufficiently compact for operation in small-practice environments, especially in the head and

neck and dental fields (Scarfe and Farman 2008, Angelopoulos 2008, Hechler 2008). The Feldkamp-Davis-Kress reconstruction formula is deduced for direct reconstruction of a three-dimensional density function from a set of two-dimensional projections (Feldkamp et al. 1984).

Interest in CBCT from all fields of dentistry is unprecedented because it has created a revolution in maxillofacial imaging, facilitating the transition of dental diagnosis from 2D to 3D images and expanding the role of imaging from diagnosis to image guidance of operative and surgical procedures by way of third-party applications software. A key feature of CBCT images is the ability to navigate through the volumetric data set in any orthogonal slice. Instead of just analyzing 2D cross-sectional images from a 3D patient, clinicians must think in 3D directions instead of 2D directions (Cevidanes et al. 2006).

1.5 Radiation Risk:

Assessment of the risks associated with the use of ionizing radiation for diagnostic imaging is an important public health issue. Most CBCT examinations impart a fraction of medical CT effective dose; however, doses vary considerably among CBCT units (Ludlow et al. 2008, 2006, and 2003). Table 1.1 shows Effective Doses from Dental and Maxillofacial X-Ray Techniques and Probability of Excess Fatal Cancer Risk per Million Examinations.

Effective Doses from Dental and Maxillofacial X-Ray Techniques and Probability of Excess Fatal Cancer Risk per Million Examinations			
Technique	Dose microSieverts	CA Risk per Million exams	Background equivalent
Panoramic – direct digital	14.2	0.8	1.7 days
Skull/Cephalometric images – indirect digital	5	0.3	17 hours
Full mouth series (PSP or F-Speed film – Rectangular Collimation)	35	2	4.3 days
Full mouth series (PSP or F-Speed film – Round collimation)	171	9	21 days
Full mouth series (D-Speed film-Round Collimation)	388	21	47 days
Single PA or Bitewing (PSP or F-Speed film-Rectangular Collimation)	2	0.1	6 hours
Single PA or Bitewing (PSP or F-Speed film-Round Collimation)	9.5	0.5	1 day
Single PA or Bitewing (D-Speed film-Round Collimation)	22	1.2	2.6 days
4 Bitewings (PSP or F-Speed film-Rectangular Collimation)	5	0.3	17 hours
4 Bitewings (D-Speed film-Round Collimation)	88	5	10 days
Tomogram (8 cm ´ 8 cm field)	10	0.5	1 day
Cone Beam CT exam (NewTom 3G/ 23 cm field of view)	68	4	8 days
Cone Beam CT exam (Galileos)	70	4	8 days
CT Maxillo-Mandibular	2100	153	256 days
CT Maxillary	1400	102	170 days

Table 1.1 Effective Doses from Dental and Maxillofacial X-Ray Techniques and Probability of Excess Fatal Cancer Risk per Million Examinations. (Ludlow et al 2008, 2006, and 2003)

Cancer induction is the most important somatic (pertaining to all cells except the germ cells), and stochastic effects (effects the probability of which, rather than their severity, is a function of radiation dose without threshold) of low-dose ionizing radiation. Carcinogenesis is considered a stochastic effect of radiation. Stochastic effects are those where the probability of which, rather than their severity, is a function of radiation dose without threshold (BEIR 1990). In sharp contrast to the case for the hereditary effects of radiation, risk estimates for leukemogenesis and carcinogenesis do not rely on animal data but can be based on experience in humans. There is a long history of a link between radiation exposure and an elevated incidence of cancer (Pierce et al. 2003, Mabuchi et al. 1994, Thompson et al. 1994, Preston et al. 1994, Ron et al. 1994). Quantitative data on cancer induction by radiation come from populations irradiated for medical purposes or exposed deliberately or inadvertently to nuclear weapons (Berrington et al. 2001, Brenner et al. 2003, Mabuchi et al. 1994, Thompson et al. 1994, Preston et al. 1994, Ron et al. 1994). Persons exposed therapeutically received comparatively high doses, and their susceptibility to the effects of radiation might have been influenced by the medical condition for which treatment was being given (Bhatia et al. 1996, Boice et al. 1979,1980,1988, Brenner et al. 2000, Coleman et al. 1996, Czesnin et al 1978, Darby et al. 1994, Howe et al. 1996, Shore et al. 1986). Those exposed to γ-rays and neutrons from nuclear weapons represent a wider cross section in terms of health and also include individuals exposed to lower doses. In both cases, dose rates were high and exposure times brief. There are two types of models estimate cancer risks

as a function of dose: the absolute risk model and the relative risk model. The absolute risk model assumes that radiation induces a "crop" of cancers over and above the natural incidence and unrelated to it (Hall 2011, 2006). The relative risk model assumes that the effect of radiation is to increase the natural incidence at all ages subsequent to exposure by a given factor. Because the natural or spontaneous cancer incidence rises significantly in old age, the relative risk model predicts a large number of radiation-induced cancers in old age (Hall 2011, 2006).

The model favored by the BEIR (Biological Effects of Ionizing Radiations) committee, for the assessment of the cancer risks from the Japanese atomic-bomb survivors is the time-dependent relative risk model. The excess incidence of cancer was assumed to be a function of dose, the square of the dose, age at exposure, and time since exposure. For some tumors, gender must be added as a variable such as in the case of breast cancer. The relative risk is a linear function of dose up to about 2 Sv (200 rem). Over the lower-dose range from 0 to 0.5 Sv (0-50 rem), there is a suggestion that the risks are slightly higher than the linear extrapolation from higher doses (Hall 2006).

Most organs or tissues of the body are unaffected by the loss of a few cells; but if the number of cells lost is sufficiently large, there is observable harm, reflecting the loss of tissue function. The probability of such harm is zero at small radiation doses, but above some level of dose, called the threshold dose, the probability increases rapidly with dose to I00%. Above the threshold, the severity of harm also increases

with dose. Effects such as this are said to be deterministic. A deterministic effect has a threshold in dose, and the severity of the effect is dose related. Radiation-induced cataracts are an example.

The outcome is very different if the irradiated cell is viable but modified. Carcinogenesis and hereditary effects fall into this category. If somatic cells are exposed to radiation, the probability of cancer increases with dose, probably with no threshold, but the severity of the cancer is not dose related. A cancer induced by 1 Gy (100 rad) is no worse than one induced by 0.1 Gy (10 rad), but of course the probability of its induction is increased. This category of effect is called stochastic. In the absence of evidence of a threshold dose, it is prudent, from a patient-policy perspective, to assume that such a risk exists (Valentin 2007, Preston 2003, UNSCEAR 2006, BEIR VII 2006). Despite a diverse collection of data for cancer in humans from medical sources, both the BEIR V and the latest UNSCEAR (United Nations Scientific Commission on Effects of Atomic Radiation) reports elected to base the risk estimates almost entirely on the data from the survivors of the atomic-bomb attacks on Hiroshima and Nagasaki. Only a few hundred excess cancer cases caused by radiation are involved, compared with many thousands of naturally occurring malignancies (Hall 2011, 2006).

Therefore the American Academy of oral and maxillofacial radiology issued a position paper (American Academy of Oral and Maxillofacial Radiology 2013) for the use of CBCT in orthodontics that is focused on minimizing or eliminating unnecessary

radiation exposure in diagnostic imaging. The purpose of radiographic imaging in orthodontics is to supplement clinical diagnosis in the pretreatment assessment of the orthodontic patient. Radiographic imaging may also be performed during treatment to assess the effects of therapy and post-treatment to monitor stability and outcome. Imaging for a specific orthodontic patient occurs in at least three 3 stages: 1) selection of the most appropriate radiographic imaging technique, 2) acquisition of appropriate images, and 3) interpretation of the images obtained. Selection of the appropriate radiographic imaging technique (or techniques) is based on the principle that practitioners who use imaging with ionizing radiation have a professional responsibility of beneficence that imaging is performed to "serve the patient's best interests." This requires that each radiation exposure is justified clinically and that procedures are applied that minimizes patient radiation exposure while optimizing maximal diagnostic benefit. The extension of this principle, referred to as the "as low as reasonably achievable" (ALARA) (NCRP 2003), to CBCT imaging is supported by the American Dental Association (ADA 2012). Justification of every radiographic exposure must be based primarily on the individual patient's presentation including considerations of the chief complaint, medical and dental history, and assessment of the physical status (as determined with a thorough clinical examination) and treatment goals.

There has been a dramatic increase in the use of CBCT in dentistry over the last decade. This technology has found particular applications in orthodontics for diagnosis and treatment planning for both adult and pediatric patients (Hechler et

al. 2008, White et al. 2009, Merret et al. 2009, Mah et al. 2010, Kapilla et al. 2011). CBCT imaging provides two unique features for orthodontic practice. The first is that numerous linear (e.g., lateral and postero-anterior cephalometric images) or curved planar projections (e.g., simulated panoramic images) currently used in orthodontic diagnosis, cephalometric analysis, and treatment planning can be derived from a single CBCT scan. This provides for greater clinical efficiency. The second, and most important, is that CBCT data can be reconstructed to provide unique images previously unavailable in orthodontic practice. Innately CBCT data are presented as inter-relational undistorted images in three orthogonal planes (i.e., axial, sagittal, and coronal); however, software techniques are readily available (e.g., maximum intensity projection and surface or volumetric rendering) that provide three-dimensional visualization of the maxillofacial skeleton, airway space and soft tissue boundaries such as the facial outline.

The position paper stated that CBCT imaging can facilitate analysis of dentofacial deformities and craniofacial anomalies and be used to simulate virtual treatments and plan orthopedic corrections and orthognathic surgeries. Computer-aided jaw surgery is increasing in use clinically because virtual plans accurately represent surgical procedures in the operating room. The position paper emphasized that effort should be exercised to minimize patient radiation exposure for any CBCT scan.

1.6 3D image analysis:

An increasing number of studies have demonstrated that computer aided surgical simulation (CASS) can predict possible surgical complications and lowers material costs while decreasing surgery duration, with comparable or better surgical outcomes (Hassfeld et al. 2001, Troulis et al. 2002, Gateno et al. 2007, Kang et al. 2010, Xia 2011, Hsu et al. 2012). However, the ability to visualize the facial asymmetry in 3D surface models does not imply the ability to quantify and precisely locate areas of asymmetry. Detailed analysis of positional as well as morphological discrepancy between the affected side and the "normal side" in an asymmetric patient is a prerequisite for ideal treatment planning.

Three-dimensional (3D) imaging and associated image analysis methods developed recently carry a potential for development in this field. The use of relatively low-dose cone beam CT (CBCT) scanners in dental practices facilitates the examination of hard tissue anatomical structures in a multi-planar view. It also provides a rich soil for the application of different image analysis techniques to further extract diagnostic information from available volumes. Creation of 3D virtual surface models from CBCT volumes, registration of those models and measurements of the surface distances between different models is a well documented approach used to study growth, treatment changes and the stability of those changes (Cevidanes et al. 2007, Cevidanes et al 2006, Cevidanes et al. 2005a, Cevidanes et al. 2005b, Cevidanes et al. 2005c).

1.6.1 Midline determination and mirroring techniques

Various approaches have been described in the literature in an attempt to use 3D imaging for the detection and quantification of craniofacial asymmetry (Maeda et al. 2006, Park et al. 2006, Katsumata et al. 2005). However, most of these techniques depend on landmark identification and manual identification of a straight ‘‘midsagittal plane’’, both of which are challenging and somewhat operator-dependent. A critical review of such techniques to test validity and reproducibility as well as clinical validity is the first step toward optimization of asymmetry assessment.

In 2000, a method to automatically define the midsagittal plane of the brain in 2D cross-sectional slices was presented (Prima et al. 2000). They presented a new method to automatically compute, reorient, and re-centre the midsagittal plane in anatomical and functional three-dimensional (3-D) brain images. This iterative approach is composed of two steps. At first, given an initial guess of the midsagittal plane (generally, the central plane of the image grid), the computation of local similarity measures between the two sides of the head allows the algorithm to identify homologous anatomical structures or functional areas, by way of a block matching procedure. The estimated plane is aligned with the center of the image grid, and the whole process is iterated until convergence (Prima et al. 2000). However, definition of the midsagittal plane in the maxillofacial area remains a challenge because the plane is a curved surface in some faces with chin deviation

and finding homologous structures in both sides of the face is not always clinically feasible.

In 2004, an alternative method for determining a symmetry plane was presented, using mirroring of the mandible in any arbitrary plane, with rigid registration of the mirrored mandible to the original image (Glerup 2005). However, this procedure did not take into consideration the mandibular morphological relationships with the maxilla and the cranial base. Taking the mandible as a free-floating shape takes the clinical significance and merit out of the resulting shape analysis. A modification of this approach that first mirrors the image and then registers on the cranial base can provide information on the entire facial structure rather than just the mandible (Cevidanes et al. 2006). The cranial base in considered a large enough stable anatomic structure for registration in adult patients. The presence of cranial base asymmetries contraindicates the use of this method (Cevidanes et al. 2006).

1.6.2 Segmentation:

The segmentation process in medical imaging could be defined as the construction of 3D virtual surface models (called segmentations) to best match the volumetric data (Grauer et al. 2009). Currently available 3D image-analysis software tools offer many manual, semiautomatic, and fully automatic segmentation techniques. For routine clinical use, a fully automated segmentation protocol is preferable because it requires only limited interaction with the user, which saves

time and also decreases variability and personal bias. Segmentation is a preparatory step for surgical planning and should be performed as quickly as possible. A simple way to segment bone in CBCT is thresholding, the technique used in commercial clinical software packages such as Dolphin, 3DMD Vultus, and Maxilim.

Thresholding classifies a voxel (element of volume in a 3D image) depending only on its intensity (Chapius et al. 2006). A certain intensity range is specified with lower and upper threshold values thus pre-selecting the skeletal components of the dataset for display & subsequent analysis. Each voxel belongs to the selected class (e.g., bone) if, and only if, its intensity level is within the specified range. The appropriate value range must be selected for each patient because bone density varies between patients, and intensity values of bone can vary between scanners.

The major limitation of thresholding is that it is prone to artifacts. These artifacts are created because different densities in a voxel are averaged and then represented by 1 CBCT number (partial volume averaging). Therefore, the CBCT numbers of thin bony walls tend to drop below the thresholding range of bone because their density is averaged with that of surrounding air. This effect causes artificial holes in 3D reconstructions of the condyles and areas of thin cortical bone, such as the internal ramus of the mandible and much of the maxilla (Hemmy et al. 1985). Segmentation of thin cortical boundaries, very closely approximated bony structures, and less dense bone should be revised manually pixel by pixel in all planes of space to ensure the required accuracy is established.

Another source of artifacts is metallic objects in the field of view (appliances such as braces, implants, surgical plates), and foreign materials such as trauma debris. The presence of metal objects in the scan field can lead to severe metal artifacts. They occur because the density of the metal is beyond the normal range that can be interpreted by the computer, resulting in incomplete attenuation profiles. Metal artifact intensity values fall into the thresholding range of bone and are included in CBCT images as pronounced linear artifacts. The morphology and position of the condyles, and internal surfaces of the ramus and the maxilla, are critical for careful virtual surgery planning because any jaw position must allow the condyles to remain in the fossae in neutral stable positions, if pain and dysfunction and an unstable result are to be avoided (Cevidanes at al. 2010).

Segmentation involves outlining of the shape of structures visible in the cross-sections of a volumetric dataset in the CBCT-3D images. The resultant surface models are basic material for image analysis and execution of virtual surgeries. Such segmentation of anatomic structures can be performed using ITK-SNAP (open source software, http://www.itksnap.org) (Yushkevich PA et al. 2006). 3D virtual models are built for each patient from a set of ~ 300 axial cross-sectional slices for each image with the image voxels reformatted for an isotropic resolution of 0.5 mm x 0.5 mm x 0.5 mm. This resolution is used because higher spatial resolution with smaller slice thickness would have exponentially increased image file size and required greater computational power and user interaction time. This decision was made having in mind the prospective use of this technology chair side for individual patients'

diagnositics. Smaller resolutions (that are clinically irrelevant) come with the cost of much longers times and/or different requirements for the needed computers to achieve the needed task.

The artifacts generated from restorative dentistry, movement of the patient, partial volume averaging, incorrect selection of Kvp / mA and threshold settings can affect the segmentation (constructed surface models) (Li P et al. in press, Luu NS et al. in press, Swennen GR et al. 2009, Xi T et al. 2013, Kim M et al. 2012). In the absence of artifacts, Luu NS et al. clearly described that when defining the true boundary of an object, at best; the line for this boundary will cross directly through the center of a voxel. At worst, when attempting to select a boundary that truly goes between voxels, one is forced to select the center of one of the surrounding voxels. In the work described in this thesis, to reduce computational time, all CBCT images were reformatted to isotropic 0.5mm voxels. The open-source image analysis techniques in these studies are robust and can be applied to smaller voxel sizes even at the micron level, at the expense of highly increased computational times. Considering quantitative approaches of mandibular asymmetry based on constructed surface models, the accuracy for the selection of a single voxel of 0.5 mm sides is reasonably proposed to be half the diagonal of the voxel or 0.43 as a geometric worst-case scenario for accuracy. As for linear measurements within the same model, given that a 2 point measurement requires the selection of two voxels, then, it is reasonable to propose a geometric worst case scenario for accuracy of two voxel half diagonal distances or approximately 0.86 mm.

The automatic segmentation procedures in ITK-SNAP use 2 methods to compute feature images based on the CBCT image's grey level intensity and boundaries. The first method causes the segmentation front to slow down near edges, or discontinuities, of intensity. The second causes the segmentation front to attract to boundaries of regions of uniform intensity. After obtaining the segmentation result, manual post-processing is normally necessary. Artifacts from metallic elements need to be removed manually afterward (Yushkevich PA et al. 2006). A 3D graphic rendering of the volumetric object allows navigation between voxels in the volumetric image and the 3D graphic representation with additional zooming, rotating and panning effects to navigate the virtual mandible.

1.6.3 Surface distance computation:

Most commercially available and academic softwares that are able to compute color-coded surface distance maps use a closest point algorithm to obtain surface distances. Closest point is a "brute force" algorithm that calculates a vertex-to-vertex Euclidean closest point distance (De Momi E et al. 1992). This method does not map corresponding surfaces based in anatomical geometry, and thus, it usually underestimates rotational and large translational movements (Paniagua et al. 2010).

The application of conventional closest point distances for mirror images in mandibles of patients with rudimentary condyles, severe occlusal table cants, or a rotated mandible, does not represent the difference between corresponding anatomical locations, but rather differences based in the minimal distances between

any point in the original and mirrored models. These clinical situations mandate the use of a more “anatomy sensitive” shape analysis technique.

Shape correspondence is a promising alternative to overcome the shortcomings of the commonly used closest point algorithm (Paniagua et al. 2010). It is one of the currently used statistical shape analysis techniques that allows measuring the surface distance between an area on one model to the corresponding anatomical area in the other model, regardless of the alignment of those models. The main shape correspondence challenges involve the representation of a population by means of correspondent point based models. Surface representation could be accomplished by several different options including, matching of template surface geometry (curvature and location)(Meyer et al. 2002), Entropy-based Particle Systems (Oguz 2009), or by SPherical HARMonic representation (SPHARM) (Gerig et al. 2001). In SPHARM the surface model is mapped in a sphere, and correspondence point based models are computed afterwards, finding the spherical harmonic basis that best fits the model (Styner et al. 2006). After surface mapping is achieved, correspondence could be based on different frameworks depending on the clinical problem at hand.

SPHARM-PDM allows for comprehensive statistical evaluations to be computed for the correspondent models as a whole or for specific regions of interest within these models. Individual case based assessment protocols were selected for the projects as group based appraisal schemes are more appropriately applied to

general trend and cross section trend data rather than specific scenario data sets.

The subtraction of mirrored from original and original asymmetric mandible models provided color-coded corresponding distance maps and maps of vectors of differences between these models. The distance maps measure the magnitude of the differences between the point-based models, while the vector maps offer directionality. To maximize the usefulness of the extensive data that SPHARM-PDM can provide, regions of interest that correspond to surgical segments could be analyzed separately. This quantitative asymmetry measure could either be communicated to the surgeon or used as an input for surgical simulation software.

Procrustes can be used to capture translational and rotational differences between each hemimandible and the mirror of the contralateral side in the three planes of space (Bookstein 1996). The 6 degrees of freedom of the differences can be calculated using rigid Procrustes alignment, which is the geometric transformation that maps and measures positional changes between point-based correspondent models (Paniagua et al. 2010).

1.7 Surgical simulation and outcome design

Facial asymmetry is a complex clinical entity that comprises two main components, a shape and a positional component. During growth, the shape discrepancies lead to compensatory positional differences resulting in disturbing the harmony of the maxillofacial complex. Clinicians need to diagnose both shape and

positional components of the asymmetry prior to the design and execution of the corrective surgery.

In the past, the inability to appreciate the interplay between maxillo-mandibular roll and yaw was a missing link in classification and diagnosis. When one diagnoses a major midline shift, a class II or class III molar relationship, or a true unilateral crossbite, quantification of the mandibular roll and yaw is essential before the quantification of actual left and right differences.

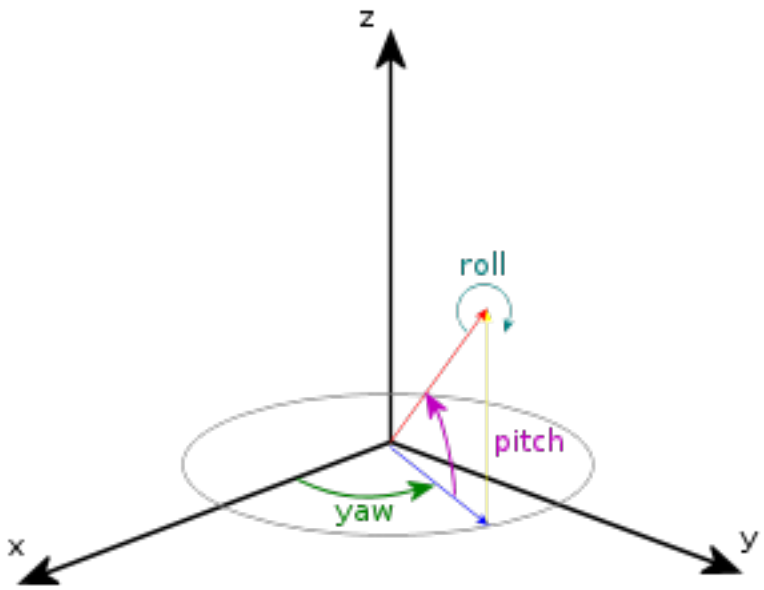

Figure 1.1. 3D analysis of orientation of the head, jaws, and dentition is incomplete without also considering 3 rotational axes of pitch, roll, and yaw in addition to planar terms antero- posterior, transverse, and vertical.

The extent of asymmetric yaw is a major determinant in whether treatment is limited to asymmetric mechanics or might extend to asymmetric extractions, unilateral bone anchors, or surgery (Ackerman et al. 2007). For surgeons to reach a "symmetric" result in the patient, first, positional asymmetries in the roll and yaw need to be corrected, and then the 3D shape asymmetry can be properly assessed and addressed. That is why the use of conventional mirror images does not adequately guide surgeons on the correction of facial asymmetries. Clearly the simplistic method fundamentally fails to compensate for positional component.

The use of the patient's own anatomy for the computation of the custom-made template might help accommodate the large gradient by which mandibular asymmetry presents clinically. It may also help to ensure that the outcome virtual template has the basic features (condylar position, relative size,...etc) that will still keep the harmony between the mandible and the rest of the maxillofacial area. This approach could also help eliminate the need to decide on a "healthy" side for the mandible to mirror and use as a template especially that the concept of a "healthy" side in an asymmetric mandible is never strictly true due to the physiological compensation processes that take place during growth.

In asymmetric faces, the lower face was affected much more frequently than the middle or upper 3rds. Upper face asymmtries constituted 5%, middle 36%, and chin deviation observed in 75% of the population. Half of patients with upper or middle asymmetry also had concomitant lower 3rd asymmetry (Severt and Proffit 1997).

That is why this and the subsequent chapters are focused on mandibular asymmetry. The projects in this dissertation are using mandibular asymmetry as a prototype that could be generalized to all types of facial asymmetries.

This thesis has described a series of multi step processes to diagnose, localize, and quantify existing mandibular asymmetries and an algorithm to design a clinically favorable outcome for the corrective surgeries of those asymmetries. Those image analysis steps were conducted on preoperative CBCT volumes.

We started by establishing the basis for asymmetry diagnosis by deciding on what mirroring method to use. We then started a series of experiments to establish the accuracy and clinical merit of SPHARM-PDM in the quantification of mandibular asymmetry. The output of asymmetry quantification using SPHARM-PDM, both quantity and direction data, could be used as an input for treatment planning of corrective surgeries of those mandibular asymmetry patients.

A novel patient-specific template that will potentially improve the surgical outcomes of corrective surgeries of mandibular asymmetries is suggested.

1.8 Thesis organization:

The following chapters will be addressing:

1) The difference between the existing landmark based mirroring technique and arbitrary mirroring followed by registration on the cranial base as a basis for the asymmetry assessment. Our null hypothesis is that there is no statistically significant

difference in the quantification of mandibular asymmetry whether *mirroring of the mandible was done around the "midsagittal plane"* vs. *arbitrary mirroring of the mandible and registration on the cranial base*

2) The use of spherical harmonic shape correspondence (SPHARM) in the assessment of mandibular asymmetry. The technology was validated in chapter 4, applied on a cohort of asymmetric patients in chapter 5, and tested on a Craniofacial Micrsomia cohort of patients to establish the boundaries of clinical usability of this technique. The hypothesis is that SPHARM is a valid algorithm for the diagnosis and localization of mandibular asymmetry.

3) The use of a custom made atlas as a template for corrective surgeries of asymmetric patients. The null hypothesis for this project was that there would be no statistically significant difference between the outcome of the corrective surgery of mandibular asymmetry patients of the current standard of care diagnostics and the use of the proposed custom made template.

Chapter 2

Comparison of two methods for quantitative assessment of mandibular asymmetry using CBCT image volumes

2.1 Introduction

Facial asymmetry is common and sometimes poses a challenge in craniofacial diagnosis and treatment planning (Proffit WR at al. 1998, Severt TR et al. 1997). It is etiologically and pathologically heterogeneous and may be localized or generalized. This wide variability in the etiology and in the presentation of the disease necessitates the management of those patients be a multifactorial stepwise decision making process. Proper assessment and quantification of the differences between the right and the left sides are crucial for diagnosis, treatment planning and follow up. Conventional posterio-anterior cephalometric radiographs used in orthodontic practice to assess asymmetry have inherent limitations as a result of superimposition, magnification and distortion.

Three dimensional imaging (3D) and associated image analysis methods developed recently carry a potential for development in this field. CBCT provides a 3rd dimension in multi-planar view using a low dose technique. Its isotropic voxel also provides equal resolution in all planes.

Creation of 3D virtual surface models from CBCT volumes, registration of those models, and measurements of the surface distances between different models is a

well documented approach used to study growth, treatment changes, and the stability of those changes (Cevidanes et al. 2005a, Cevidanes et al. 2007, Cevidanes et al. 2005b, Cevidanes et al. 2006, Xi et al 2013, Swennen 2009).

Various approaches have been described in the literature in an attempt to use 3D imaging for detection and quantification of craniofacial asymmetry (Katsumata et al. 2005, Maeda et al. 2006). However, most of these techniques depend on landmark identification and manual identification of a straight "midsagittal plane" both of which proved to be extremely challenging and operator dependent (Cevidanes et al. 2011).

Mirroring has been a focus in asymmetry research. It was researched for functional asymmetries, such as the work presented by Prima S et al. (2000). A midsagittal plane was automatically defined the midsagittal plane of the brain. Mirroring was also a part of shape analysis protocols; mandibular shape asymmetry was assessed after mirroring the mandible in any arbitrary plane with rigid registration of the mirrored mandible to the original image (Glerup et al. 2005). However, this procedure did not take into consideration the mandibular morphologic relationships with the maxilla and the cranial base. A modification of this approach, that first mirrors the image and then registers on the cranial base, can provide information on the entire facial structure rather than just the mandible (Cevidanes at al. 2006).

The aim of this experiment was to compare the degree of mandibular asymmetry, as obtained by surface distance measurement, using *mirroring of the mandible in the "midsagittal plane"* vs. *arbitrary mirroring of the mandible and registration on the cranial base*. The null hypothesis is that there is no statistically significant difference in the quantification of mandibular asymmetry whether *mirroring of the mandible was done around the "midsagittal plane"* vs. *arbitrary mirroring of the mandible and registration on the cranial base*

2.2 Materials and methods

Following a protocol approved by the Institutional Review Board for research at the University of North Carolina at Chapel Hill (Study #: 03-1647), a cohort of fifty patients with clinically detectable mandibular asymmetry were selected for this study. Clinical asymmetry was defined as more than 2 mm of chin deviation in the relation to the clinical midline of the face or the presence of cant of the occlusal plane before the start of the patient's orthodontic treatment**.**

Image acquisition:

CBCT scans of all patients were obtained using NewTom 3G cone beam scanner (AFP Imaging, Elmsford, NY). The 23 cm field of view producing 0.5mm isotropic voxel sizes was used for acquiring the image volume. Scans are obtained as a routine pre-requisite to ortho planning as part of the local gold standard treatment planning exercise. These scans were not conducted in addition to, rather as a routine part clinical assessment, avoiding additional radiation exposure to the patients

consenting to use of their anonymised datasets. The accuracy of linear measurements using NewTom CBCT machines has been well studied in the radiology litreture (Moshfeghi et al. 2012, Hassan et al. 2009, Lagravère et al. 2008, Stratemann et al. 2008)

Construction of virtual 3D models from the CBCT dataset.

Three-dimensional surface models were constructed from the CBCT volumes using segmentation tools of the Insight SNAP software (Yushkevich PA et al. 2006).

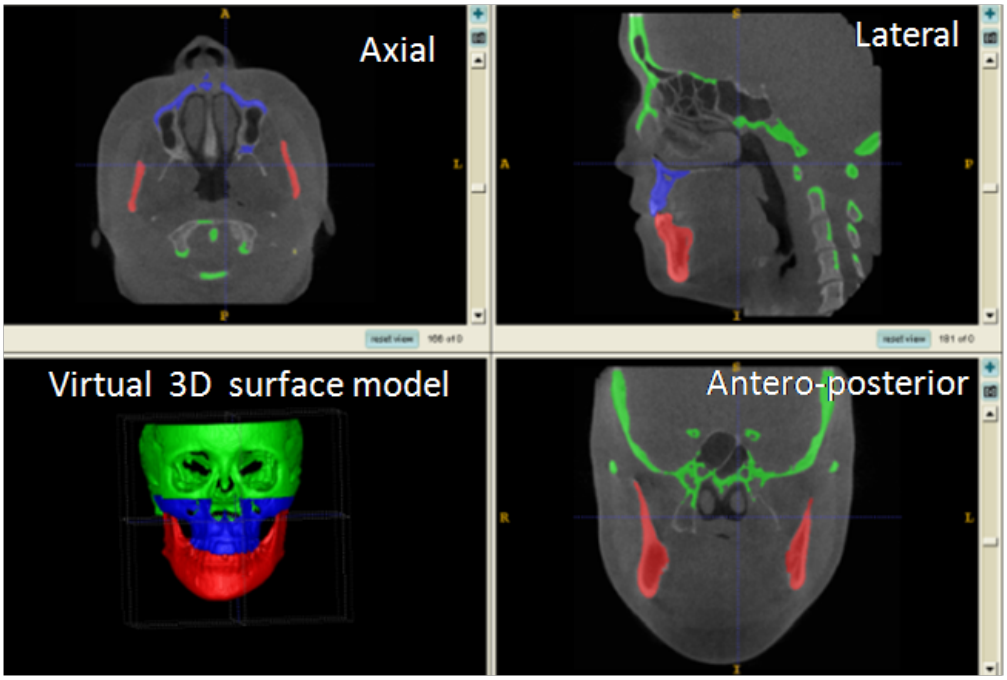

Figure 1.2. Image segmentation: Cone beam CT images are imported as DICOM files into ITK Snap. In a process known as semiautomatic segmentation, anatomical areas of interest are identified and delineated. Manual editing is performed to ensure accuracy of the segmentations. The images can be viewed in three dimensions and as axial, coronal, and sagittal slices of each image. (Mandible in red, Maxilla in blue, and cranial base in green)

3D virtual models were built for each patient from a set of ~ 300 axial cross-sectional slices for each image with the image voxels reformatted for an isotropic resolution of 0.5 mm x 0.5 mm x 0.5 mm. This resolution was used because higher spatial resolution with smaller slice thickness would have increased image file size and required greater computational power and user interaction time. Following segmentation, a 3D graphical rendering of the volumetric object allows navigation between voxels in the volumetric image and the 3D graphics with zooming, rotating and panning. As described in chapter one, considering quantitative approaches of mandibular asymmetry based on constructed surface models, the accuracy for the selection of a single voxel of 0.5 mm sides is by definition limited to the equivalent of half the diagonal of the voxel or 0.43.

Midsagittal Plane Approach

Nasion (Na), Anterior Nasal Spine (ANS), and Basion (Ba) were manually defined by the author for each patient. The midsagittal plane was defined as the plane passing through those three landmarks and was therefore used to create mirrors for both halves of the mandible. This task was performed in the CranioMaxilloFacial (CMF) software application (M.E. Müller Institute for Surgical Technology and Biomechanics, University of Bern, Switzerland.)

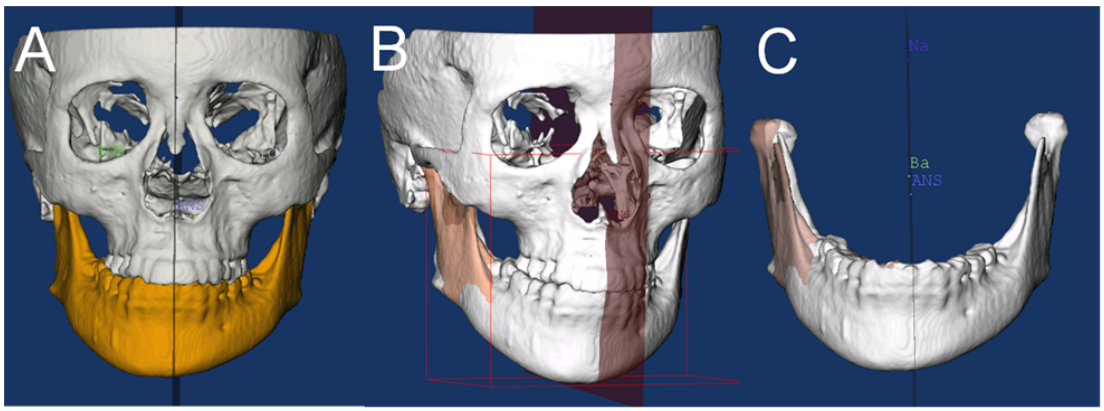

Figure 2.2. Three-dimensional image mirroring on the mid-sagittal plane: Mirroring can be a valuable technique in the treatment of asymmetries. As shown above, the mandible (A) has been colored yellow. (B) The left ramus was mirrored onto the right side using the CMF applications mirror function and the mid-saggital plane was defined for the image. (C) The right lateral ramus was then reincorporated back into the model with the right side recreated as a mirror of the left side.

Na, ANS, Ba, the midsagittal plane and the degree of asymmetry were determined five times on 22 randomly selected patients from the cohort. A randomization table was used to choose those 22 patients. Differences between repeated assessments of asymmetry served as a measure of reproducibility of midsagittal plane identification.

Arbitrary Plane plus Registration Approach

Each model of the mandibles of the 50 patients in the cohort was mirrored on an arbitrary plane. The mirroring is done by arbitrarily converting the image orientation from (**Right-Left**, Antero-Posterior and Infero-Superior) to (**Left-Right**, Antero-Posterior and Infero-Superior). The original and the arbitrarily mirrored images were then registered on the cranial base. The registration was accomplished using IMAGINE software (National Institutes of Health, Bethesda, MD; Open-source,

http://www.ia.unc.edu/dev/download/imagine/index.htm) consisting of a voxel-based registration method.

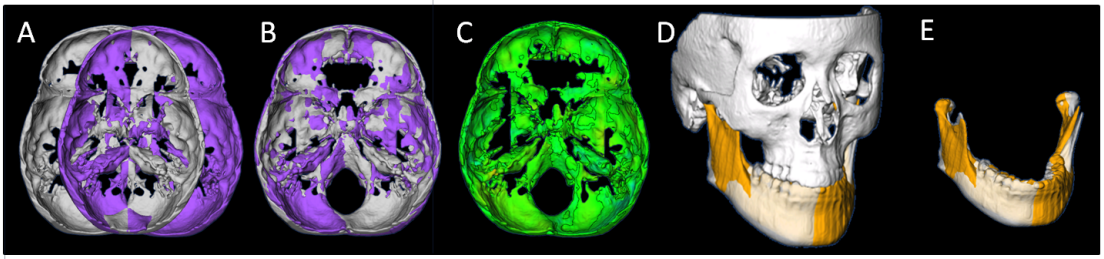

Figure 2.3. Arbitrary Plane Mirroring followed by Cranial Base Registration Approach (A) Cranial base virtual surface model for a patient (*white*) and arbitrarily mirrored image model (*purple*); (B) original model and arbitrary mirror matching on the cranial base as a result of a voxel-based registration; (C) color map of the surface distance between the registered original and arbitrary mirror models shown at 0-mm +/- 0.43mm surface distances (*green*); (D) Virtual surface model (*white*) and registered arbitrarily mirrored image model (*orange*); (E) Close-up showing mandibular asymmetry, this pair of the mandible and its mirror in now ready for surface distance computation to quanify the existing change between the left and the right sides.

This method utilizes maximization of mutual information to avoid the problems associated with observer dependent techniques such as point-to-point registration (Cevidanes et al. 2005a, Maes et al. 1997). After the software masks the maxillary and mandibular structures, it compared the grey level intensity of each voxel in the cranial base to register the two CBCT images. The rotation and translation parameters that were used to register the two grey scale images are also applied to register the 3D surface models.

CMFApp software (Chapuis J. 2006, De Momi EF et al. 2006, Chapuis et al. 2005, Chapuis J et al. 2004) was used to display the superimposed images with the two approaches: (1) Original image superimposed on image mirrored on the midsagittal

plane; and (2) Original image superimposed on image mirrored on an arbitrary plane, and then registered to the original image.

Surface distances were compared between the resultant mirrors from both approaches and the original mandible. The mean surface distances between the right and left sides were calculated for nine anatomical regions: the lateral pole, medial pole, anterior and posterior surfaces of both condyles, lateral surface of the rami and corpora of the mandible, inferior and posterior surfaces of the mandible, and anterior surface of the symphysis. Those areas were chosen to cover the medio-lateral (the lateral pole, medial pole, lateral surface of the rami and corpora of the mandible), cranio-cuadal (inferior surface of the mandible), and anterioposterior (anterior and posterior surfaces of both condyles, posterior surfaces of the mandible, and anterior surface of the symphysis) components of the existing asymmetries. The measures of surface distances were complemented by visualization of the 3-D color-coded maps.

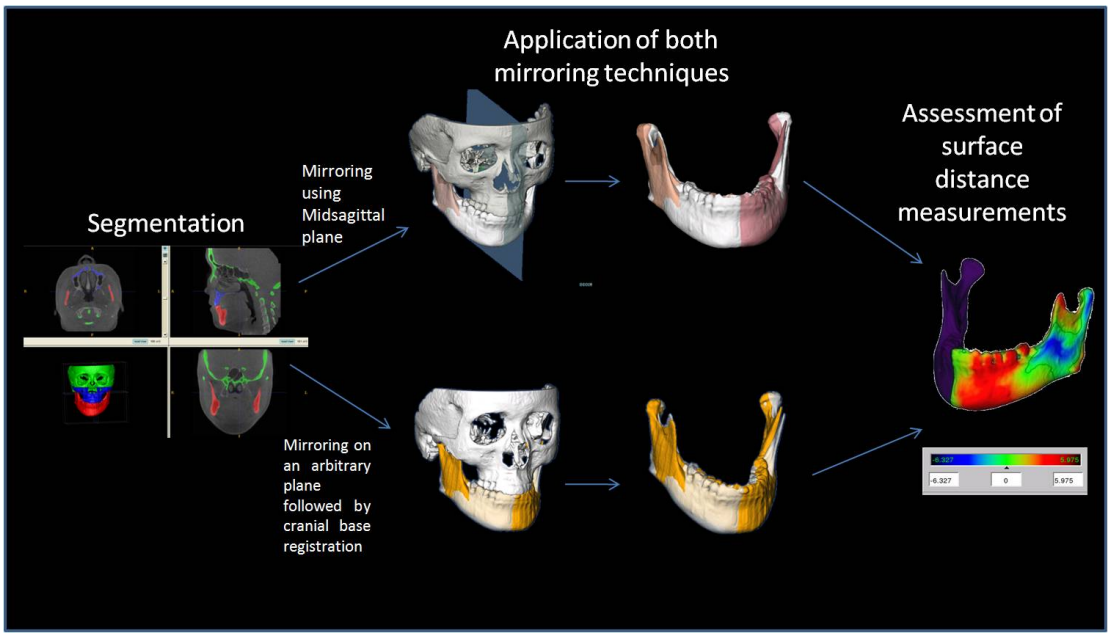

Figure 2.4. Surface distance maps show the direction of surface distance difference (Red: The hemi-mandible is larger or more lateral to the reference hemi-mandible; Blue: The hemi-mandible is smaller or more medial to the reference hemi-mandible). They also show the magnitude of the existing difference as shown in the reference bar.

Raw data was plotted to test normality. Overall Surface distance measurements proved to be normally distributed. (See Appendix one for this graph)

Paired T tests were used to assess statistical differences between the surface distance measurements obtained by the two approaches for each anatomical location. They were also used to test for differences between the measurements obtained for the right and the left sides for each approach. The Cochran-Mantel-Haenszel test was used to test for the effect of the degree of asymmetry on the difference detected between the two approaches ($\alpha = 0.05$).

2.3 Results

The variability in surface distance measurements obtained from five repeated assessments of the midsagittal plane for each subject ranged from 0 to 1.63 mm with a mean of 0.42 mm and a standard deviation of 0.18 mm. Please note that, as described in chapter one, in a $0.5mm^3$ voxel system resolution limit is determined to be 0.43mm. Measurements below that cut of point; despite being mathematically calculated, are practically insignificant. Only 5 patients had a discrepancy larger than 1mm. The paired t-tests showed no statistically significant difference in quantification of asymmetry among the five measurement sets ($p > 0.1$ for all paired comparisons, and $p = 0.44$ when pooled measurements were tested together).

Of the 18 anatomical areas measured, the mandibular ramus ($p = 0.04$), body ($p = 0.01$), and symphysis ($p = 0.005$) at the right side and the lateral pole of the condyle at the left side ($p= 0.02$) showed statistically significant differences in the mean surface distance between the two approaches. The differences in the mean surface distances ranged from 0.2 to 1.5 mm.

A positive correlation between asymmetry measurements and the discrepancy between the methods was observed at the right inferior border ($p=0.048$), left posterior border ($p=0.04$), and medial pole of left condyle ($p=0.03$).

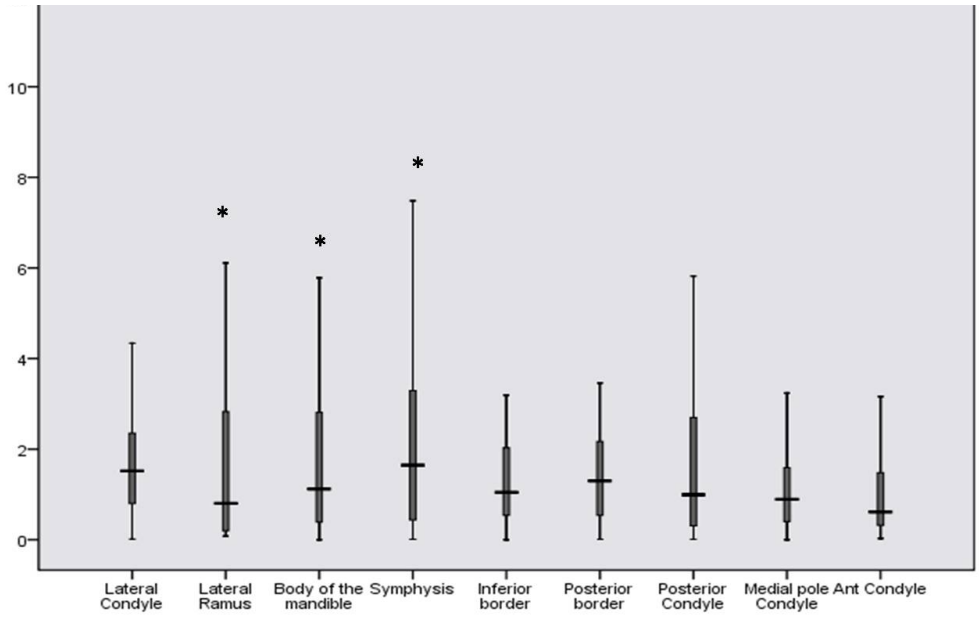

Figure 2.5. A Box plot demonstrating the mean of the absolute difference in surface distance measurements (mm) using both mirroring methods on each ROI on the Left side (* indicates statistical significance)

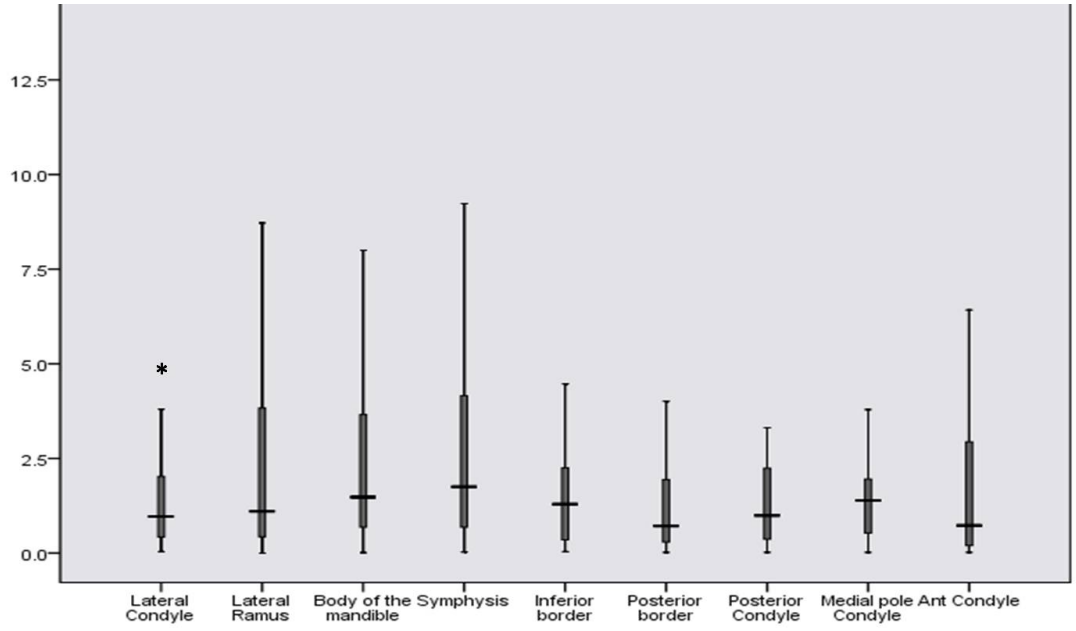

Figure 2.6. A Box plot demonstrating the mean of the absolute difference in surface distance measurements (mm) using both mirroring methods on each ROI on the right side (* indicates statistical significance)

There was no statistically significant difference in the mean of surface distance measurements between the left and the right side for all locations using the registered mirror. However, a significant difference was observed in the ramus (p=0.02), the body of the mandible (p=0.03), and the symphysis area (p=0.04) when mirroring with the midsagittal plane was used.

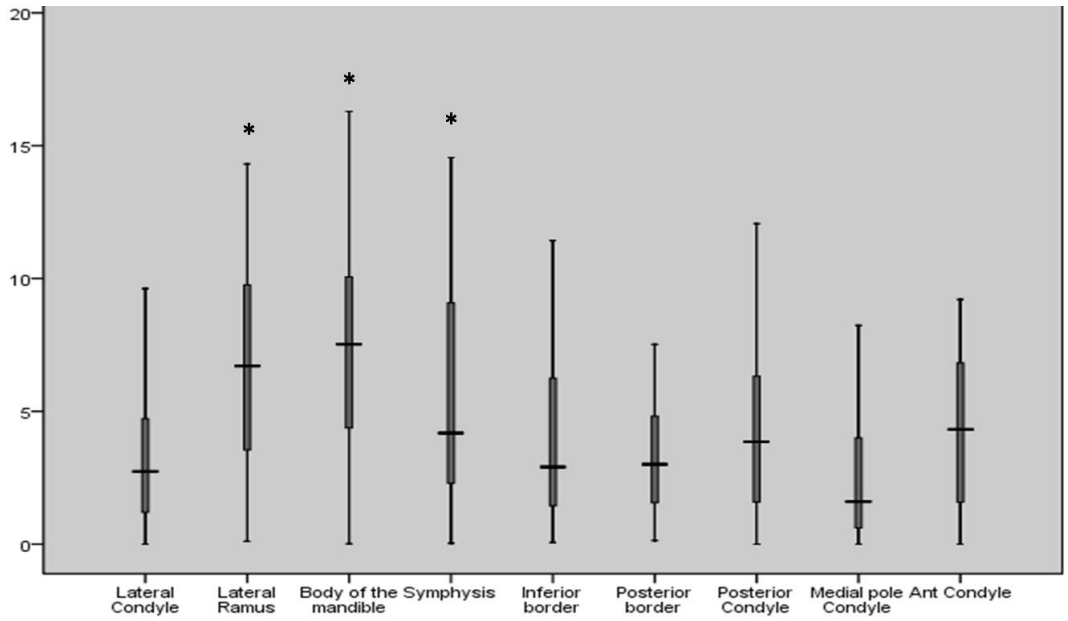

Figure 2.7. A Box plot showing the mean of the absolute difference in surface distance measurements (mm) of the left and right sides of the mandible using mirroring on the midsagittal plan. (* indicates statistical significance)

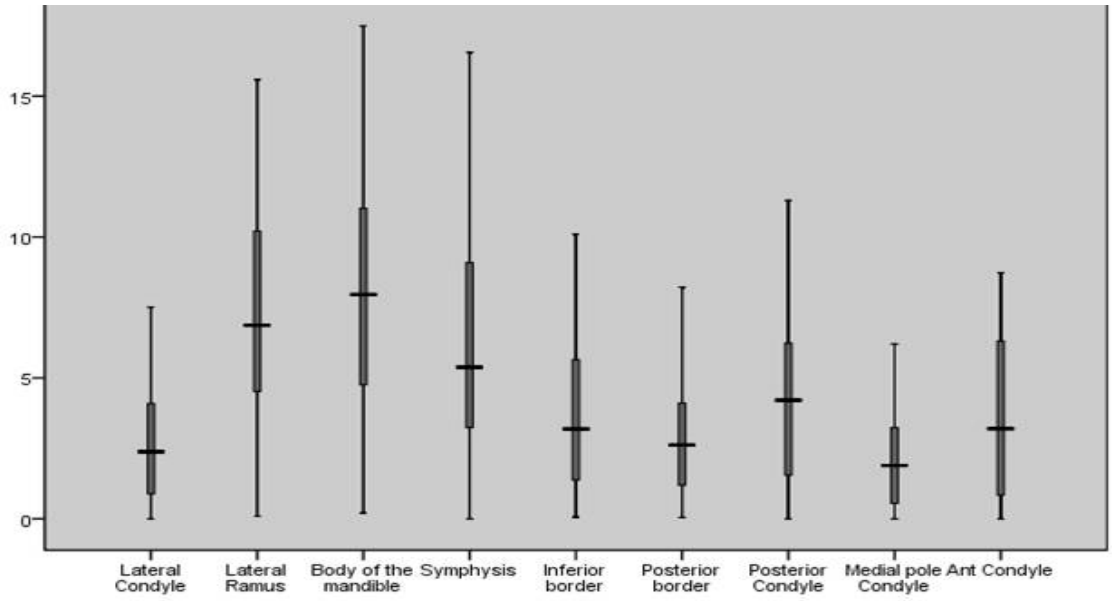

Figure 2.8. A Box plot showing the mean of the absolute difference in surface distance measurements (mm) of the left and right sides of the mandible using using arbitrary mirroring followed by registration on cranial base. (No statistical significance was detected)

These numbers are in favor of accepting the null hypothesis, particularly when the differences are set in the context of the voxel worst-case measurement scenario of a resolution limit of 0.43mm. Results showed no difference in asymmetry assessment using both mirroring techniques. However the choice of the side to be mirrored affected the outcome based on mirroring about a midsagittal plane. That indicates that arbitrary mirroring followed by registration is a more robust technique and that is does not depend on the clinicians decision of which side to mirror.

2.4 Discussion

Although PA and lateral cephalometric radiography has been, and will probably continue to be, the routine radiographic examination for any patient seeking

orthodontic\orthognathic treatment, the “inappropriateness of conventional cephalometrics” was recognized as early as 1979 (Moyers and Bookstein 1979). Those inadequacies are further accentuated when challenged with bilateral differences in the anatomy. 3D cephalometry has the potential advantage of being able to better detect and localize existing asymmetries (Adams et al. 2004). However, quantification of asymmetries using 3D cephalometry heavily depends on the operator’s understanding of 3D landmark definition and the ability to reproducibly define those landmarks (Maeda M et al. 2006, Katsumata A et al. 2005). The use of surface distance measurements between the two halves of the mandible, which served as our asymmetry quantification outcome, overcomes the need to depend on points as surrogates for real structures.

In this cohort, the use of either mirroring approach (midsagittal plane and an arbitrary plane with registration on the cranial base) provided similar results in most areas. Most of the discrepancies in surface distance measurements were located on the lateral surface of the mandible, which suggests that the medio-lateral direction is most sensitive to mirroring.

It can be hypothesized that there should be no difference in the absolute surface distance measurements based on whether the right or the left side of the mandible is being mirrored; as was tested in this project by analyzing the differences between the measurements obtained for the right and the left sides for each approach. That was true when mirroring using an arbitrary plane with registration on the cranial base, but the use of a midsagittal plane mirroring produced inconsistencies at some

locations. Furthermore, most of those locations were the same ones that showed discrepancies between the two approaches. Observation and result is supportive of the author's assertion that mirroring using an arbitrary plane with registration on the cranial base is a robust technique to be used.

The differences between the two mirroring approaches, though statistically insignificant, tended to increase with more severe asymmetries. Application of both approaches to an exclusive cohort of patients with severe asymmetries may further characterize this trend in terms of location and the cut-off point of maximal difference.

Neither approach could be applied indiscriminately to any patient. Mirroring using the midsagittal plane is difficult for patients suffering from conditions that interfere with the midline position of the points used to define the midsagittal plane, i.e., cleft palate patients. On the other hand, registration on the cranial base in patients with asymmetries involving the cranial base would also result in sub-optimal results.

Applying both mirroring approaches to patients with rudimentary condyles, severe cants, or a rotated mandible would result in a mirror image that is not aligned to the original (Fig 2.9). This complicates the interpretation of the surface distances obtained at a specified location. The measured distance would not represent the difference between corresponding anatomical locations, but rather the minimal difference between the models as computed by Closest Point algorithm used by

CMF (CranioMaxilloFacial (CMF) software application. (M.E. Müller Institute for Surgical Technology and Biomechanics, University of Bern, Switzerland.)

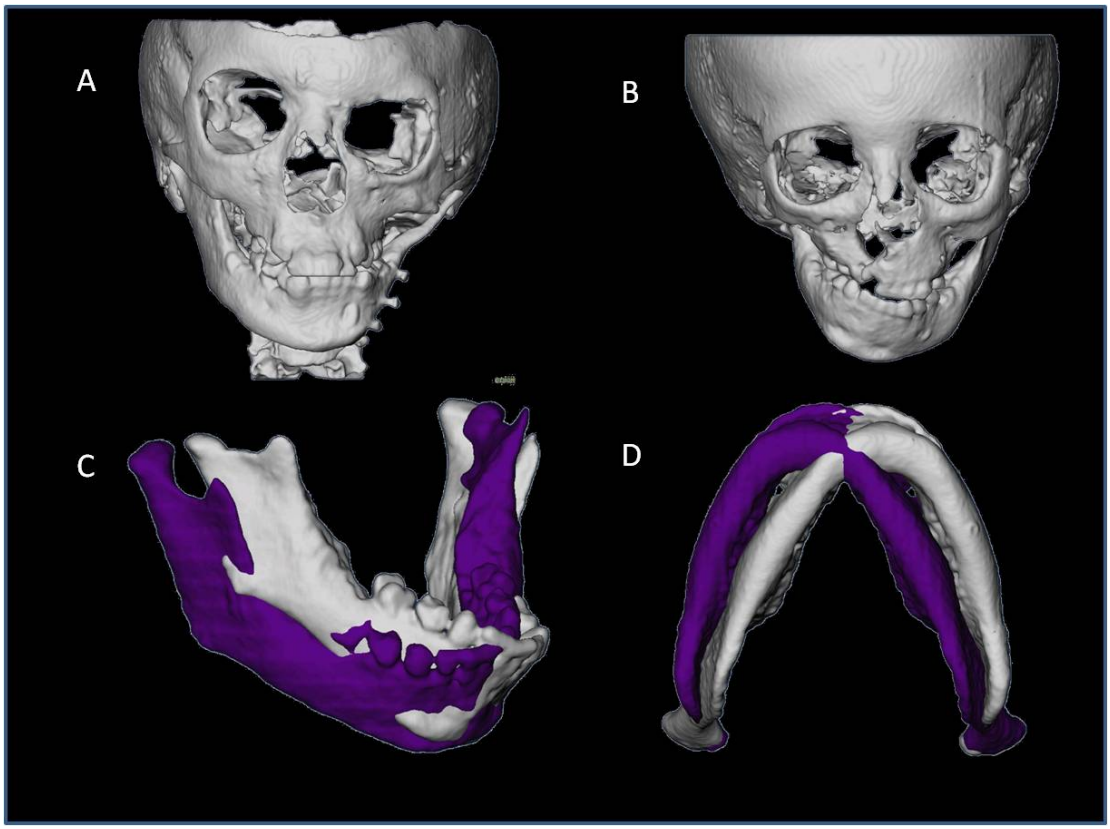

Figure 2.9. Examples of patients with challenging asymmetries for quantification. Asymmetric cranial base (A) and cleft palate (B) would interfere with both mirroring protocols. Severe cant (C) and rotation (D) is hard to deal with using CP.

2.5 Conclusion

Both mirroring using a midsagittal plane and using an arbitrary plane followed by registration on the cranial base provided similar quantification of mandibular asymmetry for most areas. One of these approaches is considered an alternative to the other when certain structural features of the patient impede the use of either approach.

Shape correspondence is a technology that allows measuring the surface distance between any area on one model to the same corresponding area in another model, regardless of the alignment of either of those models. This would avoid many of the mirroring issues alluded to above and will develope the mapping concept beyond a simple translational positional discrepancy as presented in the subsequent chapters.

Chapter 3

Background to Geometric morphometrics and shape correspondence

The geometric morphometric revolution has added to the sophistication of quantitative biological shape analysis, while at the same time making it easier to collect and analyze data to answer questions about shape of the phenotype (Zelditch et al. 2004, MacLeod and Forey 2001, Dryden and Mardia 1998, Marcus et al. 1996, Bookstein 1991, Bookstein et al. 1985).

'Geometric morphometrics' is the analysis of Cartesian geometric coordinates of morphological structures rather than linear, areal or volumetric variables. The most distinctive feature of most geometric morphometrics is that results can usually be reported using the same geometric coordinates as a pictorial representation of the morphological structure itself (Lawing et al. 2009).

Heterogeneous sets of algorithms are combined under the term geometric morphometrics. Software is available to analyze landmark points, curves, outlines (in either two dimensional (2D) or three dimensional (3D) and 3D surfaces. Details of how the geometry of objects is mathematically represented differ from one method to another. However, all geometric morphometric methods use the Cartesian coordinates of comparable features on the objects as their variables. Most methods transform the landmarks, curves or outlines of objects into 'shape coordinates,' which are new variables that can be analyzed with the full range of ordinary

multivariate statistical procedures, while others transform them into a matrix of inter-landmark distances, similar in many ways to older kinds of morphometric analysis.

The most common variety of geometric morphometrics uses landmark points that are aligned with one another using Procrustes superimposition (Rohlf & Slice, 1990, Siegel and Benson 1982, Gower 1975, Sneath 1967). Because geometric morphometric variables are Cartesian coordinates, a common coordinate system must be used to specify landmark locations on all objects. Procrustes superimposition rotates, translates and scales landmarks so that they have the same orientation and size (Rohlf and Slice 1990).

Several methods exist for the analysis of curves and outlines. Outlines can be analyzed using semi-landmarks, which are the points that fall at defined intervals along a curve between two landmarks (Bookstein 1997). Semi- landmarks can be analyzed with Procrustes superimposition like ordinary landmarks. Another outline method is perhaps the oldest type of geometric morphometrics, Fourier analysis (Younker and Erlich 1977). Fourier methods employ sine and cosine harmonic functions to describe the positions of outline coordinates. Fourier analysis can be applied to 2D outlines (Ferson et al. 1985, Younker and Erlich 1977) or 3D closed surfaces (McPeek et al. 2008, Styner et al. 2006).

Geometric methods for the analysis of 3D surfaces is a developing area, to date three approaches have been tried. The first uses a combination of landmarks and

semi-landmarks to represent the surface of a 3D object (Mitterockeret al. 2005, Wiley et al. 2005). Selected landmarks are Procrustes superimposed and the remaining surface points are transformed along with them for pictorial 'morphing.' Eigen surface is a second approach that reduces surface scan data to a grid of hundreds or thousands of surface points that are all included in the analysis as semi-landmarks (MacLeod 2008, Polly 2008, Polly and MacLeod 2008). Spherical Fourier harmonic analysis is a third approach that works on the same principal as the 2D outline Fourier method (McPeek et al. 2008, Styner et al. 2006).

The Spherical harmonic (SPHARM) description (Brechbuhler et al. 1995) is a global, fine scale description that represents shapes of spherical topology. The basis functions of the parameterized surface are spherical harmonics. SPHARM can be used to express shape deformations (Kelemen et al. 1999), and is a smooth, accurate fine-scale shape representation, given a sufficiently small approximation error. Based on a uniform icosahedron-subdivision of the spherical parameterization, a Point Distribution Model (PDM) is directly obtained from the coefficients via a linear mapping between parameter space and image coordinates (Gerig et al. 2002). Correspondence of surface points represented by SPHARM is determined by normalizing the parameterization and the object alignment to the coarse shape represented by the first order, which is an ellipsoid. Truncating the spherical harmonic series at different degrees results in object representations at different levels of detail, resulting in a multi-scale object representation (Gerig et al. 2002).

The input of the proposed shape analysis is a set of binary segmentation. These segmentations are first processed to fill any interior holes and a minimal smoothing operation. The processed binary segmentations are converted to surface meshes, and a spherical parametrization is computed for the surface meshes using an area-preserving, distortion minimizing spherical mapping. The SPHARM description is computed from the mesh and its spherical parametrization. Using the first order ellipsoid from the spherical harmonic coefficients, the spherical parametrizations are aligned to establish correspondence across all surfaces. The SPHARM description is then sampled into triangulated surfaces (SPHARM-PDM) via icosahedron subdivision of the spherical parametrization. The spherical parameterization is computed via optimizing an equal area mapping of the 3D voxel mesh onto the sphere and minimizing angular distortions.

These SPHARM-PDM surfaces are all spatially aligned using rigid Procrustes alignment. Each individual SPHARM description is composed of a set of coefficients, weighting the basis functions. Truncating the spherical harmonic series at different degrees results in object representations at different levels of detail.

Cohort differences between groups of surfaces are computed using the standard robust Hotelling T2 two sample metric (Styner et al. 2002). Statistical p-values, both raw and corrected for multiple comparisons, result in significance maps. Additional visualization of the group tests are provided via mean difference magnitude and vector maps, as well as maps of the group covariance information. The SPHARM

shape description delivers a correspondence between shapes on the boundary, which is used in the statistical analysis (Styner et al. 2002).

Correspondence of SPHARM-PDM is determined by normalizing the alignment of the spherical parameterization to an object-specific frame. This normalization is achieved by rotation of the parameterization, such that the spherical equator, 0° and 90° longitudes coincide with those of the first order ellipsoid. After this parametrization normalization, corresponding surface points across different objects possess the same parameterization. Prior to the shape analysis, the group average object is computed for each subject group, and an overall average object is computed over all group average objects. Each average structure is computed by averaging the 3D coordinates of corresponding surface points across the group. The overall average object is then used in the shape analysis as the template object. At every boundary point for each object, a distance map is computed representing the signed local Euclidean surface distance to the template object. The sign of the local distance is computed using the direction of the template surface normal. In the global shape analysis, the average of the local distances across the whole surface is analyzed with a standard group mean difference test. The local shape analysis is computed by testing the local distances at every boundary point. This results in a significance map that represents the significance of these local statistical tests and thus allows locating significant shape differences between the groups (Styner et al. 2006a, 2003,2002).

The following is the most recent version of the framework of SPHARM Correspondence as described by Styner et al. 2006:

1) Area-preserving Spherical Mapping:

The appropriate parameterization of the points of a surface description is a key problem for correspondence finding, as well as for an efficient SPHARM representation. Every point (*i*) on the surface is to be assigned a parameter vector, describing a latitude and a longitude (θi,ϕi), that are located on the unit sphere. A homogeneous distribution of the parameter space is essential for an efficient decomposition of the surface into SPHARM coefficients. Mapping of the surface to the unit sphere is created, i. e., every point on the surface is mapped to exactly one point on the sphere, and vice versa. The main idea of the procedure is to start with an initial parameterization. This initial parameterization is optimized so that every surface patch gets assigned an area in parameter space that is proportional to its area in object space. To obtain a homogeneous distribution of the parameter space over the surface, this initial parameterization is modified in a constrained optimization procedure considering two criteria:

1. Area preservation: Every object region must map to a region of proportional area in parameter space.

2. Minimal distortion: Every quadrilateral should map to a spherical quadrilateral in parameter space.

2) Surface Models from SPHARM: SPHARM-PDM:

From the SPHARM description, triangulated surfaces are computed by sampling the spherical parameterization uniformly on the virtual sphere (Styner et al. 2006b). Using a linear, uniform icosahedron subdivision, good approximation of a homogeneous sampling of the spherical parameter space and thus also of the object space is achieved.

After shape description, correspondence establishment, the next step in the shape analysis pipeline consists of testing for differences between groups at every surface location. This can be done in 2 main fashions:

- Analyzing the magnitude of the local difference vector to a template: For this option, a template needs to be first selected, usually this is the common mean of the 2 groups or the mean of separate control group. The magnitude of the difference is easily understood and results in difference maps for each subject. Also, the resulting univariate statistical analysis is quite well known and local significance can be easily computed using the Student T metric.

- Analyzing the spatial location of each point: For this option, no template is necessary and multivariate statistics of the (*x,y,z*) location is necessary.

The general workflow starts from the segmented datasets with binary labels for each structure of interest. The *SegPostProcess* program extracts a single binary label and applies methods to ensure the spherical topology of the segmentation. In the

next step, the *GenParaMesh* computes the surface mesh corresponding to the segmentation, as well as a spherical parametrization of this surface mesh via area preserving mapping. The SPHARM-PDM shape representation is then computed using the *ParaToSPHARMMesh* program, which also handles issues of alignment. These three programs have to be run on all datasets in a shape analysis study. After all SPHARM-PDM representations have been computed, the statistical testing program *StatNonParamTestPDM* computes the difference maps, the significance maps, as well as the descriptive statistics such as the mean surfaces and covariance matrixes. All these programs are command line programs without any graphical user interface (Styner et al. 2006b).

The application of the *SegPostProcess* program is optional but recommended by Styner et al. 2006, as it ensures spherical topology of the segmentation. The input to *GenParaMesh* has to be of isotropic resolution and a relative fine resolution is recommended.

GenParaMesh first extracts the surface of the input label segmentation by following the 'cracks' between the voxels of the foreground (label) and the background. The input is a surface mesh with spherical parametrization. As a first step, the raw spherical harmonic coefficients are computed only up to the first degree and the first order ellipsoid is determined. The spherical parametrization is then rotated such that the poles of the first order ellipsoid are coinciding with the poles of the parametrization. The spherical harmonic coefficients are recomputed up to the degree specified on the command line option. Additionally, the surface points

of the SPHARM are reconstructed using the icosahedron subdivision scheme (Styner et al. 2006b).

The two main parameters to choose are the maximal degree for the SPHARM computation and the subdivision level for the icosahedron subdivision. By using the '-paraOut' command line option, the spherical icosahedron subdivision, as well as local phi and theta attribute files for the quality control visualization with *KWMeshVisu* are written out (Oguz et al. 2006).

Alignment: The *ParaToSPHARMMesh* tool provides two types of alignment. The first type performs an alignment of the normalized first order ellipsoid axis to the unit-axis with the ellipsoid center located at the origin. The second alignment type is a rigid-body Procrustes alignment (Bookstien 1996), i.e. Procrustes alignment only with translation and rotation. Whereas the first alignment is object inherent, the Procrustes alignment is in need of a template, which can optionally be supplied.

Different statistical analysis could be run on the resultant corresponding models including absolute surface distances, signed surface distances and computation of vector maps.

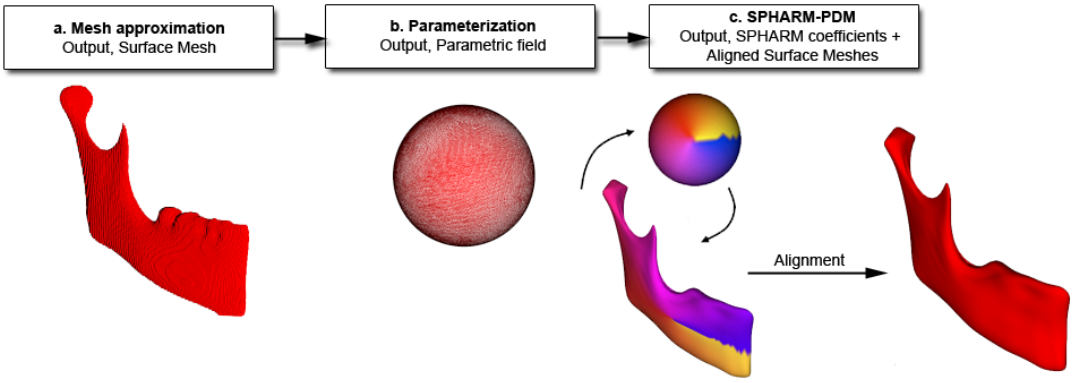

Figure 3.1. Description of shape correspondence procedures. The segmented 3-dimensional surface models of hemi-mandibles are converted into surface meshes, and a spherical parametrization is computed for the surface meshes using area-preserving and distortion-minimizing spherical mapping. The SPHARM description is computed from the mesh and its spherical parametrization. Using the first-order ellipsoid from the spherical harmonic coefficients, the spherical parametrizations establish correspondence across all surfaces. The SPHARM description is then sampled into a triangulated surface (SPHARM-PDM). The hemi-mandibles are represented using 4002 surface points.

Chapter 4

Validation of the use of SPHARM in 3D quantification using virtual mandibular asymmetries

4.1 Introduction

Treatment planning and assessment of the surgical correction of asymmetrical deformities is limited by reliance on 2D radiographs in the current clinical setting. The 2D radiographs conventionally used in mainstream orthodontic office based practice are particularly problematic when rotational or asymmetrical correction is required, since surgical jaw displacements are inherently 3-dimensional. Clinical examination and Lateral and frontal radiographs detect gross asymmetries; however, for treatment planning purposes, localization and quantification of the asymmetry is required. In 2D frontal head radiographs, the anatomic structures are overlapped. Additionally, frontal x-rays are very dependent on geometry and can give false measurements of the location, extent, and severity of mandibular asymmetry based on head tilt and rotation.

The use of cone-beam computed tomography (CBCT) or computer tomography (CT) provides the 3D imaging data necessary to generate precise knowledge of the location and the magnitude of facial asymmetry features, which are essential for the diagnosis of facial deformities and for the planning of corrective procedures. CBCT is favored is this realm because of its superior spatial resolution and lower dose compared to conventional CT scanners.

An increasing number of studies have demonstrated that computer aided surgical simulation (CASS) can predict possible surgical complications and lowers material costs while decreasing surgery duration, with comparable or better surgical outcomes (Hassfeld et al. 2001, Troulis et al. 2002, Gateno et al. 2007, Kang et al. 2010, Xia 2011, Hsu et al. 2012). However, the ability to visualize the facial asymmetry in 3D surface models does not imply the ability to quantify and precisely locate areas of asymmetry. Detailed analysis of positional as well as morphological discrepancy between the affected side and the normal side in an asymmetric patient is a prerequisite for ideal treatment planning.

Shape analysis has become of increasing interest to the Medical Image Analysis community due to its potential to precisely locate and quantify morphological changes between healthy and pathological structures. As part of the National Alliance for Medical Image Computing (http://www.na-mic.org), the Neuro-Image Research and Analysis Lab (NIRAL) at the University of North Carolina developed a comprehensive set of computing algorithms and instruments for the computation of 3D structural statistical shape analysis that have been mostly used for brain morphometry studies.

As described in the previous chapter the shape correspondence framework selected for this study was the SPHARM-PDM suite, which presents a comprehensive set of software for the computation of 3D structural statistical shape analysis (Styner et al. 2006). In summary, the SPHARM description is a hierarchical, global, multi-

scale boundary description that can only represent objects of spherical topology, proposed initially by Brechbuhler *et al.* 1995. This SPHARM shape analysis approach was further developed (SPHARM-PDM, PDM stands for Point Distribution Models) and extensively used for applications in neuroimaging (Styner et al. 2003, Gerig G et al. 2001).

The aim of this study was to determine if SPARM-shape correspondence based on segmented cone beam CT scans could correctly detect and quantify mandibular asymmetry when the two different mirroring techniques described in chapter 2 are used.

4.2 Materials and methods

Following a protocol approved by the Institutional Review Board for research at the University of North Carolina at Chapel Hill (Study #: 03-1647), twenty existing pretreatment CBCT scans, right and left mandibular morphology were compared by superimposing two image volumes. Patients ranged in age from 9 to 41 years with a mean age of 21 years. All subjects were taken from a consecutive, prospectively collected sample that sought care at UNC dentofacial deformities program and consented to participate in the project. Patients were included if they had clinically detectable asymmetry, defined as more than 2 mm of chin deviation or the presence of cant of the occlusal plan before the start of their orthodontic treatment as detected by clinical exam. Exclusion criteria were (1) history of previous jaw surgery and (2) reconstructive surgery with grafting. These patients were excluded to

minimize the confounding factors of extreme shape variability and the presence of hardware. The following 2 chapters are dedicated to the study of those cases.

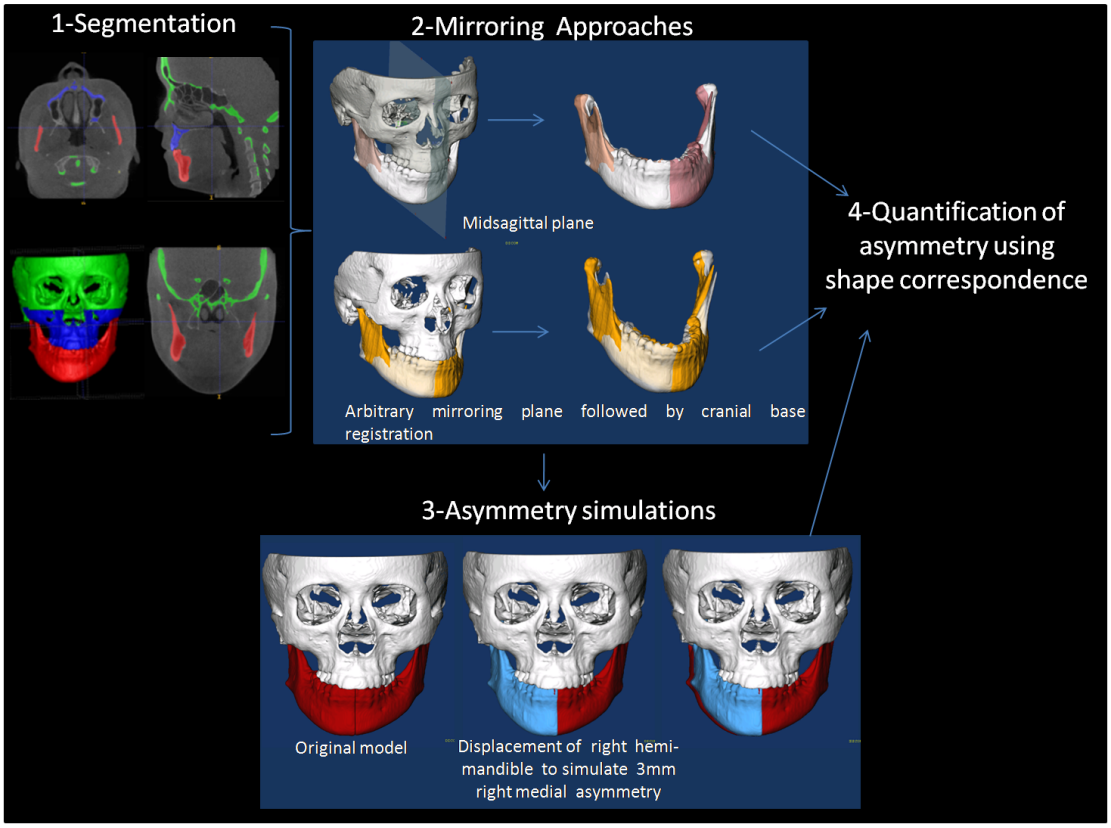

Figure 4.1. Validation of asymmetry quantification methods: (1) Cone beam CTs are taken for each patient and segmentation involves delineation of the anatomical areas of interest. (2) Visualization of the two mirroring techniques used to create mirror images for quantification of right and left side differences. (3) Simulation of asymmetry. (4) Quantification of asymmetry.

Image acquisition- NewTom 3G Cone Beam CTs (AFP Imaging, Elmsford, NY) were obtained prior to orthodontic treatment. Scans are obtained as a routine pre requisite to ortho planning as part of the local gold standard treatment planning exercise.

Construction of virtual 3D models from the CBCT dataset. The first step in this process involved segmentation of hard tissues by outlining the shape of structures visible in the axial slices of the volumetric dataset. Segmentation of anatomic structures was performed with ITK-SNAP (Yushkevich PA et al. 2006, Cevidanes et al. 2005) as described in previous chapters.

Mirroring approaches

Midsagittal Plane Approach

As described in chapter 2, Nasion (Na), Anterior Nasal Spine (ANS), and Basion (Ba) were used to define a midsagittal plane. The resultant midsagittal plane was used to create mirrors for both halves of the mandible, creating right and left hemi-mandibles

Arbitrary Plane Mirroring followed by Cranial Base Registration Approach

Models were mirrored on an arbitrary plane. Registration was then accomplished by voxel-based method on the cranial base. As described before, the registration was accomplished using IMAGINE software (National Institutes of Health,Bethesda,MD;Opensource,(http://www.ia.unc.edu/dev/download/imagine/index.htm).

The CMF software was used to display the superimposed images with the two approaches: (1) Original image superimposed to *mirrored* image on the *midsagittal plane*; and (2) Original image superimposed to *mirrored* image on an *arbitrary plane,*

and then registered to original image. A mutual-information based registration maps one image to another, using a rigid transform to evaluate within-subject changes. This task was performed using the registration pipeline within the Imagine Software developed at UNC (Cevidanes at al. 2007). Our superimposition methods are fully automated, using voxel-wise rigid registration of the cranial base instead of the current standard landmark matching method, which is observer-dependent and highly variable. After masking out maxillary and mandibular structures, the registration transform was computed solely on the grey level intensities in the cranial base. Rotation and translation parameters were calculated and then applied to register the 3D models (Cevidanes at al 2007).

Asymmetry simulation: Asymmetry simulation was performed with the CranioMaxilloFacial (CMF) software application. (M.E. Müller Institute for Surgical Technology and Biomechanics, University of Bern, Switzerland.) For each left and right hemimandible, asymmetry was simulated by translating the original models, with a known value of added asymmetric displacement (1mm x, 2mm x, 3mm x, 1mm z, 2mm z, 3mm z, 1mm x 2mm z, 2mm x 1 mm z and 3mm x 3mm z, where x is a vertical and z is a lateral plane of translation). Antero-posterior displacements (Y) were not done since they do not create asymmetries. Those numbers were chosen after consulting with an experienced orthodontist and a few surgeons at the University of North Carolina at Chapel Hill. Those clinicians decided that 2mm is a reasonable cut of point for clinically detectable asymmetry in all planes. 2mm has also been traditionally used as a “critical value” in stability studies for corrective

surgies (Proffit et al. 1987, 1991a, 1991b, 1991c, 2000, Bailey et al. 1994). The research team then decided to also test for 1mm both sides of that chosen cut of point. The 1mm displacements represent situations that are not easily detectable by clinical exam and the 3mm displacements represent asymmetries that are more easily detectable.

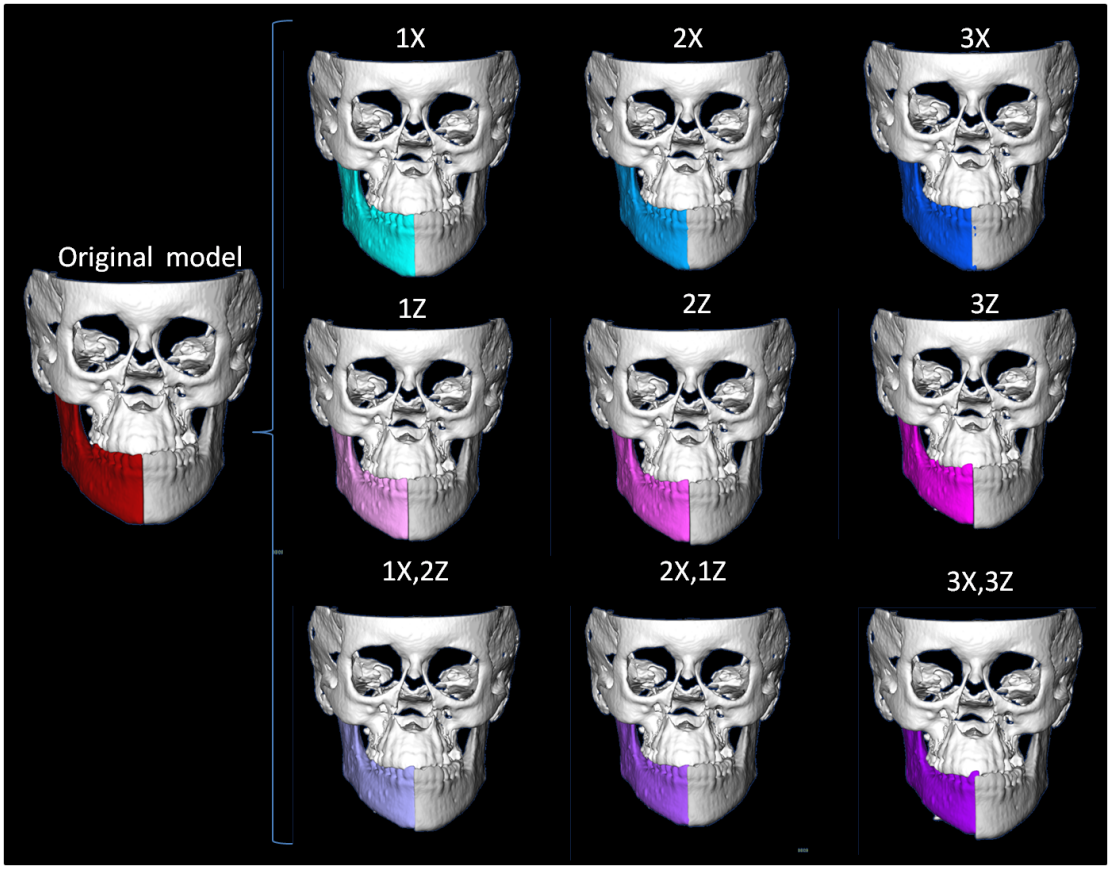

Figure 4.2. Asymmetry simulation. The segmented 3-dimensional surface models of hemi-mandibles are displaced in the lateral (X axis, yaw) and superior inferior (Z axis, roll) planes of spaces by 1, 2 and 3mm. The 9 different simulations are shown.

Asymmetric lateral and superior-inferior simulated translational movements were performed to create additional asymmetries of known magnitude (1, 2 and 3mm simulations). Simulated asymmetries were performed on the three

dimensional pretreatment models by a single examiner. After the virtual simulation of asymmetry, the mirror models were used to quantify the asymmetry and visualize the right and left side differences. This was done by changing the color and reducing the opacity of displaced models, which were superimposed with the original mirror models.

Quantification of differences between simulated asymmetries and mirror models: Shape Correspondence (SC) was employed to provide a unique and symmetric point correspondence across all measured surfaces. The correspondence was computed by mapping every point on the mandibular 3D surface models to a unique position on the unit sphere (SPHARM software, developed as part of the NAMIC consortium) (Styner at al. 2006a), followed by generating a uniformly triangulated surface based on this spherical mapping (SPHARM-PDM) (Gerig at al. 2001). Jaw asymmetry was measured for each right and left hemi-mandibles, comparing the original and the mirrored structures. First, subtraction of mirrored and original (actual) asymmetry models allowed a template for surgical corrections displaying color-coded corresponding distance maps and maps of vectors of differences between these models. Second, subtraction of mirror and simulated asymmetry models generated color-coded corresponding distance maps and maps of vectors of differences between these models. The distance maps measure the magnitude of the differences between the mirror and the simulated asymmetry point-based models, while the vector maps offer directionality. The six degrees of freedom (DOF) of the differences were calculated using rigid Procrustes alignment. The geometric

transformation that best maps the shape changes between the mirror and simulated asymmetry point-based correspondent models measured asymmetry in six DOF. The measured simulated translations with Shape correspondence/Procrustes were the absolute differences between the measurements of simulated asymmetries and the actual asymmetries: ([procrustes between each simulation translated hemimandible and original mirrored hemimandible] - [procrustes between original hemimandible and original mirrored hemimandible]).

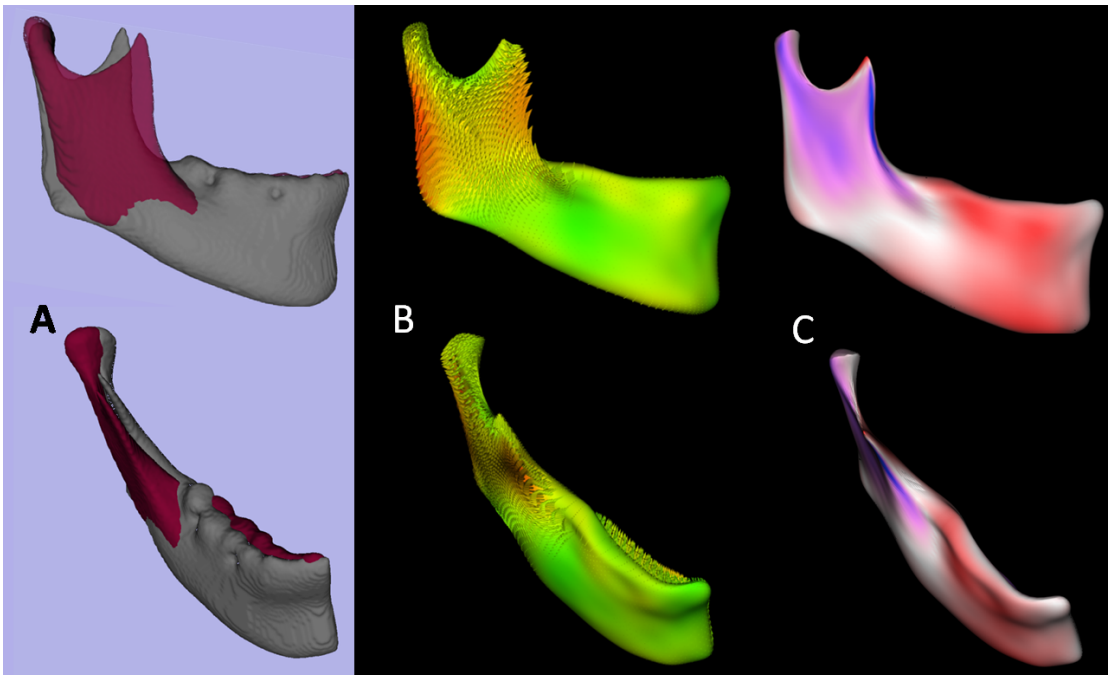

Figure 4.3. Quantification of mandibular asymmetry for a patient using Shape Correspondence. (A) original model (*grey)* and left hemi-mandible arbitrary mirror matching on the cranial base(*maroon)*; (B) Shape Correspondence can be used to quantify the right and left differences as represented in this vectorial color map of the surface distance between the registered original and arbitrary mirror models; (C) Signed color maps showing the directionality of the differences the left ramus is wider and left corpus is narrower than the right.

Statistics analysis: Three statistical methods were used to analyze the accuracy of asymmetry representation using SPHARM-PDM: (1) P ($|\bar{x}$-known$|$<0.5), the

probability that the sample mean measurement was within 0.05mm (translation) , 0.5 was choosen becuase it represents voxel size, or 5^0 (rotation) of the true value of the simulated asymmetry. Those error limits were chosen in light of clinical significance and the fact that sub-voxel values (even if calculated mathematically) are unreal for any imaging system, (2) 95% confidence interval (CI), and (3) 95% prediction interval (PI). The 95% CI provides an interval with 95% confidence that the true mean falls within the interval. The confidence interval doesn't necessarily contain the true mean. The 95% PI is an estimate of an interval that a future observation of a random variable is expected to fall within with a 95% probability. It can be considered as a "confidence interval" for prediction. The prediction interval is always wider than the confidence interval because of the additional uncertainty for prediction (Paniagua et al. 2010). All analyses were based on the decision of a normal distribution for this population depending on the shape of the graph of the raw data (See appendix one).

4.3 Results

Table 4.1 shows the results for the midsagittal plane mirroring and describes the probabilities, confidence intervals and prediction intervals for the x, y and z rotation and translations measured for the simulated asymmetries using mirroring in the midsagittal plane. Table 4.2 shows the results for the arbitrary mirroring with cranial base registration approach.

Table 4.1						
Midsagittal plane	Known asymmetry simulation	6 degrees of freedom	Mean±SD	CI (Min-Max)	PI (Min-Max)	P(|measured mean-known|<.5)
Mirror_ translation 1x	0	Rx	0.00±0.00	(0.00-0.01)	(0.00-0.01)	1
	0	Ry	0.01±0.01	(0.00-0.01)	(-0.02-0.03)	1
	0	Rz	0.01±0.01	(0.00-0.01)	(-0.01-0.02)	1
	1	Tx	1.02±0.11	(0.97-1.08)	(0.79-1.26)	1
	0	Ty	0.00±0.01	(0.00-0.01)	(-0.01-0.02)	1
	0	Tz	0.00±0.00	(0.00-0.01)	(0.00-0.01)	1
Mirror_ translation 1x_2z	0	Rx	0.01±0.01	(0.00-0.01)	(-0.01-0.03)	1
	0	Ry	0.01±0.01	(0.00-0.01)	(-0.01-0.03)	1
	0	Rz	0.01±0.01	(0.00-0.01)	(-0.01-0.03)	1
	1	Tx	1.03±0.11	(0.97-1.08)	(0.79-1.27)	1
	0	Ty	0.01±0.00	(0.00-0.01)	(-0.01-0.02)	1
	2	Tz	2.00±0.01	(1.99-2.00)	(1.99-2.01)	1
Mirror_ translation 1z	0	Rx	0.00±0.00	(0.00-0.01)	(-0.01-0.01)	1
	0	Ry	0.01±0.02	(0.00-0.02)	(-0.02-0.05)	1
	0	Rz	0.01±0.01	(0.00-0.01)	(-0.01-0.03)	1
	0	Tx	0.08±0.34	(-0.08-0.23)	(-0.64-0.80)	0.99
	0	Ty	0.01±0.01	(0.00-0.01)	(-0.01-0.02)	1
	1	Tz	1.00±0.00	(0.99-1.00)	(0.99-1.01)	1
Mirror_ translation 2x	0	Rx	0.01±0.01	(0.00-0.01)	(-0.01-0.02)	1
	0	Ry	0.00±0.01	(0.00-0.01)	(-0.01-0.02)	1
	0	Rz	0.00±0.01	(0.00-0.01)	(-0.01-0.02)	1
	2	Tx	1.97±0.11	(1.92-2.03)	(1.73-2.22)	1
	0	Ty	0.00±0.00	(0.00-0.01)	(-0.01-0.01)	1
	0	Tz	0.00±0.00	(0.00-0.01)	(0.00-0.01)	1
Mirror_ translation 2x_1z	0	Rx	0.01±0.01	(0.00-0.01)	(-0.01-0.02)	1
	0	Ry	0.01±0.01	(0.01-0.02)	(-0.02-0.04)	1
	0	Rz	0.01±0.01	(0.01-0.02)	(-0.01-0.03)	1
	2	Tx	1.97±0.11	(1.92-2.03)	(1.73-2.21)	1
	0	Ty	0.01±0.01	(0.00-0.01)	(-0.01-0.02)	1
	1	Tz	1.00±0.00	(0.99-1.00)	(0.99-1.01)	1
Mirror_ translation 2z	0	Rx	0.01±0.01	(0.00-0.01)	(-0.01-0.02)	1
	0	Ry	0.01±0.01	(0.00-0.01)	(-0.02-0.03)	1
	0	Rz	0.01±0.01	(0.00-0.01)	(-0.01-0.02)	1
	0	Tx	0.08±0.34	(-0.08-0.23)	(-0.64-0.80)	0.99
	0	Ty	0.00±0.01	(0.00-0.01)	(-0.01-0.02)	1
	2	Tz	2.00±0.00	(1.99-2.00)	(1.99-2.01)	1
Mirror_ translation 3x	0	Rx	0.01±0.00	(0.00-0.01)	(0.00-0.01)	1
	0	Ry	0.01±0.01	(0.00-0.02)	(-0.02-0.04)	1
	0	Rz	0.01±0.01	(0.00-0.01)	(-0.01-0.02)	1
	3	Tx	2.92±0.34	(2.77-3.08)	(2.21-3.64)	0.99
	0	Ty	0.00±0.01	(0.00-0.01)	(-0.01-0.02)	1
	0	Tz	0.00±0.00	(0.00-0.01)	(-0.00-0.01)	1
Mirror_ translation 3x_3z	0	Rx	0.01±0.01	(0.00-0.01)	(-0.01-0.02)	1
	0	Ry	0.01±0.01	(0.00-0.01)	(-0.01-0.02)	1
	0	Rz	0.01±0.01	(0.00-0.01)	(0.00-0.02)	1
	3	Tx	2.92±0.34	(2.77-3.08)	(2.21-2.64)	0.99
	0	Ty	0.00±0.01	(0.00-0.01)	(-0.01-0.02)	1
	3	Tz	3.00±0.00	(2.99-3.00)	(2.99-3.01)	1
Mirror_ translation 3z	0	Rx	0.01±0.01	(0.00-0.01)	(-0.01-0.02)	1
	0	Ry	0.01±0.01	(0.00-0.02)	(-0.02-0.04)	1
	0	Rz	0.01±0.01	(0.00-0.01)	(-0.01-0.02)	1
	0	Tx	0.08±0.34	(-0.08-0.24)	(-0.64-0.80)	0.99
	0	Ty	0.01±0.01	(0.00-0.01)	(-0.01-0.02)	1
	3	Tz	3.00±0.00	(2.99-3.00)	(2.99-3.01)	1

Table 4.2						
Cranial base registration	Known asymmetry simulation	6 degrees of freedom	Mean±SD	CI (Min-Max)	PI (Min-Max)	P(|measured mean-known|<.5)
Mirror_ translation 1x	0	Rx	0.01±0.00	(0.00-0.01)	(-0.01-0.02)	1
	0	Ry	0.01±0.01	(0.00-0.01)	(-0.02-0.03)	1
	0	Rz	0.01±0.01	(0.00-0.01)	(-0.01-0.02)	1
	1	Tx	1.02±0.11	(0.97-1.08)	(0.79-1.26)	1
	0	Ty	0.00±0.01	(0.00-0.01)	(-0.01-0.02)	1
	0	Tz	0.00±0.00	(0.00-0.01)	(0.00-0.01)	1
Mirror_ translation 1x_2z	0	Rx	0.01±0.01	(0.00-0.01)	(-0.01-0.03)	1
	0	Ry	0.01±0.01	(0.00-0.01)	(-0.01-0.03)	1
	0	Rz	0.01±0.01	(0.00-0.01)	(-0.01-0.03)	1
	1	Tx	1.03±0.11	(0.97-1.08)	(0.79-1.27)	1
	0	Ty	0.01±0.00	(0.00-0.01)	(-0.01-0.02)	1
	2	Tz	2.00±0.01	(1.99-2.00)	(1.99-2.01)	1
Mirror_ translation 1z	0	Rx	0.00±0.00	(0.00-0.01)	(-0.01-0.02)	1
	0	Ry	0.01±0.02	(0.00-0.02)	(-0.02-0.05)	1
	0	Rz	0.01±0.01	(0.00-0.01)	(-0.01-0.03)	1
	0	Tx	0.08±0.34	(-0.08-0.23)	(-0.64-0.80)	0.85
	0	Ty	0.01±0.01	(0.00-0.01)	(-0.01-0.02)	1
	1	Tz	1.00±0.00	(0.99-1.00)	(0.99-1.01)	1
Mirror_ translation 2x	0	Rx	0.01±0.01	(0.00-0.01)	(-0.01-0.03)	1
	0	Ry	0.00±0.01	(0.00-0.01)	(-0.01-0.02)	1
	0	Rz	0.00±0.01	(0.00-0.01)	(-0.01-0.02)	1
	2	Tx	1.97±0.11	(1.92-2.03)	(1.73-2.22)	1
	0	Ty	0.00±0.00	(0.00-0.01)	(-0.01-0.01)	1
	0	Tz	0.00±0.00	(0.00-0.01)	(0.00-0.01)	1
Mirror_ translation 2x_1z	0	Rx	0.01±0.01	(0.00-0.01)	(-0.01-0.02)	1
	0	Ry	0.01±0.01	(0.01-0.02)	(-0.02-0.04)	1
	0	Rz	0.01±0.01	(0.01-0.02)	(-0.01-0.02)	1
	2	Tx	1.97±0.11	(1.92-2.03)	(1.73-2.21)	1
	0	Ty	0.01±0.01	(0.00-0.01)	(-0.01-0.02)	1
	1	Tz	1.00±0.00	(0.99-1.00)	(0.99-1.01)	1
Mirror_ translation 2z	0	Rx	0.01±0.01	(0.00-0.01)	(-0.01-0.02)	1
	0	Ry	0.01±0.01	(0.00-0.01)	(-0.02-0.03)	1
	0	Rz	0.01±0.01	(0.00-0.01)	(-0.01-0.02)	1
	0	Tx	0.08±0.34	(-0.08-0.23)	(-0.64-0.80)	0.85
	0	Ty	0.00±0.01	(0.00-0.01)	(-0.01-0.02)	1
	2	Tz	2.00±0.00	(1.99-2.00)	(1.99-2.01)	1
Mirror_ translation 3x	0	Rx	0.01±0.00	(0.00-0.01)	(0.00-0.02)	1
	0	Ry	0.01±0.01	(0.00-0.02)	(-0.02-0.04)	1
	0	Rz	0.01±0.01	(0.00-0.01)	(-0.01-0.02)	1
	3	Tx	2.92±0.34	(2.77-3.08)	(2.21-3.64)	0.85
	0	Ty	0.00±0.01	(0.00-0.01)	(-0.01-0.02)	1
	0	Tz	0.00±0.00	(0.00-0.01)	(-0.00-0.01)	1
Mirror_ translation 3x_3z	0	Rx	0.01±0.01	(0.00-0.01)	(-0.01-0.02)	1
	0	Ry	0.01±0.01	(0.00-0.01)	(-0.01-0.02)	1
	0	Rz	0.01±0.01	(0.00-0.01)	(0.00-0.02)	1
	3	Tx	2.92±0.34	(2.77-3.08)	(2.21-3.64)	0.85
	0	Ty	0.00±0.01	(0.00-0.01)	(-0.01-0.02)	1
	3	Tz	3.00±0.00	(2.99-3.00)	(2.99-3.01)	1
Mirror_ translation 3z	0	Rx	0.01±0.01	(0.00-0.01)	(-0.01-0.02)	1
	0	Ry	0.01±0.01	(0.00-0.02)	(-0.02-0.04)	1
	0	Rz	0.01±0.01	(0.00-0.01)	(-0.01-0.02)	1
	0	Tx	0.08±0.34	(-0.08-0.24)	(-0.64-0.80)	0.85
	0	Ty	0.01±0.01	(0.00-0.01)	(-0.01-0.02)	1
	3	Tz	3.00±0.00	(2.99-3.00)	(2.99-3.01)	1

The probability that the magnitude of the asymmetry measurement difference from the known value of simulated asymmetry was less than 0.5 mm of translation or 5^0 of rotation was high for midsagittal plane mirroring (0.99-1) as well as for the arbitrary mirroring with cranial base registration (0.85-1). For this clinical application, measurements smaller than the voxel size of the image volume (0.5mm) were considered accurate. The results showed an acceptable error range in measurements calculated for both mirroring techniques with SPHARM-shape correspondence (all probabilities are above 0.84, also this lower limit was for only 5 cases using cranial base registration). All 95% confidence and probability intervals contained the hypothesized means (known asymmetry values, Tables 4.1 and 4.2). Since all the measured surface differences were within 0.5 mm of translation and 5 degrees of rotation of the real displacement. All 6 DOF for 95% CI and 95% PI contain 0; it is pretty certain that the aim of the study is fulfilled by our data.

4.4 Discussion

The results of this study demonstrate that facial asymmetry with six degrees of freedom can be accurately quantified by our method down to resolution limits of 1mm of simulated skeletal position. As discussed earlier 1mm is smaller than the clinical detectability agreed on for diagnostic and follow up for stability of corrective surgeries. This proposed rapidly developing technology might have a significant impact on future surgical procedures.

An increasing number of studies have demonstrated that computer aided surgical simulation (CASS) have lower material costs as well as decreased surgical time, comparable or better surgical outcomes, reduced complications and increased predictability of surgical complications (Hassfeld et al. 2001, Xia et al. 2000, Gateno et al. 2003, 2007, Troulis et al. 2002). It has also been utilized to allow more complex surgeries to be successfully performed in a single procedure rather than the previous multiple staged surgeries (Hassfeld et al. 2001, Xi et al. 2000, Gateno J et al. 2003, 2007, Troulis et al 2002). The ability to visualize facial asymmetry in 3D surface models does not imply the ability to quantify and precisely locate areas of asymmetry. Precise measurements rather than just general visualization are needed for a solid treatment plan; so 3D image analysis algorithms should be applied on those volumes for quantification and localization of asymmetry. Future benefits also include the fabrication of stereolithographic models and surgical splints, which have the potential to greatly reduce intra-operative time and surgical complications (Gateno et al. 2007). This is achieved by giving the surgeon the chance to go through and carefully plan the steps of the surgery virtually before the actual surgery, by providing intermediate and final splints to be used intra-operatively, and by providing a baseline for follow up. CASS helps aiding the surgeon to be guided to cut accurately & safely even if he/she can't see all the features beyond the minimal access he/she might resort to for instrument access, thus minimizing scarring and fosters better conditions for wound healing.

In this study, the use of mirroring on the midsagittal plane allowed precise and reproducible measurements of asymmetry. However, the choice of landmarks used to determine the midsagittal plane might have a marked impact on the asymmetry quantification. Manual selection of landmarks is time-consuming, as it requires great care and attention during the selection process. In addition, the result depends on availability and visibility of the anatomical landmarks and on the ability of the user to identify them.

In a particular face, symmetry is often better described by several regional symmetry axes (e.g., symmetry between jaw and midface regions often differs, for which no defining landmark set exists) (Tung-Yui et al. 2005). In severe asymmetries, as in craniofacial microsomia or cleft patients, entire regions of the anatomy might be missing or severely deranged. In these cases selection of landmarks could result in an incorrect quantification of asymmetry.

The measurements calculated for arbitrary mirroring with cranial base registration had slightly lower probabilities compared to mirroring in the midsagittal plane. It did, however, has good precision (as measured by the probabilities, 95% confidence and probability intervals) and could be used as an alternative assessment method, particularly for patients with marked mandibular asymmetry, but with relatively symmetric cranial bases. The concept of a mirroring technique using arbitrary mirroring, is possible by the subsequent voxel wise rigid registration of the cranial base. This method was validated in previous studies (Cevidanes et al. 2005).

It has been shown to be more accurate than traditional landmark methods for three-dimensional superimpositions (Gliddon et al. 2006, Xia et al. 2007). The larger the number of points used for superimposition the more accurate it becomes. If the patient's cranial base is symmetric, the use of a stable and symmetric facial structure has proven to be a reliable reference for diagnosing the facial roll and yaw components of mandibular asymmetry.

Ackerman and Proffit emphasized that valid and reliable quantification of appearance continues to elude researchers (Ackerman and Proffit 2009). Interpretation of facial asymmetry even if in 3D by subjective visual assessment of right and left differences can lead to inadequate diagnosis and mislead treatment planning. They suggested that the labial inter-commissure line and Natural Head Position are examples of orientations determined by soft tissues that should be used in the evaluation of transverse roll of the dentition (Ackerman et al. 2007). However; the labial inter-commissure line can be affected by muscular and facial animation asymmetries too (Ackerman and Ackerman 2002). In the past, the inability to appreciate the interplay between maxillo-mandibular roll and yaw was a missing link in classification and diagnosis. When one sees a major midline shift, a unilateral Class II or Class III molar relationship, or a true unilateral crossbite, quantification of the mandibular roll and yaw is essential prior to the quantification of actual left and right differences (Ackerman et al. 2007). The extent of asymmetric yaw is a major determinant in whether treatment is limited to asymmetric mechanics or might

extend to asymmetric extractions, unilateral bone anchors, or surgery (Ackerman et al. 2007).

The assessments in this study were performed as a baseline diagnosis before orthodontic preparation. However, pre-treatment diagnosis does not necessarily reflect the pre-surgical planning that might well change and evolve, depending on the orthodontics mechanics and degree of correction of the dental midlines that the clinician patient team have been able to achieve during dentoalveolar realignment therapies. The techniques developed and demonstrated in this study may be generalizable and can be applied for pre-surgical assessment.

In recent years, there has been a surge in recent years of commercially available programs for three-dimensional virtual surgery and visualization programs (De Momi et al. 2006, Gellrich et al. 2002, Hassfeld 2001, Liu et al. 2001, Junck et al. 1990, Glerup et al. 1999). The biggest drawback all these programmes share is the lack of validation. The basic algorithms used in most those programs are not fully described, resolution limits are not quoted, and the limitation in clinical use has not been demonstrated yet.

4.5 Conclusions

SPHARM-shape correspondence in combination with mirroring techniques allows visualization and quantification of the location, direction and magnitude of differences between right and left sides of the mandible down to resolution limits of 1mm of simulated skeletal position. Future efforts should be directed towards validation and development of the current tools for other craniofacial skeletal components, the occlusion and the soft tissues.

Chapter 5

3D quantification of mandibular asymmetry using the SPHARM-PDM suite: a clinical cohort study

5.1 Introduction:

Assessment of correction of skeletal discrepancies in current clinical practice is based on visual data originating from different sources: clinical examination, 3D photographic examination, Cone-Beam Computed Tomography (CBCT) and digital dental models. Correction of these deformities using orthognathic surgery involves careful repositioning the jaws, due to the unique features of each patient's deformity. Even though 3D CBCT images are now easily obtained in many dental centres, the ability to visualize the craniofacial complex in 3D does not imply the ability to quantify existing differences between sides, growth, or treatment changes in 3D. During treatment phase as well as follow up, there is a need for more precise 3D quantification and localization.

SPHARM-PDM suite, which presents a comprehensive set of algorithms for the computation of 3D structural statistical shape analysis, was developed and demonstrated in the previous 2 chapters. It proved to be able to detect the amount and direction of simulated mandibular asymmetries within the resolution of 0.5mm of the current system as determined by the used computational scheme.

The objective of the work presented in this chapter was the clinical application of this technology to assess mandibular asymmetry in a cohort of patients with a previous clinical diagnosis of mandibular asymmetry. After establishing the validity of this technology to detect the quanitity and direction of small asymmetries in a simple simulated setting, the next logical step was to establish if the proposed methodology would work for everyday clinical setting.

5.2 Materials and methods:

The cohort consisted of prospectively collected 45 pre-treatment CBCT scans from patients that sought care at UNC Dentofacial Deformities Program and consented to participate in the project. This project was approved by the University of North Carolina Ethics committee for research on human subjects (Study #: 03-1647). These scans were a subset of a bigger sample of consecutive prospectively collected images, collected in the grant "Improving Treatment Outcomes for Patients with Facial Deformity using 3D Imaging". Scans are obtained as a routine pre requisite to ortho planning as part of the local gold standard treatment planning exercise. These scans were not conducted in addition to, rather as a routine part clinical assessment, avoiding additional radiation exposure to the patients consenting to use of their anonymised datasets.

Inclusion criteria for our study were patients with clinically detectable asymmetry, defined as more than 2 mm of chin deviation or cant of the occlusal plane before the start of their orthodontic treatment. Exclusion criteria were history

of previous jaw surgery such as patients who required reconstructive surgery. The presence of hardware and the shape variability are considered confounding factors. Those will be specifically addressed next chapter.

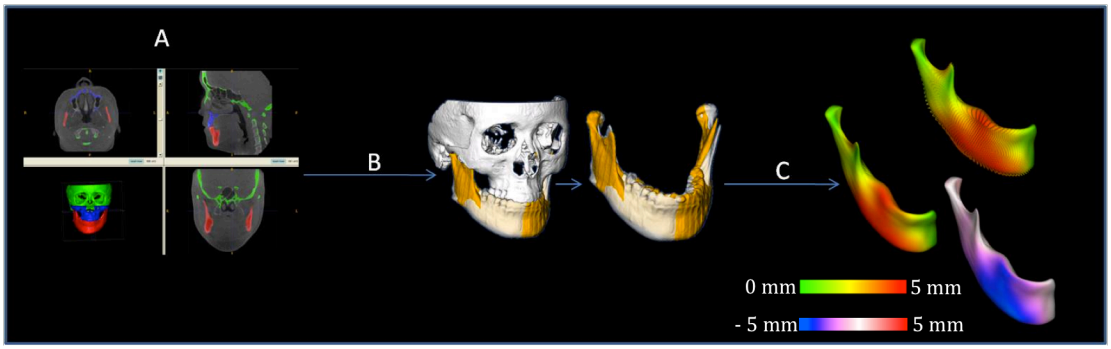

Figure 5.1. Study flowchart: After segmenting hard tissue (A), the image volume and segmentation models were mirrored by flipping left and right sides and then registering the mirrored image onto the cranial base (B). Quantification of mandibular asymmetry for a patient is done using SPHARM-PDM shape analysis (C). Original model *(white)* and left hemi-mandible arbitrary mirror matching on the cranial base (*yellow)*. Shape analysis is be used to quantify right and left differences by computing vector maps, absolute surface distance maps and signed surface distance maps of the differences between the original and arbitrary mirrored models (both registered in the cranial base). Signed distances color maps show the directionality of the differences.

Arbitrary mirroring followed by registration on the cranial base was chosen over mirroring around a midsagittal plane as they both proved to give similar results with the arbitrary mirroring technique followed by registration on the cranial base being more robust as demonstrated in chapter 2.

Image Acquisition

As in previous chapters New Tom 3G Cone-beam CTs (AFP Imaging, Elmsford, NY) with the patient in supine position were obtained prior to orthodontic treatment. Those scans are taken as a part of the diagnostic work up for patients in preperation for subsequent surgical therapy.

Construction of Virtual 3D Models from the CBCT Dataset

As described in chapter 2, segmentation of anatomic structures was performed using ITK-SNAP (open source software, http://www.itksnap.org*)(Yushkevich PA et al. 2006).*

Mirroring and cranial base registration

Models were mirrored on an arbitrary plane. Registration was then accomplished by voxel-based method on the cranial base. As described before, the registration was accomplished using IMAGINE software (National Institutes of Health,Bethesda,MD;Opensource,(http://www.ia.unc.edu/dev/download/imagine/index.htm).

Cranial base registration is important since it provides information concerning the mandibular asymmetry, relative to the face. Asymmetry was defined as the difference between each hemimandible and the mirror of the contralateral side.

Before computing correspondent point-based models using SPHARM-PDM, spherical topology of the models must be assured. This was achieved with the following pre-processing steps (Paniagua et al. 2010):

1. In order to simplify the ridges and waves of the hemimandibular segments, a Laplacian smoothing procedure was applied to each hemimandible.
2. Then a binary segmentation volume is created again from the surfaces. This was done via finding the enclosing bounding box of the shape and binarizing the cross-sections.
3. These binary segmentation volumes form the input data for the SPHARM-PDM framework.

SPHARM-PDM shape correspondence and Procrustes alignment

The UNC SPHARM-PDM shape analysis suite was employed to compute unique correspondent point based models of all the hemimandibular surfaces per patient.

The segmented 3D surface models of the hemimandibles were first converted into surface meshes, and mapped into the unit sphere using an area-preserving and distortion-minimizing spherical mapping. The SPHARM description is computed from the mesh and its spherical parameterization (Styner et al. 2003). Using the first-order ellipsoid from the spherical harmonic coefficients, the spherical parameterizations are aligned to establish correspondence across all surfaces. The SPHARM description is then sampled into triangulated surfaces (SPHARM-PDM).

Alignment of all surfaces was performed using rigid Procrustes alignment (Styner et al. 2003,2006). This rigid Procrustes alignment procedure computes an optimal linear, geometric transformation ϕ (n) that best maps the shape changes between the affected hemimandible and the mirror of the opposite healthy side based on the established correspondence (Styner et al. 2003, 2006).

A preliminary analysis was computed by subtracting the models of each hemimanadible and the mirror of the contralateral side, which were then displayed via colour-coded distance magnitude and vector maps via KWMishVisu (Oguz et al. 2006). Allowing visualization and quantification of distances between paired correspondent point-based models, indicating the direction and magnitude of disparities on each side and thus, the mirrored side discrepancies. Procrustes was used to capture translational and rotational differences between each hemimandible and the mirror of the contralateral side in the three planes of space (Bookstein 1996).

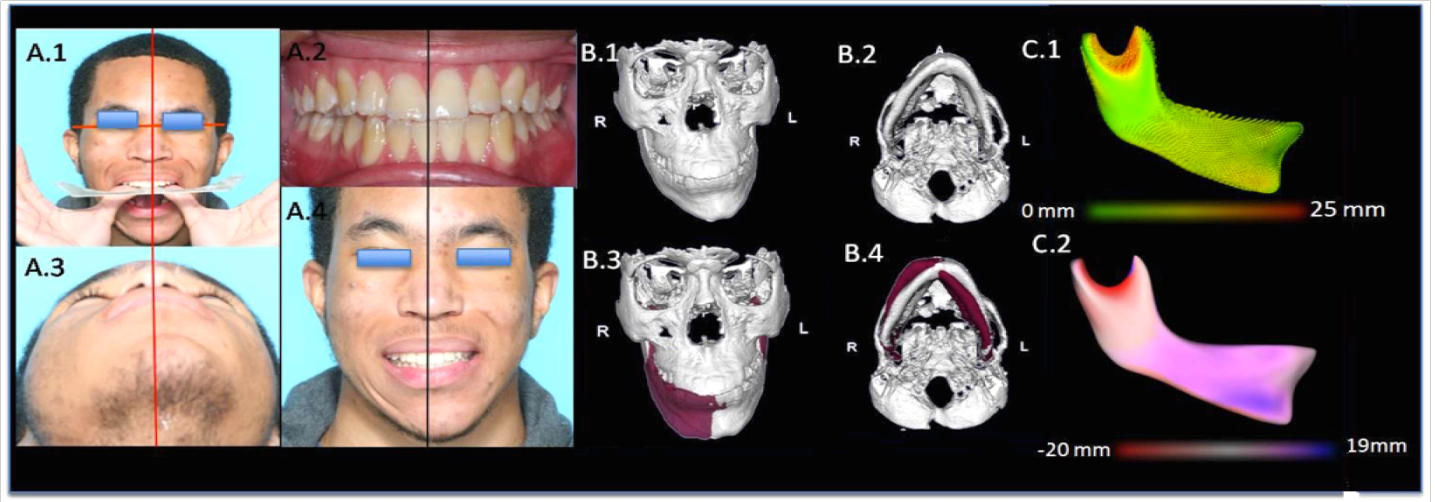

Figure 5.2. An example of 3D analysis for a patient in the cohort: Clinical photos are shown in A. Note the maxillary cant in A.1, the discrepancy in dental midline A.2, the deviation of the chine to the left in A.3 and A.4; Group B represents hard tissue surface models of the same patient. B.1 is a frontal view, B.2 is a SMV view, B.3 and B.4 are the same views respectively also showing the mirror of the mandible registered on the cranial base (Mirror model in maroon); In C is 3D analysis color maps of the right side of the mandible in relation to the mirror of the left half of the mandible, Vector maps are shown in C.1 and signed distance maps shown in C.2.

We hypothesized that there should be no difference in the absolute values of Procrustes output based on whether the right or the left side of the mandible is being mirrored. This serves as an internal validation of this methodology. Paired T test was used to test this null hypothesis. All analyses were based on the normal distribution for this population. Normality of this data was established based on the shape of the graph of the raw data (See appendix one).

5.3 Results:

The mean and standard deviation of translational differences in mm and the rotational differences in degrees between original hemimandible and the hemimmandible mirrored in the contralateral side were calculated with Procrustes alignments and are displayed in table 5.1. No statistically significant difference was observed in the absolute values of Procrustes output based on whether the right or the left side of the mandible was being mirrored. This demonstrates the consistency of Procrustes in evaluating mandibular asymmetry and the robustness of the mirroring and assessment techniques.

Table 5.1

	Tx_Left	Tx_Right	Tz_Left	Tz_Right	Rx_Left	Rx_Right	Rz_Left	Rz_Right
Mean	-0.89	-0.91	-0.33	-0.01	2.28	2.33	2.36	2.54
SD	2.47	2.51	1.94	1.80	1.79	1.73	2.03	2.14
P value	0.72		0.55		0.62		0.11	

Table 5.1 shows the average and standard deviation of translational differences in mm and rotational differences in degrees between the left hemimanadible and the mirror of the right side (_Left) and between the right side and the mirror of the left (_Right). Notice the non-significant p Value between the 2 sides. X is in mediolateral and Z is in cranio-caudal direction. Readings from the anterioposterior are not included since this plane is irrelevant for asymmetry assessment.

Location of mandibular asymmetry was heterogenous in this sample; however 8% of the cases showed characteristic larger asymmetry surface distances at the condyles, while 18% presented more marked mandibular body and ramus asymmetry. Most patients (74%) exhibited generalized asymmetric mandibular morphology with involvement of both condyle ramus and corpus.

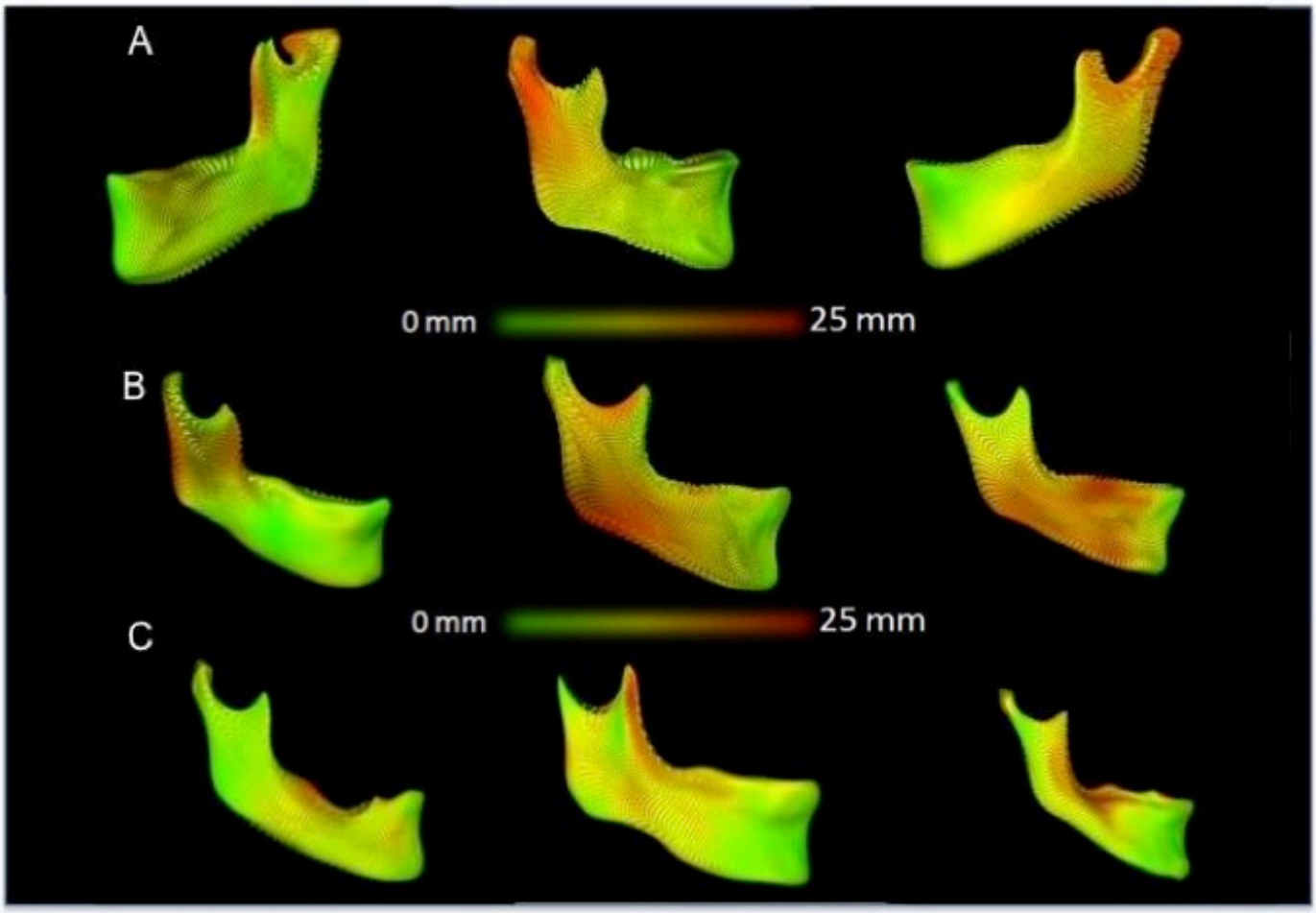

Figure 5.3. Examples of patients from the cohort with mandibular asymmetry mostly localized to the condyle (row A), or in the ramus\body of the mandible (row B), examples of generalized mandibular asymmetry are shown in row C.

Most detected asymmetries in this cohort had a translational component in the medio-lateral followed by the cranio-caudal direction. These differences ranged from 0.03-9.05 mm with a mean of (1,76± 1.99) mm, and 0.05-6.86 mm with a mean of (0.80±1.36) mm respectively. Despite being mathematically calculated all numbers smaller than 0.43mm (sub-voxel values) are not relevant clinically since they can not be observed under the resolution of the used system. When those sub-

voxel readings were excluded from the data set, the numbers reported above changed to (2.1± 1.5) mm in the medio-lateral direction and (1.34±0.8) mm cranio-caudaly.

As for the rotational component, bigger changes were detected in the yaw followed by the roll then the pitch of those heminandibles. Differences in the yaw ranged from 2.54-10.37 degrees with a mean of (2.54± 2.14) degrees while those of the roll and pitch ranged from 0.17-10.19 degrees with a mean of (2.57± 2.11) degrees, and 0.08-6.2 degrees with a mean of (2.38± 1.72) degrees.

5.4 Discussion:

Most commercially available and academic software that are able to compute color-coded surface maps use a closest point algorithm to obtain surface distance differences. Closest point is a brute force algorithm that calculates a vertex-to-vertex Euclidean closest point distance (De Momi E et al. 2006, Besl and McKay 1992). This method does not map corresponding surfaces based in anatomical geometry, and thus, it usually underestimates rotational and large translational movements.

The application of conventional closest point distances for mirror images in mandibles of patients with rudimentary condyles, severe cants, or a rotated mandible, does not represent the difference between corresponding anatomical locations, but rather differences based in the minimal distances between any point in the original and mirrored models. These clinical situations mandate the use of a more “anatomically sensitive” shape analysis technique.

Shape correspondence is a promising alternative to overcome the shortcomings of the commonly used closest point algorithm. It is one of the currently used statistical shape analysis techniques that allows measuring the surface distance between an area on one model to the corresponding anatomical area in the other model regardless of the alignment of those models. The main shape correspondence challenges involve the representation of a population by means of correspondent point based models. Surface representation could be accomplished by several different options including, matching of template surface geometry (curvature and location) (Meier and Fisher 2002), Entropy-based Particle Systems (Oguz et al. 2009), or by Spherical harmonic representation (SPHARM) (Gerig at al. 2001). In SPHARM the surface model is mapped in a sphere, and correspondence point based models are computed after finding the spherical harmonic basis that best fits the model. After surface mapping is achieved, correspondence could be based on different frameworks, depending on the clinical problem at hand.

SPHARM-PDM allows for comprehensive statistical evaluations to be computed for the correspondent models as a whole or for specific regions of interest within these models.

For asymmetry assessment and future treatment planning, an individual based analysis was chosen in this project as compared to group analysis. Group analysis is usually used to examine general trends and cross sectional tendencies; both will be

of limited utility to a unique patient focused treatment planning approach. However, to maximize the usefulness of the extensive data that SPHARM-PDM can provide, regions of interest that correspond to surgical segments could be analyzed separately.

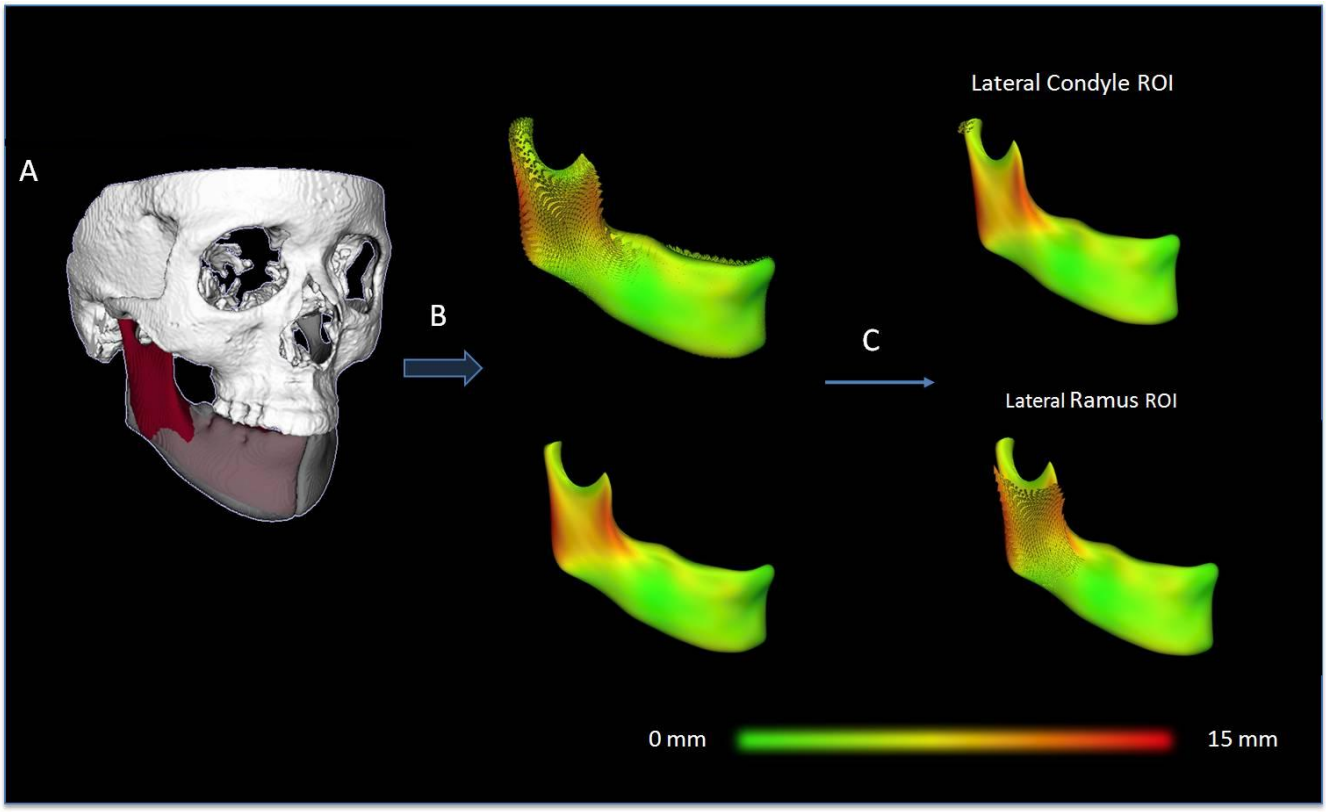

Figure 5.4. ROI analysis: (A) Hard tissue surface model for a patient showing the mirror of the left mandible registered on the cranial base (Mirror model in maroon), in (B) Vector and surface distance maps of the right side of the mandible in relation to the mirror of the left half of the mandible. Vector maps computed for specific regions of interest (Lateral pole of the condyle and lateral surface of the ramus) are shown in (C).

This quantitative asymmetry measure could then either be communicated to the surgeon directly or used as an input for surgical simulation software to produce stents and re-location guides for mobile fragments in reconstruction. Similar

applications could be developed for trauma reconstructions, mirroring the undamaged to the damaged locations to provide guides for more accurate re-location than the occlusion and pre-trauma photographic evidence.

The translational and rotational differences between mandibular halves as measured by Procrustes is an accurate representation of the location component of mandibular asymmetry; however, in patients with marked morphological differences between both hemimandibles, grafting and\or reshaping procedures might be needed. In these cases, pure shape analysis after accounting for positional differences is probably a more appropriate approach.

While this study applied shape analysis to a pretreatment assessment of mandibular asymmetry, future investigations are needed to apply the preliminary findings in this study to pre-surgical treatment planning and surgical simulation of corrective surgeries of patients with complex asymmetries to test the boundaries of the clinical usefulness of the suggested protocol.

5.5 Conclusion:

SPHARM-PDM has a promising role in individual diagnosis and quantification of mandibular asymmetry. SPHARM-PDM proved to be successful in the quantification of mandibular asymmetryies of a clinical cohort that included patients with wide range of severity, provided that those patients did not undergo previous surgeries or have additional hardware. This technology could be used to localize asymmetries to specific anatomic areas in the mandible that correspond to segments to be moved

intraoperatively during corrective surgeries. The output of asymmetry quantification using SPHARM-PDM, both quantity and direction data, could be used as an input for treatment planning of corrective surgeries of those mandibular asymmetry patients.

Three-dimensional diagnosis of mandibular asymmetry revealed the complex involvement of morphological components of the mandible and heterogeneous nature of this clinical condition.

Chapter 6

3D shape analysis of a Craniofacial Microsomia cohort

6.1 Introduction:

After SPHARM was demonstrated in a cohort of asymmetry patients, the need arises for further understanding of how the algorithm would deal with extreme cases. Extreme cases could be cases with severe asymmetries or cases with unique shape characteristics. This endeavor will establish the boundaries of clinical usefulness and will contribute to the establishment of guidelines for clinical selection criteria for this software. Craniofacial Microsomia was chosen for this project because of the vast variability of the clinical presentation of patients having this syndrome.

Craniofacial Microsomia is the most frequently encountered form of isolated facial asymmetry (Monahan et al. 2001). It primarily is a syndrome of the first branchial arch, involving underdevelopment of the temporomandibular joint, mandibular ramus, mastication muscles and the ear. Hearing loss may result from underdevelopment of the osseous components of the auditory system and a diminished or absent external auditory meatus. Occasionally, second branchial arch defects involving the facial nerve and facial muscles coexist with Craniofacial Microsomia (Gougoutas et al. 2007,Monahan et al. 2001, Rahbar et al. 2001, Horgan et al. 1995). While the exact etiology of Craniofacial Microsomia has not yet been determined, there are many theories based on embryologic, clinical and laboratory studies (Monahan et al. 2001). Development of the first branchial arch is thought to

be intimately involved with the occurrence of Craniofacial Microsomia (Bell et al. 1980). Formation of the first branchial arch occurs at approximately one month in utero, when the neural crest cells migrate into the vicinity of the developing tissues. Neural crest cells are precursor cells that develop early in fetal life and migrate throughout the head and neck region, stimulating local cell growth and differentiation. Laboratory studies suggest that an early loss of neural crest cells may be the specific factor responsible for the clinical presentation of Craniofacial Microsomia (Johnston 1991, Thomas et al. 1987). The extent of the neural crest cell loss is reflected in the degree of severity of the facial deficiency and, therefore, is thought to dictate the severity of the clinical presentation (Proffit et al. 1991). Increased incidence within families has been documented, which suggests the possibility of genetic inheritance (Berry et al. 1989).

Owing to the various clinical manifestations of the disorder, many classifications have been developed to help categorize these patients. The OMENS classification (O = orbital distortion; M = mandibular hypoplasia; E = ear anomaly; N = nerve involvement; and S = soft-tissue deficiency) is the most comprehensive and, therefore, one of the most commonly used systems (Vento et al. 1991). The OMENS system, scores five clinical manifestations of hemifacial microsomia according to dysmorphic severity on a scale from 0 to 3. It encompasses the skeletal and soft-tissue abnormalities, as well as facial nerve and extracranial problems (Cohen et al. 1991, Horgan et al. 1995). It is common for patients who have a syndrome associated with the first branchial arch to have extracranial abnormalities, such as

heart and pulmonary defects, as these systems develop simultaneously with the first arch. A type I mandible is defined as retaining normal morphologic characteristics of the ramus and condyle but diminished in size. A type II mandible demonstrates significant architectural and size distortion of the ramus, condyle, and sigmoid notch. Finally, a type III mandible shows gross distortion or complete agenesis of the ramus (Gougoutas et al. 2006).

Its variable involvement of both hard and soft tissues makes it crucial to quantify the morphological features of each patient to serve as a base for surgical planning and follow up. State-of-the-art diagnostic technology can improve the quality of life for patients who have Craniofacial Microsomia at earlier ages than was ever thought possible.

Three-dimensional (3D) data acquisition allows visualization and analysis of craniofacial anomalies in three dimensions. Both Computed tomography (CT) and Cone beam computed tomography (CBCT) could provide a three-dimensional rendition of the soft tissue of the face and an image of the underlying bone(Huisinga-Fischer et al. 2001). Researchers (Cevidanes et al. 2011, Cevidanes et al. 2005, Cevidanes et al. 2007, Cevidanes et al. 2006, AlHadidi et al. 2011, Alhadidi et al. 2012) showed that the three-dimensional data and associated image analysis in the surgical treatment plans of facial deformity patients could alter both the size and shape of the mandible. These diagnostic imaging modalities contribute to a structural assessment of the patient. They also help establish the degree of

anatomical malformation and the relationship of the deformity to the adjacent craniofacial skeleton. In addition, comparing preoperative and postoperative CT scans can be a reliable diagnostic method for confirming treatment effectiveness of hard tissue corrective surgeries.

The needed qualitative and quantitative assessment of the existing asymmetries itself and the effect of treatment have been approached in several different ways. Visual assessment of overlay of models will give the clinician a general appraisal of the clinical problem at hand and help in the localization and break down of the basic elements of the existing asymmetry and/or the short and long effect of corrective surgery (Cevidanes et al. 2005). Color-coded maps measuring pair-wise differences between 3D structures give a more precise quantitative description of the degree and the direction of the asymmetry and effect of treatment as well. Those color-coded maps could be generated using closest point algorithm or after establishing anatomic correspondence (Alhadidi et al. 2012, de Paula et al. 2013, Cevidanes et al. 2011).

This pilot work describes the use of image analysis techniques in the assessment, surgical planning and follow up of patients with craniofacial microsomia. Craniofacial Microsomia is an ideal patient group to target components of positional and morphological mandibular asymmetry because of the different degrees of complexity and severity of its clinical presentation that pose particular challenges to the computer algorithms suggested in this protocol for image analysis.

The aim of this experiment was to establish the boundaries of clinical usefulness of SPHARM in patients with severe asymmetries and structural defects.

6.2 Materials and methods:

A cohort of 11 prospective Craniofacial Microsomia patients with different degrees and classification of the disease were included in this pilot study (6 males and 5 females, age ranging from 9-15 years). This project was approved by the University of North Carolina Ethics committee for research on human subjects (Study #: 03-1647). Four of the patients in this cohort had cleft lip/palate, 2 had neural and 3 had orbital involvement. No patient was excluded as we were trying to test for extreme cases. (Fig 6.1 and Fig 6.2)

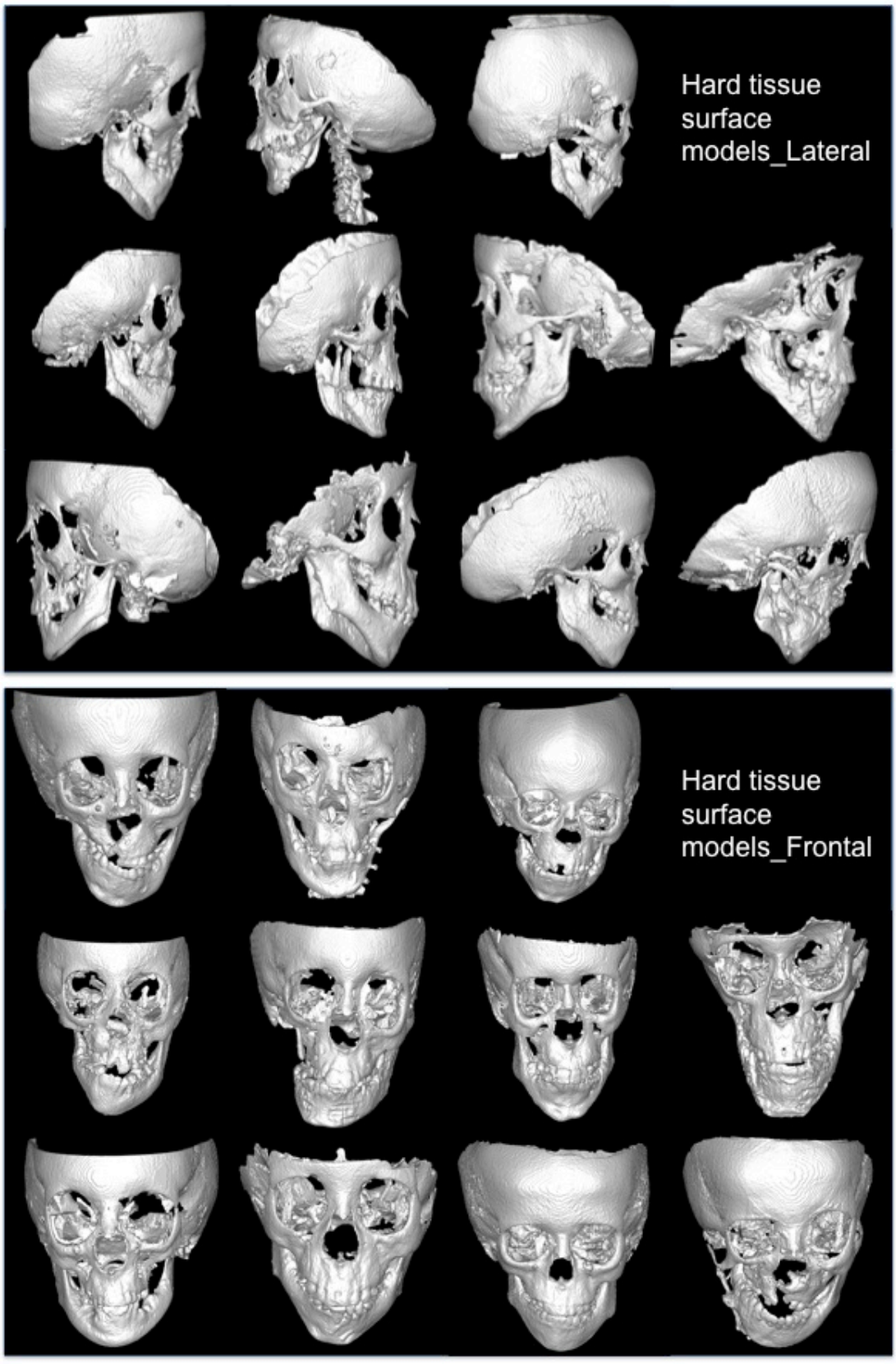

Figure 6.1. Overview of the cohort_Hard tissues

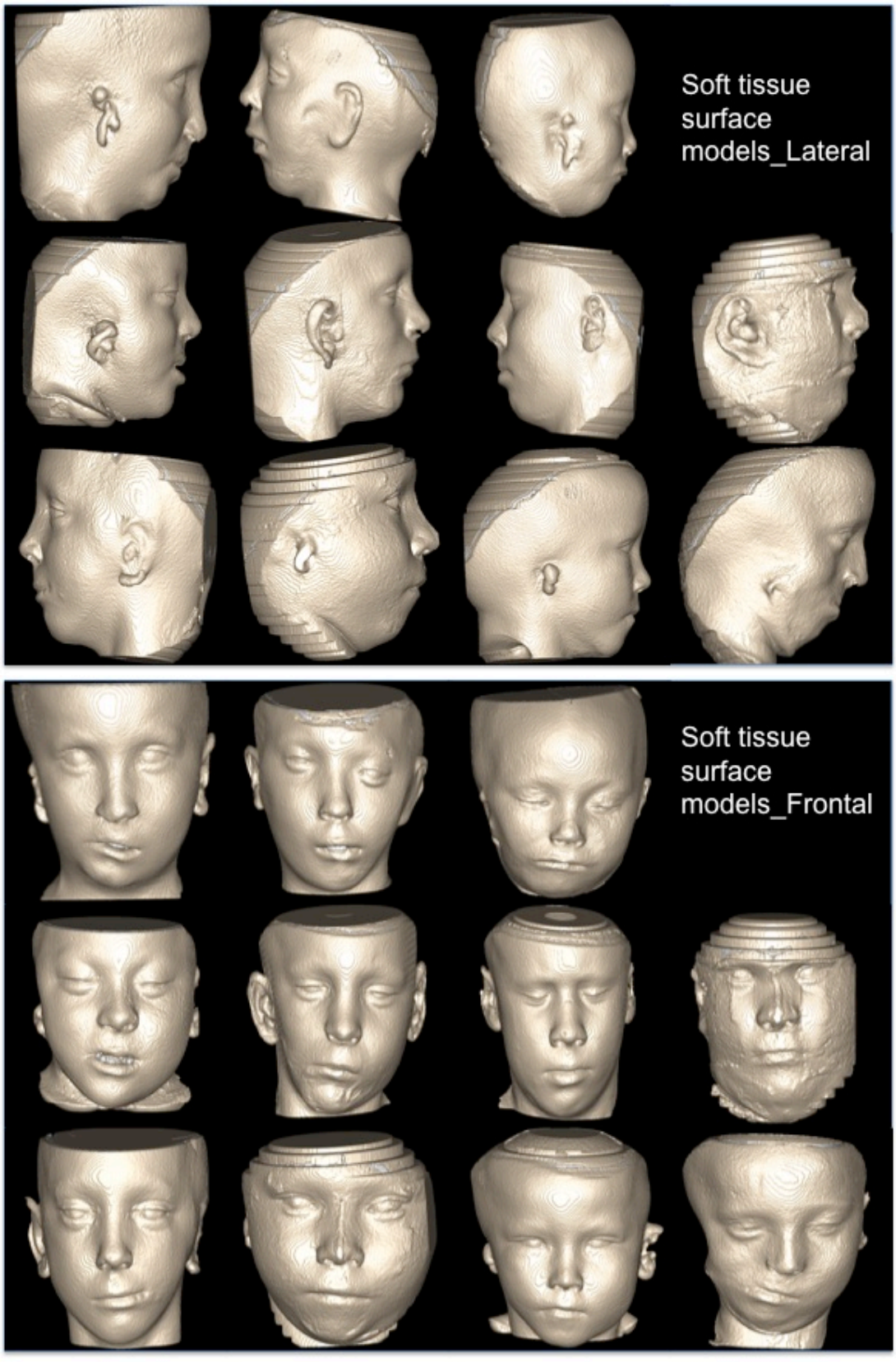

Figure 6.2. Overview of the cohort_Soft tissues

3D image analysis techniques involved construction of 3D surface models from the CBCT volumes, registration, mirroring, and quantification of asymmetry as described earlier in previous chapters.

These techniques have been previously validated and applied to craniofacial corrective surgery of a general cohort of asymmetry patients. (Cevidanes et al. 2011, Cevidanes et al. 2007, Alhadidi et al. 2012,Paniagua et al. 2010). (Fig 6.3)

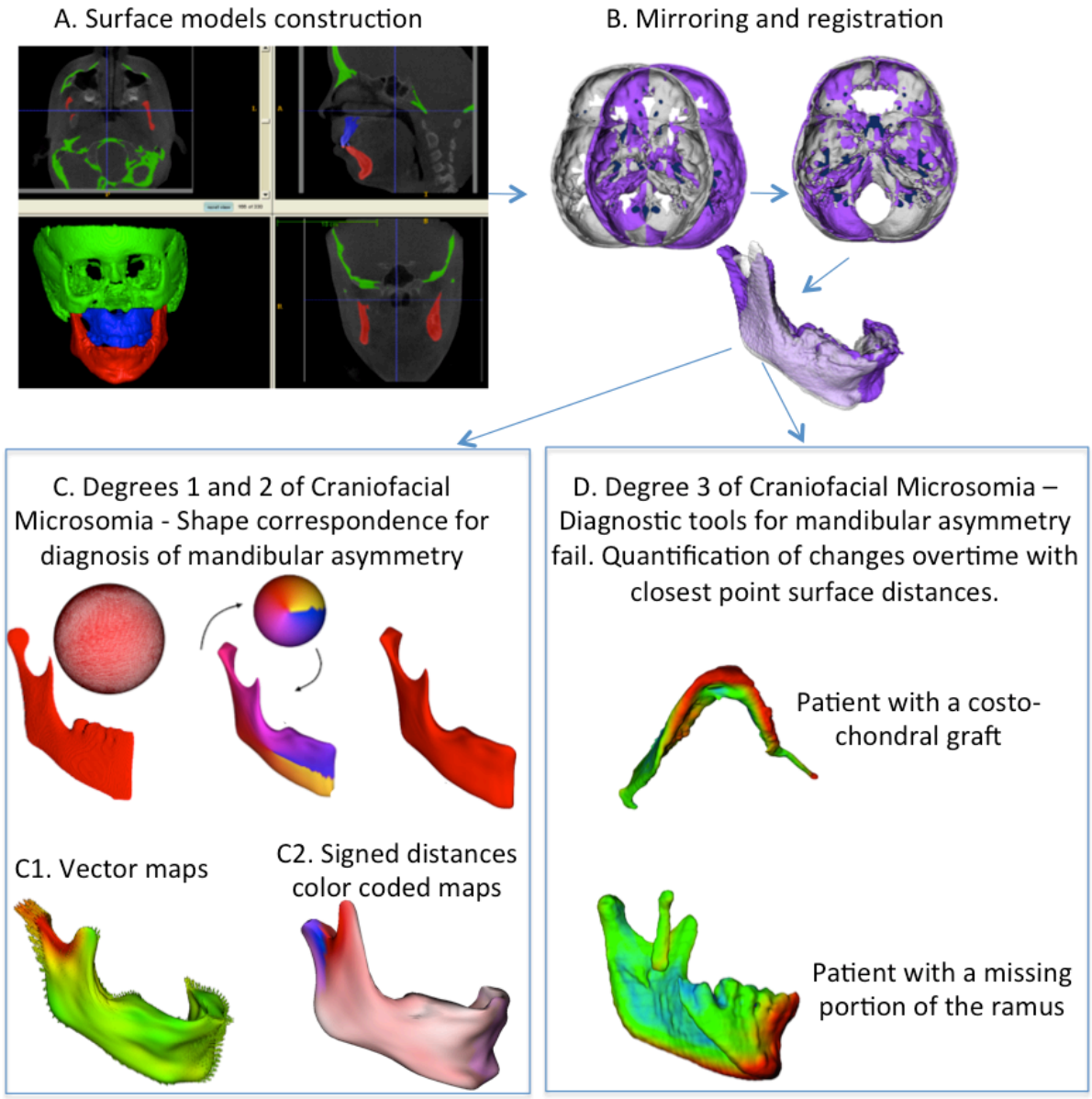

Figure 6.3. Study flowchart for quantification of mandibular asymmetry for craniofacial microsomia patients using. A. 3D surface models were constructed from CBCT images. B. Mirroring of right or left affected side. Models were registered on the cranial base to establish a common coordinate system. Overlay of the original mandibular surface model (semi-transparent grey) and left hemi-mandible mirrored on the midsagittal plane (teal); C. For degrees 1 and 2 of craniofacial microsomia shape correspondence established individual meshes of 4002 homologous surface points corresponding across left and right sides for each patient. C1. Subtraction calculations for each surface point between the affected and non affected sides of the mandibles generated 4002 vector differences, measuring the magnitude and identifying the location and direction of differences. C2. Surface-to-surface differences between right and left hemi-mandibles were also calculated as signed distances with a color-coded scale to allow quantification of morphologic variability. D. For degree 3 of craniofacial microsomia Shape Correspondence or Closest point surface distances fail to to quantify left and right differences. Longitudinal changes can still be seen as semi-transparent overlays and quantified with closest point surface distances.

Image Acquisition

New Tom 3G Cone-beam CT (AFP Imaging, Elmsford, NY) scans with large field of view (23 cm) of patients in supine position were obtained. These scans are part of the typical pretreatment diagnostic protocol for patients seen at the craniofacial clinic at the University of North Carolina at Chapel Hill. Usage of a low dose technique is of paramount importance for this young group of patients.

Construction of Virtual 3D Models from the CBCT Dataset

Segmentation of anatomic structures was performed using ITK-SNAP (open source software, http://www.itksnap.org/)(Yushkevich PA et al. 2006) *as* described before in chapter 2.

Mirroring and cranial base registration

The registration was accomplished using IMAGINE software (National Institutes of Health, Bethesda, MD; Open-source, http://www.ia.unc.edu/dev/download/imagine/index.htm) consisting of a voxel-based registration method. The original and the arbitrarily mirrored images were then registered on the cranial base as described in previous chapters.

Asymmetry was defined as the difference between each affected hemi-mandible and the mirror of the contralateral side. The term “affected hemi-mandible” is indeed not based on biological basis of the syndrome, the whole

mandible is altered by the compensatory mechanisms during growth. However, clinical wise, one side is more affected than the other. The recovery of symmetry of the face is clinically more relevant that restoring an indeal stereotype shape.

Before computing correspondent point-based models for right and left hemi-mandibles, two pre-processing steps were performed (Paniagua et al. 2010).

First, in order to simplify the small irregularities at the surfaces of the hemimandibular segments, a Laplacian smoothing procedure was applied to each hemimandible.

Secondly, a binary segmentation volume was created again from the surfaces, via finding the enclosing bounding box of the shape and binarizing the consequential cross-sections (Paniagua et al. 2010). These binary segmentation volumes are the input of the SPHARM-PDM software (open source software, http://www.nitrc.org/projects/spharm-pdm/).

SPHARM-PDM shape correspondence and Procrustes alignment

The SPHARM-PDM suite was employed to compute highly sampled point-based correspondent models for left and right anatomic structures resulting in correspondent models for the right and left hemi-mandibles. This software presents a comprehensive set of tools for the computation of 3D structural statistical shape analysis (Styner et al. 2006). The spherical harmonics (SPHARM) description is a hierarchical, global, multi-scale boundary description that can only represent objects

of spherical topology, proposed initially by Brechbühler et al. (Brechbühler et al. 1995). This shape analysis approach was further extended to SPHARM-PDM where PDM stands for Point Distribution Models and has been extensively used for applications in neuroimaging (Gerig et al. 2001, Styner et al. 2003).

A preliminary analysis was computed by subtracting the virtual models of each hemimandible and the mirror of the contralateral side and each "difference vector map" was displayed via color-coded distance magnitude and vector maps. Vector maps provided visualization and quantification of distances between paired correspondent point-based models, indicating the direction and magnitude of discrepancies between each side and its mirror opposite.

Procrustes was used to capture translational and rotational differences between each hemi-mandible and the mirror of the contralateral side in the three planes of space.

The SPHARM-PDM software quantified right and left differences for only 6 of the 11 patients in this study (Fig 6.4).

Shape correspondence could not be established for the remaining 5 patients because of structural reasons: 2 patients did not have a condyle on the affected side, 2 were grafted, and one was wearing a distraction osteogenesis appliance when the CBCT was taken since treatment of those patients started at an outside institution. The presence of either graft material or any hardware will distort the shape of the

affected hemimandible and that will disturb the presence of coorepondent points between this hemimandible and the contralateral side.

For patients where SPHARM could not be computed, color-coded surface maps for follow up were generated based on closest point algorithm (CP). Closest point is a brute force algorithm that calculates a vertex-to-vertex Euclidean closest point distance, where correspondent point-based models are not necessary for the quantification of changes (Cevidanes et al. 2011). CP cannot quantify existing asymmetry in those patients as explained in chapters 4 and 5.

6.3 Results:

Translational differences in mm and the rotational differences in degrees between original hemimandible and the hemimandible mirrored in the contralateral side calculated with Procrustes alignments are displayed for each of the 6 successful cases in table 6.1.

Table 6.1

Pt #	Tx	Ty	Tz	Rx	Ry	Rz
1	-4.57	3.91	-0.53	7.59	16.69	5.33
2	2.83	2.04	-0.23	4.26	2.55	1.89
3	-14.15	1.56	0.98	1.83	5.88	1.96
4	-2.21	-1.61	1.45	3.88	-4.21	3.83
5	-4.99	6.71	-2.86	2.94	14.62	17.99
6	-0.28	-2.51	-0.96	3.46	4.41	4.63

Table 6.1 shows the translational differences (T) in mm and the rotational differences (R) in degrees between original hemimandible and the hemimandible mirrored in the contralateral side calculated with Procrustes alignments in X, Y, and Z planes.

Right and left differences for individual diagnosis and treatment planning were quantified by color-coded surface distances and vector maps. Overlay of both hemimandibles allowed visual assessment of size and shape differences in 3D between the affected and non-affected sides. Color-coded maps were quantified and graphically display the location, amount and direction of those differences. Color-coded maps computed via closest point algorithm were used to follow up 2 of the cases in which shape corrspondence could not be established because of the discontinuity and the gross distortion of the mandible or the presence of a graft (Fig 6.5 and 6.6).

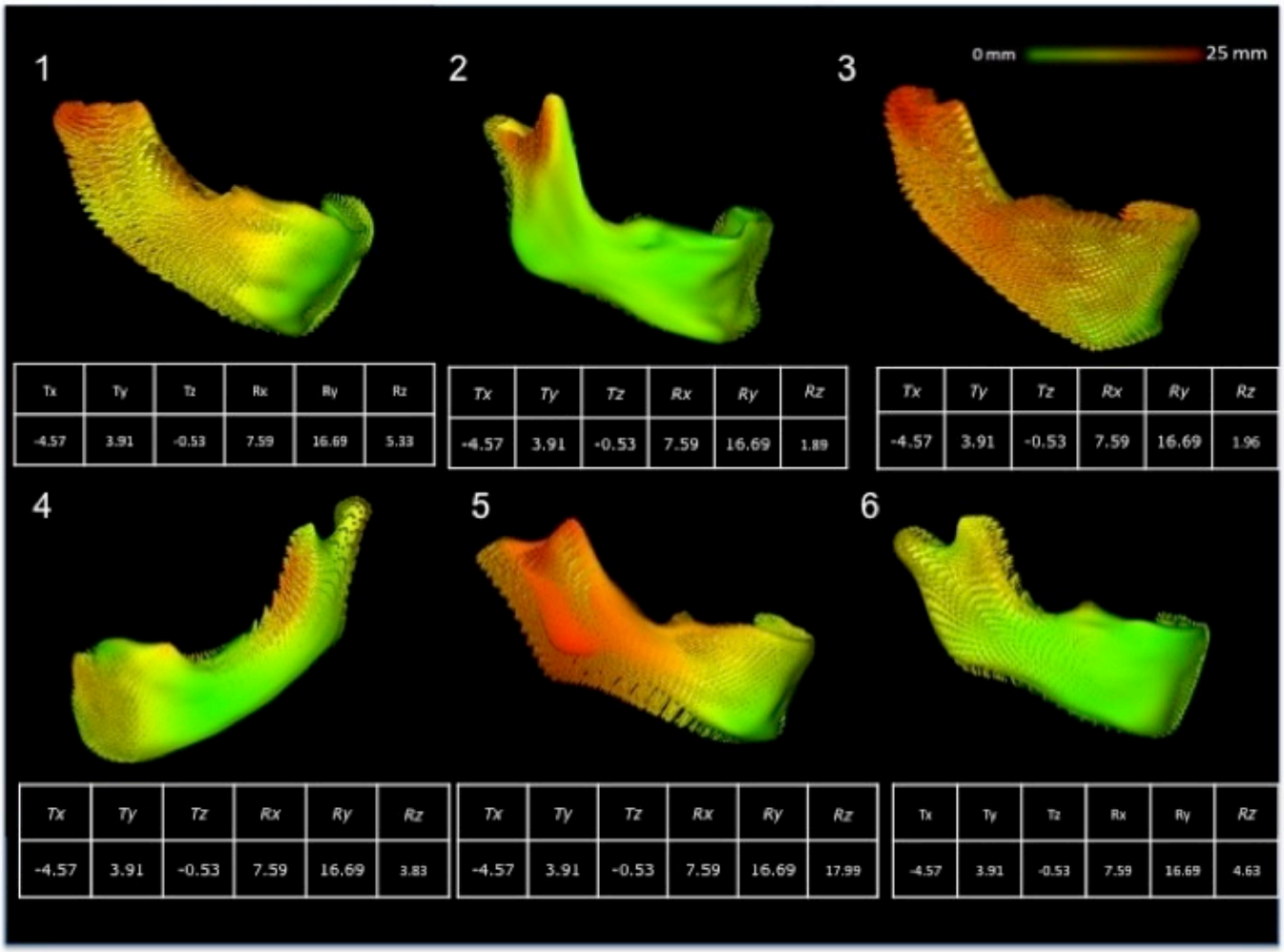

Figure 6.4. Six patients with degree 1 or 2 of craniofacial microsomia for which shape correspondence of the mandible morphology was adequately established. Vector maps quantify the location and direction of the right to left side differences. The vectors are displayed at a 0.5 size scale to facilitate visualization. The color-code is standardized at a maximum of 25mm to allow comparisons of severity of asymmetry.

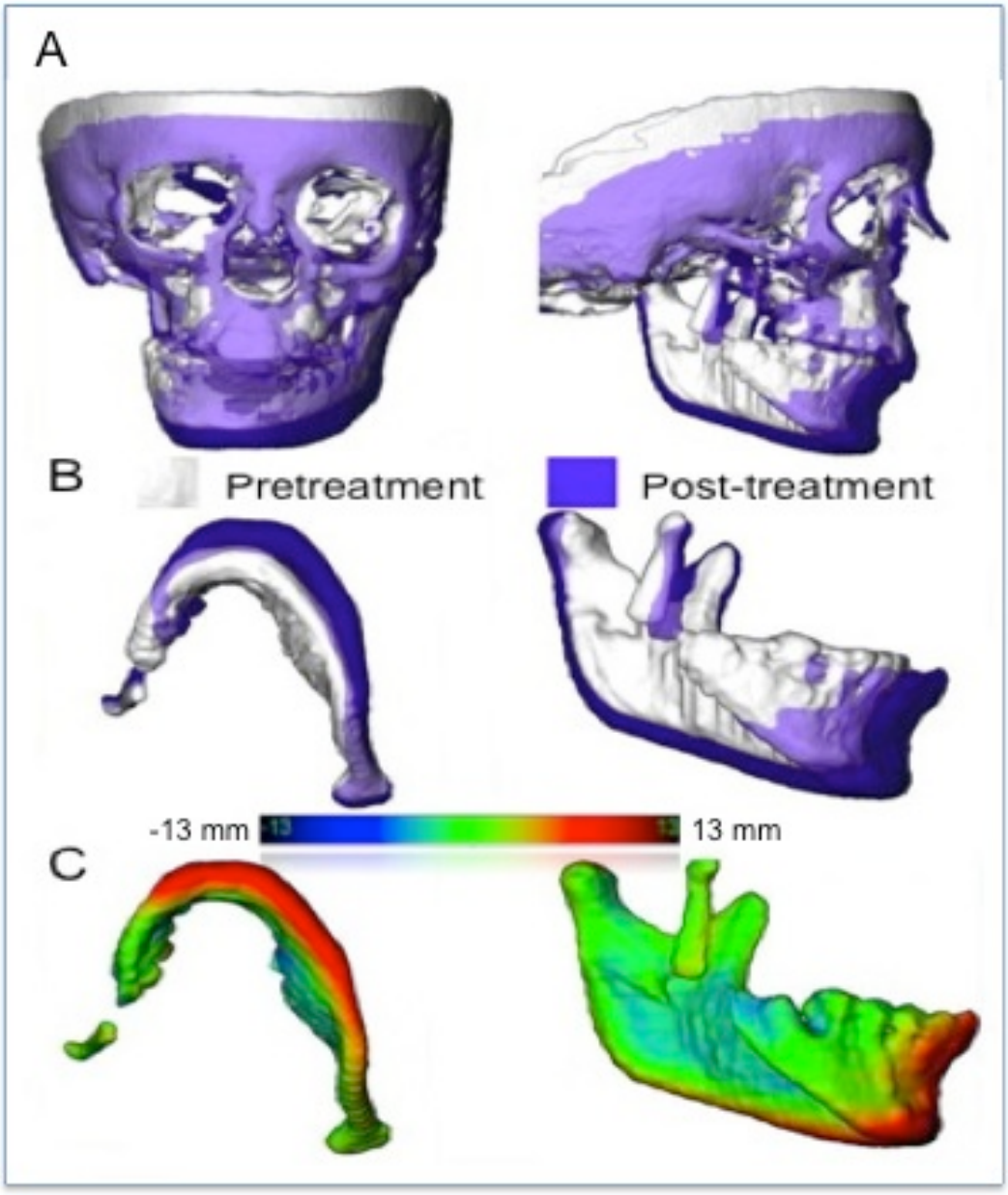

Figure 6.5. Patient with degree 3 of craniofacial microsomia for whom the proposed shape analysis methodology fails to establish correspondence between the left and right anatomic structures because anatomic structures may be partially of completely missing. Note that this patient presented with a missing part of the right mandible corpus and ramus. A. Semi-transparent overlays can still be used to visualize longitudinal differences. B. Close-up of the longitudinal differences with mandibular growth and treatment with a phase I orthopedic functional appliance. D. Quantification of longitudinal follow up using closest point algorithm.

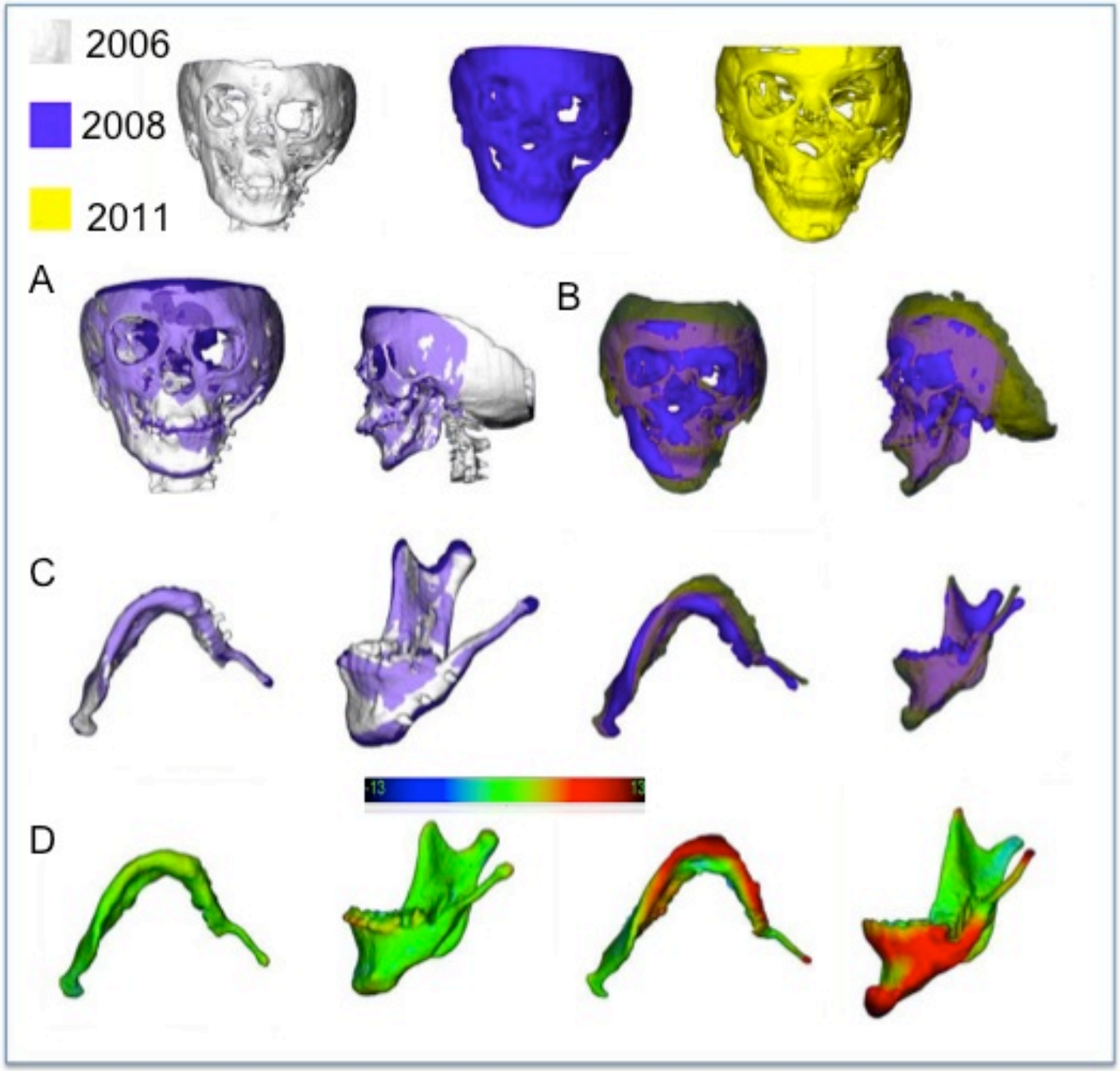

Figure 6.6. Another patient with degree 3 of craniofacial microsomia who presented with a costo-chondral graft on the left side. Note that the costo-chondral graft has a more lateral orientation, characteristic of the rib morphology. For this reason the shape analysis methodology fails to establish correspondence between the left and right anatomic structures. A. Semi-transparent overlays between pre-treatment and 2 year-follow up; B. Semi-transparent overlays between the 2 year-follow up and at splint removal after mandibular advancement surgery; C. Close-up of the longitudinal differences with mandibular growth and treatment. D. Quantification of longitudinal follow up using closest point algorithm.

6.4 Discussion:

The mandibular asymmetry component was assessed in craniofacial microsomia patients for whom quantification of left and right differences have been a very challenging clinical problem up to now. The same methods have potential applications to assess midface asymmetries as well and this methodology has also been applied to evaluate surgical correction and changes in the maxilla and the mandible (de Paula et al. 2013).

This Chapter reports results of an automated method to quantify mandibular asymmetry. The major advantage of the methodology presented in this study is that shape analysis allows measuring morphologic differences regardless of positional differences. Diagnosis and treatment of mandibular asymmetry are particularly challenging because there are two components of left and right differences: true morphological differences and positional/alignment distortions resulting from mandibular displacements relative to the maxilla and cranial base during growth. This positional component of asymmetry can lead to incorrect diagnosis of left and right differences that can be very misleading for clinicians when using mirroring techniques. For example, the mandible can present a vertical roll/tilt on one side as compensatory growth response relative to maxillary excess on one side (positional component of the asymmetry) without a true left and right morphological difference. The methodology used in this study allowed us to measure surface distances between left and right sides of the mandible and identify differences

between corresponding anatomical areas, regardless of positional alignment of those models.

The SPHARM-PDM suite quantified right and left differences for 6 patients in this study. However, shape correspondence (SPHARM) failed to establish right and left correspondence for 5 patients each of whom did not present corresponding right and left structures. Two patients did not have a condyle on the affected side, 2 were grafted, and one was wearing a distraction osteogenesis appliance when the CBCT was taken. If no anatomical correspondence exists, as in instances when there is a complete loss or an external augmentation of a certain structure, the software kept attempting to assign corresponding points between left and right structures, but those points were not present. That led to the software crashing after days of trails without being able to give an output. The issue was not how big the difference between the two halves of the examined asymmetric mandibles was as long as there is not any major distortion in the overall shape of anatomic areas of the mandible.

For these reasons, when all anatomic structures are not present, the left and right sides do not present corresponding structures the SPHARM-PDM suite cannot be indicated for use. A different approach should then be considered in an attempt to help those patients. The use of average mandibular shapes to act as a template for corrective surgeries will be addressed in the next chapter.

Patients with complete missing parts of the mandible or existing grafts are still considered a challenge from the diagnostic point of view. Techniques to quantify the amount of asymmetry in those patients are still lacking.

Closest point, which is used in most commercially available and academic software bundles, is a brute force algorithm that calculates a vertex-to-vertex Euclidean closest point distance(De Momi E et al. 2006, Besl et al. 1992). This method does not map corresponding surfaces based in anatomical geometry, and thus, it usually underestimates rotational and large translational movements. Hence this methods is rendered useless for quantification of asymmetries in extreme cases but could potentially be used for longitudinal follow up. Anatomical shape correspondence data such as the one computed using SPHARM-PDM, that is usually used to overcome the disadvantages of closest point method, also cannot be used in these patients because of the lack of similar anatomical areas in both halves of the mandible (Lack of anatomic correspondence).

The soft tissue component of craniofacial microsomia is considered a determinant factor in the management of the disease (Meyer-Marcotty et al. 2011). However 3D evaluation of the soft tissue faces multiple challenges. The lack of a clinically useful stable reference soft tissue points makes it hard to interpret the results of the computed color-coded maps. The reading might be the result of disease or treatment or might just be the result of movement of tissues due to different muscle tonality. Prediction of soft tissue behavior after orthognathic

surgery is also a challenging task. The spring theory used to predict this behavior does not accurately depict the true nature of the soft tissue in the head and neck (Kaipatur et al. 2009, Koh et al. 2004).

This issue also faces forensic experts when attempting facial reconstruction. Forensic facial reconstruction aims at estimating the facial appearance associated with an unidentified skull specimen. Classically estimation is generally based on tabulated average values of soft tissue thicknesses measured at a sparse set of landmarks on the skull. Traditional 'plastic' methods apply modeling clay or plasticine on a cast of the skull, approximating the estimated tissue depths at the landmarks and interpolating in between (Tyrell et al. 1997). Currently computerized techniques mimic this landmark interpolation procedure. Those techniques use a flexible statistical model of a dense set of facial surface points, combined with an associated sparse set of skull-based landmarks (Claes et al. 2006). Furthermore, estimated properties of the skull specimen (BMI, age and gender, e.g.) are incorporated as conditions on the reconstruction by removing property-related shape variation from the statistical model. Modeling in these techniques is combining population dependents variation and correlation of skin surface shape and tissue depth calculated from a facial database (Claes et al. 2006).

The diagnostic information of the color-coded distance maps of the areas of left and right differences for each patient allowed the surgeons to quantify the amount by which each surgical segment needed to be moved or augmented to

achieve a reasonably symmetric outcome. The use of vector maps further elucidated the diagnosis of areas of bone deficiency or formation. Those vector maps added directionality to the amount of differences quantified by the surface distance color-coded maps. The vector maps can also be potentially useful for planning distraction osteogenesis.

6.5 Conclusion:

3D image analysis quantifies positional and shape components in the diagnosis and treatment planning of mandibular asymmetry for patients with degree 1 or 2 of craniofacial microsomia. Correspondent based points fail to quantify complex dysmorphologies in patients with a missing ramus or grafts. This novel methodology may better guide clinicians' choice of therapeutic approaches in functional orthopedics, distraction osteogenesis and/or complex surgeries.

Chapter 7

The use of a custom made atlas as a template for corrective surgeries of asymmetric patients: Proof of principle and a multi-center end user survey

7.1 Introduction:

Computational anatomy (CA), the mathematical study of anatomy, is rapidly emerging as a discipline focused on the precise study of the biological variability of human anatomy. Although the study of structural variability of such manifolds can certainly be traced back to the beginnings of modern science, in his influential treatise “On Growth and Form”, Thompson (1917) had the clearest vision of what lay ahead, namely:

“In a very large part of morphology, our essential task lies in the comparison of related forms rather than in the precise definition of each; and the deformation of a complicated figure may be a phenomenon easy of comprehension, though the figure itself may have to be left unanalyzed and undefined. This process of comparison, of recognizing in one form a definite permutation or deformation of another, apart altogether from a precise and adequate understanding of the original “type” or standard of comparison, lies within the immediate province of mathematics and finds its solution in the elementary use of a certain method of the mathematician. This method is the Method of Coordinates, on which is based the Theory of Transformations.”

Computational anatomy has three principal aspects (Grenander and Miller 1998, Miller et al. 1997, 2002, Thompson and Toga 2002): (i) automated construction of anatomical manifolds of points, curves, surfaces, and subvolumes; (ii) comparison of these manifolds; and (iii) the statistical codification of the variability of anatomical shape and structure via probability laws allowing for the inference of structural disease and functional responses on the geometries.

Towards the construction of anatomical manifolds, the general area of the mathematical codification of biological and anatomical structure has expanded rapidly over the past several decades. Atlases supporting neuromorphometric analyses are becoming available with many anatomical samples. Deformable and active models are being used for generating one-dimensional manifold curves in two to three dimensions (Bartesaghi and Sapiro 2001, Cachia et al. 2003, Feldmar et al. 1997, Khaneja et al. 1998, Lorigo et al. 2001, Montagnat et al. 2001, Rettmann et al. 2002, Thirion and Goudon 1995, 1996, Vaillant and Davatzikos 1997).

Towards comparison of anatomical manifolds, because of the fundamental structural variability of biological shape there has been great emphasis by groups on the study of anatomical shape via vector and metric comparison. The earliest vector mapping of biological coordinates via landmarks and dense imagery was pioneered in the early 1980s and continues by Andresen et al. (2000), Bookstein (1978, 1991, 1996a,b, 1997), Avants and Gee (2004), Bajcsy and Kovacic (1989), Bajcsy et al. (1983), Dann et al. (1989), Gee (1999), Gee and Bajcsy (1999), and Gee and Haynor

(1999). Comparison via vector maps based on dense imagery is being carried on by many of the aforementioned groups.

Concerning inference on statistical representations of shape, studies in computational anatomy of growth, atrophy, and disease have exploded since the advent of automated methods for manifold construction. Applications to growth and statistical atlas building are evidenced by Andresen et al. (2000), Joshi et al. (2004), Paus et al. (1999), Sowell et al. (2003), Thompson et al. (2000), Toga et al. (1996), and Vaillant et al. (2004).

In facial asymmetry diagnosis two aspects have been considered a potential source of bias, the choice of a " healthy side" to use as a reference and the isolation of the shape and location component. Stability of orthognathic surgery depends on the surgical technique used, on the postoperative location of the condyles and on the torque applied on the rami in mandibular corrective surgeries. This pilot study is intended to explore an algorithm that would calculate a mean shape from asymmetric mandibles and their mirror, thus utilizing data from both sides of the mandible. Both shape and location inputs of both hemimandibles are utilized in the calculation of the resultant average. This individual computed mandible is to be used as a template to guide plan virtual orthognathic surgeries.

The purpose of this study was to evaluate the utility of a patient-specific atlas as a template for corrective surgeries for patients suffering from mandibular

asymmetry. This template will enhance the predictability and reproducibility of the surgical outcomes of those corrective surgeries.

7.2 Material and methods:

Data:

Twenty patients with history of favorable clinical outcome of the correction of their mandibular asymmetry were chosen for this pilot study. Favorable outcome was decided based on post-operative clinical exam, post operative dental casts, and clinical photographs. This project was approved by the University of North Carolina Ethics committee for research on human subjects (Study #: 03-1647). Existing CBCT volumes for those patients were used under the terms of the ethics approval. Those CBCT were taken before and 6 weeks after corrective surgery of each patient using NewTom 3G cone beam CT (AFP Imaging, Elmsford, NY). The 12" field of view producing 0.5 mm isotropic voxel sizes was used for acquiring the image volume. These scans are part of a bigger sample of consecutive prospectively collected images, collected in the grant "Improving Treatment Outcomes for Patients with Facial Deformity using 3D Imaging".

Segmentation:

Segmentation was performed with ITK-SNAP (Yushkevich PA et al. 2006) as in all previous chapters.

Mirroring and rigid registration on the cranial base:

As described in previous chapters, registration was accomplished via the voxel-based registration software IMAGINE (National Institutes of Health, Bethesda, MD; Open-source, http://www.ia.unc.edu/dev/download/imagine/index.htm).

Atlas formation:

Surface models for both the mandible and its registered mirror were used to compute an atlas using deformable fluid registration. To facilitate deformable registration, a surface-wise, geometry sensitive smoothing was performed to remove noisy artifacts from the data typically visible around the dental line from metallic artifacts (Paniagua et al. 2010). We used an iterative mean-curvature evolution algorithm (Meyer et al. 2000) that smoothes the surface mesh using a relaxation operator. The total smoothing in the data was less than half a voxel on average, thus representing the mandibular surface accurately. The resulting meshes are scan-converted into binary volumes and then deformably registered using a greedy fluid flow algorithm (Joshi et al. 2004).

AtlasWerks, used for patient-specific atlas building in this project, is an open-source (BSD license) software package for medical image atlas generation. AtlasWerks atlas formation is based on greedy fluid registration in a diffeomorphic deformation setting (Joshi et al. 2004). Most registration algorithms make the assumption that similar structures are present in both images; therefore it is desirable that the deformation field be smooth and invertible (so that every point in

one image has a corresponding point in the other). Such smooth, invertible transformations are called diffeomorphisms. This well-known viscous fluid model accommodates large-distance, nonlinear deformations of small subregions of the target image. Fig (7.1)

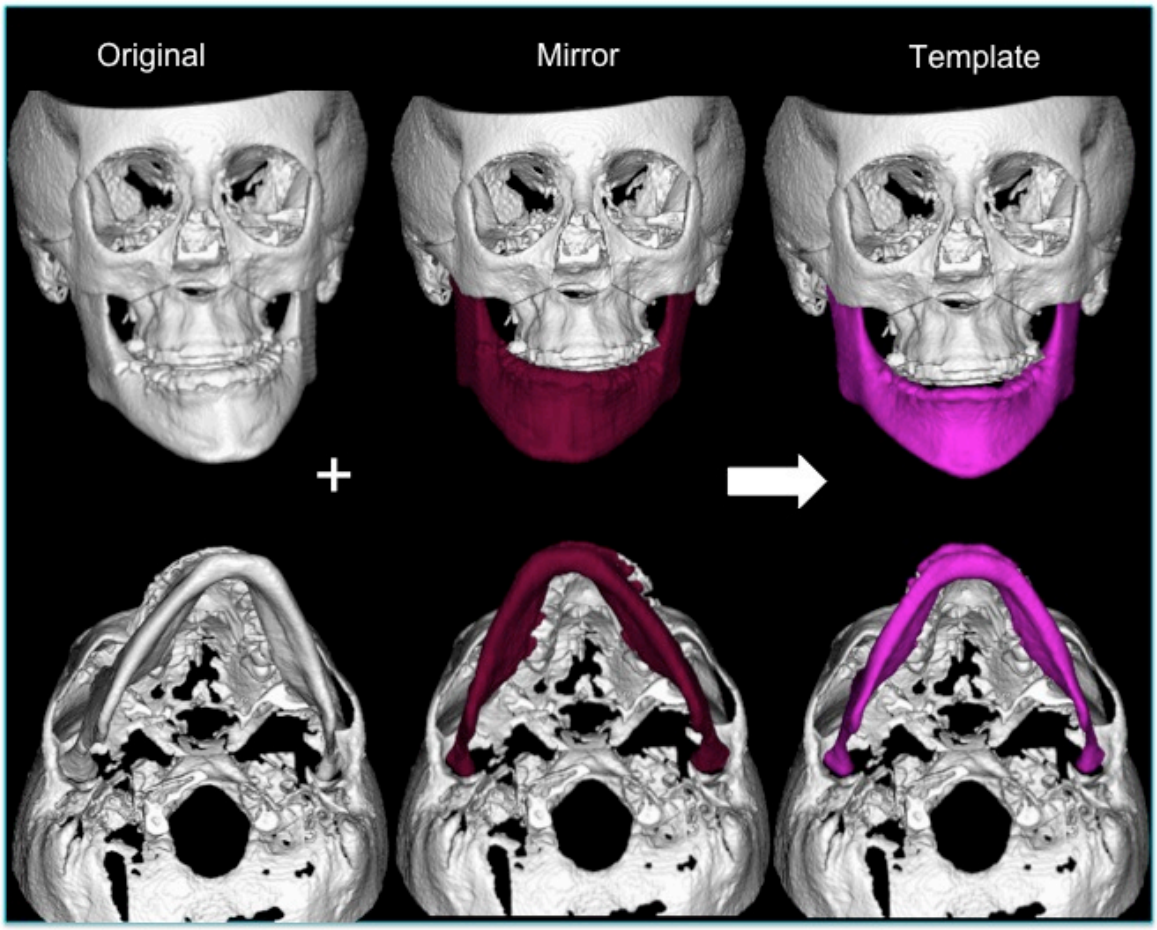

Figure 7.1. Atlas formation: The original mandible (white) and its registered mirror (maroon) are both used to compute an atlas (pink) that will serve subsequently as a template for surgical simulation

Surgical simulation:

Corrective surgery was simulated by the author, using the atlas computed as a template, using 3DSlicer. 3DSlicer is an open-source free software (http://www.slicer.org/) that allows cutting, panning, and rotation of displayed models. The ROI module was used to simulate surgical cuts via clip boxes. The maxilla was cut through a Le Fort I level, and then it was moved to align the occlusal plane and get an acceptable profile for each patient. Autorotation of the mandible was then simulated if needed. The mandibular BSSO surgical cuts were simulated simultaneously on both the mandible and the template. The resultant surgical segments were then registered using surface registration to the corresponding anatomical region at the template. The mandibular segments were merged at the final position using the merge model functionality of 3DSlicer. Fig (7.2) The author did not have any supplemental records for the patients to help guide the virtual surgey.

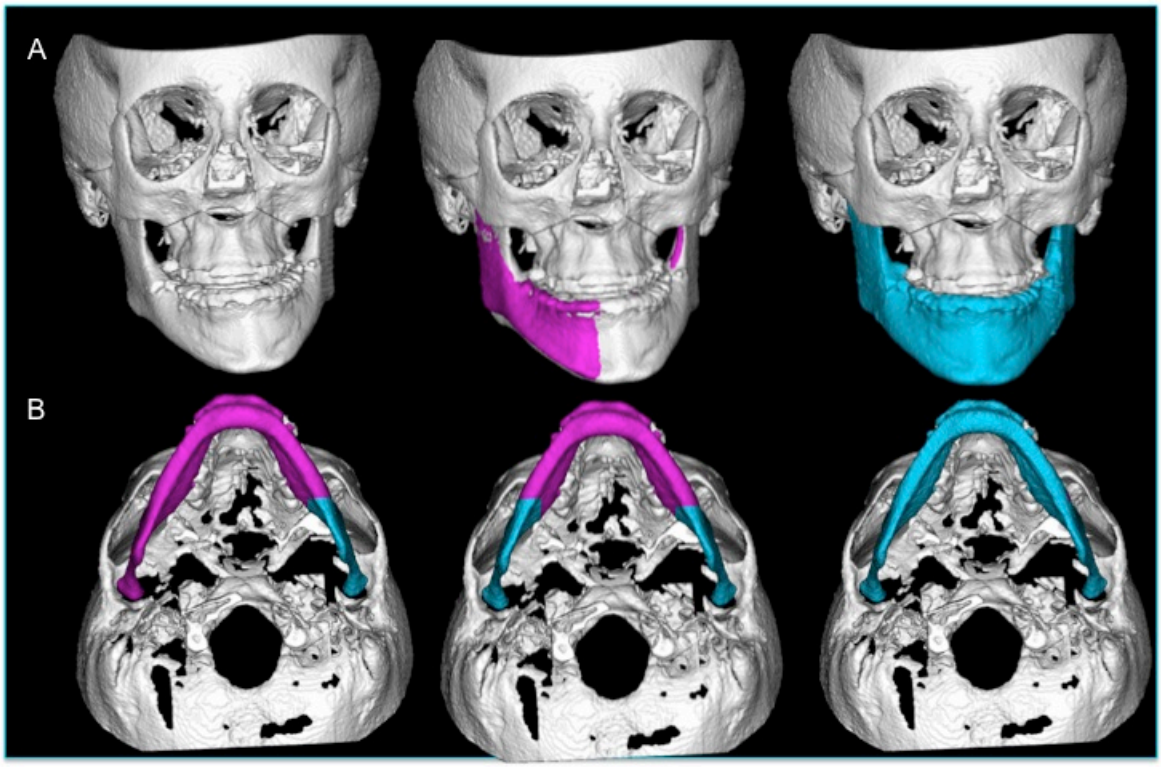

Figure 7.2. Surgical simulation: The original mandible (white) is overlaid over the computed template (pink) to guide moving the surgical segments in 3DSlicer. As shown in row (B) the surgical segments were moved to match the position of the template leading to the virtual outcome mandible (blue).

Initial validation of virtual surgeries:

For the first 3 patients, the differences between the virtual simulated outcome and the actual surgical outcome were computed using UNC SPHARM-PDM toolbox (Styner et al. 2006) to quantitatively measure the difference between the outcome of the template simulation and the actual desirable surgical outcome. Rigid Procrustes alignment procedure computes an optimal linear, geometric transformation ϕ (n) that best maps the shape changes between the affected hemimandible and the mirror of the opposite healthy side based on the established correspondence (Styner et al. 2003, 2006). The 6 degrees of freedom (DOF) of the

differences between the virtual and the actual outcome mandibles were calculated using rigid Procrustes alignment. Composite overlays were used for visual assessment of results. Fig (7.3)

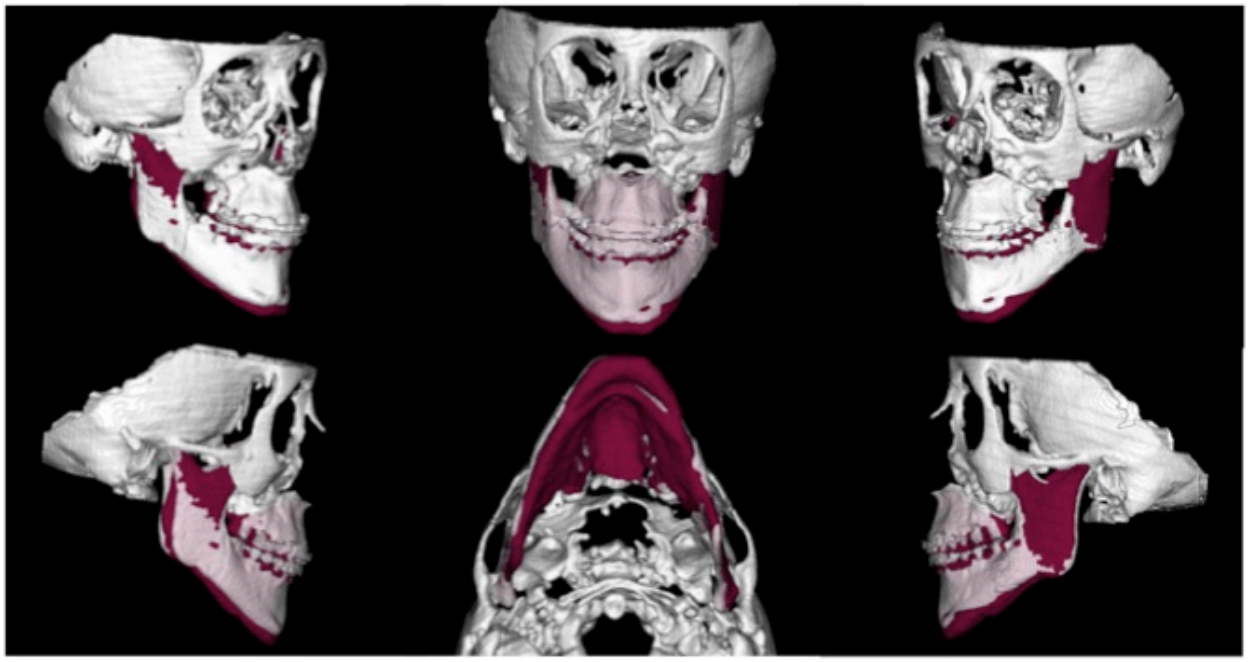

Figure 7.3. Composite overlays: The asymmetry correction differences between the actual post surgery mandible (white) and the virtual outcome mandible (maroon) are minimal as shown in this overlay. Comparisons are done at the condyle, ramus, and chin levels.

Multi-centre observation sessions:

After approval by the Kings College London (KCL Ref: **BDM/12/13-28.**) and the University of North Carolina Ethics committee for research on human subjects (UNC Ref: **12-1685**), a multi-centre online survey using "Qualtrics" was conducted to gain clinical feedback of 20 surgeons/orthodontists comparing both treatment planning and treatment outcomes.

Sample Size calculation: The power calculation was obtained using the one sample mean power analysis program in SAS (version 9.2). The proposed project aimed to determine the extent to which knowledgeable observers rate simulated surgical outcomes predicted for each of 20 cases as equal to or better than the actual outcome observed for each case. In the absence of any existing data, we hypothesize that observers would rate the simulated result as equivalent to or better than the actual result in 50% of the 20 cases. We tested the null hypothesis that the mean percentage of times each of 20 observers rate the simulated outcome as equal to or better than the observed outcome for 20 cases is 0.5, using the assumption that the standard deviation of the 20 observer scores is 0.10. Under these conditions, we will have a power of 0.84 to reject the null hypothesis, if the observed mean value differs from 0.5 by 0.07.

Observers' recruitment: Practicing university clinicians and residents in Oral and Maxillofacial surgey and Orthodontic departments from the University of Jordan, University of Michigan, University of North Carolina at Chapel Hill, and King's College London were invited by e-mail to participate in the survey. Potential participants were invited to the survey by email and were sent the link for the survey upon their agreement to participate. Clinicians responding to the e-mail invitation were asked to compare images of skeletal surface models of actual outcomes to models of simulated outcomes with reference to preoperative models of each patient. The two scenarios were randomized without any indication that they belong to the same patient. In essence that gave the study 40 apparent cases to be examined. The

survey was designed with the help of a statistician and a psychologist. The psychologist gave feedback toward the wording of the questions as well as the appearance of the preoperative and postoperative models.

Please refer to description of patients included in the survey in the appendices.

The following is an excerpt showing the use of the same clinical case in both real and surgical modalities, with the survey questions shown.

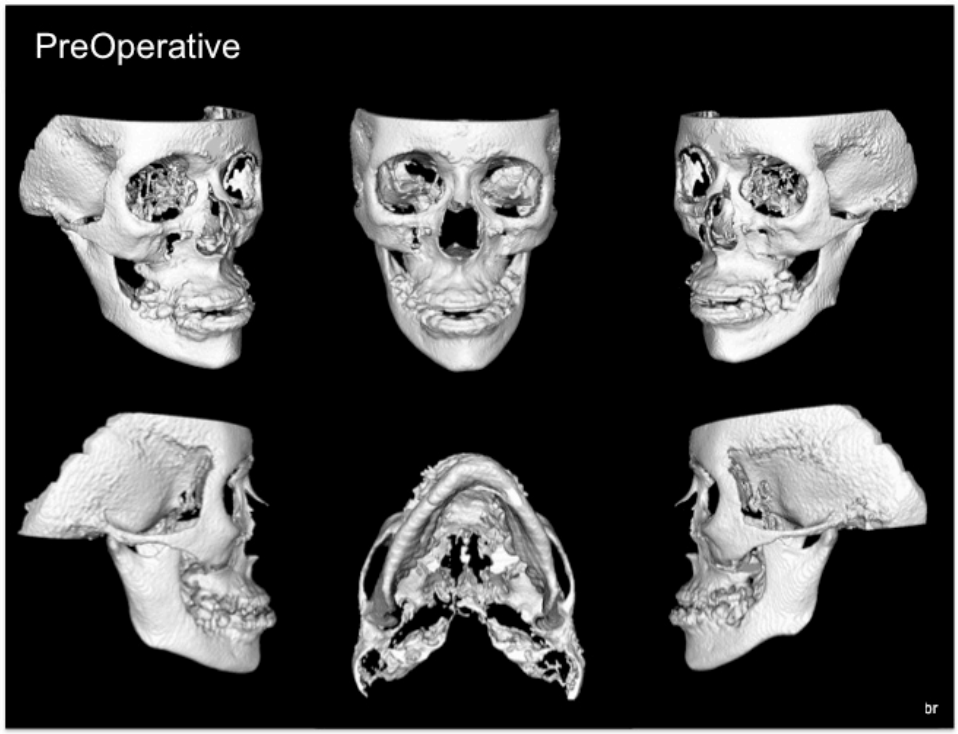
PreOperative
br

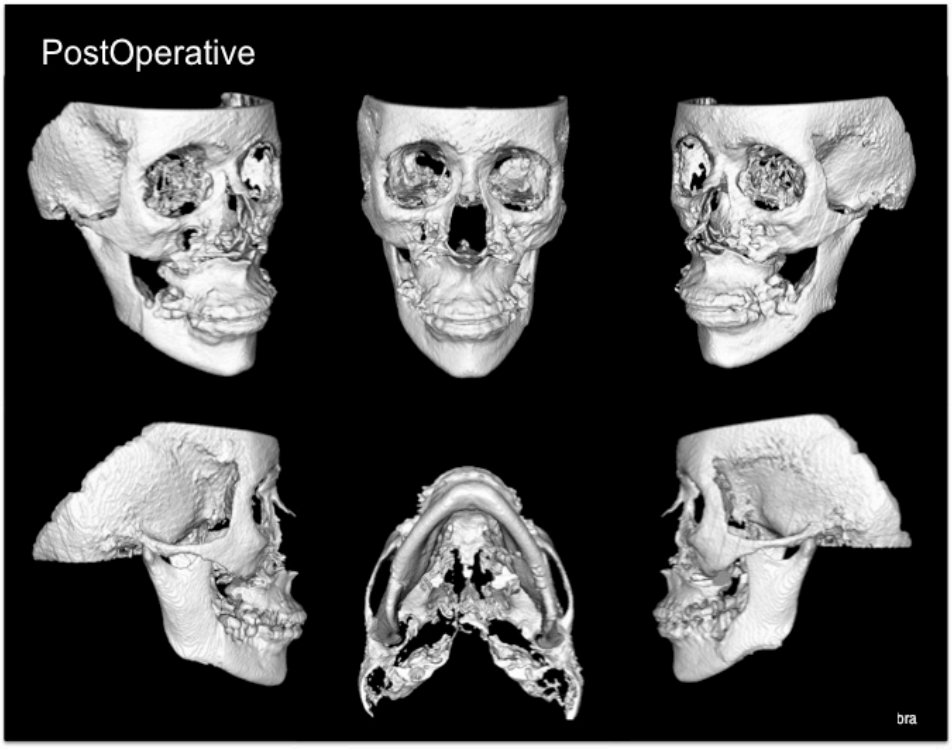
PostOperative
bra

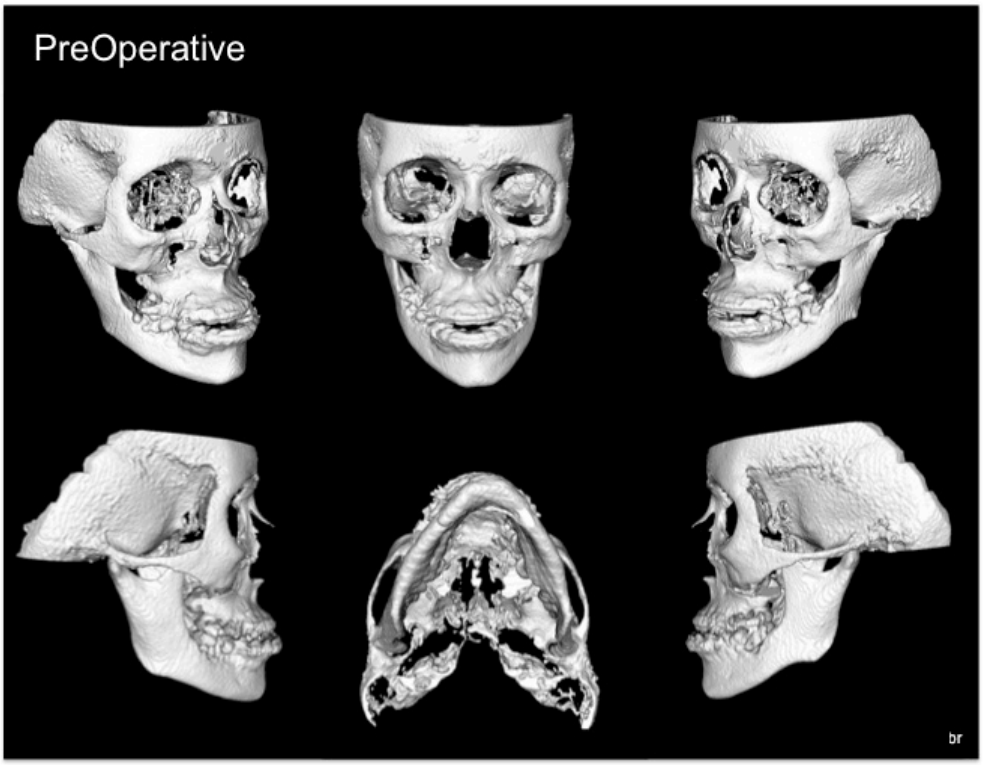
PreOperative
br

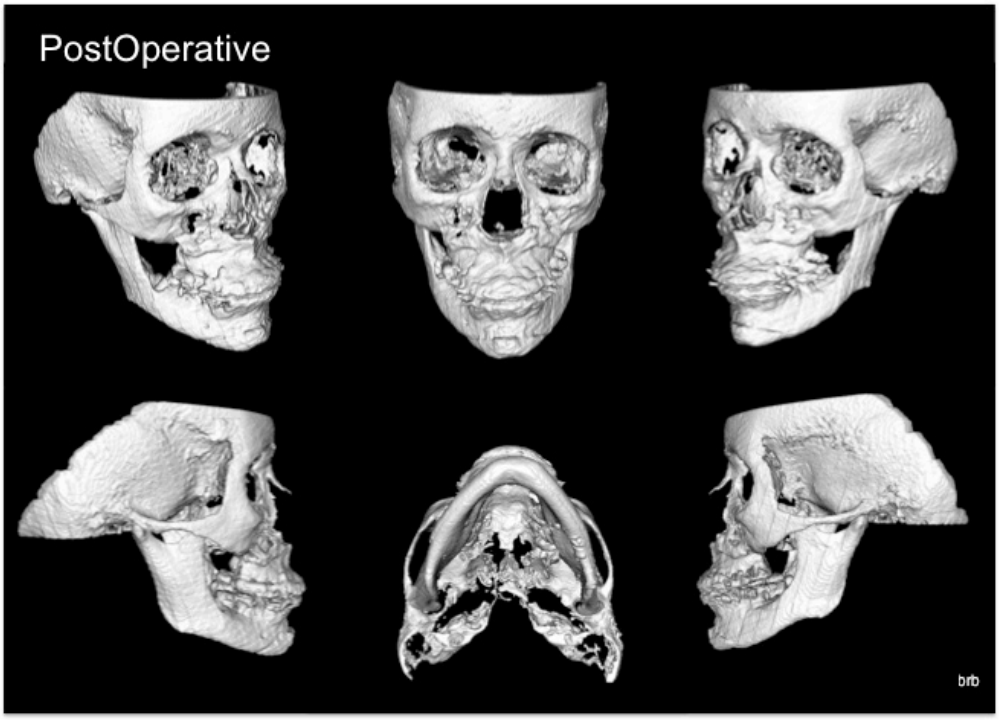
PostOperative
brb

Questions:

•The chin position in these Post Operative models is:

A. In the Midline

B. slightly deviated

C. Markedly deviated

•Regarding the vertical length of the Rami, do you think they are:

A. The same length

B. Slightly different

C. Markedly different

•Looking at the SMV view, the mediolateral position of the body of the mandible on both sides is:

A. Identical

B. Slightly different

C. Markedly different

•The overall Post Operative result is:

A. Very Good

B. Acceptable

C. Poor

Statistical analysis:

Two-sided and one-sided paired T test were used to test the following research questions:

1) Are the results of the computer assissted simulation equal to conventional planning as rated by clinicians who participated in the survey?

2) Are the results of the computer assissted simulation better to conventional planning as rated by clinicians who participated in the survey?

To test for the effect of confounding factors such as the difficulty of the case as well as the individual observer on the results a mixed effect model was used.

The levels of significance were set at 0.05 for P values.

7.3 Results:

Initial validation of virtual surgeries:

The detected differences between the virtual simulated outcome and the actual surgical outcome in the 3 patients from the 20 patient cohort, as characterized in 6 degrees of freedom, were smaller than 2 mm of translation and 5 degrees of rotation. This indicates that the location of the synthesized template is similar to the desired clinical outcome. The condyles in the virtual postoperative mandible were centered in the glenoid fossae and the rami have reasonable torque.

These signs reflect the feasibility of the suggested surgical movements and the long-term stability of the surgical outcome.

Multi-centre observation sessions:

23 clinicians participated in the multi-center observation sessions. More clinicians rated the simulated outcome to be “Good”, whereas the actual surgical outcomes were rated as “fair” and “poor”. This was true for regional appraisal for the chin, Rami, and body of the mandible as well as the overall assessment of the outcome of surgeries (Fig 7.4 through 7.7).

	1(Good)	2(Fair)	3(Poor)
Simulated	270	162	28
Actual	186	197	77

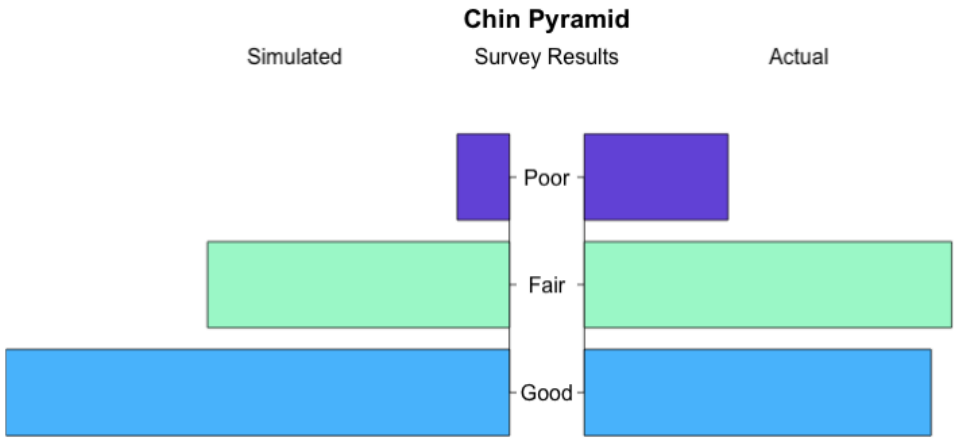

Figure 7.4 shows the distribution of clinicians’ responses for the chin results

	1(Good)	2(Fair)	3(Poor)
Simulated	191	199	69
Actual	142	220	98

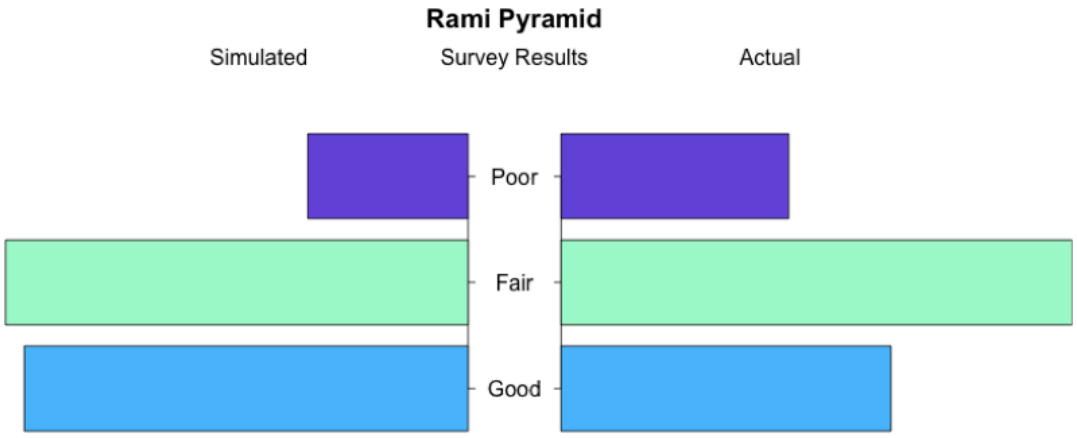

Figure 7.5 shows the distribution of clinicians' responses for the Rami results

	1(Good)	2(Fair)	3(Poor)
Simulated	184	208	68
Actual	126	249	85

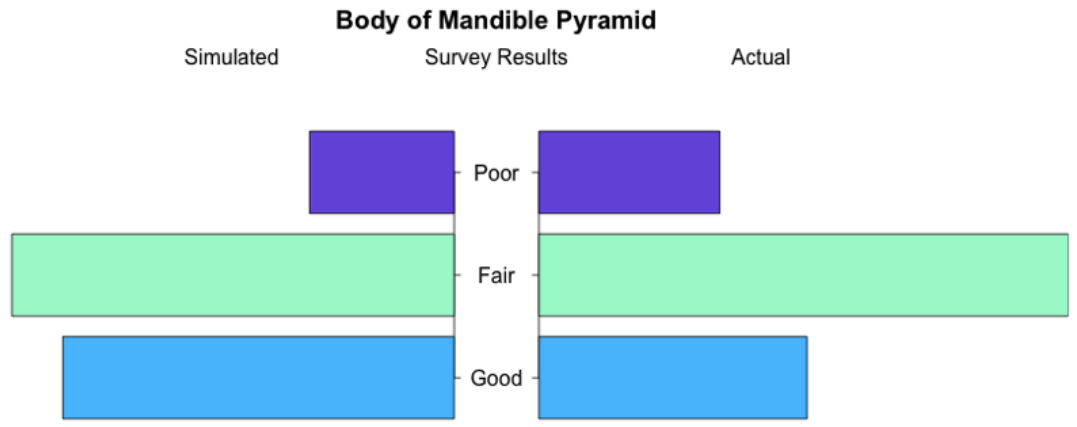

Figure 7.6 shows the distribution of clinicians' responses for the body of the mandible results

	1(Good)	2(Fair)	3(Poor)
Simulated	287	153	19
Actual	206	206	46

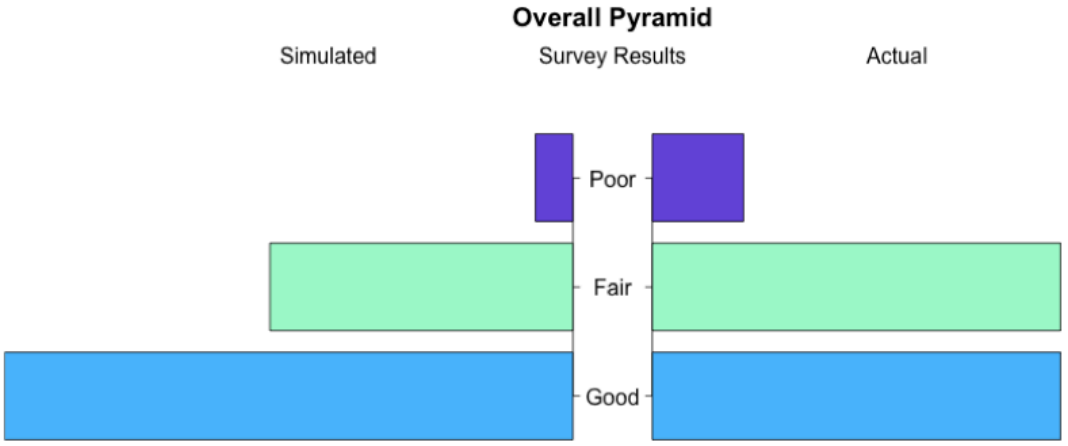

Figure 7.7 shows the distribution of clinicians' responses for the overall appraisal of the surgical outcome

Paired T test showed that those differences observed between the simulated outcome and the actual outcome are statistically significant for all areas of the mandible (except the body of the mandible in the two-sided paired T test) and for the overall appraisal as well (Table 7.1).

Paired T-test P-values:

	Two-Sided	One-Sided
Chin	0.0008643	0.0004322
Rami	0.03209	0.01605
Body of Mandible	0.09384	0.04692
Overall	0.004705	0.002353

Table 7.1 shows paired T test P values for differences observed between the simulated outcome and the actual outcome

The one sided paired T test results support the assertion that the simulated outcome based on the proposed template is better than the actual outcome planned by conventional methods as decided by our 23 observers.

Furthermore, we re-interrogated the dataset considering whether the degree of surgical challenge influenced the results using mixed effect model. The general linear mixed model is used for the regression analysis of correlated data. The correlation arises because subjects may contribute multiple responses to the data set. The model assumes a continuous outcome variable that is linearly related to a set of explanatory variables; it expands on the ordinary linear regression model by allowing one to incorporate lack of independence between observations and to model more than one error term (Cnaan et al. 1997).

The model indicated that the gains of computer-assisted simulation tend to be greater for *difficult* cases. The gain was mostly seen in the correction of the body of the mandible then the chin then the Ramus correction.

The model also included observers as random variables and showed that some observers are more lenient regardless of the location of the mandible being test or the planning approach being used. Further analysis of the 5 most strict and 5 most lenient observers did not show any pattern as the two groups had orthodontist and surgeons, senior and junior clinicians, as well as observers from the 4 institutions included in this study.

7.4 Discussion:

Treatment planning and assessment of the surgical correction of asymmetrical deformities is limited by reliance on 2D radiographs in the current clinical setting. The 2D radiographs conventionally used in orthodontic practice are particularly problematic when rotational or asymmetrical correction is required since surgical jaw displacements are inherently 3-dimensional. The use of cone-beam computed tomography (CBCT) or computer tomography (CT) provides the 3D imaging data necessary to generate precise knowledge of the location and the magnitude of facial asymmetry features, which are essential for the diagnosis of facial deformities and for the planning of corrective procedures.

The current available computer aided surgical simulation software for surgical simulation the operator freehandedly moves mandibular surgical segments for

asymmetry corrections. Those movement decisions are subjective and carry the risk of under-treating the existing asymmetry in one of the planes of space or unbalancing position and shape corrections of the existing problem. The introduction of a template in the pipeline used in this project is intended to guide surgeons in the correction of the location differences between the left and right side of the mandible in all 3 planes of space.

Atlas construction has been conventionally used for group studies where deviation in size or shape in a particular anatomical structure from the "average" of the population indicates disease (Miller et al. 2001,2004; Beg et al. 2005). The use of the patient's own anatomy for the computation of the custom-made template accommodates the large gradient by which mandibular asymmetry presents clinically. It ensures that the outcome virtual template has the basic features (condylar position, relative size,…etc) that will still keep the harmony between the mandible and the rest of the maxillofacial area. This approach will also help eliminate the need to decide on a "healthy" side for the mandible to mirror and use as a template especially that the concept of a "healthy" side in an asymmetric mandible is never strictly true due to the physiological compensation processes that take place during growth.

7.5 Conclusions:

This is a novel use of patient-specific atlas construction that will potentially improve the surgical outcomes of corrective surgeries and therefore the quality of life of patients with craniofacial anomalies presented as facial asymmetry. The data of this project demonstrated that the outcome of virtual surgeries planned based on this custom made template is superior to the actual surgical outcome as planned by current conventional methods. The results also suggest that the use of this template is even more helpful in more severe asymmetry cases.

As the virtual surgeries were planned based on computed template only, following this protocol might help reduce the chair side time needed to collect conventional diagnostic aid for treatment planning and will tremendously augment those records.

As intermediated and final surgical wafers can be designed and printed based on our virtual surgeries and then used in the theatre. The actual surgeries done based on planning based upon the custom-made atlas will hopefully eliminate subjectivity from surgical plans and increase the reproducibility of treatment planning of surgical correction of facial asymmetries. This approach has the potential to optimize the outcome of craniofacial corrective surgeries for asymmetric patients.

A double-blinded clinical trial is needed to establish the clinical merit of the suggested custom-made template. The trial with 2 arms, a control group where the surgeon would use intermediate and final surgical wafers designed based on a

conventional mock surgery and an intervention group where the surgeon uses surgical wafers designed based on the virtual surgeries based on the designed custom made template. Technology for occlusion detection and finer virtual surgical cuts is still needed to refine the virtual surgeries.

Chapter 8

Conclusions

8.1 conclusions

1. The first project investigated the difference between the currently used mirroring technique using a midsagittal plan and a new suggested technique using mirroring on an arbitrary plane. As proved by the results of chapter 2, both mirroring using a midsagittal plane and using an arbitrary plane followed by registration on the cranial base provided similar quantification of mandibular asymmetry for most areas, however mirroring using an arbitrary plane followed by registration on the cranial base proved to be more consistent.

2. SPHARM-PDM was adopted, modified, and tested for its clinical merit to diagnose, localize, and quantify existing mandibular asymmetries. We started with testing for the accuracy of this technology in detecting the quantity and direction of small-simulated asymmetries, then we moved on to testing in a clinical cohort with more severe asymmetries and more complex presentation with asymmetries in all planes. We then decided to push the envelope and test the algorithm for a Craniofacial Microsomia cohort. Based on this series of experiments, we can conclude that SPHARM-PDM can accurately diagnose, localize, and quantify existing mandibular asymmetries in both simulated and real clinical setting unless there is major shape discrepancy between the tow halves of the mandible such as in cases where the

whole condyle and big part of the ramus is missing or in patient with distraction osteogenesis hardware or big grafts.

3. A custom made template was designed and validated to be used as a guide to treatment plan corrective surgeries. As per the feedback of 23 clinicians who participated in our multi center end-user observation sessions, the simulated outcome based on the proposed template is better than the actual outcome planned by conventional methods. The results also proved that the gain of computer-assisted simulation tend to be greater for *difficult* cases.

Chapter 9

Future work

9.1 Future work:

1. There is still a lack of solutions to quantify and localize asymmetry in mandible with large missing areas or big grafts.

2. A double-blinded clinical trial is needed to establish the clinical merit of the suggested custom-made template. The trial with 2 arms, a control group where the surgeon would use intermediate and final surgical wafers designed based on a conventional mock surgery and an intervention group where the surgeon uses surgical wafers designed based on the virtual surgeries based on the designed custom made template. Technology for occlusion detection and finer virtual surgical cuts is still needed to refine the virtual surgeries.

3. Trials to compute such custom-made templates for the more complex shapes of the maxilla and other midface structure are needed to help plan surgeries of midface asymmtries.

4. Trials to compute average gender-specific, age-specific templates to guide correction of class II, and class III skeletal relationships.

5. An attempt to simplify the suggested diagnostic process by grouping all the included algorithms in a universal user-friendly graphic interface.

Chapter 10

Bibliography

Ackerman JL, Proffit WR, Sarver DM, Ackerman MB, Kean MR. Pitch, roll, and yaw: describing the spatial orientation of dentofacial traits. Am J Orthod Dentofacial Orthop. 2007 Mar;131(3):305-10.

Ackerman JL, Proffit WR. A not-so-tender trap. Am J Orthod Dentofacial Orthop. 2009 Nov;136(5):619-20

Adams GR. Physical attractiveness, personality, and social reactions to peer pressure. Journal of Psychology 1977;96(2d Half):287-96.

Alhadidi A, Cevidanes LHS, Mol A, Ludlow J, Styner MA. 3D Analysis of Facial Asymmetry based on Midsaggital Plane Computation. J Dent Res. 2009;88(Spec Issue A):311.

AlHadidi A, Cevidanes L, Mol A, Ludlow J, Styner M. Comparison of two methods for quantitative assessment of mandibular asymmetry using cone beam computed tomography image volumes. Dentomaxillofac Radiol. 2011 Sep;40(6):351-7. doi: 10.1259/dmfr/13993523.

Alhadidi A, Cevidanes LH, Paniagua B, Cook R, Festy F, Tyndall D. 3D quantification of mandibular asymmetry using the SPHARM-PDM tool box. Int J Comput Assist Radiol Surg. 2012 Mar;7(2):265-71. doi: 10.1007/s11548-011-0665-2. Epub 2011 Nov 17.

American Academy of Oral and Maxillofacial Radiology. Clinical recommendations regarding use of cone beam computed tomography in orthodontic treatment. Position statement by the American Academy of Oral and Maxillofacial Radiology. Oral Surg Oral Med Oral Pathol Oral Radiol. 2013 Aug; 116(2):238-57. doi:10.1016/j.oooo.2013.06.002.

American Dental Association Council on Scientific Affairs. The use of cone-beam computed tomography in dentistry: an advisory statement from the American Dental Association Council on Scientific Affairs. J Am Dent Assoc. 2012 Aug;143(8):899-902.

Andresen, P.R., Bookstein, F.L., Conradsen, K., Ersbll, B.K., Marsh, J.L., Kreiborg, S. Surface-bounded growth modeling applied to human mandibles. IEEE Trans. Med. Imaging. 2000; 19, 1053 – 1063.

Angelopoulos C. Cone beam tomographic imaging anatomy of the maxillofacial region. Dent Clin North Am. 2008 Oct;52(4):731-52, vi. doi: 10.1016/j.cden.2008.07.002.

Avants, Brian, and James C. Gee. "Geodesic estimation for large deformation anatomical shape averaging and interpolation." Neuroimage 2004; 23:S139-S150.

Bailey L', Cevidanes LH, Proffit WR. Stability and predictability of orthognathic surgery.Am J Orthod Dentofacial Orthop. 2004 Sep;126(3):273-7.

Bajcsy, R., Lieberson, R., Reivich, M. A computerized system for the elastic matching of deformed radiographic images to idealized atlas images. J. Comp. Assist. Tomogr. 1983; 7, 618–625.

Bajcsy, R., Kovacic, S. Multiresolution elastic matching, computer vision. Graph. Image Process. 1989; 46, 1–21.

Barton DJ, Clark SJ, Eleazer PD, Scheetz JP, Farman AG. Tuned-aperture computed tomography versus parallax analog and digital radiographic images in detecting second mesiobuccal canals in maxillary first molars. Oral Surg Oral Med Oral Pathol Oral Radiol Endod. 2003 Aug;96(2):223-8.

Bartesaghi, A., Sapiro, G. A system for the generation of curves on 3d brain images. Hum. Brain Mapp. 2001; 14, 1–15.

Beg MF, Miller MI, Trouvé A., Younes L. Computing large deformation metric mappings via geodesic flows of diffeomorphisms. International Journal of Computer Vision 2005;61(2):139-57.

BEIR, VII. "Phase 2.(2006) Health Risks from Exposure to Low Levels of Ionizing Radiation: BEIR VII Phase 2." 270.

Berry G. Note on congenital defect (coloboma) of the lower lid. Lond Ophthalmol Hosp Rep 1989;12:255.

Berscheid, E., & Walster, E. Physical attractiveness. In L. Berkowitz (Ed.). Advances in experimental social psychology 1974;7: 156–213.

Besl PJ, McKay ND. A Method for Registration of 3-D Shapes. IEEE Transactions on Pattern Analysis and Machine Intelligence 1992; 14: 239-256.

Bhatia S, Robison LL, Oberlin O, et al.: Breast cancer and other second neoplasms after childhood Hodgkin's disease. N Engl J Med 1996; 334:745-751.

Boice JD Jr, Land CE, Shore RE, Norman JE, Tokunaga M: Risk of breast cancer following low-dose exposure. Radiology 13 1979; 1:589-597.

Boice JD, Hutchison GB: Leukemia in women following radiotherapy for cervical cancer: Ten-year follow-up of an international study. J Natl Cancer Inst 1980; 65:115-129.

Boice JD Jr, Engholm G, Kleinman RA, et al.: Radiation dose and second cancer risk in patients treated for cancer of the cervix. Radiat Res 1988; 116:3-55.

Bookstein, F.L. Morphometric tools for landmark data: geometry and biology. Cambridge: Cambridge University Press. 1991

Bookstein, F.L. Biometrics, biomathematics and the morphometric synthesis. Bull. Math. Biol. 1996;58:313–365.

Bookstein, F.L. Landmark methods for forms without landmarks: morphometrics of group differences in outline shape. Med. Image Anal. 1997a; 1:225–243.

Bookstein, F.L. Shape and the information in medical images: a decade of the morphometric synthesis. Comput. Vis. Image Und. 1997b; 66, 97–118.

Bookstein, F.L., Chernoff, B., Elder, R., Humphries, J., Smith, G. & Strauss, R. Morphometrics in evolutionary biology. Philadelphia: Academy of Natural Sciences (Special Publication, No. 15). 1985

Bookstein, Fred L., "Landmark methods for forms without landmarks: localizing group differences in outline shape," Mathematical Methods in Biomedical Image Analysis, 1996., Proceedings of the Workshop on , 1996; 21-22: 279-289. doi: 10.1109/MMBIA.1996.534080

Bookstein, F.L. The Measurement of Biological Shape and Shape Change. Lect. Notes Biomath.1978; vol. 24. Springer-Verlag, New York.

Bookstein, F.L., 1991. Morphometric Tools for Landmark Data: Geometry and Biology. Cambridge Univ. Press, Cambridge, UK.

Bookstein, F.L. Biometrics, biomathematics and the morphometric synthesis. Bull. Math. Biol. 1996a;58, 313–365.

Bookstein, F.L. Landmark methods for forms without landmarks: morphometrics of group differences in outline shape. Med. Image Anal. 1996b;1:225–243.

Bookstein, F.L. Shape and the information in medical images: a decade of the morphometric synthesis. Comput. Vis. Image Understand. 1997; 66: 97118.

Brand, J. W., et al. Radiation Protection in Dentistry. NCRP 2003. No. 145. Report.

Brechbühler C, Gerig G, Kübler O. Parametrization of Closed Surfaces for 3-D Shape Description. Comput Vision Image Understanding 1995;61(2):154.

Brenner DJ, Curtis RE, Hall EJ, Ron E: Second malignancies in prostate patients after radiotherapy compared with surgery. Cancer 2000; 88:398-406.

Brooks M, Pomiankowski A. Symmetry is in the eye of the beholder. Trends Ecol. Evol. 1994; 9:201–2

Bruce, V., & Young, A. W. (1998). In the eye of the beholder. Oxford: Oxford University Press.

Bull, R., & Rumsey, N. (1988) . The social psychology of facial appearance. New York: Springer-Verlag.

Bushberg, J., et al. "The Essential Physics of Diagnostic Radiology." (2001).

Cachia, A., Mangin, J.F., Riviere, D., Kherif, F., Boddaert, N., Andrade, A., Papadopoulos-Orfanos, D., Poline, J.B., Bloch, I., Zilbovicius, M., Sonigo, P., Brunelle, F., Regis, J. A primal sketch of the cortex mean curvature: a morphogenesis based approach to study the variability of the folding patterns. IEEE Trans. Med. Imaging 2003; 22:754 – 765.

Carter L, Farman AG, Geist J, Scarfe WC, Angelopoulos C, Nair MK, Hildebolt CF, Tyndall D, Shrout M; American Academy of Oral and Maxillofacial Radiology. American Academy of Oral and Maxillofacial Radiology executive opinion statement on performing and interpreting diagnostic cone beam computed tomography. Oral Surg Oral Med Oral Pathol Oral Radiol Endod. 2008 Oct;106(4):561-2. doi: 10.1016/j.tripleo.2008.07.007.

Cevidanes LH, Alhadidi A, Paniagua B, Styner M, Ludlow J, Mol A, Turvey T, Proffit WR, Rossouw PE. Three-dimensional quantification of mandibular asymmetry through cone-beam computerized tomography. Oral Surg Oral Med Oral Pathol Oral Radiol Endod. 2011 Jun;111(6):757-70. Epub 2011 Apr 16.

Cevidanes LH, Bailey LJ, Tucker GR,Jr, Styner MA, Mol A, Phillips CL, et al. Superimposition of 3D cone-beam CT models of orthognathic surgery patients. Dentomaxillofac Radiol. 2005 Nov;34(6):369-75.

Cevidanes LH, Bailey LJ, Tucker SF, Styner MA, Mol A, Phillips CL, et al. Three-dimensional cone-beam computed tomography for assessment of mandibular changes after orthognathic surgery. Am J Orthod Dentofacial Orthop. 2007 Jan;131(1):44-50.

Cevidanes LH, Franco AA, Gerig G, Proffit WR, Slice DE, Enlow DH, et al. Comparison of relative mandibular growth vectors with high-resolution 3-dimensional imaging. Am J Orthod Dentofacial Orthop. 2005 Jul;128(1):27-34.

Cevidanes LH, Franco AA, Gerig G, Proffit WR, Slice DE, Enlow DH, et al. Assessment of mandibular growth and response to orthopedic treatment with 3-dimensional magnetic resonance images. Am J Orthod Dentofacial Orthop. 2005 Jul;128(1):16-26.

Cevidanes LH, Styner MA, Proffit WR. Image analysis and superimposition of 3-dimensional cone-beam computed tomography models. Am J Orthod Dentofacial Orthop. 2006 May;129(5):611-8.

Chapuis J , Rudolph T, Borgesson B, De Momi E, Pappas I, Hallermann W, Schramm A, et al. 3D surgical planning and navigation for CMF surgery .SPIE Medical imaging, San Diago, California, USA. 2004 February .

Chapuis J. Computer- aided cranio-maxillofacial surgery [dissertation]. Switszerland: University of Bern; 2006.

Chapuis J, Ryan P, Blaeuer M, Langlotz F, Hallermann W, Schramm A, et al. A new approach for 3D computer-assisted orthognathic surgery—first clinical case. Int Congr Ser. 2005 5;1281:1217-22.

Chapuis J, Schramm A, Pappas I, Hallermann W, Schwenzer-Zimmerer K, Langlotz F, Caversaccio M. A new system for computer-aided preoperative planning and Intraoperative navigation during corrective jaw surgery.IEEE Trans Inf Technol Biomed. 2007 May;11(3):274-87.

Chew MT. Spectrum and management of dentofacial deformities in a multiethnic Asian population. Angle Orthod. 2006 Sep;76(5):806-9.

Claes P, Vandermeulen D, De Greef S, Willems G, Suetens P. Craniofacial reconstruction using a combined statistical model of face shape and soft tissue depths: methodology and validation. Forensic Sci Int. 2006 May 15;159 Suppl 1:S147-58. Epub 2006 Mar 15.

Cohen MM Jr. A critique of the OMENS classification of hemifacial microsomia. Cleft Palate Craniofac J 1991;28:77.

Coleman CN: Second malignancy after treatment of Hodgkin's disease: An evolving picture. J Clin Oncol 1986; 4:821-824.

Committee on the Biological Effects of Ionizing Radiation: Health Effects of Exposure of Low Levels of Ionizing Radiations. Washington, DC, National Academy of Sciences, National Research Council. 1990

Concar D. Sex and the symmetrical body. New Sci. 1995; 146:40–44

Cunningham, M. R., Roberts, A. R., Barbee, A. P., Druen, P. B., & Wu, C.-H. (1995). Their ideas of beauty are, on the whole, the same as ours: Consistency and variability in the cross-cultural perception of female physical attractiveness. Journal of Personality and Social Psychology, 1995; 68:261–279.

Cunningham, M. R. Measuring the physical in physical attractiveness: Quasi-experiments on the sociobiology of female facial beauty. Journal of Personality and Social Psychology, 1986;50:925–935.

Curry III, Thomas S., James E. Dowdey, and Robert C. Murry Jr. Christensen´s physics of diagnostic radiology 4 Ed. Lippincott Williams & Wilkins, 1990.

Czesnin K, wronkowski Z: Second malignancies of the irradiated area in patients treated for uterine cervix cancer. Gynecol Oncol 1978; 6:309-315.

Dann, R., Hoford, J., Kovacic, S., Reivich, M., Bajcsy, R. Evaluation of elastic matching systems for anatomic (CT, MR) and functional (PET) cerebral images. J. Comp. Assist. Tomogr. 1982;13:603–611.

Darby SC, Reeves G, Key T, Doll R, Stovall M: Mortality in a cohort of women given x-ray therapy for metropathia haemorrhagica. Int J Cancer 1994; 56:793-801.

De Momi EF, Chapuis JF, Pappas IF, Ferrigno GF, Hallermann WF, Schramm AF, et al. Automatic extraction of the mid-facial plane for cranio-maxillofacial surgery planning. Int J Oral Maxillofac Surg. 2006;35(7):636-42.

De Paula L, Ruellas A, Paniagua B, Styner M, Turvey T, Zhu H, et al. One-year assessment of surgical outcomes in Class III patients using cone beam computed tomography. Int J Oral Maxillofac Surg. 2013 Jun;42(6):780-9. doi: 10.1016/j.ijom.2013.01.002. Epub 2013 Feb 8.

Dion, K. K., Berscheid, E., & Walster, E. (1972). What is beautiful is good. Journal of Personality and Social Psychology, 1972; 24:285–290.

Dryden, I.L. & Mardia, K.V. (1998). Statistical analysis of shape. New York: John Wiley and Sons.

Eagly, A. H., Ashmore, R. D., Makhijani, M. G., & Longo, L. C. What is beautiful is good, but. . .:A meta-analytic review of research on the physical attractiveness stereotype. Psychological Bulletin, 1991; 110:109–128.

Effects of Ionizing Radiation: United Nations Scientific Committee on the Effects of Atomic Radiation: UNSCEAR 2006 Report to the General Assembly, with Scientific Annexes. Scientific Annexes C, D and E. UN, 2009.

Farkas LG, Posnick JC, Hreczko TM, Pron GE. Growth patterns of the nasolabial region: a morphometric study. Cleft Palate Craniofac J. 1992 Jul;29(4):318-24.

Farkas LG, Posnick JC, Hreczko TM, Pron GE. Growth patterns in the orbital region: a morphometric study. Cleft Palate Craniofac J. 1992 Jul;29(4):315-8.

Farkas LG, Posnick JC, Hreczko TM. Growth patterns of the face: a morphometric study.Cleft Palate Craniofac J. 1992 Jul;29(4):308-15.

Farkas LG, Posnick JC, Hreczko TM. Anthropometric growth study of the head. Cleft Palate Craniofac J. 1992 Jul;29(4):303-8.

Feldkamp,Davis, Kress, “Practical cone-beam algorithm,” J. Opt. Soc. Am. 1984;A 1:612–619.

Feldmar, J., Ayache, N., Betting, F. 3D–2D projective registration of free-form curves and surfaces. Comput. Vis. Image Underst. 1997;65:403 – 424.

Ferrario VF, Sforza C, De Franco DJ.Mandibular shape and skeletal divergency. Eur J Orthod. 1999 Apr;21(2):145-53.

Ferrario V F, Sforza C, Ciusa V, Dellavia C, Tartaglia G M. The effect of sex and age on facial asymmetry in healthy subjects: a cross-sectional study from adolescence to mid-adulthood. Journal of Oral and Maxillofacial Surgery. 2001;59: 382–388

Ferson, S.F., Rohlf, F.J. & Koehn, R.K. Measuring shape variation of two-dimensional outlines. Syst. Zool. 1985;34:59–68.

Fong JH, Wu HT, Huang MC, Chou YW, Chi LY, Fong Y, Kao SY.Analysis of facial skeletal characteristics in patients with chin deviation. J Chin Med Assoc. 2010 Jan;73(1):29-34.

Frieze, I. H., Olson, J. E., & Russell, J. (1991). Attractiveness and income for men and women in management. Journal of Applied Social Psychology. 1991; 21:1039–1057.

Gangestad, S.W., Thornhill, R., and Yeo, R.A. Facial attractiveness, developmental stability, and fluctuating asymmetry. Ethology and Sociobiology. 1994;15:73–85.

Gangestad, S.W., and Thornhill, R. The evolutionary psychology of extrapair sex: the role of fluctuating asymmetry. Evolution and Human Behavior 1997; 18:69–88.

Gangestad SW, Simpson JA. 2000. The evolution of human mating: tradeoffs and strategic pluralism. Behav. Brain Sci. 2000; 23:573–87.

Gateno J, Teichgraeber JF, Xia JJ. Three-dimensional surgical planning for maxillary and midface distraction osteogenesis. J Craniofac Surg. 2003 Nov;14(6):833-9.

Gateno J, Xia JJ, Teichgraeber JF, Christensen AM, Lemoine JJ, Liebschner MA, et al. Clinical feasibility of computer-aided surgical simulation (CASS) in the treatment of complex cranio-maxillofacial deformities. J Oral Maxillofac Surg. 2007 Apr;65(4):728-34.

Gee, J.C. On matching brain volumes. Pattern Recognit. 1999; 32:99 – 111.

Gee, J.C., Bajcsy, R.K. Elastic matching: continuum mechanical and probabilistic analysis. In: Toga, A.W. (Ed.), Brain Warping. 1999;183–196.

Gee, J., Haynor, D. Numerical methods for high-dimensional warps. In: Toga, A.W. (Ed.), Brain Warping. 1999;101 – 113.

Gellrich N, Schramm A, Hammer B,Rojas S, Cufi D, Lagreze W, Schmelzeisen R. Computer assisted secondary reconstruction of unilateral posttraumatic orbital deformity. Plast Reconstr Surg 2002: 110: 1417–1429.

Gerig G, Styner M, Jones D, Weinberger D, Lieberman J. Shape analysis of brain ventricles using Spharm. MMBIA Proceedings. IEEE 2001;171-8.

Gougoutas AJ, Singh DJ, Low DW, Bartlett SP. Hemifacial microsomia: clinical features and pictographic representations of the OMENS classification system. Plast Reconstr Surg. 2007 Dec;120(7):112e-120e.

Gower, J.C. (1975). Generalized procrustes analysis. Psychometrika 1975; 40:33–51.

Glerup N. Asymmetry measures in medical image analysis [dissertation]. Department of Innovation IT, University of Copenhagen; April 29, 2005.

Glerup, N. Nielsen, M. Sporring, J. Kreiborg, S. Journal title Proceedings- SPIE the international society for optical engineering 1999; 5370 (1):274-282

Gliddon MJ, Xia JJ, Gateno J, Wong HT, Lasky RE, Teichgraeber JF, et al. The accuracy of cephalometric tracing superimposition. J Oral Maxillofac Surg. 2006 Feb;64(2):194-202.

Grammer, K., and Thornhill, R. Human (Homo sapiens) facial attractiveness and sexual selection—the role of symmetry and averageness. Journal of Comparative Psychology 1994; 108:233–242.

Grauer D, Cevidanes LS, Proffit WR. Working with DICOM craniofacial images. Am J Orthod Dentofacial Orthop. 2009 Sep;136(3):460-70. doi: 10.1016/j.ajodo.2009.04.016.

Grenander, U., Miller, M.I., 1998. Computational anatomy: an emerging discipline. Q. Appl. Math. 1998; 56:617–694.

Hall, E. J. and A. J. Giaccia (2012). Radiobiology for the radiologist. Philadelphia, Wolters Kluwer Health/Lippincott Williams & Wilkins.

Hassan B, van der Stelt P, Sanderink G. Accuracy of three-dimensional measurements obtained from cone beam computed tomography surface-rendered images for cephalometric analysis: influence of patient scanning position. Eur J Orthod. 2009 Apr;31(2):129-34. doi: 10.1093/ejo/cjn088. Epub 2008 Dec 23. 9994.

Hassfeld S, Muhling J. Computer assisted oral and maxillofacial surgery--a review and an assessment of technology. Int J Oral Maxillofac Surg. 2001 Feb;30(1):2-13. Review.

Hechler SL. Cone-beam CT: applications in orthodontics. Dent Clin North Am. 2008 Oct;52(4):809-23, vii. doi: 10.1016/j.cden.2008.05.001.

Hemmy DC, Tessier PL. CT of dry skulls with craniofacial deformities: accuracy of three-dimensional reconstruction. Radiology. 1985 Oct;157(1):113-6.

Holtel MR. Emerging technology in head and neck ultrasonography. Otolaryngol Clin North Am. 2010 Dec;43(6):1267-74, vii. doi: 10.1016/j.otc.2010.08.003.

Horgan, JE, Padwa BL, LaBrie RA, Mulliken JB. OMENS-Plus: analysis of craniofacial and extracraniofacial anomalies in hemifacial microsomia. Cleft Palate Craniofac J 1995;32(5):405-12.

Howe GR, Mclaughlin J: Breast cancer mortality between 1950 and I 987 after exposure to fractionated moderate- dose-rate ionizing radiation in the Canadian Fluoroscopy cohort study and a comparison with breast cancer mortality in the atomic bomb survivors study. Radiat Res 1996; 145:694- 707.

Huisinga-Fischer C, Zonneveld F, Vaandrager J, Prahl-Andersen B. CT-based size and shape determination of the craniofacial skeleton: a new scoring system to assess bony deformities in hemifacial microsomia. J Craniofac Surg. 2001 Jan;12(1):87-94.

Johnston MC, Bronsky PT. Animal models for human craniofacial malformations. J Craniofac Genet Dev Biol. 1991 Oct-Dec;11(4):277-91.

Jones D, Hill K. Criteria of facial attractiveness in five populations. Hum. Nat. 1993; 4: 271–96.

Joshi, S., Davis, B., Jomier, M., and Gerig, G., "Unbiased dffeomorphic atlas construction for computational anatomy," NeuroImage 2004; 23 (1): 151.

Junck L, Moen JG, Hutchins GD,Brown MB, Kuhl DE. Correlation methods for the centering, rotation and alignment of functional brain images. J Nuclear Med 1990: 3: 1220–1226.

Kaipatur N, Flores-Mir C. Accuracy of computer programs in predicting orthognathic surgery soft tissue response. J Oral Maxillofac Surg. 2009 Apr;67(4):751-9. doi: 10.1016/j.joms.2008.11.006.

Kapila S, Conley RS, Harrell WE Jr. The current status of conebeam computed tomography imaging in orthodontics. Dentomaxillofac Radiol. 2011;40:24-34.

Katsumata A, Fujishita M, Maeda M, Ariji Y, Ariji E, Langlais RP. 3D-CT evaluation of facial asymmetry. Oral Surg Oral Med Oral Pathol Oral Radiol Endod. 2005 Feb;99(2):212-20.

Kelemen A, Székely G, Gerig G. Elastic model-based segmentation of 3-D neuroradiological data sets. IEEE Trans Med Imaging. 1999 Oct;18(10):828-39. 2(2):151-61.

Khaneja, N., Grenander, U., Miller, M.I., 1998. Dynamic programming generation of curves on brain surfaces. Pattern Anal. Mach. Intell. 1998; 20:1260 – 1264.

Kim M, Huh KH, Yi WJ, Heo MS, Lee SS, Choi SC. Evaluation of accuracy of 3D reconstruction images using multi-detector CT and cone-beam CT. Imaging Sci Dent. 2012; 42: 25-33.

Koh C, Chew MT. Predictability of soft tissue profile changes following bimaxillary surgery in skeletal class III Chinese patients. J Oral Maxillofac Surg. 2004 Dec;62(12):1505-9.

Kowner R. Facial asymmetry and attractiveness judgment in developmental perspective. J. Exp. Psychol. Hum. Percept. Perform. 1996; 22:662–75

Lagravère MO, Carey J, Toogood RW, Major PW. Three-dimensional accuracy of measurements made with software on cone-beam computed tomography images. Am J Orthod Dentofacial Orthop. 2008 Jul;134(1):112-6. doi: 10.1016/j.ajodo.2006.08.024.

Langlois, J. H., Ritter, J. M., Roggman, L. A., & Vaughn, L. S. Facial diversity and infant preferences for attractive faces. Developmental Psychology, 1991; 27:79–84.

Langlois, J. H., & Roggman, L. A. Attractive faces are only average. Psychological Science, 1990;1:115–121.

Langlois JH, Roggman LA, Musselman L. What is average and what is not average about attractive faces? Psychol. Sci. 1994; 5:214–20

Lee MS, Chung DH, Lee JW, Cha KS. Assessing soft-tissue characteristics of facial asymmetry with photographs. Am J Orthod Dentofacial Orthop. 2010 Jul;138(1):23-31. doi: 10.1016/j.ajodo.2008.08.029.

Li P, Tang Y, Li J, Shen L, Tian W, Tang W. Establishment of sequential software processing for a biomechanical model of mandibular reconstruction with custom-madeplate. Comput Methods Programs Biomed. (In press)

Liang H, Tyndall DA, Ludlow JB, Lang LA, Nunn ME. Accuracy of mandibular cross-sectional imaging with tuned- aperture computed tomography (TACT), iteratively reconstructed TACT, and multidirectional, linear, and transverse panoramic tomography. Oral Surg Oral Med Oral Pathol Oral Radiol Endod. 2001 May;91(5):594-602.

Liu Y, Collins RT, Rothfus WE Robust midsagittal plane extraction from normal and pathological 3-D neuroradiology images. IEEE Trans Med Imaging 2001: 20: 175–192.

Lorigo, L.M., Faugeras, O.D., Grimson, W.E., Keriven, R., Kikinis, R., Nabavi, A., Westin, C.F. Curves: curve evolution for vessel segmentation. Med. Image Anal. 2001; 5:195 – 206.

Ludlow JB, Ivanovic M. Comparative dosimetry of dental CBCT devices and 64-slice CT for oral and maxillofacial radiology. Oral Surg Oral Med Oral Pathol Oral Radiol

Endod. 2008 Jul;106(1):106-14. doi: 10.1016/j.tripleo.2008.03.018. Epub 2008 May 27.

Ludlow JB, Davies-Ludlow LE, Brooks SL, Howerton WB. Dosimetry of 3 CBCT devices for oral and maxillofacial radiology: CB Mercuray, NewTom 3G and i-CAT. Dentomaxillofac Radiol. 2006 Jul;35(4):219-26. Erratum in: Dentomaxillofac Radiol. 2006 Sep;35(5):392.

Ludlow JB, Davies-Ludlow LE, Brooks SL. Dosimetry of two extraoral direct digital imaging devices: NewTom cone beam CT and Orthophos Plus DS panoramic unit. Dentomaxillofac Radiol. 2003 Jul;32(4):229-34.

Luu NS, Mandich MA, Flores-Mir C, El-Bialy T, Heo G, Carey JP, Major PW. The validity,reliability, and time requirement of study model analysis using cone-beam computed tomography– generated virtual study models. Orthod Craniofac Res. (in press)

Mabuchi K, Soda M, Ron E, Tokunaga M, Ochikubo S, Sugimoto S, Ikeda T, Terasaki M, Preston DL, Thompson DE. Cancer incidence in atomic bomb survivors. Part I: Use of the tumor registries in Hiroshima and Nagasaki for incidence studies. Radiat Res. 1994 Feb;137(2 Suppl):S1-16.

MacLeod, N. & Forey, P.L. (2001). Morphology, shape, and phylogeny. London: Taylor & Francis.

MacLeod, N. Understanding morphology in systematic contexts: 3D specimen ordination and 3D specimen recognition. In The new taxonomy. 2008; 143–210.

Mah JK, Huang JC, Choo H. Practical applications of conebeam computed tomography in orthodontics. J Am Dent Assoc. 2010;141(suppl 3):7S-13S.

Maeda M, Katsumata A, Ariji Y, Muramatsu A, Yoshida K, Goto S, et al. 3D-CT evaluation of facial asymmetry in patients with maxillofacial deformities. Oral Surg Oral Med Oral Pathol Oral Radiol Endod. 2006 Sep;102(3):382-90.

Maes F, Collignon A, Vandermeulen D, Marchal G, Suetens P. Multimodality image registration by maximization of mutual information. IEEE Trans Med Imaging. 1997 Apr;16(2):187-98.

Marcus, L.F., Corti, M., Loy, A., Naylor, G.J.P. & Slice, D.E. (1996). Advances in morphometrics. New York: Plenum.

Masood Y, Masood M, Zainul NN, Araby NB, Hussain SF, Newton T. Impact of malocclusion on oral health related quality of life in young people. Health Qual Life Outcomes. 2013 Feb 26;11:25. doi: 10.1186/1477-7525-11-25.

Masood M, Masood Y, Saub R, Newton JT. Need of minimal important difference for oral health-related quality of life measures. J Public Health Dent. 2012 Sep 21. doi: 10.1111/j.1752-7325.2012.00374.x.

McPeek, M.P., Shen, L., Torrey, J.Z. & Farid, H. The tempo and mode of 3-dimensional morphological evolution in male reproductive structures. Am. Nat. 2008; 171:E158–E178.

Mealey, L., and Bridgstock, R. Symmetry and perceived facial attractiveness: a monozygotic co-twin comparison. Journal of Personality and Social Psychology 1999;76:151–158.

Merrett SJ, Drage NA, Durning P. Cone beam computed tomography: a useful tool in orthodontic diagnosis and treatment1199 planning. J Orthod. 2009;36:202-210.

Meier D, Fisher E. Parameter space warping: shape-based correspondence between morphologically different objects. IEEE Trans Med Imaging. 2002 Jan;21(1):31-47

Meyer-Marcotty P, Stellzig-Eisenhauer A, Bareis U, Hartmann J, Kochel J. Three-dimensional perception of facial asymmetry. Eur J Orthod. 2011 Dec;33(6):647-53. doi: 10.1093/ejo/cjq146. Epub 2011 Feb 25.

Meyer M, Desbrun M, Schröder P, Barr AH. Discrete differential-geometry operators for triangulated 2-manifolds. 2002; 3(2):52-58.

Miller, M., Banerjee, A., Christensen, G., Joshi, S., Khaneja, N., Grenander, U., Matejic, L. Statistical methods in computational anatomy. Stat. Methods Med. Res. 1997; 6: 267–299.

Miller, M.I., Massie, A., Ratnanather, J.T., Botteron, K.N., Csernansky, J.G. Bayesian construction of geometrically based cortical thickness metrics. NeuroImage 2000; 12:676–687.

Miller MI, Younes L. Group actions, homeomorphisms, and matching: A general framework. International Journal of Computer Vision 2001;41(1):61-84.

Miller. Computational anatomy: Shape, growth, and atrophy comparison via diffeomorphisms. Neuroimage 2004;23, Supplement 1(0):S19.

Mitteröcker, P., Gunz, P. & Bookstein, F.L. Heterochrony and geometric morphometrics: a comparison of cranial growth in Pan paniscus versus Pan troglodytes. Evol. Dev. 2005; 7:244–258.

Monahan R, Seder K, Patel P, Alder M, Grud S, O'Gara M. Hemifacial microsomia. Etiology, diagnosis and treatment. J Am Dent Assoc. 2001 Oct;132(10):1402-8.

Montagnat, J., Delingette, H., Ayache, N., 2001. A review of deformable surfaces: topology, geometry and deformation. Image Vis. Comput. 2001;19:1023 – 1040.

Moshfeghi M, Tavakoli MA, Hosseini ET, Hosseini AT, Hosseini IT. Analysis of linear measurement accuracy obtained by cone beam computed tomography (CBCT-NewTom VG). Dent Res J (Isfahan). 2012 Dec;9(Suppl 1):S57-62.

Moyers RE, Bookstein FL. The inappropriateness of conventional cephalometrics. Am J Orthod 1979 6;75(6):599-61

Murshid ZA, Amin HE, Al-Nowaiser AM. Distribution of certain types of occlusal anomalies among Saudi Arabian adolescents in Jeddah city. Community Dent Health. 2010 Dec;27(4):238-41.

Nguyen T, Cevidanes L, Paniagua B, Zhu H, Koerich L, De Clerck H. Use of shape correspondence analysis to quantify skeletal changes associated with bone-anchored Class III correction. Angle Orthod. 2013 Jul 25.

Newton JT, Prabhu N, Robinson PG. The impact of dental appearance on the appraisal of personal characteristics. The International Journal of Prosthodontics 2003;16(4):429-34.

O'Grady K, Antonyshyn O. Facial asymmetry: three-dimensional analysis using laser surface scanning. Plast Reconstr Surg 1999: 104: 928–937.

Oguz I. Groupwise shape correspondence with local features. 2009 PhD dissertation, University of North Carolina. (http://webcat.lib.unc.edu/record=b6135448~S1)

Palmer AC, Strobeck C. Fluctuating asymmetry: measurement, analysis, pattern. Annu. Rev. Ecol. Syst. 1986;17:391–421.

Paniagua B, Cevidanes L, Walker D, Zhu H, Guo R, Styner M. Clinical application of SPHARM-PDM to quantify temporomandibular joint osteoarthritis. Comput Med Imaging Graph. 2011 Jul;35(5):345-52. doi: 10.1016/j.compmedimag.2010.11.012. Epub 2010 Dec 24.

Paniagua B, Cevidanes L, Zhu H, Styner M. Outcome quantification using SPHARM-PDM toolbox in orthognathic surgery. Int J Comput Assist Radiol Surg. 2011 Sep;6(5):617-26. doi: 10.1007/s11548-010-0539-z. Epub 2010 Dec 16.

Park SH, Yu HS, Kim KD, Lee KJ, Baik HS. A proposal for a new analysis of craniofacial morphology by 3-dimensional computed tomography. Am J Orthod Dentofacial Orthop. 2006 May;129(5):600.e23,600.e34.

Parsons PA. Fluctuating asymmetry: an epigenetic measure of stress. Biol. Rev. 1990; 65:131–45.

Perrett, D.I., May, K.A., and Yoshikawa, S. Facial shape and judgements of female attractiveness. Nature 1994; 368:239–242.

Pierce DA, Preston DL: Radiation-related cancer risks at low doses among atomic bomb survivors. Radiation Research 2003; 154:178-186.

Polak M. 2003. Developmental Instability: Causes and Consequences. New York: Oxford Univ. Press

Polly, P.D. Developmental dynamics and G-matrices: can morphometric spaces be used to model phenotypic evolution? Evol. Biol. 2008;35:1–20. (Online DOI 10.1007/s11692-008-9020-0).

Polly, P.D. & MacLeod, N. Locomotion in fossil Carnivora: an application of eigen surface analysis for morphometric analysis of 3D surfaces. Palaeontol. Electron. 2008; 11:1–13.

Ponyi S, Szabó G, Nyilasi J. Asymmetry of mandibular dimensions in European skulls. Proc Finn Dent Soc. 1991;87(3):321-7.

Preston DL, Pierce DA, Shimizu Y, Ron E, Mabuchi K. Dose response and temporal patterns of radiation-associated solid cancer risks. Health Phys. 2003 Jul; 85(1):43-6. Review.

Preston DL, Kusumi S, Tomonaga M, Izumi S, Ron E, Kuramoto A, Kamada N, Dohy H, Matsuo T, Matsui T [corrected to Matsuo T], et al. Cancer incidence in atomic bomb survivors. Part III. Leukemia, lymphoma and multiple myeloma, 1950-1987. Radiat Res. 1994 Feb;137(2 Suppl):S68-97. Erratum in: Radiat Res 1994 Jul;139(1):129.

Prima S, Ourselin S, Ayache N. Computation of the mid-sagittal plane in 3D images of the brain. Computer Vision â€" ECCV 2000. 2000:685-701.

Proffit WR, Jackson TH, Turvey TA.Changes in the pattern of patients receiving surgical-orthodontic treatment. Am J Orthod Dentofacial Orthop. 2013 Jun;143(6):793-8. doi: 10.1016/j.ajodo.2013.01.014.

Proffit WR, Fields HW Jr, Moray LJ. Prevalence of malocclusion and orthodontic treatment need in the United States: estimates from the NHANES III survey. Int J Adult Orthodon Orthognath Surg. 1998;13(2):97-106.

Proffit WR, Turvey TA, Phillips C.The hierarchy of stability and predictability in orthognathic surgery with rigid fixation: an update and extension. Head Face Med. 2007 Apr 30;3:21.

Proffit WR, Turvey TA, Phillips C. The hierarchy of stability and predictability in orthognathic surgery with rigid fixation: an update and extension. Head Face Med. 2007 Apr 30;3:21.

Proffit WR, Turvey TA, Phillips C. Orthognathic surgery: a hierarchy of stability. Int J Adult Orthodon Orthognath Surg. 1996;11(3):191-204.

Proffit WR, Phillips C, Dann C 4th, Turvey TA. Stability after surgical-orthodontic correction of skeletal Class III malocclusion. I. Mandibular setback. Int J Adult Orthodon Orthognath Surg. 1991;6(1):7-18.

Proffit WR, Phillips C, Prewitt JW, Turvey TA. Stability after surgical-orthodontic correction of skeletal Class III malocclusion. 2. Maxillary advancement. Int J Adult Orthodon Orthognath Surg. 1991;6(2):71-80.

Proffit WR, Phillips C, Turvey TA. Stability after surgical-orthodontic corrective of skeletal Class III malocclusion. 3. Combined maxillary and mandibular procedures. Int J Adult Orthodon Orthognath Surg. 1991;6(4):211-25.

Proffit WR, Phillips C, Turvey TA. Stability following superior repositioning of the maxilla by LeFort I osteotomy. Am J Orthod Dentofacial Orthop. 1987 Aug;92(2): 151-161

Paus, T., Zijdenbos, A., Worsley, K., Collins, D., Blumenthal, J., Giedd, J., Rapoport, J., Evans, A., 1999. Structural maturation of neural pathways in children and adolescents: in vivo study. Science 1999; 283:1908–1911.

Proffit, William R., Henry W. Fields Jr, and David M. Sarver. Contemporary orthodontics. Elsevier Health Sciences, 2012.

Proffit WR, White RP. Surgical-orthodontic treatment. St. Louis: Mosby–Year Book, 1991:27-8.

Radon, J. "On determination of functions by their integral values along certain multiplicities." Ber. der Sachische Akademie der Wissenschaften Leipzig,(Germany) 1917; 69: 262-277.

Rahbar R, Robson C, Mulliken J, Schwartz L, Dicanzio J, Kenna M, et al. Craniofacial, temporal bone, and audiologic abnormalities in the spectrum of hemifacial microsomia. Arch Otolaryngol Head Neck Surg. 2001 Mar;127(3):265-71.

Rashedi B, Tyndall DA, Ludlow JB, Chaffee NR, Guckes AD. Tuned aperture computed tomography (TACT) for cross-sectional implant site assessment in the posterior mandible. J Prosthodont. 2003 Sep;12(3):176-86.

Reyneke JP, Tsakiris P, Kienle F.A simple classification for surgical treatment planning of maxillomandibular asymmetry. Br J Oral Maxillofac Surg. 1997 Oct;35(5):349-51.

Rettmann, M.E., Han, X., Xu, C., Prince, J.L. Automated sulcal segmentation using watersheds on the cortical surface. NeuroImage 2002; 15:329 – 344.

Rhodes G. 1996. Superportraits: Caricatures and Recognition. Hove, UK: Psychol. Press

Rhodes G, Chan J, Zebrowitz LA, Simmons LW. 2003. Does sexual dimorphism in human faces signal health? Proc. R. Soc. Lond. Ser. B Biol. Sci. 2003; 270:S93–95.

Rhodes G, Halberstadt J, Brajkovich G. Generalization of mere exposure effects to averaged composite faces. Soc. Cogn. 2001; 19:57–70

Rhodes G, Halberstadt J, Jeffery L, Palermo R. The attractiveness of average faces is not a generalised mere exposure effect. Soc. Cogn. 2005a;23:205–17

Rhodes G, Harwood K, Yoshikawa S, Nishi- tani M, McLean I. The attractiveness of average faces: cross-cultural evidence and possible biological basis. In Facial Attrac-tiveness: Evolutionary, Cognitive and Social Perspectives, 2002; 35–58.

Rhodes G, Hickford C, Jeffery L. Sex- typicality and attractiveness: Are supermale and superfemale faces super-attractive? Br. J. Psychol. 2000; 91:125–40

Rhodes G, Jeffery L, Watson TL, Clifford CWG, Nakayama K. Fitting the mind to the world: face adaptation and attractiveness aftereffects. Psychol. Sci. 2003;14:558–66

Rhodes G, Lee K, Palermo R, Weiss M, Yoshikawa M, McLean I. Attractiveness of own-race, other-race and mixed-race faces. Perception 20055b;34:319–40.

Rhodes G, Proffitt F, Grady JM, Sumich A. Facial symmetry and the perception of beauty. Psychon. Bull. Rev. 1998;5:659–69.

Rhodes G, Roberts J, Simmons L. Reflections on symmetry and attractiveness. Psychol. Evol. Gend. 1999a;1:279–95

Rhodes G, Simmons L, Peters M. Attractiveness and sexual behaviour: Does attractiveness enhance mating success? Evol. Hum. Behav. 2005c; 26:186–201.

Rhodes G, Sumich A, Byatt G. Are average facial configurations attractive only because of their symmetry? Psychol. Sci. 1999b;10:52–58

RhodesG, TremewanT . Averageness, exaggeration, and facial attractiveness. Psychol. Sci. 1996; 7:105–10

Rhodes G, Yoshikawa S, Clark A, Lee K, McKay R, Akamatsu S. Attractiveness of facial averageness and symmetry in non-Western cultures: in search of biologically based standards of beauty. Perception 2001b;30:611–25.

Rhodes G, Zebrowitz LA. Facial Attractiveness: Evolutionary, Cognitive, and Social Perspectives. Westport, CT: Ablex. 2002; 311.

Rhodes G, Zebrowitz LA, Clark A, Kalick S, Hightower A, McKay R. Do facial averageness and symmetry signal health? Evol. Hum. Behav. 2001c; 22:31–46.

Rikowski A, Grammer K. Human body odour, symmetry and attractiveness. Biol. Sci. 1999;266:869–74.

Robinson S, Suomalainen A, Kortesniemi M. Mu-CT. Eur J Radiol. 2005 Nov;56(2):185-91.

Rohlf, J.L. & Slice, D. Extensions of the Procrustes method for the optimal superimposition of landmarks. Syst. Zool. 1990; 39:40–59.

Rohr K. Landmark-based image analysis: Using geometric and intensity models. 2001; 21.ID: 421870969.

Ron E, Preston DL, Mabuchi K, Thompson DE, Soda M. Cancer incidence in atomic bomb survivors. Part IV: Comparison of cancer incidence and mortality. Radiat Res. 1994 Feb;137(2 Suppl):S98-112.

Samman N, Tong AC, Cheung DL, Tideman H.Analysis of 300 dentofacial deformities in Hong Kong. Int J Adult Orthodon Orthognath Surg. 1992;7(3):181-5.

Samuels CA, Butterworth G, Roberts T, Graupner L, Hole G. Facial aesthetics—babies prefer attractiveness to symmetry. Perception 1994;23:823–31.

Scarfe WC, Farman AG. What is cone-beam CT and how does it work? Dent Clin North Am. 2008 Oct;52(4):707-30, v. doi: 10.1016/j.cden.2008.05.005.

Seehra J, Fleming PS, Newton T, DiBiase AT. Bullying in orthodontic patients and its relationship to malocclusion,self-esteem and oral health-related quality of life. J Orthod. 2011 Dec;38(4):247-56; quiz 294. doi: 10.1179/14653121141641.

Seehra J, Newton JT, Dibiase AT. Interceptive orthodontic treatment in bullied adolescents and its impact on self-esteem and oral-health-related quality of life. Eur J Orthod. 2013 Oct;35(5):615-21. doi: 10.1093/ejo/cjs051. Epub 2012 Jul 28.

Seeram, E. "Computed tomography-physical principles, clinical applications, and quality control. St. Louis: Saunders." (2009).

Severt TR, Proffit WR. The prevalence of facial asymmetry in the dentofacial deformities population at the university of north carolina. Int J Adult Orthodon Orthognath Surg. 1997;12(3):171-6.

Shore RE, Hildreth N, Woodard E, Dvoretsky P, HempelmannL, Pasternack B: Breast cancer among women given x-ray therapy for acute postpartum mastitis. J Natl Cancer Inst 1986;77:689-696.

Siegel, A.F. & Benson, R.H. (1982). A robust comparison of biological shapes. Biometrics 1982;38:341–350.

Sneath, P.H. Trend-surface analysis of transformation grids. J. Zool. (Lond.) 1967;151:65–122.

Sowell, E.R., Peterson, B.S., Thompson, P.M., Welcome, S.E., Henkenius, A.L., Toga, A.W. Mapping cortical change across the human life span. Nat. Neurosci. 2003; 6: 309–315.

Stratemann SA, Huang JC, Maki K, Miller AJ, Hatcher DC. Comparison of cone beam computed tomography imaging with physical measures. Dentomaxillofac Radiol. 2008 Feb;37(2):80-93. doi: 10.1259/dmfr/3134

Styner M, Oguz I, Xu S, Brechbuehler C, Pantazis D, Levitt JJ, et al. Framework for the Statistical Shape Analysis of Brain Structures using SPHARM-PDM. Insight J. 2006;(1071):242-250.

Styner, M. Jomier, M. Gerig, G. Closed and open source neuroimage analysis tools and libraries at UNC. 3rd IEEE International Symposium on Biomedical Imaging: Nano to Macro, 6-9 April 2006, Arlington, VA pp 702-705.

Styner M, Gerig G, Lieberman J, Jones D, Weinberger D. Statistical shape analysis of neuroanatomical structures based on medial models. Med Image Anal 2003;7(3):207.

Symons, D. (1979). The evolution of human sexuality. New York: Oxford University Press.

Swaddle JP,Cuthilll C. Asymmetry and human facial attractiveness—symmetry may not always be beautiful. Proc. R. Soc. Lond. Ser. B Biol. Sci. 1995; 261:111–16.

Swennen GR, Mollemans W, De Clercq C, Abeloos J, Lamoral P, Lippens F, Neyt N, Casselman J, Schutyser F.A cone-beam computed tomography triple scan procedure to obtain a three-dimensional augmented virtual skull model appropriate for orthognathic surgery planning. J Craniofac Surg. 2009; 20: 297-307.

Thirion, J., Goudon, A. Computing the differential characteristics of isointensity surfaces. Comput. Vis. Image Underst. 1995; 61:190–202.

Thomas JT, Frias JL. The heart in selected congenital malformations: a lesson in pathogenetic relationships. Ann Clin Lab Sci 1987;17:207-10.

Thompson DE, Mabuchi K, Ron E, Soda M, Tokunaga M, Ochikubo S, Sugimoto S, Ikeda T, Terasaki M, Izumi S, et al. Cancer incidence in atomic bomb survivors. Part II: Solid tumors, 1958-1987. Radiat Res. 1994 Feb;137(2 Suppl):S17-67. Review. Erratum in: Radiat Res 1994 Jul;139(1):129.

Thompson, P.M., Toga, A.W., 2002. A framework for computational anatomy. Comput. Vis. Sci. 2002;5:1–12.

Thompson, P.M., Giedd, J.N., Woods, R.P., MacDonald, D., Evans, A.C., Toga, A.W. Growth patterns in the developing brain detected by using continuum mechanical tensor maps. Nature 2000;404:190–193.

Thornhill, R., and Gangestad, S.W. Human facial beauty: averageness, symmetry and parasite resistance. Human Nature 1993; 4:237–269.

Thornhill, R., Gangestad, S.W., and Comer, R. Human female orgasm and mate fluctuating asymmetry. Animal Behaviour 1995; 50:1601–1615.

Thornhill, R., & Gangestad, S. W. Facial attractiveness. Trends in Cognitive Sciences, 1999;3:452–460.

Thornhill R, Moller AP. Developmental stability, disease and medicine. Biol. Rev. Camb. Philos. Soc. 1997; 72:497–548

Toga, A.W., Thompson, P.M., Payne, B.A., 1996. Modeling morphometric changes of the brain during development. In: Thatcher, R.W., Lyon, G.R., Krasnegor, N. (Eds.), Developmental Neuroimaging: Mapping the Development of the Brain and Behavior. Academic Press, New York.

Troulis MJ, Everett P, Seldin EB, Kikinis R, Kaban LB. Development of a three-dimensional treatment planning system based on computed tomographic data. Int J Oral Maxillofac Surg. 2002 Aug;31(4):349-57.

Tung-Yui W, Jing-Jing F, Tung-Chin W. A Novel Method of Quantifying Facial Asymmetry. H U Lemke, K Inamura, K Doi, M W Vannier, and A G Farman, editors, Computer Assisted Radiology and Surgery, Berlin, Germany. 2005 June.

A.J. Tyrell, M.E Evison, A.T. Chamberlain, M.A. Green, Forensic three-dimensional facial reconstruction: historical review and contemporary developments, J. Forensic Sci. 1997;42:653-661.

Vaillant M, Miller MI, Younes L, Trouvé A. Statistics on diffeomorphisms via tangent space representations. Neuroimage. 2004;23 Suppl 1:S161-9.

Vaillant, M., Davatzikos, C. Finding parametric representations of the cortical sulci using an active contour model. Med. Image Anal. 1997;1:295 – 315.

Valentin J; International Commission on Radiation Protection. Managing patient dose in multi-detector computed tomography (MDCT). ICRP Publication 102. Ann ICRP. 2007; 37(1):1-79, iii.

Vento RA, LaBrie RA, Mulliken JB. The O.M.E.N.S. classification of hemifacial microsomia. Cleft Palate Craniofac J 1991;28:68-76.

Watson PM, Thornhill R. Fluctuating asymmetry and sexual selection. Trends Ecol. Evol. 1994;9:21–25

Webber RL, Horton RA, Underhill TE, Ludlow JB, Tyndall DA. Comparison of film, direct digital, and tuned-aperture computed tomography images to identify the location of crestal defects around endosseous titanium implants. Oral Surg Oral Med Oral Pathol Oral Radiol Endod. 1996 Apr;81(4):480-90.

White SC, Pae EK. Patient image selection criteria for cone beam computed tomography imaging. Semin Orthod. 2009;15:19-28.

White, Stuart C., and Michael J. Pharoah. Oral radiology: principles and interpretation. Elsevier Health Sciences, 2008.

Wiley, D., Amenta, N., Alcantara, D., Ghosh, D., Kil, Y.J., Delson, E., Harcourt-Smith, W., St.John, K., Rohlf, F.J. & Hamann, B. Evolutionary morphing. Proc. IEEE Vis. Conf. 2005; 431–438.

Xi T, van Loon B, Fudalej P, Bergé S, Swennen G, Maal T. Validation of a novel semiautomated method for three-dimensional surface rendering of condyles using cone beam computed tomography data. Int J Oral Maxillofac Surg. 2013; 42:1023-9.

Xia J, Samman N, Yeung RW, Shen SG, Wang D, Ip HH, et al. Three-dimensional virtual reality surgical planning and simulation workbench for orthognathic surgery. Int J Adult Orthodon Orthognath Surg. 2000 Winter;15(4):265-82.

Xia J, Ip HH, Samman N, Wang D, Kot CS, Yeung RW, et al. Computer-assisted three-dimensional surgical planning and simulation: 3D virtual osteotomy. Int J Oral Maxillofac Surg. 2000 Feb;29(1):11-7.

Xia JJ. Accuracy of the computer-aided surgical simulation (CASS) system in the treatment of patients with complex craniomaxillofacial deformity: A pilot study. Journal of oral and maxillofacial surgery. 2007 -02;65(2):248-54.

Younker, J.L. & Erlich, R. Fourier biometrics – harmonic amplitudes as multivariate shape descriptors. Syst. Zool. 1977;26:336–342.

Yushkevich PA , Piven J, Hazlett HC, Smith RG, Ho S, Gee JC, et al. User-guided 3D active contour segmentation of anatomical structures: Significantly improved efficiency and reliability. NeuroImage.2006;31 (3):1116-28.

Zebrowitz LA, Voinescu L, Collins MA. “Wide-eyed” and “crooked-faced”: determinants of perceived and real honesty across the life span. Personal. Soc. Psychol. Bull. 1996;22: 1258–69

Zelditch, M.L., Swiderski, D.L., Sheets, H.D. & Fink, W.L. (2004). Geometric morphometrics for biologists: a primer. Amsterdam: Elsevier.

Appendix 1

Raw data for the projects described in this dissertation

Surface distances were compared between the resultant mirrors from both approaches and the original mandible of 50 patients. The mean surface distances between the right and left sides were calculated for nine anatomical regions Different colors): the lateral pole, medial pole, anterior and posterior surfaces of both condyles, lateral surface of the rami and corpora of the mandible, inferior and posterior surfaces of the mandible, and anterior surface of the symphysis.

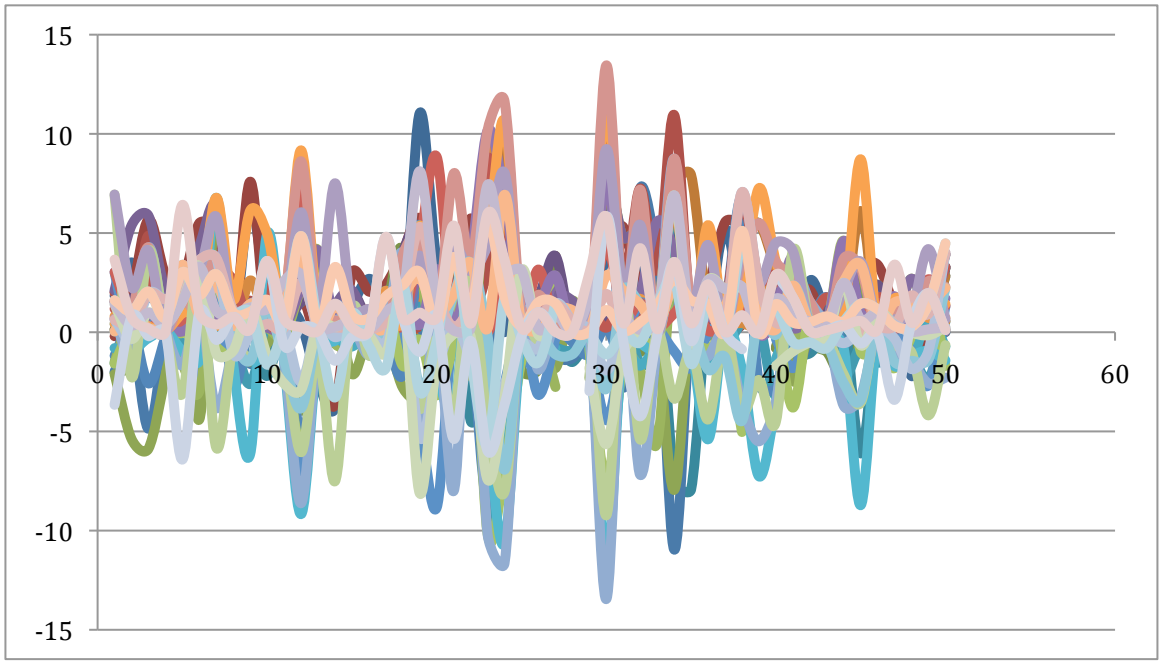

Raw data of chapter 2 (different color represents surface distance differences at all anatomic regions). X axis is case #, and Y axis is surface distance measurments in mm

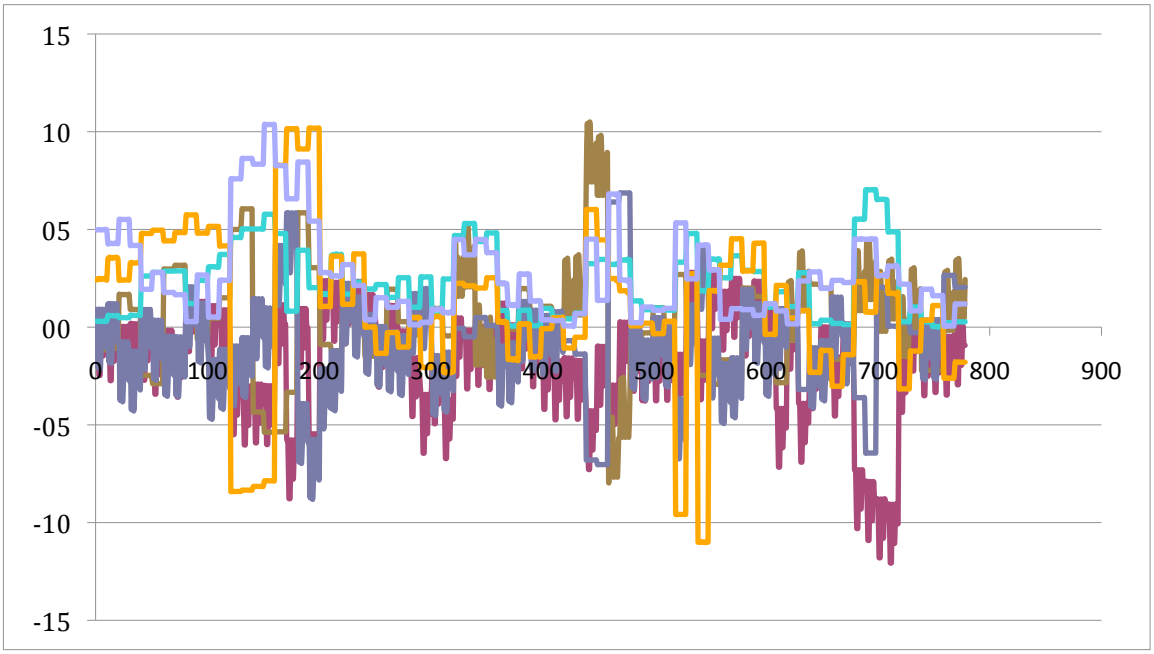

Raw data of chapter 4, all 9 simulations for each hemimandible of a 20 patient sample using the 2 mirroring techniques (different colors represent the differences in mms and degree in X,Y, and Z for all hemimandibles). X axis is case #, and Y axis is surface distance measurments in mm.

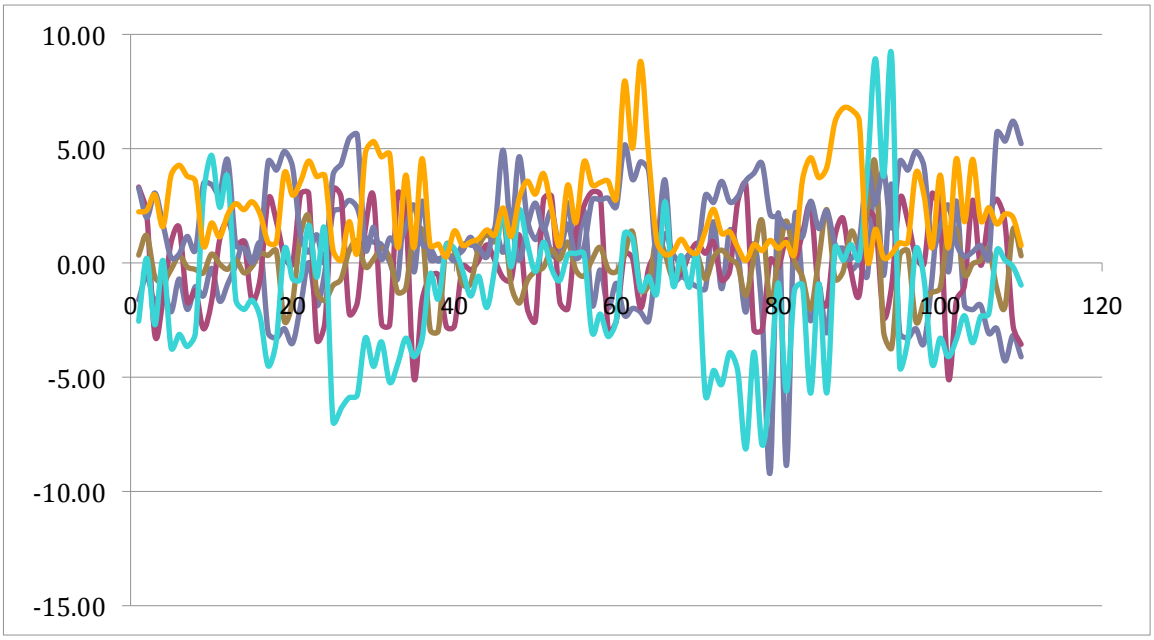

Raw data of chapter 5, values of Procrustes output for all the right and the left side mirrored models. (Different colors represent the differences in mms and degree in X,Y, and Z for all hemimandibles). X axis is case #, and Y axis is surface distance measurments in mm.

Appendix 2

Ethical approval application for the multi-center survey

For office use only **Research Ethics Reference Number:** **Date Received:**

King's College London (KCL) College Research Ethics Committees (CREC)
RESC/REP[1] Application Form A (for full RESC/REP meeting review)

Name of Researcher:	Abeer AlHadidi
Title of Study:	The use of a custom made atlas as a template for corrective surgeries of asymmetric patients
Name of review Subcommittee/Panel:	Biomedical Sciences, Dentistry, Medicine and Natural & Mathematical Sciences Research Ethics Subcommittee (**BDM RESC**)

Preparatory Notes: It is strongly advised that prior to completing this application form you consult the Staff & Student Research Project Briefing Page (www.kcl.ac.uk/innovation/research/support/ethics/applications/briefingpage.aspx) for advice on what kinds of projects require ethical approval from the KCL College Research Ethics Committee (CREC) system, the different application methods, as well as the appropriate application route to take. Once you have consulted the above and established the appropriate application procedure for your project, assuming you are clear that your project requires ethical review by CREC through the full Research Ethics Subcommittee (RESC)/Research Ethics Panel (REP) meeting review procedure, you should continue and complete the RESC/REP Application Form A accordingly.

Summary of application procedures for ethical review through the KCL CREC system:

The KCL CREC system has **two** different procedures for applying for ethical approval:

1. The online electronic application system for low risk research – submission of a short electronic online application form.
2. Full RESC/REP meeting review using the RESC/REP Application Form(s) – submission of the full Word application form(s).

Which of the two above application procedures you use will depend on factors such as the School you are applying from, your status as a researcher (eg. undergraduate, taught postgraduate, MPhil/PhD, staff member), and the risk level of the project in question. Certain applicants will be eligible to make an application through the online electronic application system for low risk research (which does **not** involve completing the RESC/REP Application Form A). In such cases, a shorter electronic application form is completed and submitted online, which then goes for review through an automated system.

Those applicants/projects not eligible for the online low risk electronic application system, will instead need to make an application using RESC/REP Application Form A, which will then be reviewed either at a full RESC or REP meeting. This form should be completed for all applications that are being submitted to the Biomedical Sciences,

[1] CREC is the over-arching committee responsible for the implementation of the College's research ethics system and procedures. The actual ethical review of studies that fall under the review remit of CREC is undertaken by three research ethics subcommittees (RESCs) and five research ethics panels (REPs): http://www.kcl.ac.uk/innovation/research/support/ethics/committees/index.aspx

Dentistry, Medicine and Natural & Mathematical Sciences (BDM) RESC, Psychiatry, Nursing & Midwifery (PNM) RESC, Social Sciences & Public Policy, Arts & Humanities, Law and King's Learning Institutes (SSHL) RESC and the five School based Research Ethics Panels (REPs). This form is for all projects that will involve collecting new data from human participants, or where the project will involve the further analysis of pre-existing data (where the data being accessed is either sensitive or could be used to identify specific individuals). In cases where a research project does not involve collecting new data from human participants or further analysis of pre-existing data, but for other reasons it has been agreed that the project requires ethical approval from CREC (for example the potential environmental, social impact/implications of the project on the local human community), the RESC/REP Application Form A should be completed.

Note for Undergraduate and Taught Postgraduate students from the Schools of Social Science & Public Policy, Arts & Humanities, Law and King's Learning Institute (KLI).
Undergraduate and Taught Postgraduate students from the Schools of Social Science & Public Policy, Arts & Humanities, Law and KLI may be eligible for the shorter, online electronic application system for low risk research. In the first instance consult the Low Risk Screening Tool to determine your eligibility for the online low risk system: www.kcl.ac.uk/innovation/research/support/ethics/applications/lowrisk/lowriskscreeningtool.aspx
Where your project is eligible for the online low risk system, you do **not** need to complete the RESC/REP Application Form(s).

The RESC/REP Application Form A is divided into four parts. Depending on the nature of your project, you will need to complete either some or all of these parts. Guidance on which parts need to be completed for which types of project is provided on the application form and in the associated guidelines. Failure to complete the required parts may lead to delays in the review of your application.

PART ONE: TO BE COMPLETED BY ALL APPLICANTS

Please read the guidelines before filling in the application form and refer to the specific guidelines about each section when completing the form. (www.kcl.ac.uk/innovation/research/support/ethics/applications/apply.aspx)

RESC/REP Meeting Dates, Deadlines & Submission Requirements: Refer to the Deadline Calendar (http://www.kcl.ac.uk/innovation/research/support/ethics/calendar.aspx) for the submission deadlines for your RESC/REP and the number of copies to submit (including electronic versions if applicable).

All applications should be submitted **by 5pm on the deadline day.**

All Research Ethics Subcommittee (RESC) applications should be submitted to the Research Ethics Office, 5.11 Franklin Wilkins Building, (Waterloo Bridge Wing), Waterloo Campus, King's College London, Stamford Street, London SE1 9NH.

All Research Ethics Panel (REP) applications should be submitted to Dan Butcher, K0.58 Ground Floor Strand Building, King's College London, The Strand, London WC2R 2LS.

Applicants from the Schools of Biomedical Sciences, Dentistry, Medicine, Natural & Mathematical Sciences, Nursing & Midwifery and the Institute of Psychiatry.	
Review Subcommittee:	**Tick One**
Biomedical Sciences, Dentistry, Medicine and Natural & Mathematical Sciences Research Ethics Subcommittee (**BDM RESC**)	√☐
Psychiatry, Nursing & Midwifery Research Ethics Subcommittee (**PNM RESC**)	☐

Applicants from the Schools of Social Science & Public Policy, Arts & Humanities, Law, KLI and Central Departments.	
NOTE: Applicants from the Schools of Social Science & Public Policy, Arts & Humanities, Law, KLI and Central Departments will either need to apply to the SSHL RESC **or** to the appropriate departmental REP, depending on the risk level of the project in question. To determine which risk level your project is, and consequently whether you will need to apply to the SSHL RESC or one of the five REPs, please see here: www.kcl.ac.uk/innovation/research/support/ethics/committees/sshl/index.aspx	
Review Subcommittee or Panel:	**Tick One**
Social Sciences & Public Policy, Arts & Humanities and Law Research Ethics Subcommittee (**SSHL RESC**) – Note that only 'high risk' applications should be submitted to SSHL RESC	☐
Arts & Humanities Research Ethics Panel (**A&H REP**) – non high risk applications only	☐
Education & Management Research Ethics Panel (**E&M REP**) – non high risk applications only	☐
Geography, Social Science, Health & Medicine Research Ethics Panel (**GSSHM REP**) – non high risk applications only	☐
Law & Department of Political Economy Research Ethics Panel (**Law REP**) – non high risk applications only	☐
War Studies Group Research Ethics Panel (**WSG REP**) – non high risk applications only	☐

IMPORTANT: RESEARCHER DECLARATION REGARDING APPLICATION REQUIREMENTS FOR THE UK HEALTH DEPARTMENTS' RESEARCH ETHICS SERVICE

Before completing the RESC/REP Application Form A all researchers must agree to the below declaration, to confirm that they have consulted the list of criteria in the Guidelines for RESC/REP Application Form A outlining the circumstances where ethical review from a Research Ethics Committee from within the UK Health Departments' Research Ethics Service may be required.

SECTION 1. APPLICANT DETAILS

1.1 RESEARCHER

Researcher's Name: Abeer AlHadidi

Researcher's Department & School: Dental institute

Status:

☐ **Undergraduate** ☐ **Taught Postgraduate** √**MPhil / PhD/ Specialist Doctorate** ☐ **Staff Research**

If Student:

Name of course/qualification: PhD

If Staff:

Researcher's Post:

1.2 CONTACT DETAILS

Email: (Please use your KCL email address where possible) Alhadidi.Abeer@kcl.ac.uk

Telephone number: (919) 966-1161

Address: School of dentistry, Manning drive & Columbia St. , CB#7450, Chapel Hill, NC 27599

1.3 SUPERVISOR - COMPLETE FOR ALL STUDENT PROJECTS (Including PhD)

Name of Supervisor: Richard Cook

Supervisor's Post: Senior Lecturer/Honorary Consultant

Supervisor's Department (if different to student): Biomaterials, Tissue Engineering & Imaging, Floor 17 Tower Wing Guy's site, London, SE1 9RT.

Supervisor's email address: richard_james.cook@kcl.ac.uk

1.4 OTHER INVESTIGATORS, COLLABORATORS, ORGANISATIONS

List any other investigators/collaborators involved with the study, and ensure that their role (e.g. collaborator, gatekeeper) and responsibilities within the project are explained. You should include any draft/preliminary approach letters to gatekeeper organisations and confirm that you will have permission letters available for inspection if requested for audit purposes.

NB: For other investigators/collaborators specify if their employer is not King's College London.

Dr. Lucia Cevidanes

University of Michigan

School of Dentistry
1011 N. University
Ann Arbor, MI 48109-1078
734-763-6933

E-mail: luciacev@umich.edu

and

Dr. Donald Tyndall, Professor, UNC-CH School of Dentistry

The University of North Carolina at Chapel Hill,

167 Brauer Hall,
UNC-CH School of Dentistry
UNC Chapel Hill
Diagnostic Sciences

SECTION 2. PROJECT DETAILS	
2.1 Project Title	The use of a custom made atlas as a template for corrective surgeries of asymmetric patients
2.2 Projected Start Date of Project This should be when you intend to start work with participants.	November 2012
2.3 Expected Completion Date of Project Please note: Ethical approval must cover the duration of the study, up to the end of data collection. See the guidelines for further details.	October 2013
2.4 Sponsoring Organisation Your sponsor will be assumed to be King's College London unless stated otherwise. **NB: Do not put 'N/A'.**	
2.5 Funder (e.g. self-funded, King's College London, ESRC, AHRB, EU)	Self-funded

2.6 OTHER INFORMATION RELATING TO RISK

Will the study place the researcher at any risk greater than that encountered in his/her daily life? (e.g. interviewing alone or in dangerous circumstances, or data collection outside the UK)**.**

Yes ☐ **No** √

If applicable:

Does the study involve the using a Medical Device outside of the CE mark approved method of use? (see guidelines) If you are using a medical device 'off label' (outside of the approved method of use) then a risk assessment needs to be completed. For further information on medical devices see the Medicines and Healthcare Products Regulatory Agency web pages: http://www.mhra.gov.uk/Publications/Regulatoryguidance/Devices/index.htm and http://www.mhra.gov.uk/Publications/Regulatoryguidance/Devices/GuidanceontheECMedicalDevicesDirectives/index.htm

Yes ☐ **No** √

If you have ticked yes to either of the above:

☐ **Yes,** and I have completed a risk assessment which has been co-signed by the Head of Department/ I have discussed the risks involved with my supervisor or Head of Department and agreed a strategy for minimising these risks.

2.7 OTHER PERMISSIONS, ETHICAL APPROVALS & CRIMINAL RECORDS BUREAU CLEARANCE REQUIRED

ANOTHER REVIEWING BODY/PERMISSIONS - Are any other approvals by another reviewing body (including other ethics committees, gatekeepers and peer review) required? If yes, give details and say when these will be obtained. In cases where ethical or legal permissions are required from local organisations or gatekeepers, it is the researchers' responsibility to ensure that these have been obtained prior to commencing the study. If they have already been obtained you should provide a copy of the approval with the application otherwise you will need to supply it when ready.

YES √ **NO** ☐ An ethical approval application has been submitted to the University of North Carolina at chapel hill to cover the USA sites participating in this project. - Appended

CRIMINAL RECORDS BUREAU – If you think Criminal Records Bureau clearance might be necessary for your project, ensure you have contacted the Criminal Records Bureau directly to confirm whether or not this is the case. You will need to ensure you have the appropriate and necessary Criminal Records Bureau clearance for your study prior to commencing recruitment or data collection. You may wish to consult with the relevant 'gatekeeper' organisation in which you are undertaking the study with respect to this issue.

If Criminal Records Bureau clearance is required for your study, please confirm that clearance will be sought before commencement of the project. **YES** ☐ **NA** √

SECTION 3. AIMS, OBJECTIVES & NATURE OF STUDY

Provide the academic/scientific justification of the study as well as detailing and explaining the principal research question, objectives and hypotheses to be tested.

Applications to the BDM and PNM RESC should include a full list of references/citations to back up the academic/scientific justification of the study. Note that sufficient information must be provided to allow the Committee to locate any sources to which you refer.

Asymmetry occurs in 40% of dentofacial patients with Class III or long face problems, and in 28% of mandibular deficiency patients[1]. Normally, the right side of the human face is slightly larger, and when an asymmetric mandible is observed in patients with mandibular deficiency or excess, there is a >80% chance that the chin will be off to the left[2, 3]. When excessive vertical growth of the maxilla occurs, left and right asymmetries are equally probable. Furthermore, correcting maxillary asymmetry usually involves moving one side up (and perhaps the other side down) to correct a canted occlusal plane and usually is done in conjunction with mandibular surgery. For the maxillary component of asymmetry surgery, downward movement of the maxilla is in the stability problematic category.

Quantification of right and left side differences is not possible in 2D imaging, and it is also a challenge in 3D analysis. Definition of the midsagittal plane[4], registration of the mirrored image[5], and measurement of the asymmetry [6]demand further investigation. While we anticipate that all subjects present some degree of asymmetry, we have no information on the degree to which asymmetrical corrections contribute to undesirable maxillo-mandibular rotations. In the surgical correction of dentofacial deformity, it frequently is necessary to change ramus length more on one side than the other, even in patients whose major problem is not an overt asymmetry. It is not possible to measure this accurately on cephalometric radiographs or with conventional mirroring techniques. Because there was no appropriate way to measure asymmetry, data on asymmetry was previously limited.

Facial asymmetry is a complex clinical entity that comprises two main components, a shape and a positional component. During growth, the shape discrepancies lead to compensatory positional differences resulting in disturbing the harmony of the maxillofacial complex. Clinicians need to diagnose both shape and positional components of the asymmetry prior to the design and execution of the corrective surgery. The use of conventional mirror images does not adequately guide surgeons on the correction of facial asymmetries because it does not compensate for the positional component.

We have previously shown that the choice of mirroring orientation (mid-sagittal plane vs arbitrary plane and registration) affects the 3D localization of asymmetry[7]. In the current study, we present the application of registration methods to correct positional components of facial asymmetry and use 3D templates to aid in the surgical planning. AtlasWerks, used for patient-specific atlas building in this project, is an open-source (BSD license) software package for medical image atlas generation. AtlasWerks atlas formation is based on greedy fluid registration in a diffeomorphic deformation setting [8]. This well- known viscous fluid model accommodates large-distance, nonlinear deformations of small subregions of the target image. Corrective surgery was simulated using the atlas computed as a template, using 3DSlicer (http://www.slicer.org/).

The purpose of this study is to evaluate the utility of a patient-specific atlas as a template for corrective surgeries for patients suffering from mandibular asymmetry. This template will enhance the predictability and reproducibility of the surgical outcomes of those corrective surgeries.

References :

1. Severt TR, Proffit WR. The prevalence of facial asymmetry in the dentofacial deformities population at the university of north carolina. Int J Adult Orthodon Orthognath Surg 1997;12(3):171-6.

2. Proffit WR, Fields HW,Jr, Moray LJ. Prevalence of malocclusion and orthodontic treatment need in the united states: Estimates from the NHANES III survey. Int J Adult Orthodon Orthognath Surg 1998;13(2):97-106.

3. Proffit W, Bailey L, Phillips C, Turvey TA. Long-term stability of surgical open-bite correction by le fort I osteotomy. The Angle Orthodontist JID - 0370550 0829.

4. Prima S, Ourselin S, Ayache N. Computation of the mid-sagittal plane in 3D images of the brain. Computer Vision â€" ECCV 2000 2000:685-701.

5. Rohr K. Landmark-based image analysis : Using geometric and intensity models. Dordrecht; Boston: Kluwer Academic Publishers; 2001. ID: 421870969.

6. Nanna Glerup. Asymmetry measures in medical image analysis. Department of Innovation IT, University of Copenhagen; April 29, 2005.

7. AlHadidi A, Cevidanes L, Mol A, Ludlow J, Styner M. Comparison of two methods for quantitative assessment of mandibular asymmetry using cone beam computed tomography image volumes. Dento Maxillo Facial Radiology JID - 7609576 1013(0250-832; 0250-832).

8. Joshi S, Davis B, Jomier M, Gerig G. Unbiased diffeomorphic atlas construction for computational anatomy. NEUROIMAGE} 2004};23}(Suppl. 1}):S151-S160}.

SECTION 4. STUDY DESIGN/METHODOLOGY, DATA COLLECTION & ANALYSIS

Provide a brief outline of the step-by-step procedure of your proposed study in lay language, in no more than 1 page where possible. Extensive research protocols that have been prepared for funding bodies or similar organisations are likely to be of too technical a nature, or will provide more information than is necessary for ethical review/approval. Please ensure you focus on using non-technical lay language throughout, outlining clearly and simply the methodology to be used in your study. (For applications to the BDM and PNM RESCs it is strongly recommended that you provide the Committee with a flowchart diagram demonstrating step by step the process of the study. An example of a flow chart that can be used can be seen below.)

A multi-centre online survey using "Qualtrics" will be conducted to gain clinical feedback of upto 100 surgeons/orthodontists comparing both treatment planning and treatment outcomes. Clinicians from the Universities of Michigan, UNC, and KCL will be invited by e mail to participate in the survey. Clinicians responding to the e mail invitation will be asked to compare images of skeletal surface models of actual outcomes to models of simulated outcomes in reference to preoperative models of each patient. The 2 scenarios are going to be randomized without any indication that they belong to the same patient. In essence that makes the survey contain "40 patients". Potential participants are going to be invited to the survey by email and will be sent the link for the survey upon their agreement to participate. We plan a second reminder e mail shot at 1 month to boost participation and a second reminder 1 month later if necessary. No other communications are proposed. The custodian of the data is Dr. Cevidanes Uof Michigan. The original data was acquired under a previous study (**Study #:** 03-1647_ Former IRB Number DENT-2063), wherein, each patient consented for CBCT x ray acquisition during their routine treatment planning and its subsequent user for these developmental purposes. This project is a secondary data analysis of that dataset, by new clinicians and colleagues. Data used in this project is de-identified with no HIPPA identifiers.

- Invitation Email:

"Dear Dr.,

You have been invited to participate in a research comparing the surgical outcome of two surgical techniques for the correction of mandibular asymmetry. The following is a link to an electronic survey that has preoperative and post operative models for 40 patients. After each set of preoperative and post operative figures, you will be asked to evaluate the surgical correction for symmetry of certain areas in the mandible and also and will be asked to give an overall appraisal of the surgical outcome. The survey will take almost 30 minutes and does not have to be completed in one sitting. The questionnaires will be analyzed through Qualtrics©. Your participation is voluntary and you will not receive any financial compensation for answering the survey. Your participation and answers will remain completely confidential, but they will be aggregated to the results.

The team will be happy to share the methodology and the results of the project once the responses are collected and analyzed.

P.S Do not hesitate to contact the research team if you have any questions through

Abeer Alhadidi (email: Alhadida@dentistry.unc.edu)

We appreciate your time and expert opinion.

Many thanks,
The research team

The following is anynomous link to the survey, however in real time each participant is going to get and individualized link for further analysis of results

https://unc.qualtrics.com/SE/?SID=SV_6gMVmQc3FE4H2u0

Study Flowchart:-

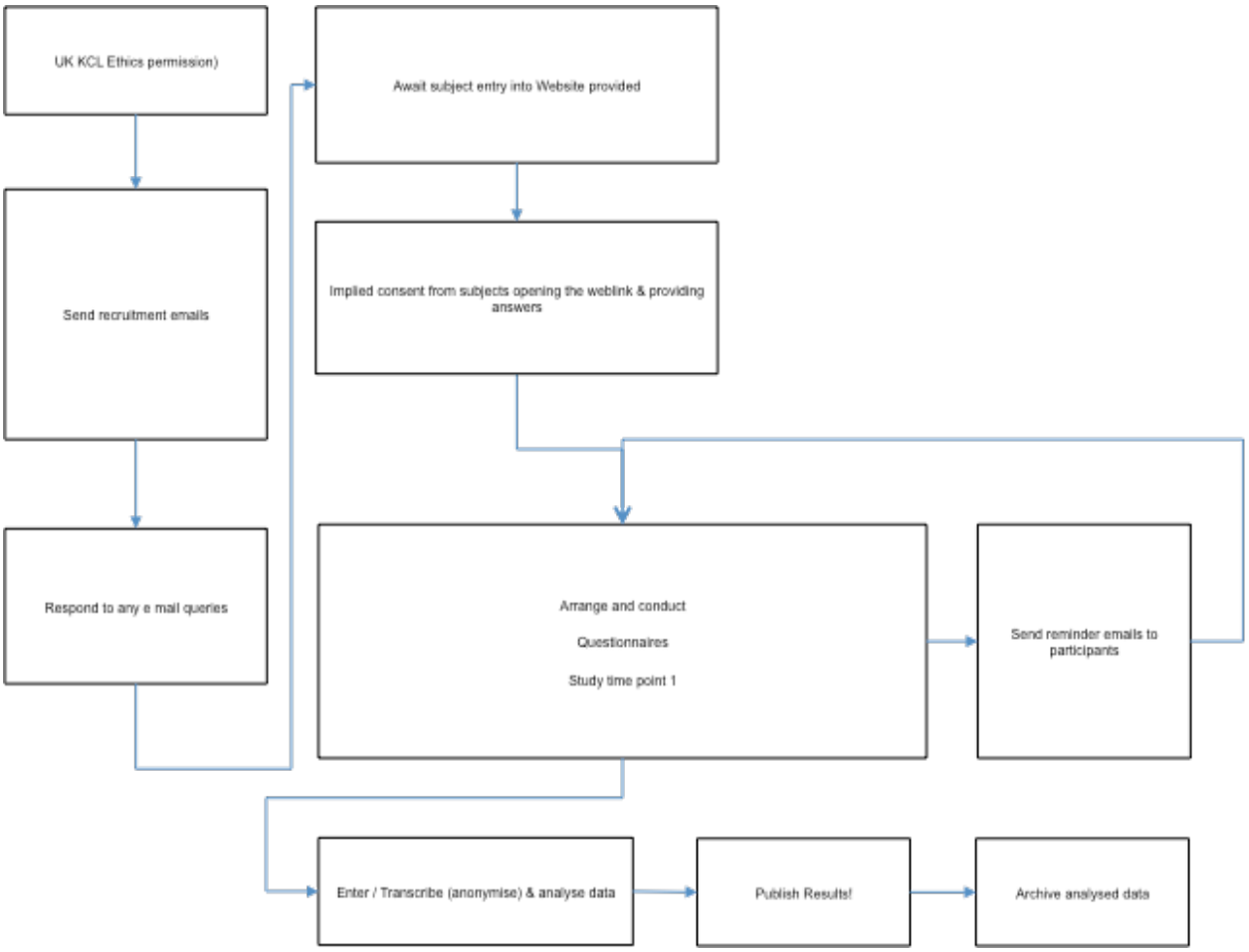

PART TWO: PROJECTS INVOLVING PRIMARY DATA COLLECTION

THIS PART OF THE APPLICATION FORM MAY NOT APPLY TO ALL PROJECTS. See below for guidance.	
DOES YOUR PROJECT INVOLVE THE COLLECTION OF NEW/PRIMARY DATA FROM HUMAN PARTICIPANTS? No	
YES	If you answer **'yes'** to the above question: **Part Two** of the application form is specifically tailored towards your project. Please continue below to **Section 5: Risk Checklist,** completing all sections within **Part Two:**
NO	If you answer **'no'** to the above question, but your study involves the further analysis of pre-existing data (where the data is sensitive or could lead to the identification of individuals from the dataset), continue directly to **Part Three**.

SECTION 5. RISK CHECKLIST

Complete the checklist ticking 'Yes' to any of the questions relevant to your study. The associated section of the Guidelines for RESC/REP Application Form A provides further details on the circumstances where it is appropriate to tick 'Yes' for each question.

Note that where you have ticked '**Yes**' to a question below, you will need to specifically address the ethical issues raised in Section 7.3 of the application form. See the guidelines for further details on what kinds of issues might need addressing, as well as how to decide whether you need to tick 'Yes' or 'No' to the various questions in the Risk Checklist.

		Yes	No
A	Does the study involve **participants who are particularly vulnerable** or unable to give informed consent or in a dependent position (e.g. vulnerable children, your own students, over-researched groups, people with learning difficulties, people with mental health problems, young offenders, people in care facilities, including prisons)?	☐	√
B	Will participants be asked to take part in the study without their consent or knowledge at the time or will **deception** of any sort be involved (e.g. covert observation of people in non-public places)?	☐	√
C	Is there a risk that the highly sensitive nature of the research topic might lead to **disclosures** from the participant concerning their own involvement in illegal activities or other activities that represent a threat to themselves or others (e.g. sexual activity, drug use, or professional misconduct)?	☐	√
D	Could the study induce **psychological stress or anxiety**, or produce humiliation or cause harm or negative consequences beyond the risks encountered in normal life?	☐	√
E	Does the study involve **imaging techniques** such as MRI scans or ultrasound?	☐	√
F	Does the study involve sources of **non-ionising radiation** (e.g. lasers)?	☐	√
G	Does the study involve **physically intrusive procedures**, use of bodily materials, or DNA/RNA analysis? (see Guidelines for RESC/REP Application Form B for more details)	☐	√

If 'yes', continue below and ensure you have also completed the RESC/REP Application Form B form, in accordance with the associated Guidelines:

		Yes	No
G1:	Does the study involve the use or collection of **bodily materials** or **tissue** from a **human being?** (see Guidelines for RESC/REP Application Form B for more details)	☐	☐
G2:	Does the study involve **DNA or RNA** analysis of any kind? (see Guidelines for RESC/REP Application Form B for more details)	☐	☐

G3:	Are substances or products to be administered (such as **food substances** or **drugs**)? (see Guidelines for RESC/REP Application Form B for more details)	☐	☐
G4:	Does the study involve **only moderately** intrusive procedures (taking less than 40ml blood, collecting bodily waste, cheek swabs)? (see Guidelines for RESC/REP Application Form B for more details)	☐	☐
G5:	Are invasive, intrusive or potentially harmful procedures **not already covered** by items **G1** – **G4** to be used in this study? (see Guidelines for RESC/REP Application Form B for more details)	☐	☐

SECTION 6. PARTICIPANTS

6.1 PROJECTED NUMBER OF PARTICIPANTS

Where relevant, (for example because the age ranges of participant samples differ) duplicate and complete the text below for each sub-population of your study.

Number: maximum of 100 participants **If applicable:** How many will be male and female . N/A

Justification for the sample size: Between the centres conducting the trial, the maximum number of candidates can be 100 – we are hoping for a 50% response rate but the minimum for statistical significance is 10.

The lower age limit will be assumed to be 16 years of age unless specified otherwise. If an upper age limit is needed you must provide a justification. N/A

Upper Age Limit: **Lower age limit:**

6.2 SELECTION CRITERIA

The subject pools are identified as Trainers and Training Dental Specialists in Orthodontics and maxillofacial surgery...the two professional groups who will be likely to use the programme and its output data in treatment planning the clinical interventions for their future patients. No other society groups are appropriate for the study. Any clinician within the dental schools involved, who is training to be or has become a specialist in facial reconstruction and rebuilding will be a potential subject – as these are the only groups likely to use the method if validated.

6.3 RECRUITMENT

Describe how participants will be (i) identified and (ii) approached.

(i) Participants will be identified from current appropriate departmental staff lists in the participating institutions.

(ii) Approach will solely be via an e mail as outlined and in the text above. Potential subjects will be invited to log into a web address to conduct the survey – indicating consent. Partially filled surveys will be rejected as reversal of consent and data eliminated. All responses are anonymous.

SECTION 7. ETHICAL CONSIDERATIONS

7.1 INFORMED CONSENT

Describe the process you will use to ensure your participants are freely giving fully informed consent to participate. This will **always** include the provision of an information sheet and will normally require a consent form unless it is a purely self-completion questionnaire based study or there is a justification for not doing so (this must be clearly stated). Templates for Information Sheets and consent forms are available here (www.kcl.ac.uk/innovation/research/support/ethics/applications/apply.aspx) and should be filled in and modified where necessary.

The study is a purely self-completion questionnaire based study, participation being invited via e mail (as above), describing the process but intentionally omitting the hypothesis to eliminate subject bias. Subjects going to the website do so of their own will and therefore indicate consent to provide answers to the questions posed. Only completed forms will be analysed and incomplete survey data will be rejected as implying withdrawal of consent. The submitted data is anonymous and will be analysed by number of answers to questions rather than individual's patterns of answering – making it impossible to identify individuals or groups from within the data pool. Consequently, as the invitation e mail and website are self-leading and self explanatory, no further documentation is thought necessary in this case by the applicants. Further information is available upon request by e mail to Dr Alhadidi as noted in the invitation e-mail above.

7.2 RIGHT OF WITHDRAWAL

(Participants should be able to withdraw from the research process at any time and also should be able to withdraw their data if it is identifiable as theirs and should be told when this will no longer be possible (e.g. once it has been included in the final report). Please describe the exact arrangements for withdrawal from participation and withdrawal of data depending on your study design).

No recipient is obliged to complete or enter into the study, however submission of a completed survey is taken as consent for data analysis and final publication. Similarly, incomplete submissions will be discarded, being interpreted as withdrawal of consent and all data eliminated from the analyses.

7.3 RISK CHECKLIST – Questions ticked as 'Yes'

Where you have ticked **'Yes'** on the **Risk Checklist** in **Section 5**, provide details of relevant qualifications and experience **with reference to the issues mentioned in those questions of the Risk Checklist**. This **must** include the researcher and/or supervisor as well as other collaborators (if applicable) involved in those sections marked as presenting risk. **(**Do not submit a c.v.)

You must also specifically address the ethical issues raised from those sections here:

NB:

If you ticked 'Yes' to any point in G1 – G5 of the checklist, you must also complete and submit the RESC/REP Application Form B form.

7.4 OTHER ETHICAL ISSUES

Please consider what other ethical issues there are that have not already been addressed elsewhere in the form. **Please note that all research projects have some ethical considerations, even if this only relates to how confidentiality will be maintained. PLEASE DO NOT LEAVE THIS SECTION BLANK.**

Further, **if applicable**, add the professional code of conduct you intend to follow in your research.
http://www.kcl.ac.uk/innovation/research/support/ethics/training/codes.aspx

No recipient is obliged to complete or enter into the study, however submission of a completed survey is taken as consent for data analysis and final publication. Similarly, incomplete submissions will be discarded, being interpreted as withdrawal of consent and all data eliminated from the analyses. As there ins no direct meeting of participants and researchers and all data is anonymised, the researchers feel there are no other ethical issues raised by the study design.

7.5 BENEFITS & RISKS

Describe any expected benefits to the research participant (e.g. will participants receive a copy of the final report?): There are no benefits to the participants other than contribution to research within Kings & allied Colleges.

Describe any possible risks to the research participant: For example:

What is the potential for adverse effects resulting from study participation, e.g.

- **participants suffering pain, discomfort, distress, inconvenience or changes to lifestyle.**
- **sensitive, embarrassing or upsetting topics being discussed/raised.**

Identify the potential for each of above and state how you will minimise risk and deal with any untoward incidents/adverse reactions**.**

Given the survey nature of the design of the anonymous trial no such opportunities exist.

7.6 CRIMINAL OR OTHER DISCLOSURES REQUIRING ACTION

Is it possible that criminal or other disclosures requiring action (e.g. evidence of professional misconduct) could be made during this study?

YES ☐ **NO** √

If yes, detail what procedures will be put in place to deal with these issues. In certain circumstances there may be a need for disclosures to be communicated beyond the research team. The limits to confidentiality must be made clear to participants at the outset. The Information Sheet should make it clear to potential participants under which circumstances action may be taken by the researcher.

SECTION 8. FINANCIAL INCENTIVES, EXPENSES AND COMPENSATION

8.1 Will travelling expenses be given? If yes, this should be stated on the Information Sheet

YES ☐ **NO** √ no travel involved

8.2 Is any reward, apart from travelling expenses to be given to participants? If yes, please provide details and a justification for this. It is recommended that participants are informed of the compensation on the information sheet.

YES ☐ **NO** √

8.3 Is the study in collaboration with a pharmaceutical company or an equipment or medical device manufacturer? If yes, please give the name of the company and indicate what arrangements exist for compensating patients or healthy volunteers for adverse effects resulting from their participation in the study (in most cases, the Committee will only approve protocols if the pharmaceutical company involved confirms that it abides by APBI (The Association of the British Pharmaceutical Industry) guidelines. A copy of the indemnification form (Appendix Form Two) should be submitted with the application.

YES ☐ **NO** √

8.4 No fault compensation scheme If your study is based in the UK, you **must** offer the No-fault compensation scheme to participants unless there is a clear justification for not doing so. (If this is the case, this must be stated and you should bear in mind that the RESC/REP reserves the right to make this a condition of approval).

YES, I am making the scheme available to participants √

NO, the study is based outside the UK and so the scheme is not applicable ☐

NO, the study is within the UK but the No-fault compensation scheme is not offered for the following reason:

PART THREE: PROJECTS INVOLVING FURTHER ANALYSIS OF PRE-EXISTING DATA

THIS PART OF THE APPLICATION FORM MAY NOT APPLY TO ALL PROJECTS. See below for guidance.	
DOES YOUR PROJECT INVOLVE THE FURTHER ANALYSIS OF PRE-EXISTING (SENSITIVE/IDENTIFIABLE) DATA, WHERE THIS DATA WAS ORIGINALLY OBTAINED FROM HUMAN PARTICIPANTS? Yes	
YES	If you answer **'yes'** to the above question: **Part Three** of the application form is specifically tailored towards your project. Note that not all projects involving the further analysis of pre-existing data (sometimes referred to as secondary data analysis) require formal ethical review through the CREC system. For example, projects analysing secondary data in the public domain (such as books, journals and other literary resources) do not require CREC ethical approval. Similarly, projects analysing non-sensitive, fully anonymous/anonymized data do not require CREC ethical approval. Further guidance can be found here: http://www.kcl.ac.uk/innovation/research/support/ethics/training/existingdata.aspx If your project involves the further analysis of pre-existing data, where this data could be deemed sensitive, or could lead to the identification of an individual from the original set of participants, you will need to complete all sections within **Part Three**. If so please continue to **Section 9** below.
NO	If you answer **'no'** to the above question continue directly to **Part Four** below.

SECTION 9. FURTHER ANALYSIS OF PRE-EXISTING (SENSITIVE/IDENTIFIABLE) DATA

9.1 ACCESS TO THE DATA

Provide details of any permissions that may be required to gain access to the dataset to be analysed. Where such permissions are required from individuals, institutions or bodies who own/are responsible for the dataset, provide written evidence that such permissions have been obtained. Although such permission can be obtained prior to gaining a CREC ethical approval, note that full access to and analysis of the data should not commence until full ethical approval has been granted from CREC.

If there are any limitations or conditions imposed by the owners of the data related to how the data is accessed, stored, analysed, please outline these as appropriate.

The custodian of the de-identified 3D virtual surface models to be included in this study is Dr, Cevidanes, one of the primary mentors at the USA sites. Dr. Cevidanes has granted access to this data that contains no direct or indirect identifying information.

9.2 DATA TO BE ACCESSED & DATA ANALYSIS

Provide details of exactly what sort of pre-existing data will be accessed, whether the data is quantitative (e.g. interviews, focus group transcripts, field note observations) or qualitative (e.g. statistical data), how it was collected from participants at the time, and how the data will be analysed.

Anonymous CBCT scans from the original study will be used to build the virtual 3D models used for the online survey.

9.3 CONSENT FROM ORIGINAL PARTICIPANTS

Clarify what consent was taken from the participants at the time the data was collected, and outline how the consent taken is in accordance with the way in which you will be accessing, analysing and (where appropriate) publishing the results of your own analysis.

All subjects signed informed consents at the time of data acquisition, The consent forms clarified that interpretation of CBCT data sets would be performed for academic purposes and would not include contain any individual identifiers, during data analysis and publication.

9.4 SENSITIVE NATURE OF DATA

Where the data to be accessed is deemed 'sensitive' please outline why you believe this to be the case, and any associated ethical issues you feel this might raise. Provide details as to procedures/protocols in place to address these issues.

The original CBCTs are part of patients' records however those are anonymized and coded for this secondary analysis.

9.5 ANONYMITY/CONFIDENTIALITY OF DATA

Provide details of the degree of anonymity of the data you will have access to. If the data you will access contains identifiable data, state what this data will be. If the data you will access has been anonymized, clarify how this has been done (bear in mind that combinations of demographic data can still identify individual participants from the original dataset, particularly for small sample sizes).

Virtual models used for the survey has been anonymized and given number codes. This information is saved in a master excel sheet stored in the principle investigator's computer. That document and the computer are both password protected.

PART FOUR: TO BE COMPLETED BY ALL APPLICANTS

THIS PART OF THE APPLICATION FORM MUST BE COMPLETED BY ALL APPLICANTS

SECTION 10. DATA PROTECTION, CONFIDENTIALITY, DATA AND RECORDS MANAGEMENT, DISSEMINATION

10a. Confirm that all processing of personal information related to the study will be in full compliance with the Data Protection Act 1998 (DPA) *including the Data Protection Principles).*

YES √☐ **NO** ☐

Where your study involves processing personal information outside the European Economic Area, confirm that you will ensure compliance with the DPA. See the following page of the Governance section of the website for guidance on the DPA: http://www.kcl.ac.uk/aboutkings/governance/dataprotection/guidance.aspx

YES ☐ **N/A** √

10b. What steps will be taken to ensure the confidentiality of personal information? Give details of anonymisation procedures and of physical and technical security measures. Please note: to make data truly anonymous **all information** that could potentially identify a participant needs to be removed in addition to names. **NB: Personally identifiable data held on mobile devices must be encrypted** : http://www.kcl.ac.uk/college/policyzone/index.php?id=222

Data used in this project is de-identified with no HIPPA identifiers. Virtual models used for the survey has been anonymized and given number codes. This information is saved in a master excel sheet stored in the principle investigator's computer. That document and the computer are both password protected.

10c. Who will have access to personal information relating to this study? Confirm that any necessary wider disclosures of personal information (for instance to colleagues beyond the study team, translators, transcribers, auditors etc) have been properly explained to study participants. Further guidance on the above issues can be found at the following link: http://www.kcl.ac.uk/innovation/research/support/ethics/training/feedback.aspx

Only the Principle investigator will have access to the responses of the survey. http://software.unc.edu/qualtrics/ can only be accessed with a student specific user name and password.

10d. Data and records management responsibilities during the study. The 'Principal Investigator' is the named researcher for staff projects and the supervisor for student projects.

I confirm that the Principal Investigator will take full responsibility for ensuring appropriate storage and security for all study information including research data, consent forms and administrative records and that, where appropriate, the necessary arrangements will be made in order to process copyright material lawfully.

YES √☐ **NO** ☐

Further, provide a **specific physical location** at which research data will be stored **during** the study.
School of Dentistry. The University of North Carolina at Chapel Hill

10e. Data management responsibilities <u>after</u> the study.

State **how long** study information (including research data, consent forms and administrative records) will be retained for:

3 years

State in **what format(s)** the information will be retained (for example, as physical and/or electronic copies):

Electronic copy

State the **specific physical location where** the data will be stored (for example, where within King's College London):

School of Dentistry. The University of North Carolina at Chapel Hill

See the Information Management pages of the website for further guidance on how research data should be managed during and after your project: http://www.kcl.ac.uk/library/using/info-management/rdm/res-guide.aspx and http://www.kcl.ac.uk/library/using/info-management/rdm/index.aspx

Will data be archived for use by other researchers?

NO √

YES (in anonymised form) ☐ If you intend to retain or share **anonymised** data with other researchers, you must make this clear on the information sheet.

YES (in identifiable form) ☐ If you intend to retain or share **identifiable** data with other researchers, you must ensure that these arrangements are detailed in the Information Sheet and that explicit participant consent to do so will be obtained.

10f. Research dissemination

Dissemination plans:

If you intend that the research findings will be disseminated, please give details of how you will achieve this. Forms of dissemination might include an examined dissertation/thesis, peer reviewed journal, internal report, public report, press release to media, conference/seminar presentation. Where possible it is best practice to report back research findings to the participants, and ensure that findings are made available to a wide audience.

This work is going to be a part of a PhD dissertation. The findings are hopefully going to be hopefully published in peer-reviewed journals and presented in national and international meetings in the fields of Radiology, Orthodontics, Surgery, and dental research.

Other ethical issues related to dissemination:

Provide details of any other ethical issues or risks that may arise as a result of the dissemination of the research findings. For example, if there are any anticipated limitations or restrictions on how the research findings might be disseminated or published (perhaps imposed by researcher funders, sponsors or collaborating bodies) provide details. If the dissemination of findings might present risks to the participants, outline these risks and how they will be minimised.

There are no particular ethical issues when it comes to dissemination of this work.

SECTION 11. AUTHORISING SIGNATURES

11.1 RESEARCHER/APPLICANT

I undertake to abide by accepted ethical principles and appropriate code(s) of practice in carrying out this study. The information supplied above is to the best of my knowledge accurate. I have read the Application Guidelines and clearly understand my obligations and the rights of participants, particularly as regards obtaining valid consent. I understand that I must not commence research with human participants until I have received full approval from the ethics committee.

Signature … A.M.H **…… Date……15-10-2012…….**

11.2 SUPERVISOR AUTHORISATION FOR STUDENT PROJECTS (including PhD)

I confirm that I have read this application and will be acting as the student researcher's supervisor for this project. The proposal is viable and the student has appropriate skills to undertake the research. Participant selection and recruitment procedures, including the Information Sheet(s) to be provided and the manner of obtaining informed consent, are appropriate and the ethical issues arising from the project have been addressed in the application. I understand that research with human participants must not commence without full approval from the ethics committee.

If applicable:

The student has read an appropriate professional code of ethical practice √

The student has completed a risk assessment form ☐

Name of Supervisor: Dr Richard Cook

Signature 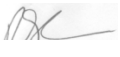 **Date 25/10/12**

Name of Medical Supervisor:

Medical Supervisor's MDU/MPS (or other insurance provider) number:

……

Signature of Medical Supervisor:

……. **Date**……..

11.4 DECLARATION BY COLLEGE RADIATION PROTECTION OFFICER (if appropriate – see the Guidelines)

For studies involving use of non-ionising radiation: Declaration by College Radiation Protection Officer who has given advice on exposure risks.

I am satisfied that the type and degree of radiation exposure are appropriate for the research being undertaken, and that appropriate procedures are in place to minimise any associated risk:

Signature of College Radiation Protection Officer:

……. **Date**……..

SECTION 12. INFORMATION SHEET AND CONSENT FORM

Remember to submit your information sheet(s) for participants and consent form (if necessary) with your application. Failure to do so will cause delays to your applications. A template Information Sheet and Consent Form can be found here: www.kcl.ac.uk/innovation/research/support/ethics/applications/apply.aspx

Information Sheet(s) and Consent Form(s) for participants should be composed according to the guidelines available at the above page. **The text in red should be deleted or modified as appropriate. If the language in the template is not suitable for your intended participant group it can be modified**. Where a consent form is not required (e.g. submission of an anonymous questionnaire which implies consent to the data being used), the template Consent Form may be deleted. Please refer to the guidelines for further information.

Submission Checklist	**Tick box** (where applicable)
RESC/REP Application Form A	√
RESC/REP Application Form B (where applicable)	
Information Sheet	
Consent Form (where applicable)	
Recruitment documents (e.g. recruitment email, posters, flyers or advertisements)	√
Measures to be used (e.g. questionnaires, surveys, interview/focus group topic guides/schedules/example questions as appropriate)	
Approach letters to 'gatekeeper' organisations (where applicable)	
Evidence of any other approvals or permissions (where applicable)	
Appendices (where applicable) UNC Ethics Ctee statement of Agreement of Ethical position of the study.	√

THE UNIVERSITY of NORTH CAROLINA at CHAPEL HILL

To: Lucia Cevidanes , Orthodontics

From: Office of Human Research Ethics

Date: 9/06/2012

RE: Notice of IRB Exemption
Exemption Category: 4.Existing data, public or deidentified,2.Survey, interview, public observation
Study #: 12-1685

Study Title: The use of a custom made atlas as a template for corrective surgeries of asymmetric patients

This submission has been reviewed by the Office of Human Research Ethics and was determined to be exempt from further review according to the regulatory category cited above under 45 CFR 46.101(b).

Study Description:

Purpose: The purpose of this study was to evaluate the utility of an individualized atlas as a template for corrective surgeries for patients suffering from mandibular asymmetry.

Participants: Cone beam CT scan of patients who undergone corrective surgeries for mandibular asymmetry

Procedures (methods):

An online clinical survey (using Qualtrix) will show separately the virtual craniofacial surface models of the actual outcome of jaw surgery and the simulated outcome of surgery for 20 patients.

The survey questions are designed to determine the clinician's appraisal of the overall

correction of asymmetry and the correction of specific anatomic regions as well.

Regulatory and other findings:

A limited waiver of HIPAA is granted for the purpose of identifying records containing PHI to be included in Exempt Category 4 research. According to this category of exemption, no direct or indirect identifying information may be recorded and included with your data. Please be advised that you may need to clear your activities with the custodian of the records before accessing PHI.

Investigator's Responsibilities:

If your study protocol changes in such a way that exempt status would no longer apply, you should contact the above IRB before making the changes. The IRB will maintain records for this study for 3 years, at which time you will be contacted about the status of the study.

Researchers are reminded that additional approvals may be needed from relevant "gatekeepers" to access subjects (e.g., principals, facility directors, healthcare system).

CC:
Don Tyndall, Diagnostic Science and General Dentistry

Appendix 3

Preoperative models of patients included in the survey:

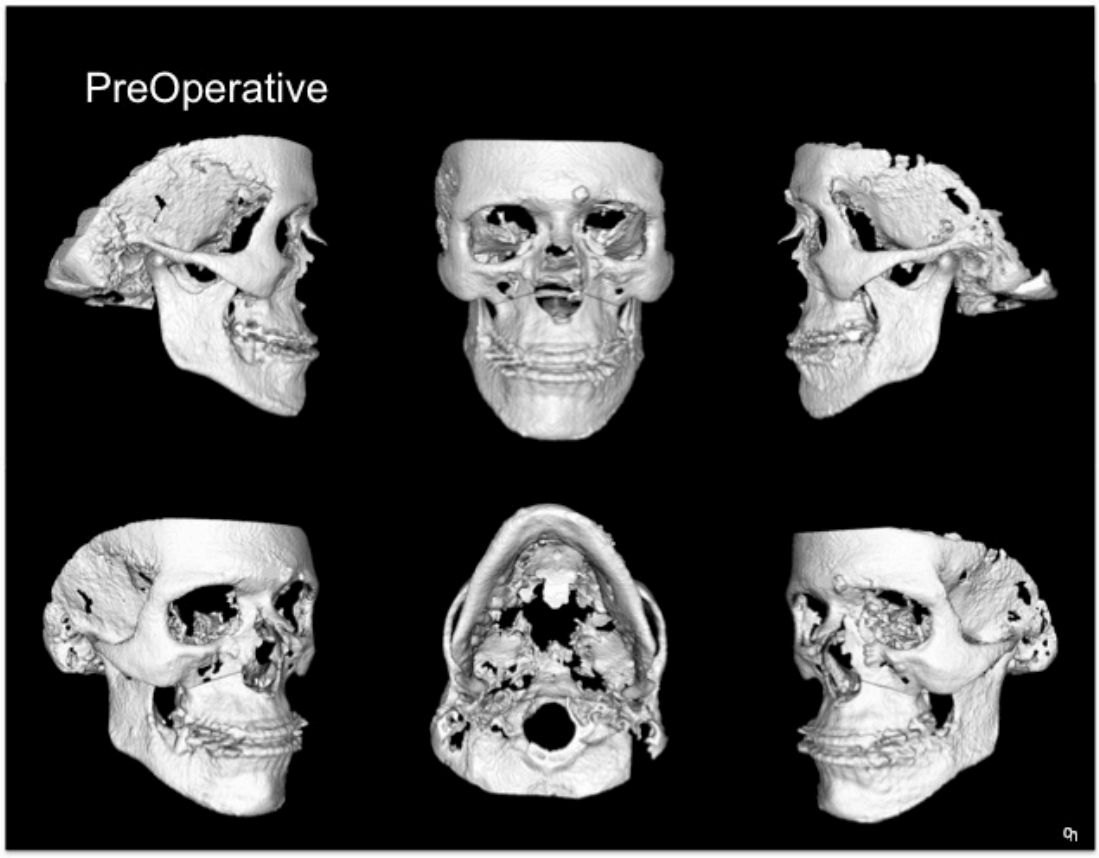

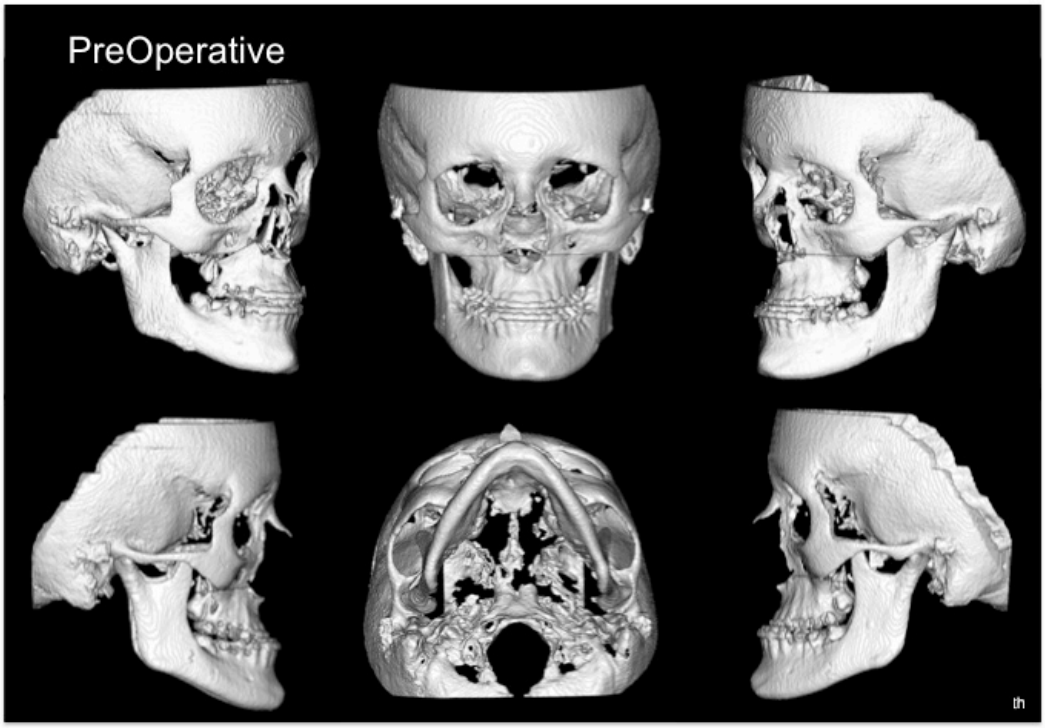
PreOperative
th

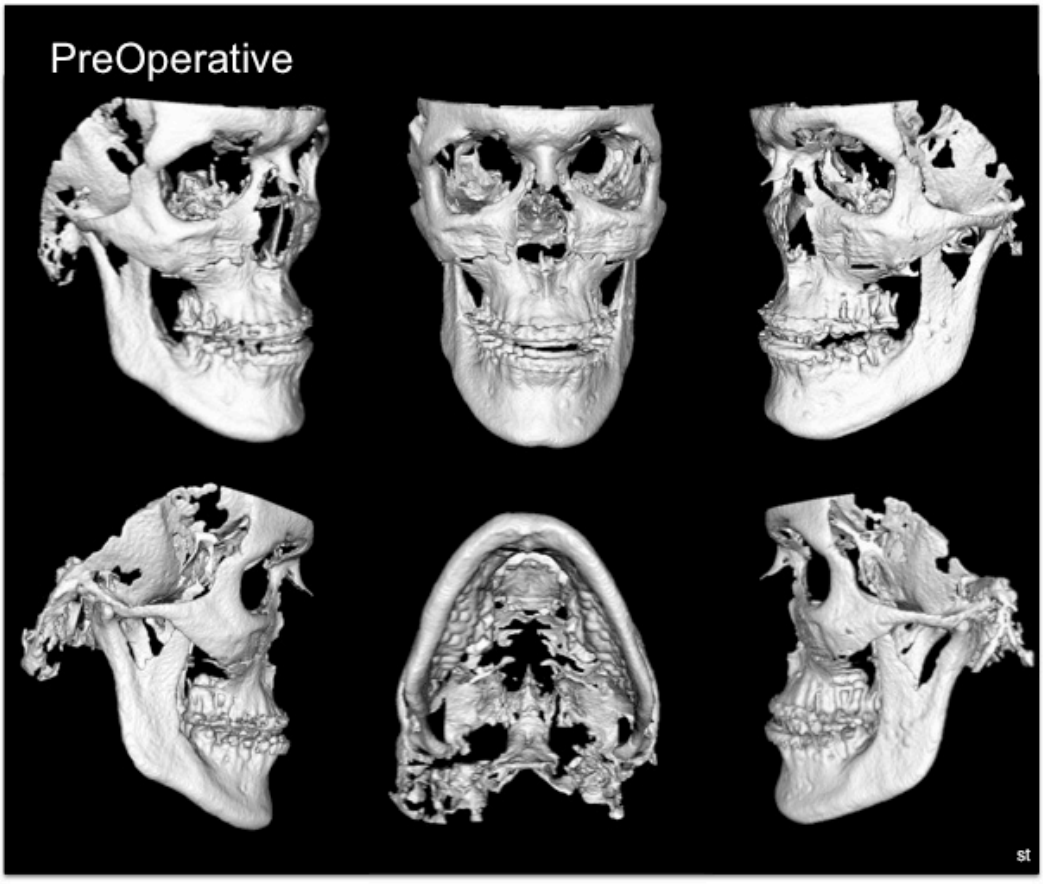
PreOperative
st

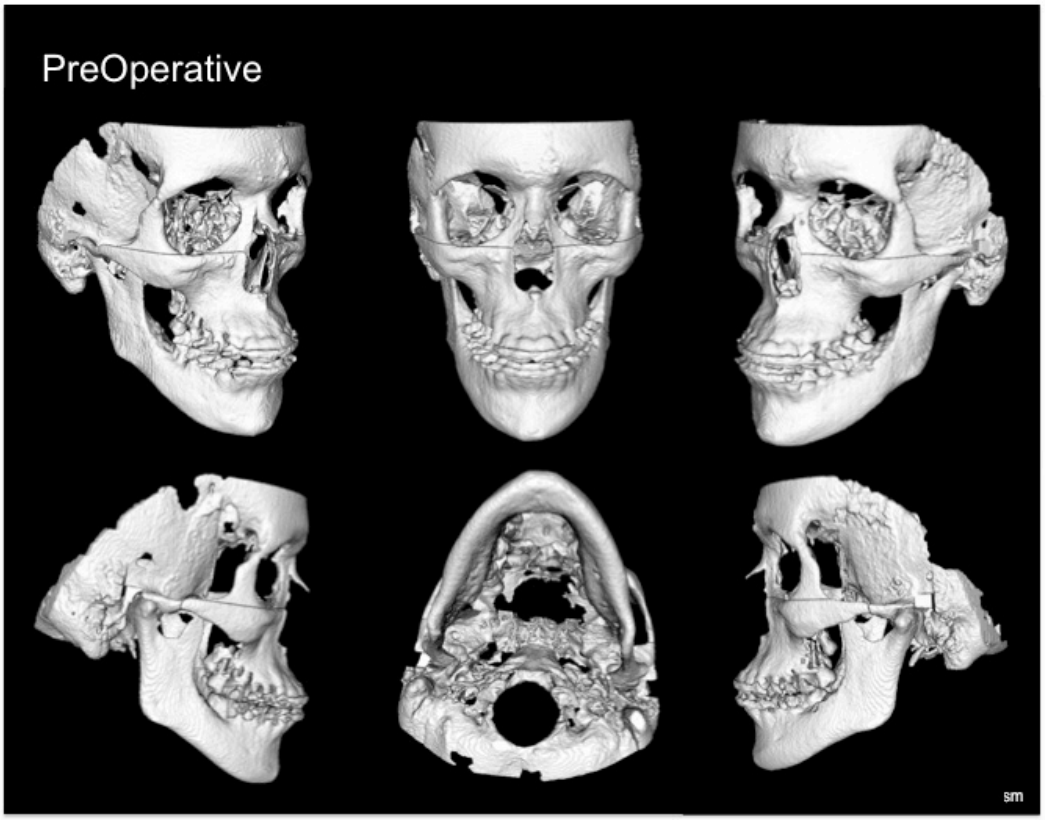
PreOperative
sm

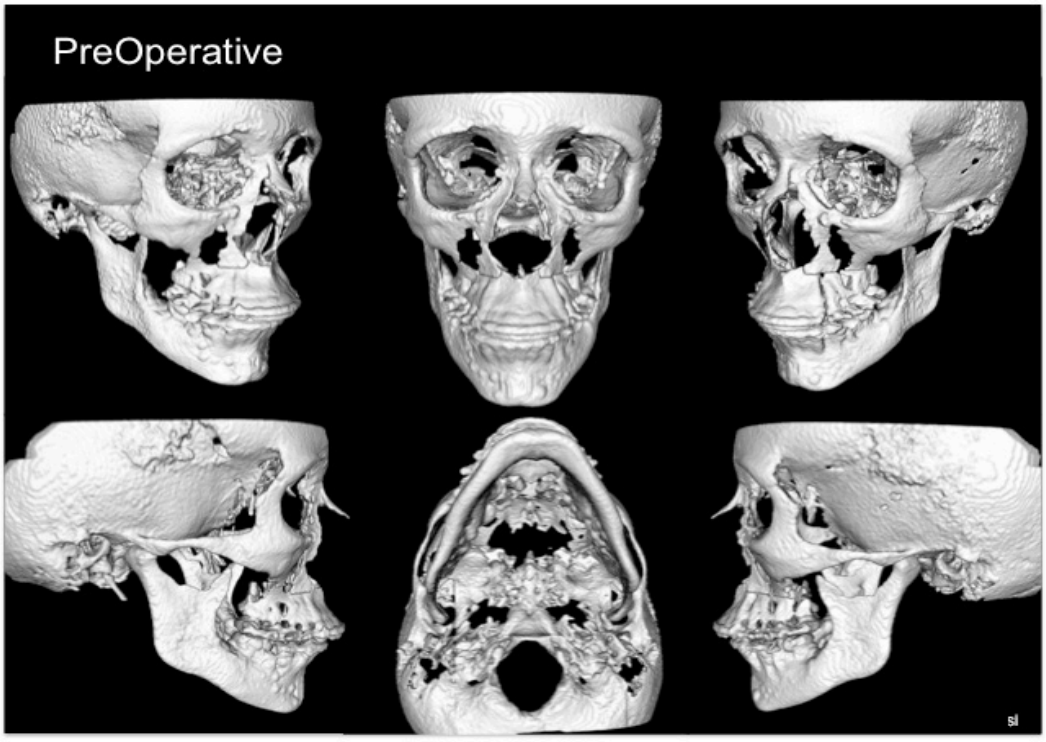
PreOperative
sl

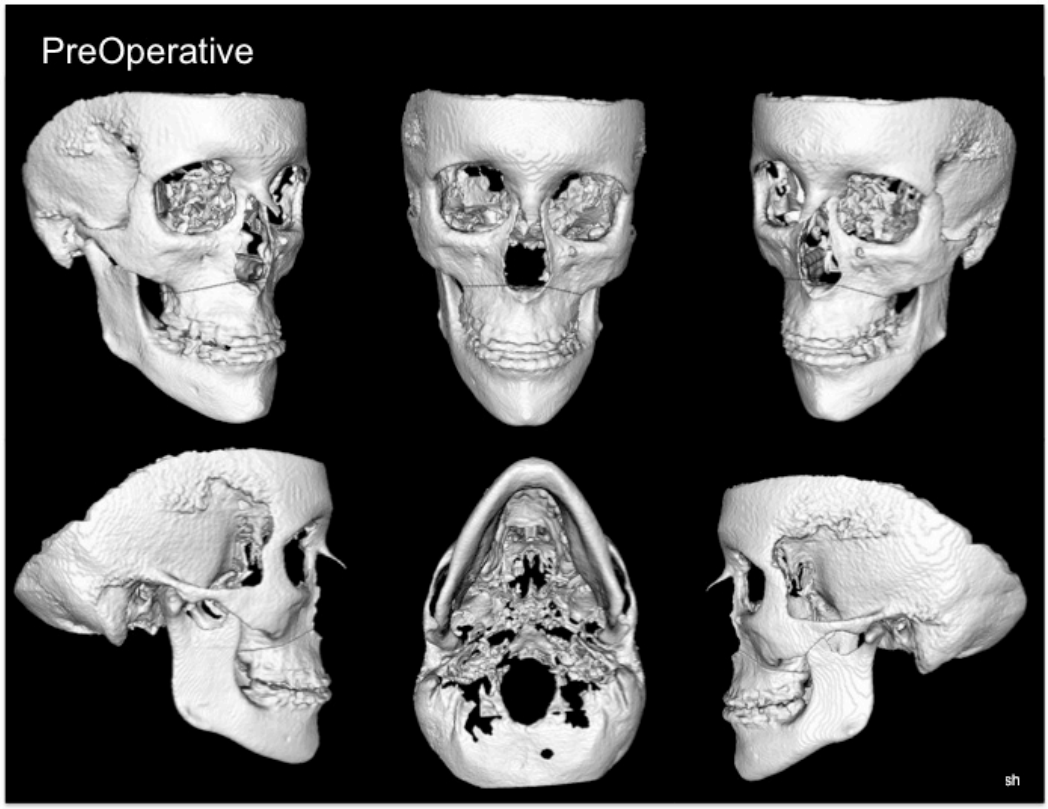
PreOperative
sh

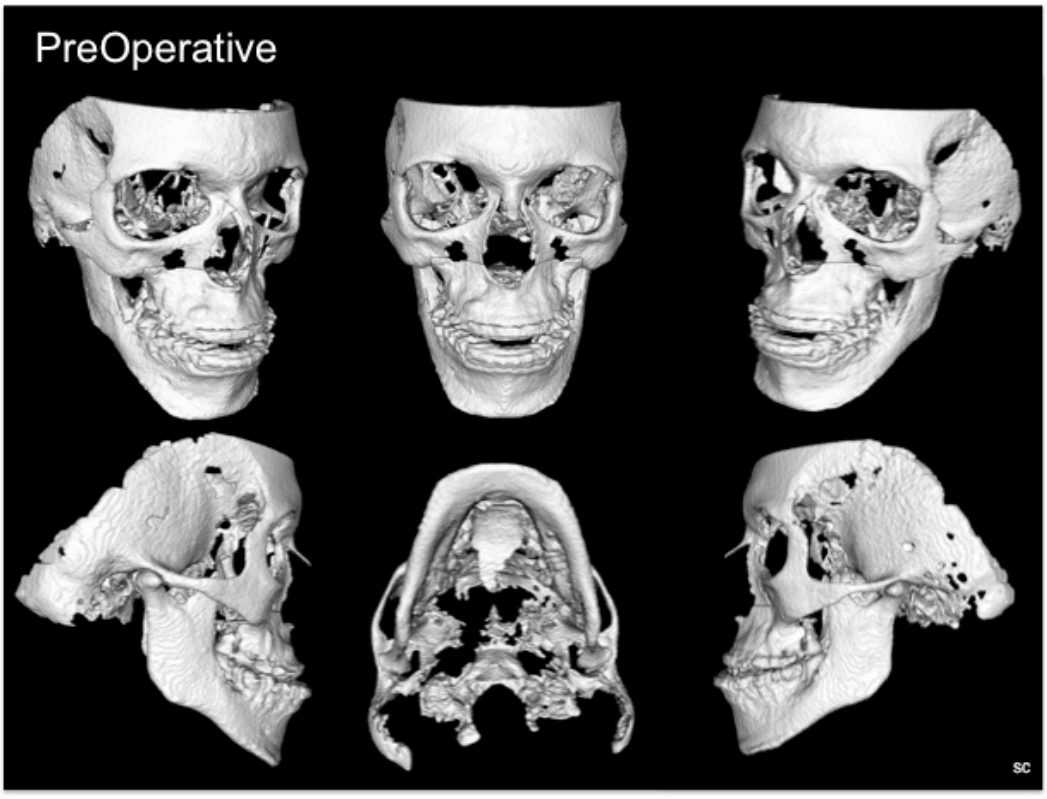
PreOperative
sc

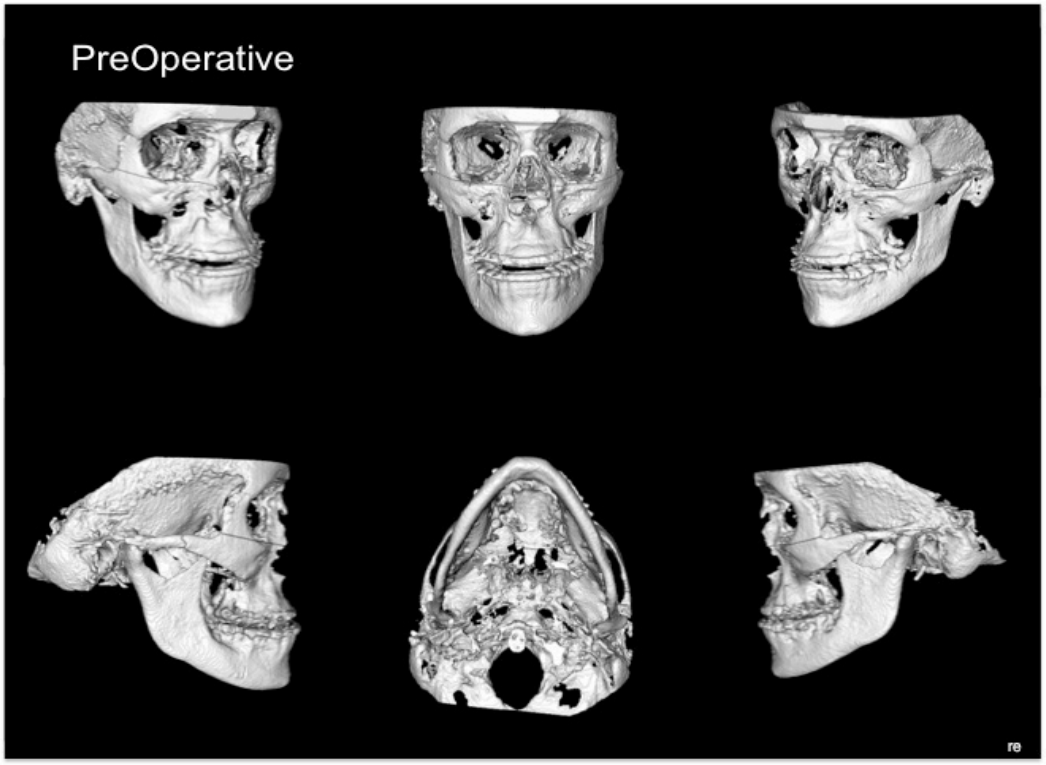
PreOperative
re

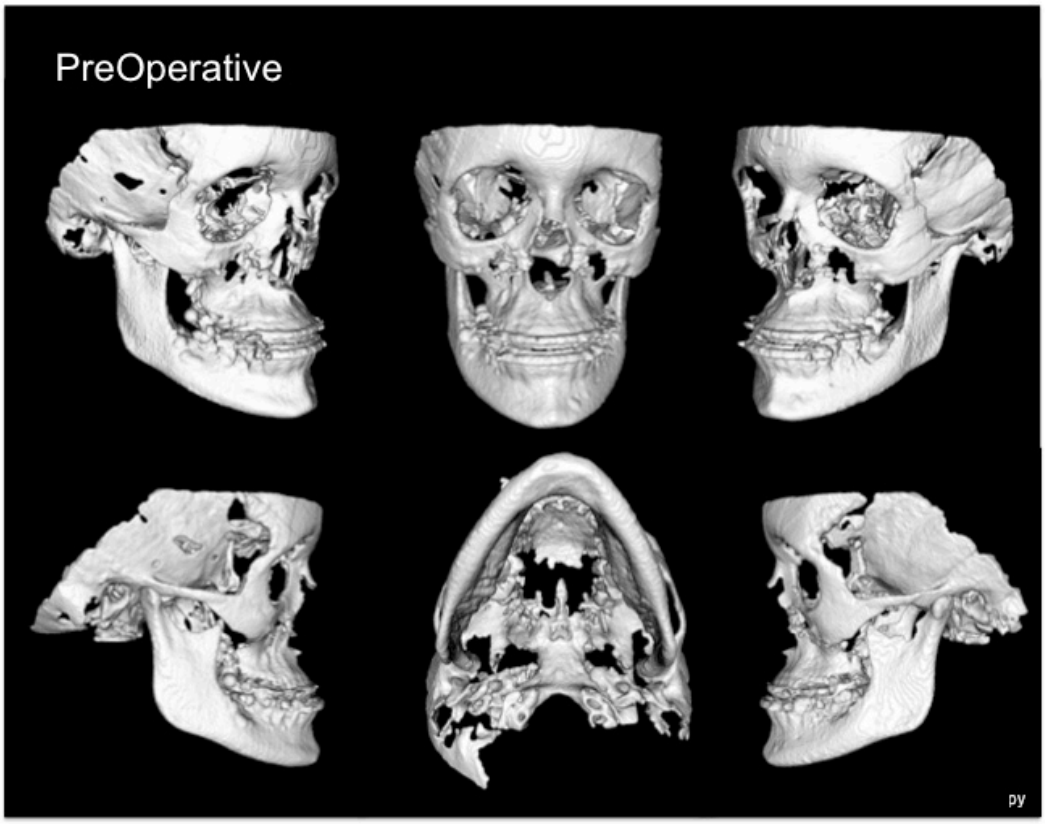
PreOperative
py

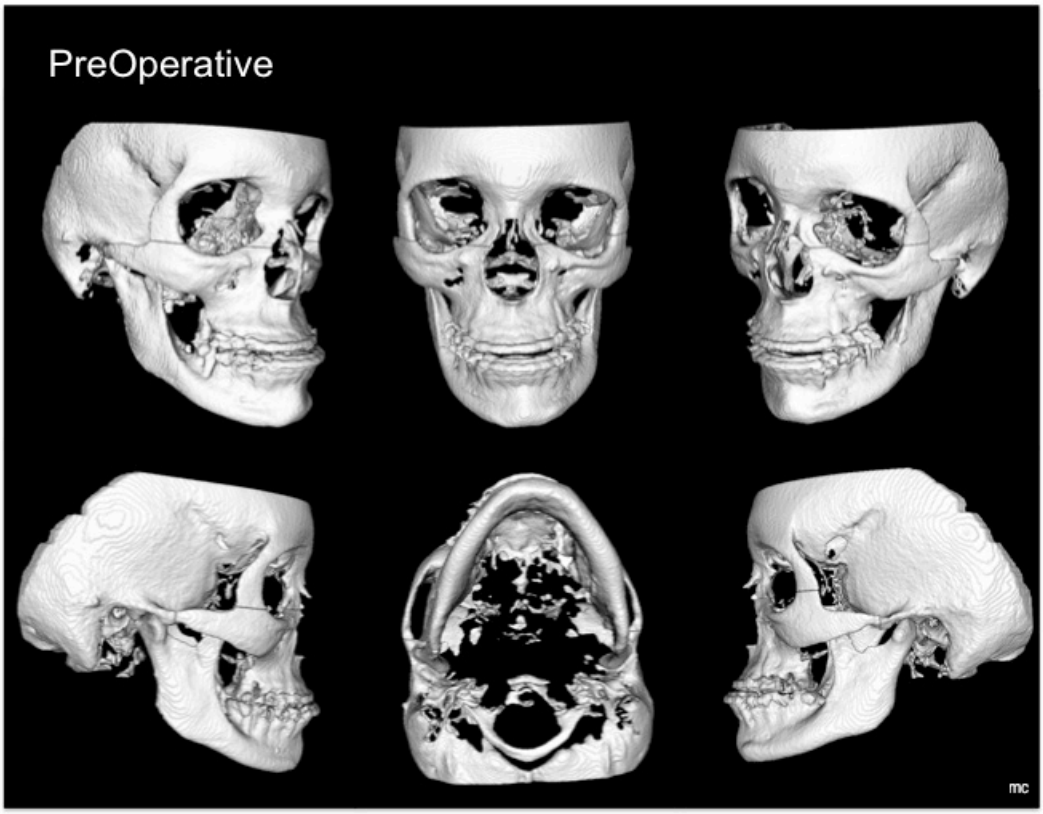
PreOperative
mc

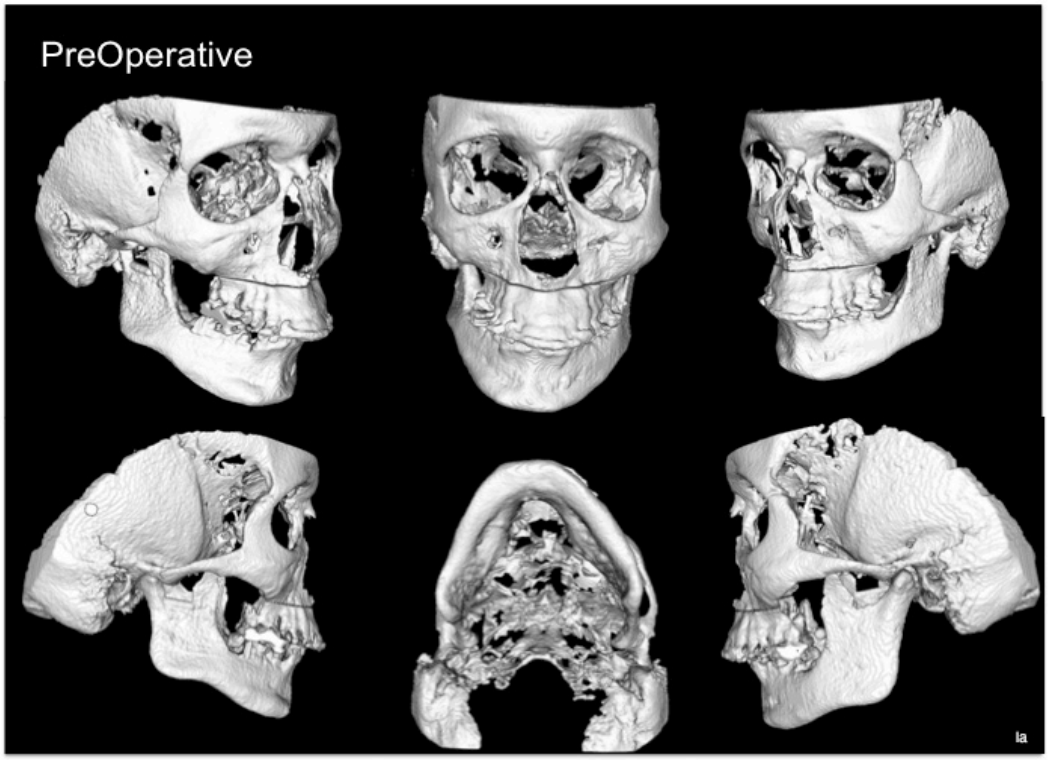
PreOperative
la

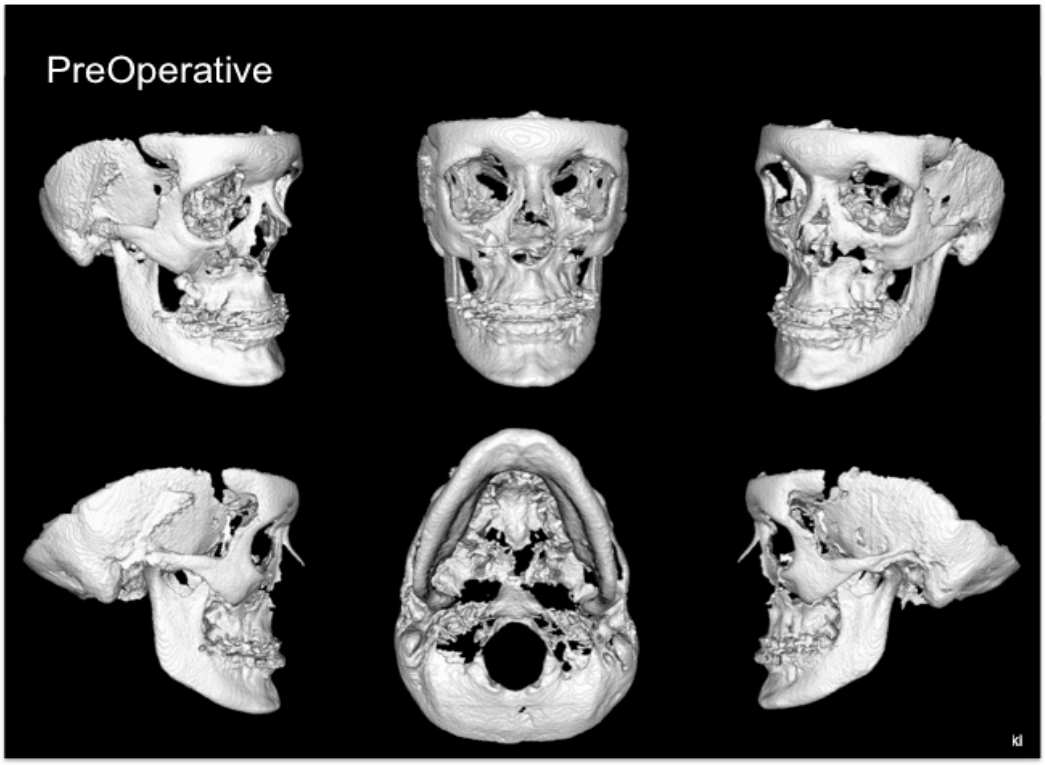
PreOperative
kl

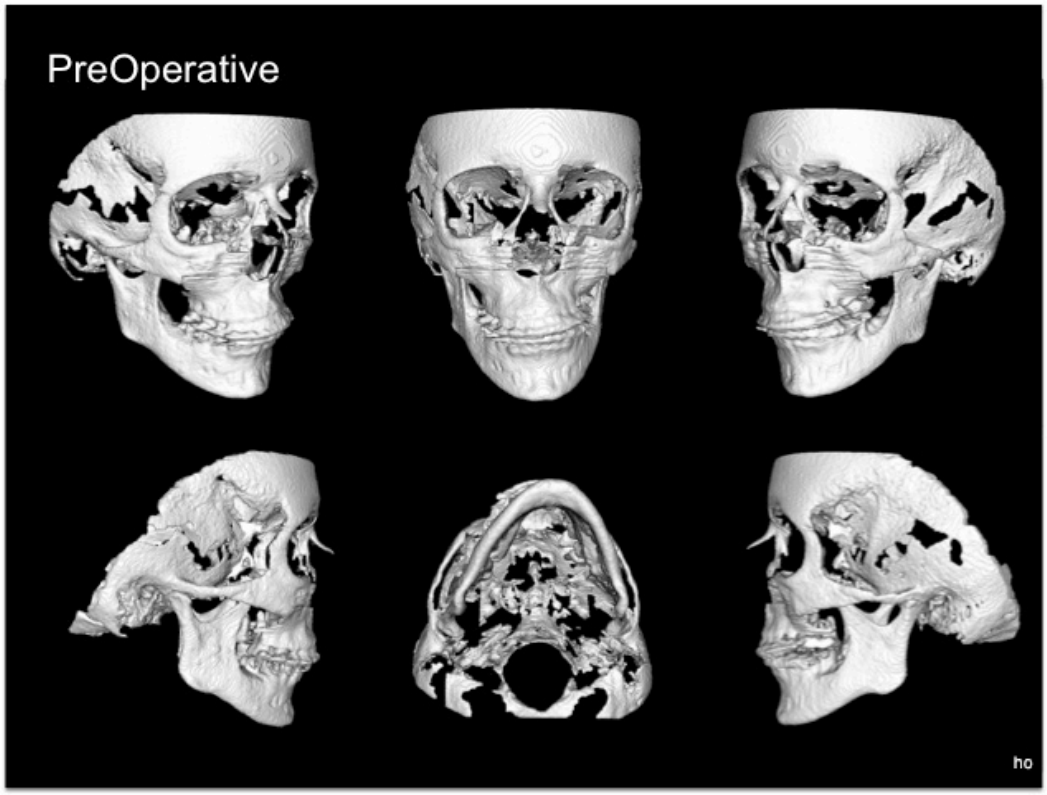
PreOperative
ho

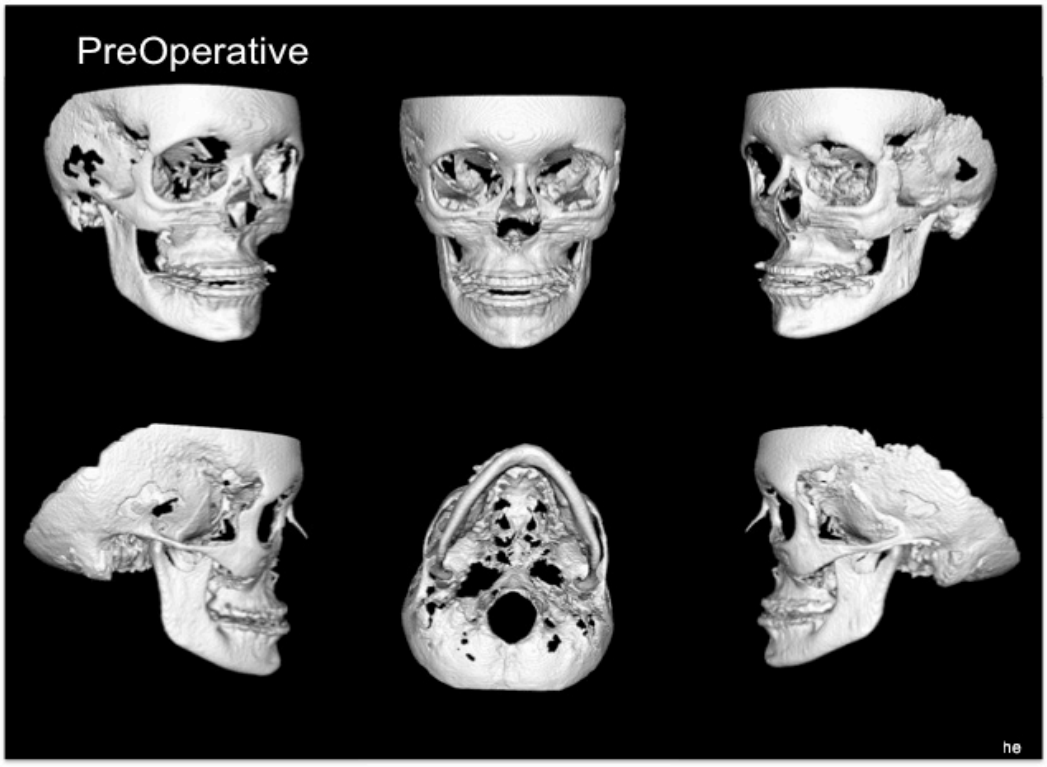
PreOperative
he

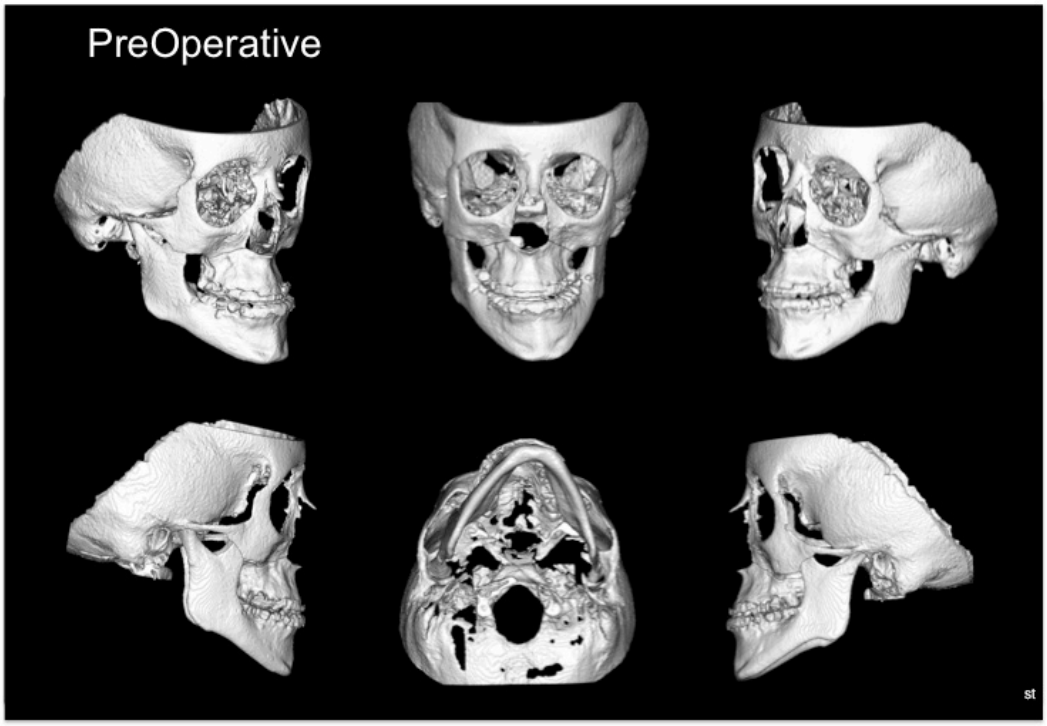
PreOperative
st

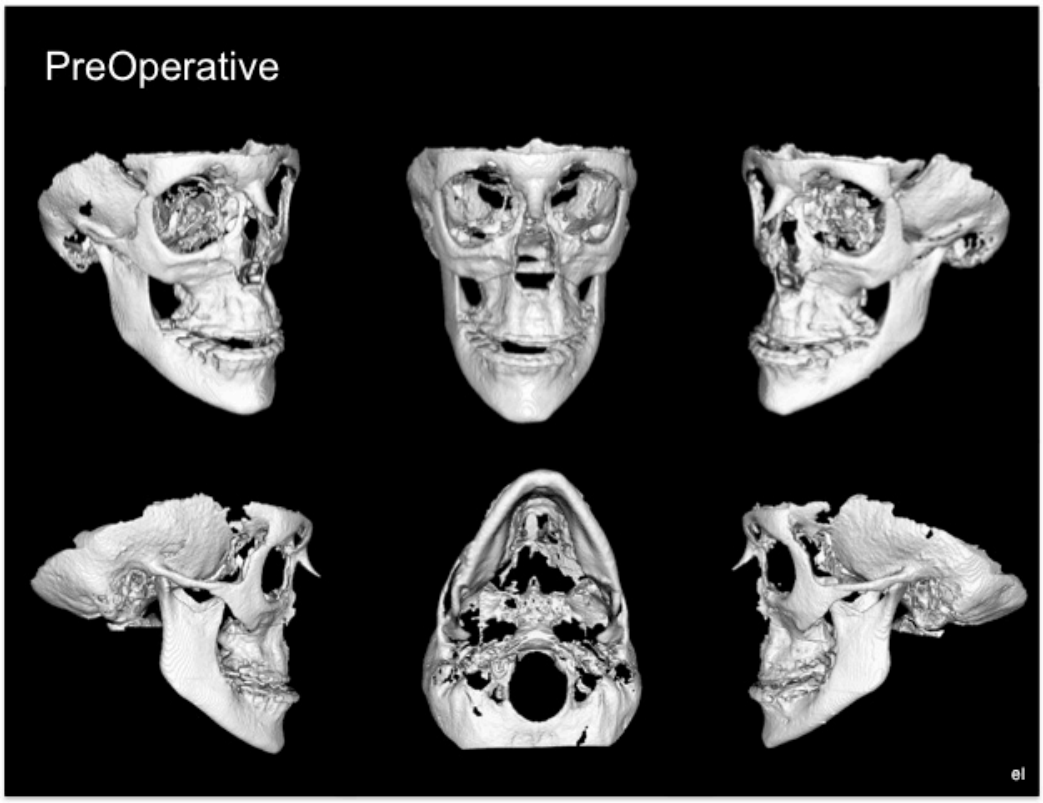
PreOperative
el

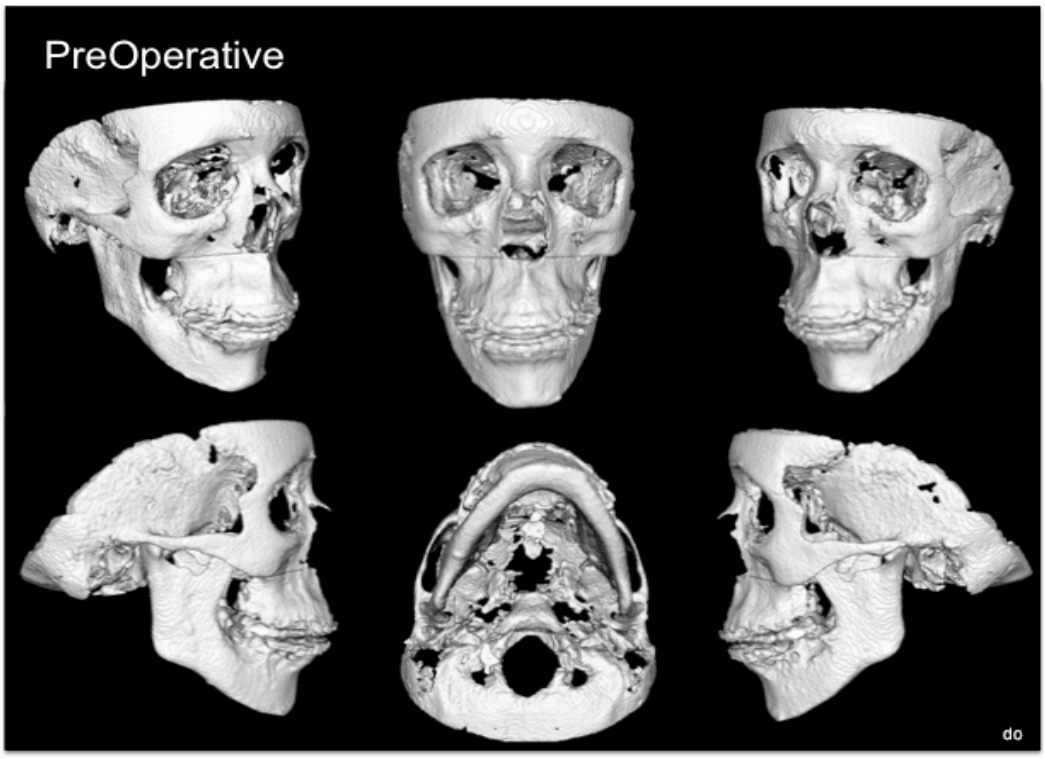
PreOperative
do

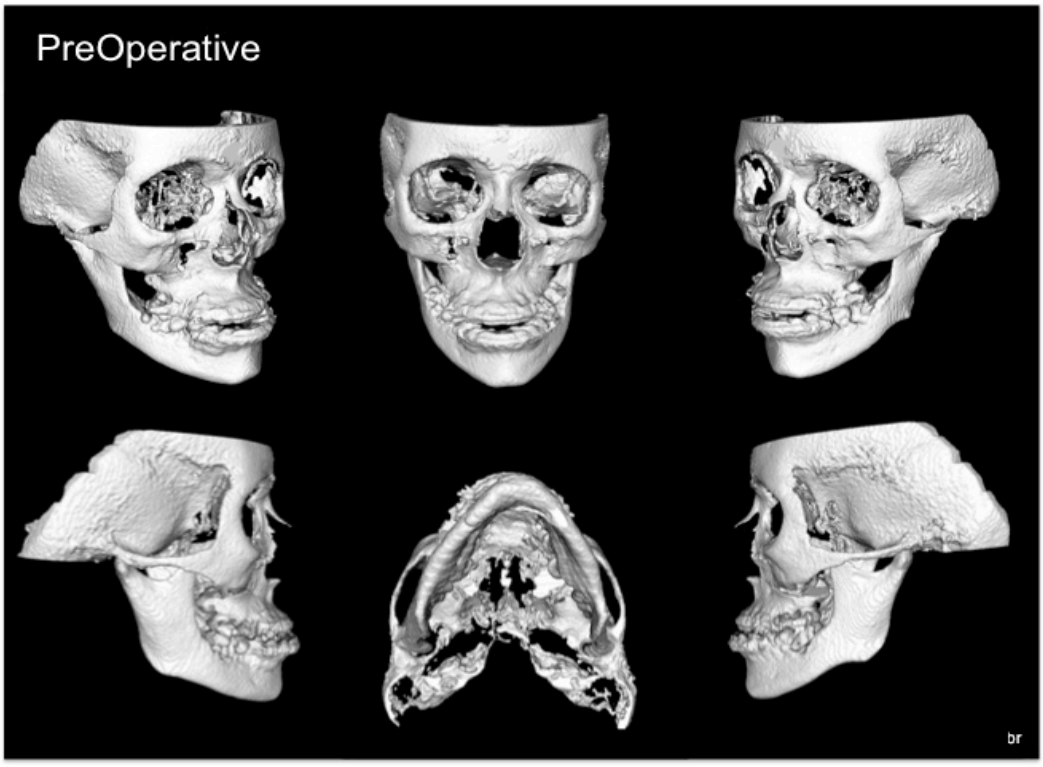
PreOperative
br

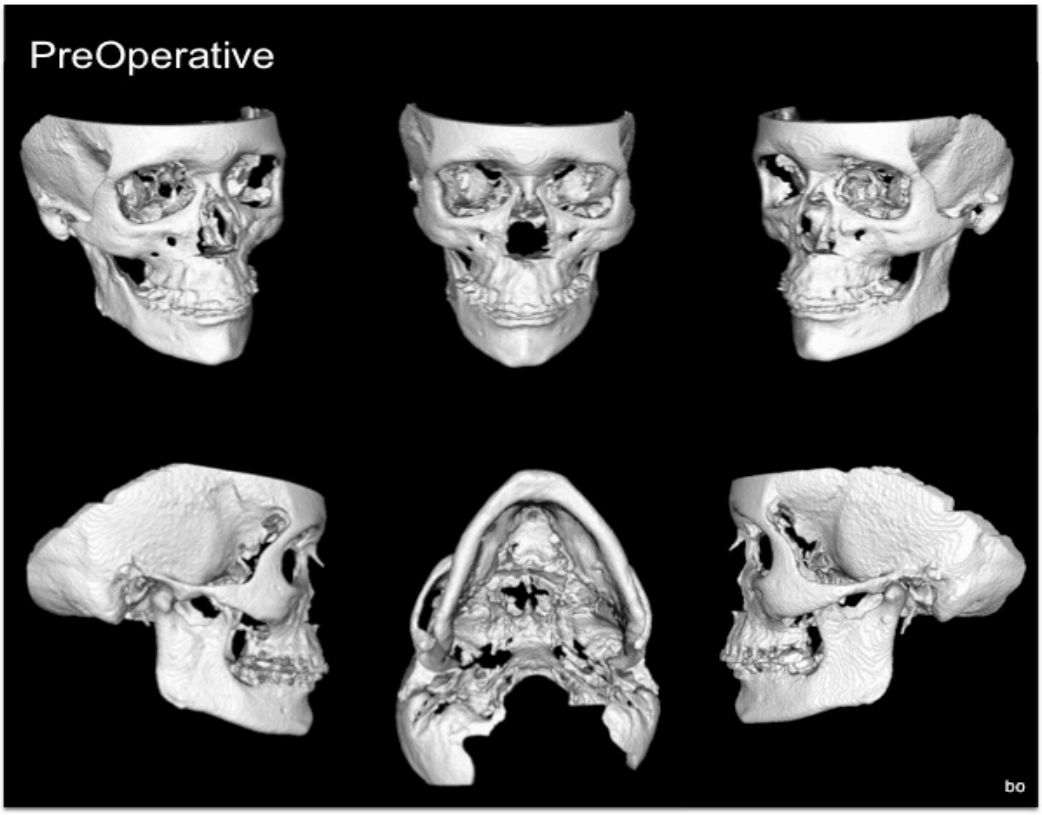
PreOperative
bo

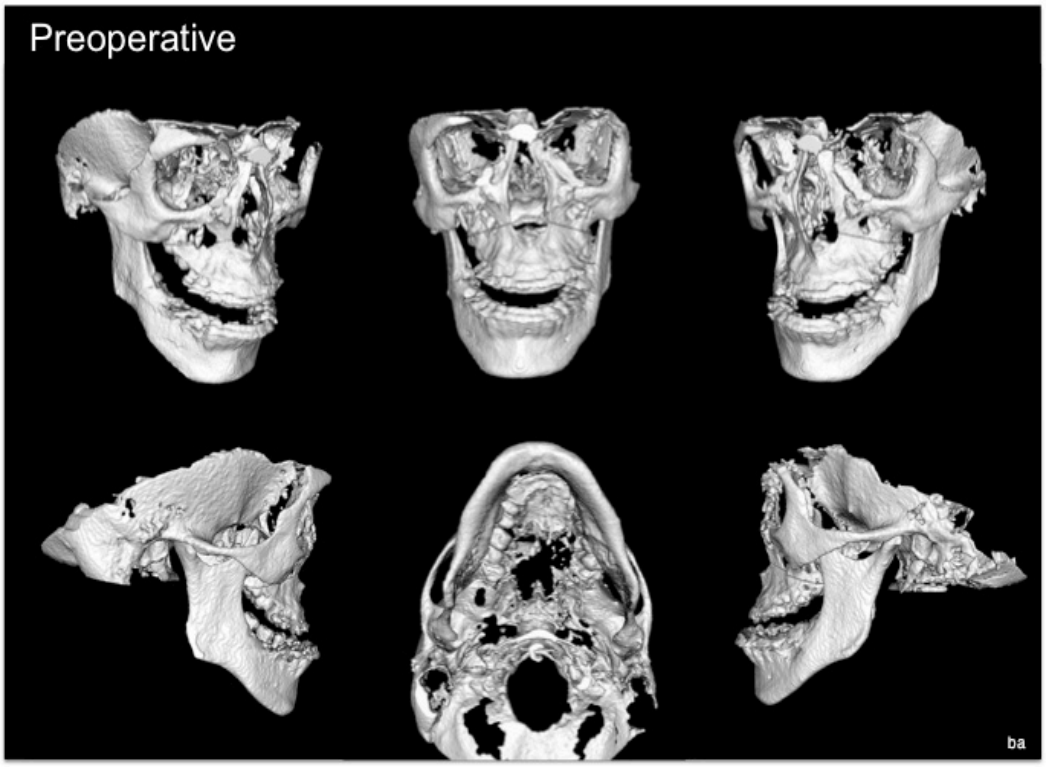
Preoperative
ba

Appendix 4:

Papers published out of this work:

Int J CARS (2012) 7:265–271
DOI 10.1007/s11548-011-0665-2

ORIGINAL ARTICLE

3D quantification of mandibular asymmetry using the SPHARM-PDM tool box

Abeer AlHadidi · Lucia H. Cevidanes · Beatriz Paniagua · Richard Cook · Frederic Festy · Donald Tyndall

Received: 5 July 2011 / Accepted: 25 October 2011 / Published online: 17 November 2011

Abstract
Purpose Pretreatment diagnosis of mandibular asymmetry in orthognathic surgery patients can be improved by quantitative shape modeling and analysis. The UNC SPHARM-PDM (University of North Carolina Spherical Harmonics—Point Distribution Model) toolbox was applied to a cohort of patients and the results were evaluated.
Methods Three-dimensional (3D) virtual surface models are constructed from CBCT scans of each patient in the cohort by segmentation. Mirroring on a sagittal arbitrary plane is used to flip the left and right sides of each image. An automatic voxel-based registration on the cranial base is used to align the volume and its mirror for comparison. SPHARM-PDM is used to compute correspondent models for each hemimandible and the mirror of the contralateral side. Procrustes analysis was used to evaluate discrepancies between each pair of models to assess asymmetry. Mandibular asymmetry was also located and quantified by computing corresponding surface distances between each hemimandible (left and right sides) and the mirror of the contralateral side.
Results There were no statistically significant differences in surrogates for mandibular asymmetry assessment based on right or the left side mirroring. Those surrogates are the rotational and translational differences between each hemimandible and the mirror of the contralateral side in 3 planes of space (the absolute values of Procrustes registration output in 6 degrees of freedom). Absolute and signed distance maps between each hemimandible and the mirror of the contralateral side located and quantified areas of asymmetry diagnosis for each patient. Even though mandibular condyle asymmetry was observed in 8% of the cases and mandibular asymmetry along areas of the ramus and mandibular corpus was noted in 17.8% of the cases, the remaining 74.2% showed generalized morphological and positional asymmetry at the condyle, the ramus and mandibular corpus.
Conclusion Three-dimensional diagnosis of mandibular asymmetry revealed the complex involvement of morphological components of the mandible and the heterogeneous nature of this clinical condition. SPHARM-PDM has a promising role in the individual diagnosis and quantification of mandibular asymmetry.

Keywords Mandibular asymmetry · Shape correspondence · SPHARM-PDM · Statistical shape analysis

A. AlHadidi (✉)
University of Jordan, Amman, Jordan
e-mail: Alhadida@dentistry.unc.edu

L. H. Cevidanes
University of Michigan, Ann Arbor, MI, USA

B. Paniagua · D. Tyndall
University of North Carolina at Chapel Hill, Chapel Hill, NC, USA

R. Cook · F. Festy
King's College London Dental Institute, London, UK

Introduction

Treatment planning and assessment of the surgical correction of asymmetrical deformities are limited by reliance on 2D radiographs in the current clinical setting. The 2D radiographs conventionally used in orthodontic practice are particularly problematic when rotational or asymmetrical correction is required since surgical jaw displacements are inherently three dimensional. Clinical examination and frontal radiographs detect gross asymmetries; however, for treatment planning purposes, localization and quantification of

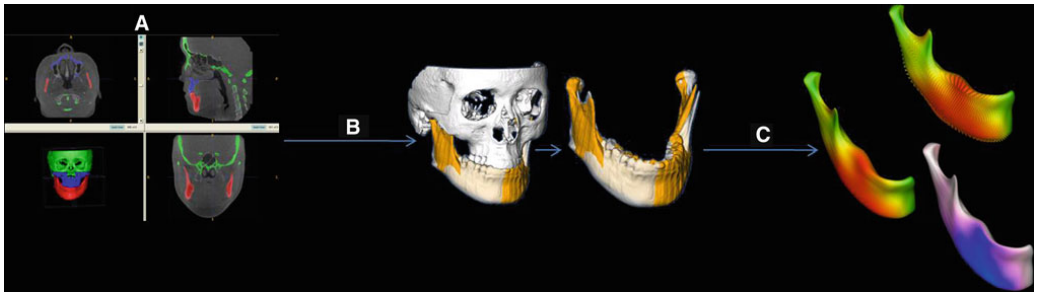

Fig. 1 After segmenting hard tissue (**a**), the image volume and segmentation models were mirrored by flipping *left* and *right* sides and then registering the mirrored image onto the cranial base (**b**). Quantification of mandibular asymmetry for a patient is done using SPHARM-PDM shape analysis (**c**). Original model *white* and *left* hemi-mandible arbitrary mirror matching on the cranial base *yellow*. Shape analysis is used to quantify *right* and *left* differences by computing vector maps, absolute surface distance maps and signed surface distance maps of the differences between the original and arbitrary mirrored models (both registered in the cranial base). Signed distances color maps show the directionality of the differences

the asymmetry are required. In 2D frontal head radiographs, the anatomic structures are overlapped. Additionally, frontal X-rays are very dependent on geometry and can give false measurements of the location, extent, and severity of mandibular asymmetry.

The use of cone-beam computed tomography (CBCT) or spiral computer tomography (CT) provides the 3D imaging data necessary to generate precise knowledge of the location and the magnitude of facial asymmetry features, which are essential for the diagnosis of facial deformities and for the planning of corrective procedures. An increasing number of studies have demonstrated that computer-aided surgical simulation (CASS) can predict possible surgical complications and lowers material costs while decreasing surgery duration, with comparable or better surgical outcomes [1–3]. However, the ability to visualize the facial asymmetry in 3D surface models does not imply the ability to quantify and precisely locate areas of asymmetry. Detailed analysis of positional as well as morphological discrepancy between the affected side and the normal side in an asymmetric patient is a prerequisite for ideal treatment planning.

Shape analysis has become of increasing interest to the medical image analysis community due to its potential to precisely locate and quantify morphological changes between healthy and pathological structures. As part of the National Alliance for Medical Image Computing (http://www.na-mic.org), the Neuro-Image Research and Analysis Lab (NIRAL) at the University of North Carolina developed a comprehensive set of tools for the computation of 3D structural statistical shape analysis that have been mostly used for brain morphometry studies.

The shape correspondence framework selected for this study is SPHARM-PDM toolbox, which presents a comprehensive set of tools for the computation of 3D structural statistical shape analysis [4]. In summary, the SPHARM description is a hierarchical, global, multi-scale boundary description that can only represent objects of spherical topology, proposed initially by Brechbuhler et al. [5]. This SPHARM shape analysis approach was further developed (SPHARM-PDM, PDM stands for Point Distribution Models) and extensively used for applications in neuroimaging [6,7].

In previous work we established the accuracy of SPHARM-PDM to quantify the direction and degree of simulated known amounts of mandibular asymmetry [8]. The objective of the work presented in this manuscript is the clinical application of this technology to assess mandibular asymmetry in a cohort of patients with a previous clinical diagnosis of mandibular asymmetry.

Materials and methods

The cohort consisted on 45 pretreatment CBCT scans from patients that sought care at our Dentofacial Deformities Program and consented to participate in the project. This project was approved by a university committee for research on human subjects. These scans are part of a bigger sample of consecutive prospectively collected images, collected in the grant "Improving Treatment Outcomes for Patients with Facial Deformity using 3D Imaging". Inclusion criteria for our study were patients with clinically detectable asymmetry, defined as more than 2 mm of chin deviation or cant of the occlusal plan before the start of their orthodontic treatment. Exclusion criteria were history of previous jaw surgery and patients who required reconstructive surgery, as graft planning. Figure 1 shows an overview of the methodological framework.

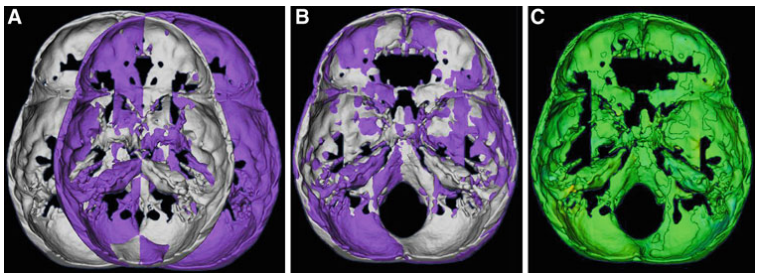

Fig. 2 Arbitrary plane mirroring followed by cranial base registration: cranial base virtual surface model for a patient *white* and arbitrarily mirrored image model *purple* before registration in (**a**); the original model and arbitrary mirror matching on the cranial base as a result of a voxel-based registration (**b**); in **c** a color map of the surface distance between the registered original and arbitrary mirror models shown at 0 mm surface distances *green*

Image acquisition

New Tom 3G Cone-beam CTs (AFP Imaging, Elmsford, NY) with the patient in supine position were obtained prior to orthodontic treatment.

Construction of virtual 3D models from the CBCT dataset

Segmentation involved outlining of the shape of structures visible in the cross-sections of a volumetric dataset in the CBCT-3D images. Segmentation of anatomic structures was performed using ITK-SNAP (open-source software, http://www.itksnap.org) [9]. 3D virtual models were built for each patient from a set of ∼300 axial cross-sectional slices for each image with the image voxels reformatted for an isotropic resolution of 0.5 mm × 0.5 mm × 0.5 mm. This resolution was used because higher spatial resolution with smaller slice thickness would have increased image file size and required greater computational power and user interaction time. After segmentation with ITK-SNAP tool, a 3D graphic rendering of the volumetric object allowed navigation between voxels in the volumetric image and the 3D graphic representation with zooming, rotating, and panning.

Mirroring and cranial base registration

Each model was mirrored on an arbitrary sagittal plane. The mirroring is done by arbitrarily converting the image orientation from (Right-Left, Antero-Posterior, and Infero-Superior) to (Left-Right, Antero-Posterior, and Infero-Superior). The original and the arbitrarily mirrored images were then registered on the cranial base. The registration was accomplished using IMAGINE software (National Institutes of Health, Bethesda, MD; Open-source, http://www.ia.unc.edu/dev/download/imagine/index.htm) consisting on a voxel-based registration method. This method utilizes maximization of mutual information to avoid the problems associated with observer-dependent techniques. After the software masks the maxillary and mandibular structures, it compares the gray-level intensity of each voxel in the cranial base to register the two CBCT images. The rotation and translation parameters that are used to register the two gray scale images are also applied to register the 3D surface models (Fig. 2).

Cranial base registration is important since it provides information of the mandibular asymmetry relative to the face. Asymmetry was defined as the difference between each hemimandible and the mirror of the contralateral side.

Before computing correspondent point-based models using SPHARM-PDM, spherical topology of the models must be assured, which is achieved with the following preprocessing steps. In order to simplify the ridges and waves of the hemimandibular segments, a Laplacian smoothing procedure was applied to each hemimandible. Then, a binary segmentation volume is created again from the surfaces. This was done via finding the enclosing bounding box of the shape and binarizing the cross-sections. These binary segmentation volumes are the input of the SPHARM-PDM framework.

SPHARM-PDM shape correspondence and Procrustes alignment

The UNC SPHARM-PDM shape analysis toolbox was employed to compute unique correspondent point-based models of all the hemimandibular surfaces per patient.

The segmented 3D surface models of the hemimandibles are first converted into surface meshes, and mapped into the unit sphere using an area-preserving and distortion-minimizing spherical mapping. The SPHARM description is computed from the mesh and its spherical parameterization. Using the first-order ellipsoid from the spherical harmonic coefficients, the spherical parameterizations are aligned to establish correspondence across all surfaces. The SPHARM description is then sampled into triangulated surfaces (SPHARM-PDM). Alignment of all surfaces

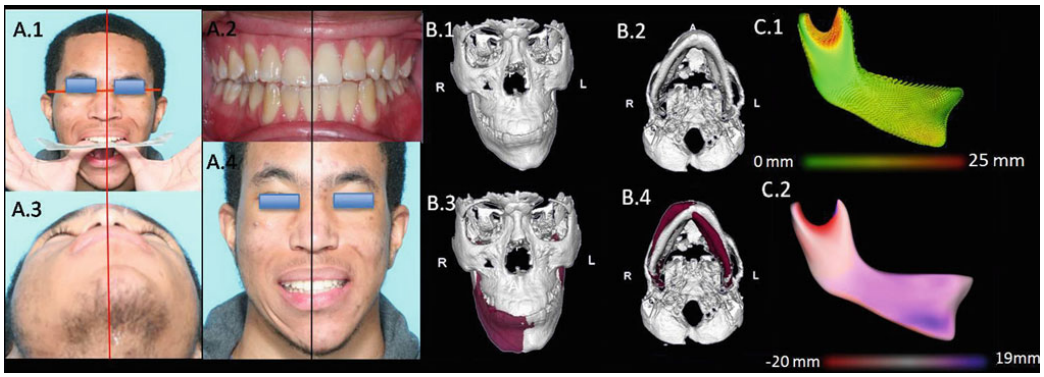

Fig. 3 An example of 3D analysis for a patient in the cohort: clinical photographs are shown in **A**. Note the maxillary cant in *A.1*, the discrepancy in dental midline *A.2*, the deviation of the chine to the *left* in *A.3* and *A.4*; Group **B** represents hard tissue surface models of the same patient. *B.1* is a frontal view, *B.2* is a SMV view, *B.3* and *B.4* are the same views, respectively also showing the mirror of the mandible registered on the cranial base (Mirror model in *maroon*); In **C** is 3D analysis color maps of the *right* side of the mandible in relation to the mirror of the *left* half of the mandible, Vector maps are shown in *C.1* and signed distance maps shown in *C.2*

was performed using rigid Procrustes alignment. This rigid Procrustes alignment procedure computes an optimal linear, geometric transformation $\phi(n)$ that best maps the shape changes between the affected hemimandible and the mirror of the opposite healthy side based on the established correspondence [10].

A preliminary analysis is computed by subtracting the models of each hemimandible and the mirror of the contralateral side and displayed via color-coded distance magnitude and vector maps. Vector maps provide visualization and quantification of distances between paired correspondent point-based models, indicating the direction and magnitude of each side and the mirrored side discrepancies. Figure 3 shows an example of this analysis. Procrustes was used to capture translational and rotational differences between each hemimandible and the mirror of the contralateral side in the three planes of space.

We hypothesize that there should be no difference in the absolute values of Procrustes output based on whether the right or the left side of the mandible is being mirrored. This serves as an internal validation of this methodology. Paired T test was used to test this null hypothesis.

Results

The average and standard deviation of translational differences in mm and the rotational differences in degrees between original hemimandible and the hemimandible mirrored in the contralateral side calculated with Procrustes alignment are displayed in Table 1. No statistically significant difference was observed in the absolute values of Procrustes output based on whether the right or the left side of the mandible is being mirrored. This demonstrates the consistency of Procrustes in evaluating mandibular asymmetry.

Location of mandibular asymmetry was heterogenous in this sample; however, 8% of the cases showed characteristic larger asymmetry surface distances at the condyles, while 17.8% presented more marked mandibular body and ramus asymmetry. Most patients (74.2%) exhibited generalized asymmetric mandibular morphology with the involvement of both condyle ramus and corpus (Fig. 4).

Most detected asymmetries in this cohort had translational component in the medio-lateral followed by the cranio-caudal direction. These differences ranged from 0.03 to 9.05 mm with a mean of (1.76 $\pm$ 1.99) mm, and

Table 1 The average and standard deviation of translational differences in mm and rotational differences in degrees between the left heminadible and the mirror of the right side (_Left) and between the right side and the mirror of the left (_Right)

	Tx_Left	Tx_Right	Tz_Left	Tz_Right	Rx_Left	Rx_Right	Rz_Left	Rz_Right
Average	−0.89	−0.91	−0.33	−0.01	2.28	2.33	2.36	2.54
SD	2.47	2.51	1.94	1.80	1.79	1.73	2.03	2.14
P value	0.72		0.55		0.62		0.11	

Notice the non-significant *P* value between the 2 sides. *X* is in medio-lateral and *Z* is in cranio-caudal direction. Readings from the anterioposterior are not included since this plane is irrelevant for asymmetry assessment

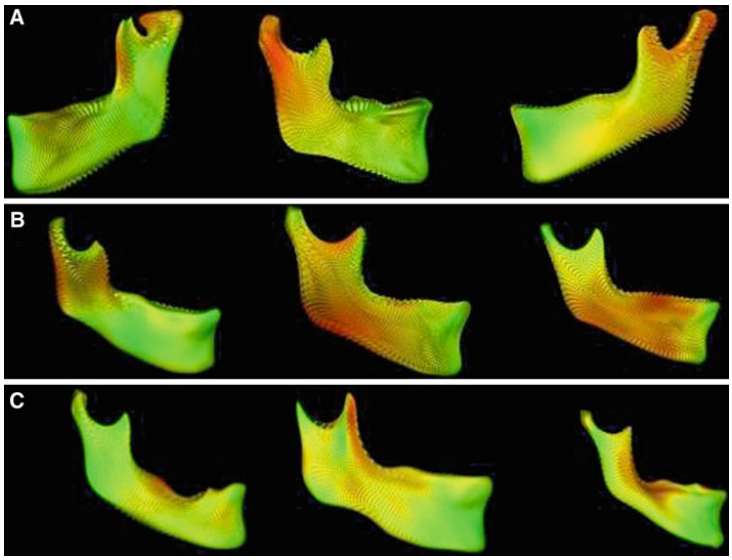

Fig. 4 Examples of patients from the cohort with mandibular asymmetry mostly localized to the condyle (*row* **a**), or in the ramus\body of the mandible (*row* **b**), examples of generalized mandibular asymmetry are shown in (*row* **c**)

0.05–6.86 mm with a mean of (0.80 ± 1.36) mm, respectively. As for the rotational component, bigger changes were detected in the yaw followed by the roll then the pitch of those hemimandible. Differences in the yaw ranged from 2.54 to 10.37 degrees with a mean of (2.54 ± 2.14) degrees while those of the roll and pitch ranged from 0.17 to 10.19 degrees with a mean of (2.57 ± 2.11) degrees, and 0.08–6.2 degrees with a mean of (2.38 ± 1.72) degrees.

Discussion

Most commercially available and academic software that are able to compute color-coded surface maps use closest point algorithm to obtain surface distances. Closest point is a brute force algorithm that calculates a vertex-to-vertex Euclidean closest point distance [11,12]. This method does not map corresponding surfaces based in anatomical geometry, and thus, it usually underestimates rotational and large translational movements.

The application of conventional closest point distances for mirror images in mandibles of patients with rudimentary condyles, severe cants, or a rotated mandible does not represent the difference between corresponding anatomical locations, but rather differences based in the minimal distances between any point in the original and mirrored models. These clinical situations mandate the use of a more "anatomy sensitive" shape analysis technique.

Shape correspondence is a promising alternative to overcome the shortcomings of the commonly used closest point algorithm. It is one of the currently used statistical shape analysis techniques that allows measuring the surface distance between an area on one model to the corresponding anatomical area in the other model regardless the alignment of those models. The main shape correspondence challenges involve the representation of a population by means of correspondent point-based models. Surface representation could be accomplished by several different options including, matching of template surface geometry (curvature and location) [13], entropy-based Particle Systems [14], or by Spherical harmonic representation (SPHARM) [6]. In SPHARM the surface model gets mapped in a sphere, and correspondence point-based models are computed after finding the spherical harmonic basis that best fits the model. After surface mapping is achieved, correspondence could be based on different frameworks depending on the clinical problem on hand.

SPHARM-PDM allows for comprehensive statistical evaluations to be computed for the correspondent models as a whole or for specific regions of interest within these models. For asymmetry assessment and future treatment planning, an individual-based analysis was chosen in this project when compared to group analysis. Group analysis is usually used to examine general trends and cross-sectional tendencies, both those will be of limited utility to a "patient per patient" treatment planning approach.

To maximize the usefulness of the extensive data that SPHARM-PDM can provide, regions of interest that correspond to surgical segments could be analyzed separately (Fig. 5). This quantitative asymmetry measure could either be communicated to the surgeon or used as an input for surgical simulation software.

The translational and rotational differences between mandibular halves as measured by Procrustes are an accurate

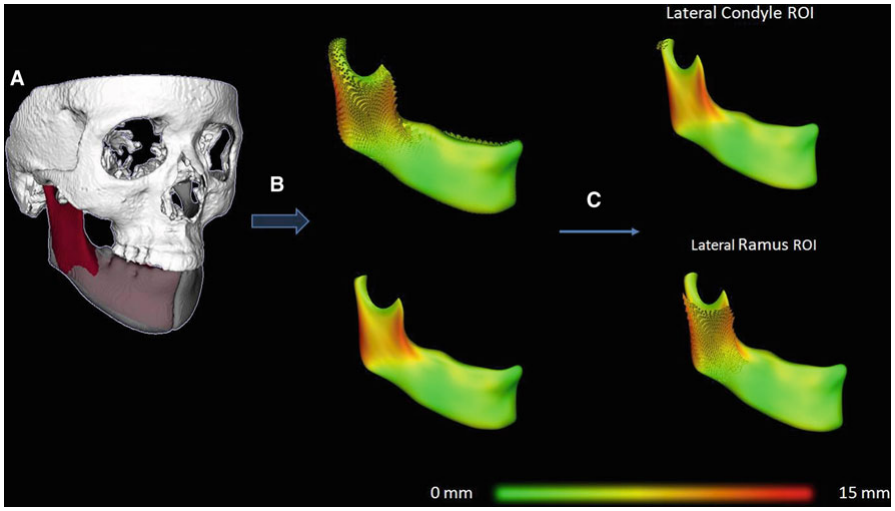

Fig. 5 ROI analysis: **a** hard tissue surface model for a patient showing the mirror of the *left* mandible registered on the cranial base (Mirror model in *maroon*), in **b** vector and surface distance maps of the *right* side of the mandible in relation to the mirror of the *left* half of the mandible. Vector maps computed for specific regions of interest (lateral pole of the condyle and lateral surface of the ramus) are shown in (**c**)

representation of the location component of mandibular asymmetry; however, in patients with marked morphological differences between both hemimandibles, grafting and\or reshaping procedures might be needed. In these cases, pure shape analysis after accounting for positional differences is a better approach.

While this study applied shape analysis to a pretreatment assessment of mandibular asymmetry, future investigations are needed to apply the preliminary findings in this study to presurgical treatment planning and surgical simulation of corrective surgeries of patients with complex asymmetries.

Conclusion

SPHARM-PDM has a promising role in individual diagnosis and quantification of mandibular asymmetry. Three-dimensional diagnosis of mandibular asymmetry revealed the complex involvement of morphological components of the mandible and heterogeneous nature of this clinical condition.

Conflict of interest None.

References

1. Hassfeld S, Muhling J (2001) Computer assisted oral and maxillofacial surgery—a review and an assessment of technology. Int J Oral Maxillofac Surg 30(1):2–13
2. Troulis MJ, Everett P, Seldin EB, Kikinis R, Kaban LB (2002) Development of a three-dimensional treatment planning system based on computed tomographic data. Int J Oral Maxillofac Surg 31(4):349–357
3. Gateno J, Xia JJ, Teichgraeber JF, Christensen AM, Lemoine JJ, Liebschner MA, Gliddon MJ, Briggs ME (2007) Clinical feasibility of computer-aided surgical simulation (CASS) in the treatment of complex cranio-maxillofacial deformities. J Oral Maxillofac Surg 65(4):728–734
4. Styner M, Oguz I, Xu1 S, Brechbuhler C, Pantazis D, Levitt J, Shenton M, Gerig G (2006) Framework for the statistical shape analysis of brain structures using spharm-pdm. Insight J. http://www.insightjournal.org/
5. Brechbühler C, Gerig G, Kübler O (1995) Parametrization of closed surfaces for 3-D shape description. Comput Vis Image Underst 61:154
6. Gerig G, Styner M, Jones D, Weinberger D, Lieberman JA (2001) Shape analysis of brain ventricles using spharm. Math Methods Biomed Image Anal MMBIA (2001):171–178
7. Styner M, Gerig G, Lieberman J, Jones D, Weinberger D (2003) Statistical shape analysis of neuroanatomical structures based on medial models. Med Image Anal 7:207
8. Cevidanes LH, Alhadidi A, Paniagua B, Styner M, Ludlow J, Mol A, Turvey T, Proffit WR, Rossouw PE (2011) Three-dimensional quantification of mandibular asymmetry through cone-beam computerized tomography. Oral Surg Oral Med Oral Pathol Oral Radiol Endod 111(6):757–770
9. Yushkevich PA, Piven J, Hazlett HC, Smith RG, Ho S, Gee JC, Gerig G (2006) User-guided 3D active contour segmentation of anatomical structures: significantly improved efficiency and reliability. Neuroimage 31(3):1116–1128
10. Styner M, Gerig G, Lieberman J, Jones D, Weinberger D (2003) Statistical shape analysis of neuroanatomical structures based on medial models. Med Image Anal 7:207
11. Besl PJ, McKay ND (1992) A method for registration of 3-D shapes. IEEE Trans Pattern Anal Mach Intell 14:239–256

12. De Momi E, Chapuis J, Pappas I, Ferrigno G, Hallermann W, Schramm A, Caversaccio M. Automatic extraction of the mid-facial plane for cranio-maxillofacial surgery planning. Int J Oral Maxillofac Surg JID-8605826 0829
13. Meier D, Fisher E (2002) Parameter space warping: shape-based correspondence between morphologically different objects. IEEE Trans Med Imaging 21(1):31–47
14. Oguz I (2009) Groupwise shape correspondence with local features. PhD dissertation, University of North Carolina. (http://webcat.lib.unc.edu/record=b6135448~S1)

The use of a custom made atlas as a template for corrective surgeries of asymmetric patients

Abeer AlHadidi[a]; Lucia H Cevidanes[b]; Richard Cook[c]; Frederic Festy[c]; Donald Tyndall[d]; Beatriz Paniagua[e]

[a] Faculty of Dentistry, University of Jordan. [b] School of Dentistry, University of Michigan. [c] The Dental institute, King's College London. [d] School of Dentistry, University of North Carolina at Chapel hill. [e] Neuro Image Research and Analysis Laboratories, Department of Psychiatry, University of North Carolina at Chapel hill

Aim: The use of conventional mirror images does not adequately guide surgeons on the correction of facial asymmetries. The purpose of this study was to evaluate the utility of an individualized atlas as a template for corrective surgeries for patients suffering from mandibular asymmetry. The patient-specific atlas is calculated from both the original asymmetric mandible and the mirror of the same mandible registered on the cranial base. **Material and Method:** Three patients with history of favorable clinical outcome of the correction of their mandibular asymmetry were chosen for this pilot study. CBCT were taken before and 6 weeks after corrective surgery using NewTom 3G. Each volume was mirrored and rigidly registered on the cranial base. Surface models for both the mandible and its registered mirror were used to compute an atlas using deformable fluid registration. Corrective surgery was simulated based of the resulting atlas. Differences between the virtual simulated outcome and the actual surgical outcome were computed using UNC SPHARM-PDM toolbox. **Results:** The detected differences between the virtual simulated outcome and the actual surgical outcome, as characterized in 6 degrees of freedom, were smaller than 2 mm of translation and 5 degrees of rotation. This indicates that the location of the synthesized template is similar to the desired clinical outcome. **Conclusions:** The construction of patient-specific atlases using non-rigid registration has the potential to optimize and increase the predictability of the outcome of craniofacial corrective surgeries for asymmetric patients.

Medical Imaging 2012: Biomedical Applications in Molecular, Structural, and Functional Imaging, edited by Robert C. Molthen, John B. Weaver, Proc. of SPIE Vol. 8317, 83171Y · © 2012 SPIE · CCC code: 1605-7422/12/$18
doi: 10.1117/12.911048

Proc. of SPIE Vol. 8317 83171Y-1

Introduction:

Asymmetry occurs in 40% of dentofacial patients with Class III or long face problems, and in 28% of mandibular deficiency patients[1]. Normally, the right side of the human face is slightly larger, and when an asymmetric mandible is observed in patients with mandibular deficiency or excess, there is a >80% chance that the chin will be off to the left[2, 3]. When excessive vertical growth of the maxilla occurs, left and right asymmetries are equally probable. Furthermore, correcting maxillary asymmetry usually involves moving one side up (and perhaps the other side down) to correct a canted occlusal plane and usually is done in conjunction with mandibular surgery. For the maxillary component of asymmetry surgery, downward movement of the maxilla is in the stability problematic category.

Quantification of right and left side differences is not possible in 2D imaging, and it is also a challenge in 3D analysis. Definition of the midsagittal plane[4], registration of the mirrored image[5], and measurement of the asymmetry [6]demand further investigation. While we anticipate that all subjects present some degree of asymmetry, we have no information on the degree to which asymmetrical corrections contribute to undesirable maxillo-mandibular rotations. In the surgical correction of dentofacial deformity, it frequently is necessary to change ramus length more on one side than the other, even in patients whose major problem is not an overt asymmetry. It is not possible to measure this accurately on cephalometric radiographs or with conventional mirroring techniques. Because there was no appropriate way to measure asymmetry, data on asymmetry was previously limited.

Facial asymmetry is a complex clinical entity that comprises two main components, a shape and a positional component. During growth, the shape discrepancies lead to compensatory positional differences resulting in disturbing the harmony of the maxillofacial complex. Clinicians need to diagnose both shape and positional components of the asymmetry prior to the design and execution of the corrective surgery. The use of conventional mirror images does not adequately guide surgeons on the correction of facial asymmetries because it does not compensate for the positional component.

We have previously shown that the choice of mirroring orientation (mid-sagittal plane vs arbitrary plane and registration) affects the 3D localization of asymmetry[7]. In the current study, we present the application of registration methods to correct positional components of facial asymmetry and use 3D templates to aid in the surgical planning.

The purpose of this study is to evaluate the utility of a patient-specific atlas as a template for corrective surgeries for patients suffering from mandibular asymmetry. This template will enhance the predictability and reproducibility of the surgical outcomes of those corrective surgeries.

Methods:

Data:

Three patients with history of favorable clinical outcome of the correction of their mandibular asymmetry were chosen for this pilot study. Favorable outcome was decided based on post-operative clinical exam, post operative dental casts, and photos.

CBCT were taken before and 6 weeks after corrective surgery of each patient using NewTom 3G cone beam CT (Aperio Services, Sarasota, Fla). The 12" field of view producing 0.5 mm isotropic voxel sizes was used for acquiring the image volume.

Segmentation:

Virtual 3D models were created by segmenting or outlining the shape of anatomical areas of interest in the cross-sections of the volumetric dataset from the CBCT images. Segmentation was performed with ITK-SNAP open source software [8]. The 3D models were then built from a set of ~ 300 axial cross-sectional slices with image voxels reformatted for an isotropic resolution of 0.5 mm x 0.5 mm x 0.5 mm. This resolution was used because higher spatial resolution with smaller slice thickness would have increased image file size and required greater computational power and user interaction time.

Mirroring and rigid registration:

The mirroring of the presurgery dataset was done by arbitrarily converting the image orientation from (Right-Left, Antero-Posterior and Infero-Superior) to (Left-Right, Antero-Posterior and Infero-Superior). The original and the arbitrarily mirrored images were then registered on the cranial base. The registration was accomplished via the voxel-based registration software IMAGINE (National Institutes of Health, Bethesda, MD; Open-source, http://www.ia.unc.edu/dev/download/imagine/index.htm). This method utilizes maximization of mutual information to avoid the problems associated to observer dependent techniques. After the software masks out maxillary and mandibular structures, it compares the grey level intensity of each voxel in the cranial base to register the two CBCT images. The rotation and translation parameters that are used to register the two CBCT grey scale images are also applied to register the 3D surface models. Fig (1)

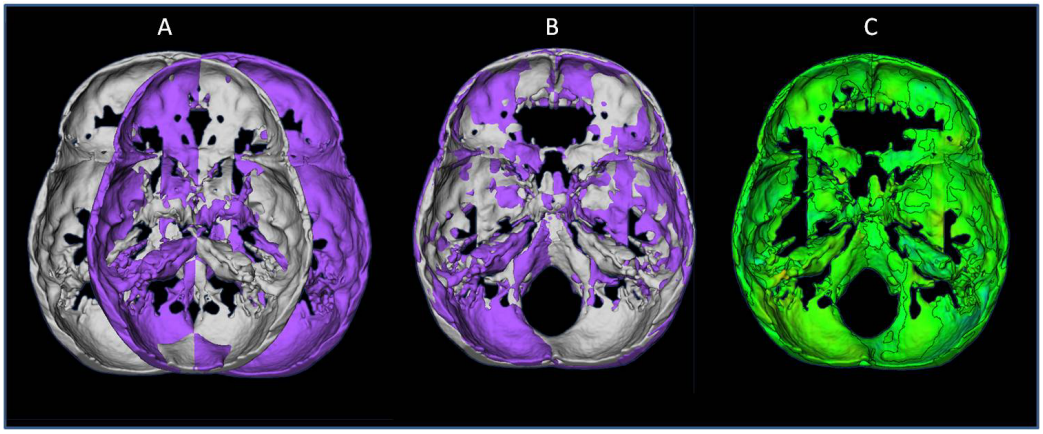

Fig 1. Arbitrary plane mirroring followed by cranial base registration: Cranial base virtual surface model for a patient (*white*) and arbitrarily mirrored image model (*purple*) before registration in A; the original model and arbitrary mirror matching on the cranial base as a result of a voxel-based registration (B); in (C) a color map of the surface distance between the registered original and arbitrary mirror models shown at 0 mm surface distances (*green*).

Atlas formation:

Surface models for both the mandible and its registered mirror were used to compute an atlas using deformable fluid registration. To facilitate deformable registration, a surface-wise, geometry

sensitive smoothing is performed to remove noisy artifacts from the data typically visible around the dental line. We used an iterative mean-curvature evolution algorithm[9] that smoothes the surface mesh using a relaxation operator, such that the vertices are repositioned according to $V_i^{t+1} = (1-\lambda)V_i^t + \lambda V_i^t$ where V is the position of the i^{th} vertex, t is the number of iterations, $\lambda \varepsilon [0, 1]$ is a smoothing parameter, and V_i^t is the average vertex position, which is the average position of neighboring triangle centers weighted by the triangle areas. Note that the inflation has to be done in small increments to avoid introducing topological changes. The total smoothing in the data was less than half a voxel on average, thus representing the mandibular surface accurately. The resulting meshes are scan-converted into binary volumes and then deformably registered using a greedy fluid flow algorithm.

AtlasWerks, used for patient-specific atlas building in this project, is an open-source (BSD license) software package for medical image atlas generation. AtlasWerks atlas formation is based on greedy fluid registration in a diffeomorphic deformation setting [10]. This well- known viscous fluid model accommodates large-distance, nonlinear deformations of small subregions of the target image. Fig (2)

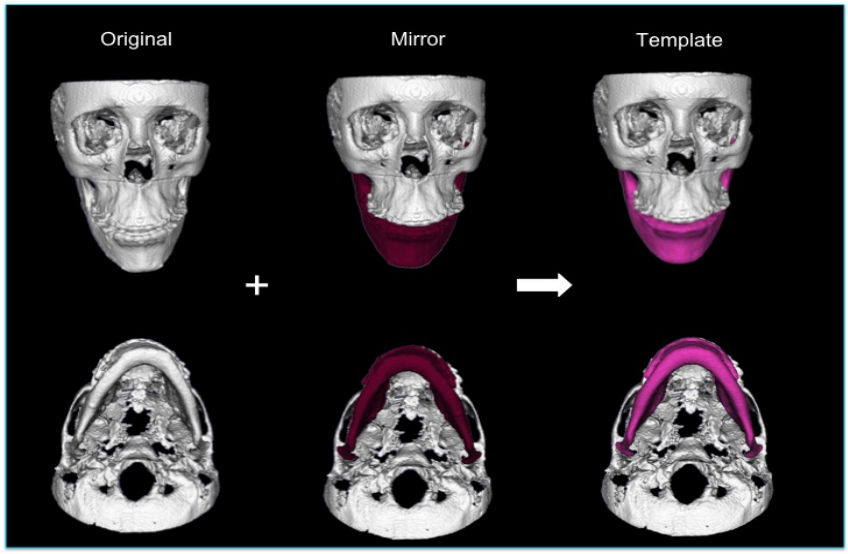

Fig 2. Atlas formation: The original mandible (white) and its registered mirror (maroon) are both used to compute an atlas (pink) that will serve subsequently as a template for surgical simulation

Surgical simulation:

Corrective surgery was simulated using the atlas computed as a template, using 3DSlicer. 3DSlicer is an open-source free software (http://www.slicer.org/) that allows cutting, panning, and rotation of displayed models. The ROI module was used to simulate surgical cuts via clip boxes. The surgical cuts were simulated simultaneously on both the mandible and the template. The resultant surgical segments were then registered using surface registration to the corresponding anatomical region at the template. The mandibular segments were merged at there final position using the merge model functionality of 3DSlicer. Fig (3)

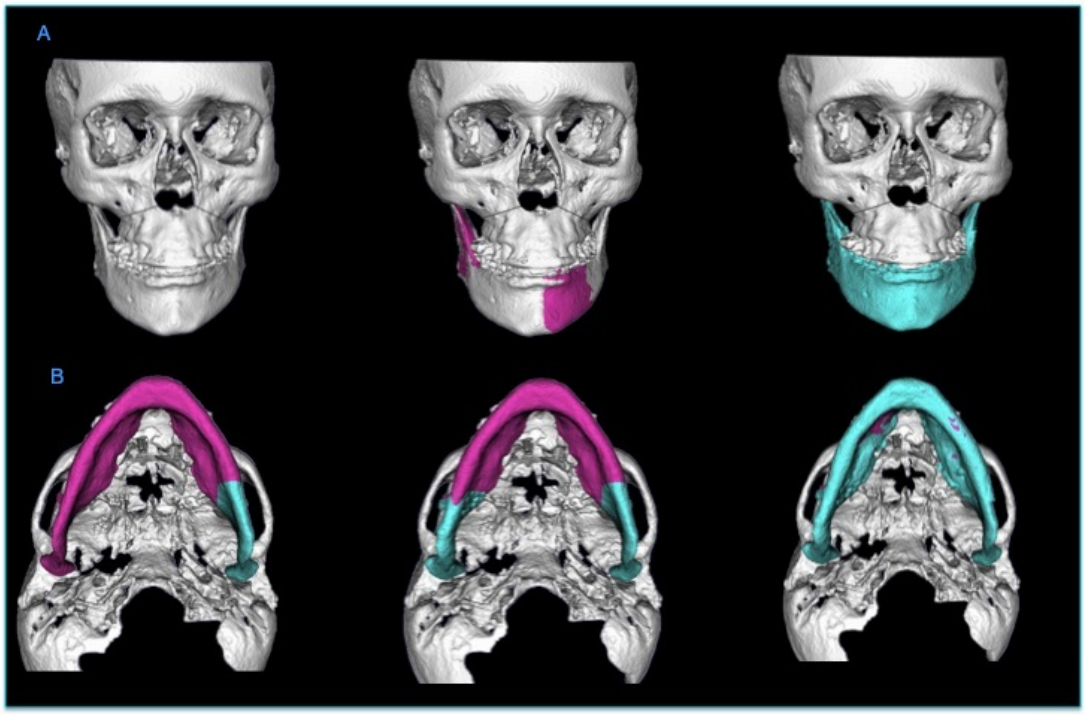

Fig 3. Surgical simulation: The original mandible (white) is overlaid over the computed template (pink) to guide moving the surgical segments in 3DSlicer. As shown in row (B) the surgical segments were moved to match the position of the template leading to the virtual outcome mandible (blue).

Differences between the virtual simulated outcome and the actual surgical outcome were computed using UNC SPHARM-PDM toolbox[11]. The segmented 3D surface models of surgical segments of the mandible in both the virtual and the actual setting are first converted into surface meshes, and

mapped into the unit sphere using an area-preserving and distortion-minimizing spherical mapping. The SPHARM description is computed from the mesh and its spherical parameterization. Using the first-order ellipsoid from the spherical harmonic coefficients, the spherical parameterizations are aligned to establish correspondence across all surfaces. The SPHARM description is then sampled into correspondent triangulated surfaces (SPHARM-PDM)[12]. Discrepancies between the correspondent based models of each surgical segment were aligned using rigid Procrustes alignment. This rigid Procrustes alignment procedure computes an optimal linear, geometric transformation φ (*n*) that best maps the shape changes between the affected hemimandible and the mirror of the opposite healthy side based on the established correspondence The 6 degrees of freedom (DOF) of the differences between the virtual and the actual outcome mandibles were calculated using rigid Procrustes alignment. Composite overlays were used for visual assessment of results. Fig (4)

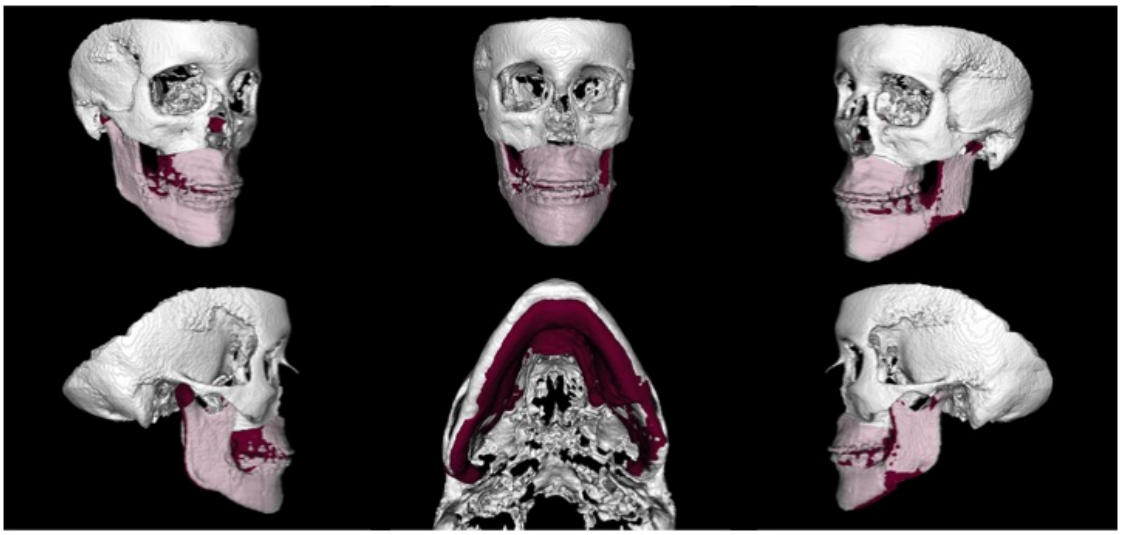

Fig 4. Composite overlays: The asymmetry correction differences between the actual post surgery mandible (white) and the virtual outcome mandible (maroon) are minimal as shown in this overlay. Comparisons are done at the condyle, ramus, and chin levels.

Results:

The detected differences between the virtual simulated outcome and the actual surgical outcome, as characterized in 6 degrees of freedom, were smaller than 2 mm of translation and 5 degrees of rotation. This indicates that the location of the synthesized template is similar to the desired clinical

outcome. The condyles in the virtual postoperative mandible were centered in the glenoid fossae and the rami have reasonable torque. These signs reflect the feasibility of the suggested surgical movements and the long-term stability of the surgical outcome.

Discussion:

Treatment planning and assessment of the surgical correction of asymmetrical deformities is limited by reliance on 2D radiographs in the current clinical setting. The 2D radiographs conventionally used in orthodontic practice are particularly problematic when rotational or asymmetrical correction is required since surgical jaw displacements are inherently 3-dimensional. The use of cone-beam computed tomography (CBCT) or computer tomography (CT) provides the 3D imaging data necessary to generate precise knowledge of the location and the magnitude of facial asymmetry features, which are essential for the diagnosis of facial deformities and for the planning of corrective procedures.

An increasing number of studies have demonstrated that computer aided surgical simulation (CASS) can predict possible surgical complications and lowers material costs while decreasing surgery duration, with comparable or better surgical outcomes[13-15]. However in the current available software for surgical simulation the operator freehandedly move mandibular surgical segments for asymmetry corrections. Those movement decisions are subjective and carry the risk of under-treating the existing asymmetry in one of the planes of space or unbalancing position and shape corrections of the existing problem. The introduction of a template in the pipeline used in this project guides surgeons in the correction of the location differences between the left and right side of the mandible in the 3 planes of space.

Atlas construction has been conventionally used for group studies where deviation in size or shape in a particular anatomical structure from the "average" of the population indicates disease[16-18]. The use of the patient's own anatomy for the computation of the custom-made template accommodates the large gradient by which mandibular asymmetry presents clinically. It ensures that the outcome virtual template has the basic features (condylar position, relative size,…etc) that will still keep the

harmony between the mandible and the rest of the maxillofacial area. This approach will also help eliminate the need to decide on a "healthy" side for the mandible to mirror and use as a template especially that the concept of a "healthy" side in an asymmetric mandible is never strictly true due to the physiological compensation processes that take place during growth.

This pilot study will act as a proof of concept and a base for a multi-centre clinical survey to be conducted to get clinical feedback of 20 surgeons/orthodontists comparing our novel patient-specific atlas driven corrective surgeries with real surgery outcomes. Clinicians will be comparing surface models of actual surgical outcome to models of simulated outcome in reference to surface models and preoperative photos of each patient in a 20 patients cohort. Both scenarios will be compared using questions targeted to specific sub-regions in the mandible and its comparative position in space.

Conclusions:

This is a novel use of patient-specific atlas construction that will potentially improve the surgical outcomes of corrective surgeries and therefore the quality of life of patients with Craniofacial anomalies presented as facial asymmetry. It will also reduce the chair side time needed to collect conventional diagnostic aid for treatment planning and will tremendously augment those records. This custom-made atlas will hopefully eliminate subjectivity from surgical plans and increase the reproducibility of treatment planning of surgical correction of facial asymmetries. This approach has the potential to optimize the outcome of craniofacial corrective surgeries for asymmetric patients.

References :

1. Severt TR, Proffit WR. The prevalence of facial asymmetry in the dentofacial deformities population at the university of north carolina. Int J Adult Orthodon Orthognath Surg 1997;12(3):171-6.

2. Proffit WR, Fields HW,Jr, Moray LJ. Prevalence of malocclusion and orthodontic treatment need in the united states: Estimates from the NHANES III survey. Int J Adult Orthodon Orthognath Surg 1998;13(2):97-106.

3. Proffit W, Bailey L, Phillips C, Turvey TA. Long-term stability of surgical open-bite correction by le fort I osteotomy. The Angle Orthodontist JID - 0370550 0829.

4. Prima S, Ourselin S, Ayache N. Computation of the mid-sagittal plane in 3D images of the brain. Computer Vision â€" ECCV 2000 2000:685-701.

5. Rohr K. Landmark-based image analysis : Using geometric and intensity models. Dordrecht; Boston: Kluwer Academic Publishers; 2001. ID: 421870969.

6. Nanna Glerup. Asymmetry measures in medical image analysis. Department of Innovation IT, University of Copenhagen; April 29, 2005.

7. AlHadidi A, Cevidanes L, Mol A, Ludlow J, Styner M. Comparison of two methods for quantitative assessment of mandibular asymmetry using cone beam computed tomography image volumes. Dento Maxillo Facial Radiology JID - 7609576 1013(0250-832; 0250-832).

8. Yushkevich PA, Piven J, Hazlett HC, Smith RG, Ho S, Gee JC, Gerig G. User-guided 3D active contour segmentation of anatomical structures: Significantly improved efficiency and reliability. NeuroImage JID - 9215515 1006.

9. Meyer M, Desbrun M, Schröder P, Barr AH. Discrete differential-geometry operators for triangulated 2-manifolds. 2002.

10. Joshi S, Davis B, Jomier M, Gerig G. Unbiased diffeomorphic atlas construction for computational anatomy. NEUROIMAGE} 2004};23}(Suppl. 1}):S151-S160}.

11. Styner M, Oguz I, Xu S, Brechbuehler C, Pantazis D, Levitt JJ, Shenton ME, Gerig G. Framework for the statistical shape analysis of brain structures using SPHARM-PDM. 2006.

12. Styner M, Gerig G, Lieberman J, Jones D, Weinberger D. Statistical shape analysis of neuroanatomical structures based on medial models. Med Image Anal 2003;7(3):207.

13. Troulis MJ, Everett P, Seldin EB, Kikinis R, Kaban LB. Development of a three-dimensional treatment planning system based on computed tomographic data. (0901-5027 (Print); 0901-5027 (Linking)).

14. Hassfeld S, Muhling J. Computer assisted oral and maxillofacial surgery--a review and an assessment of technology. (0901-5027 (Print); 0901-5027 (Linking)).

15. Gateno J, Xia JJ, Teichgraeber JF, Christensen AM, Lemoine JJ, Liebschner MA, Gliddon MJ, Briggs ME. Clinical feasibility of computer-aided surgical simulation (CASS) in the treatment of complex cranio-maxillofacial deformities. (0278-2391 (Print); 0278-2391 (Linking)).

16. I. M, Miller. Computational anatomy: Shape, growth, and atrophy comparison via diffeomorphisms. Neuroimage 2004;23, Supplement 1(0):S19.

17. Beg MF, Miller MI, TrouvÃ© A, Younes L. Computing large deformation metric mappings via geodesic flows of diffeomorphisms. International Journal of Computer Vision 2005;61(2):139-57.

18. Miller MI, Younes L. Group actions, homeomorphisms, and matching: A general framework. International Journal of Computer Vision 2001;41(1):61-84.